

Conduction and Dielectric Relaxation Mechanisms in Oil Sands Influencing Electrical Heating

By

Tinu Mary Abraham

A thesis submitted in partial fulfillment of the requirements for the degree of

Doctor of Philosophy

in

Chemical Engineering

Department of Chemical & Materials Engineering

University of Alberta

©Tinü Mary Abraham, 2016

Abstract

Electrical heating has been proposed in the past as an alternative to conventional water based thermal methods for reducing viscosity of bitumen in oil sands reservoirs. This could reduce or even eliminate water use and associated problems like inefficient heat transfer in the reservoir, poor bitumen recovery as well as produced water treatment issues in the oil sands processing plant. However, four decades since its initial ideation, electrical heating of oil sands is still not commercialized. The reasons are rooted in a lack of understanding about the dynamic electrical heat generation mechanisms in oil sands. This has led to over-dependence of electrical heating on water, resulting in non-uniform and discontinuous heating of the reservoir, as well as overheating of electrodes leading to failure during field trials. This research study therefore gave importance to understanding the dynamic electrical heat generation mechanisms in heterogeneous oil sands as a function of their composition, microstructural arrangement and heating temperatures. The first approach was to determine conduction and dielectric relaxation mechanism in oil sands using impedance spectroscopy studies conducted between 1Hz and 1 MHz and at temperatures between 20 and 200°C. These studies revealed an array of conduction and polarization mechanisms. When water content of oil sands was high (>5%) present as connected water channels, dc conduction was the dominant mechanism via which electrical energy was dissipated as heat. On the other hand when it was low (<5%), water was assumed to be present in isolation at the interface between bitumen and silica grains resulting in interfacial or Maxwell Wagner (MW) polarizations which showed dielectric relaxations between 1 kHz and 1 MHz. Oil sands with least water content (<1%) showed a dominance of conduction relaxations via charge hopping mechanisms following Jonscher's law owing to the presence of silica grains having conduction through grain and grain boundaries. They also showed dominance of dipole relaxations in bitumen between 100 kHz and 1 MHz. These bitumen relaxations were present in all oil sands irrespective of their water content but were revealed only in cases where water was low. Temperature based studies revealed that beyond 120°C all oil sands behaved similarly, revealing a dominance of conduction relaxations due to silica and dipole relaxations due to bitumen, irrespective of the initial water and clay contents making them low loss heterogeneous dielectrics. Results from the second research approach linking heating patterns to the dynamic electrical behaviour of oil sands shed light on important operational strategies that could be implemented while carrying out electrical heating. A resonant autotransformer was used for electrically heating, probing and controlling the heating

process via capacitive heating configuration. The studies revealed that joule or ohmic heating could be most suitable for high water content (>5%) oil sands having dominance of dc conduction. Frequency tuned capacitive heating would be useful for oil sands showing a dominant loss peak due to MW polarizations (1 to 5% water). Whereas capacitive or dielectric heating set at the relaxation frequency of bitumen molecules would be most suitable for oil sands with least water content (<1%). Pure capacitive heating could also be most suitable beyond 120°C for all oil sands as they showed similar electrical behavior therefore suggesting that as temperature changes, operational strategies should be varied to catch up with changing electrical behaviour of oil sands. This research study therefore sheds new light on the electrical heat generation mechanisms which could influence efficient electrical heating of oil sands. These findings are expected to improve oil sands extraction process, resulting in cost reduction coupled with reduced impact on environment due to reduction in water usage, and carbon emissions.

Preface

This thesis is composed of a patent and a series of papers that have either been published in journal or conference proceeding. The following is a statement of contributions made to the jointly authored patent and papers contained in this thesis:

1. Abraham Tinu, Afacan Artin, Dhandharia Priyesh, Thundat Thomas, Conduction and Dielectric Relaxation in Athabasca Oil Sands with Application to Electrical Heating in *Energy & Fuels* 2016, 30 (7), 5630–5642. Abraham was responsible for conducting experiments, data analysis and writing paper. Afacan and Dhandharia helped with data analysis and proof reading. Thundat provided proof reading. This paper forms Chapters 3 and 4 of this thesis.
2. Abraham Tinu, Van Neste C.W., Afacan Artin, Thundat Thomas, Dielectric Relaxation-Based Capacitive Heating of Oil Sands in *Energy & Fuels*, 2016, 30 (3), 1987-1996. Abraham was responsible for conducting experiments and writing the paper. Afacan helped with experimental design and proof reading. Van Neste helped with construction of an experimental tool and proof reading. Thundat provided proofreading. This paper forms Chapters 5, 6 and 7 of this thesis.
3. Abraham Tinu, Gaikwad Rohan, Hande Aharnish, Van Neste C. W., Hawk J. E., Phani Arindam, Afacan Artin, Thundat Thomas, In Situ Heating of Oil Sands Using an Electrical Standing Wave Resonance Excitation Approach, *Proceedings of the World Heavy Oil Congress 2015*. March 24-26, 2015; Edmonton, Alberta, Canada. Abraham was responsible for conducting majority of the experiments, data analysis and writing the paper and oral presentation at the conference. Gaikwad conducted some oil sands characterization related experiments and proof reading. Hande and Phani helped with data discussion and proof reading. Van Neste and Hawk helped in construction of an experimental tool and proof reading. Afacan helped in experimental design and proof reading. Thundat provided proof reading. This paper forms Chapter 6 and 7 of this thesis.
4. C.W. Van Neste, Thomas Thundat, J.E. Hawk, Tinu Abraham, Jacob H. Masliyah, Jonathan Backs, Richard Hull, Arindam Phani, Resonant Dielectric Heating, US 2015/0129587 A1, May 14th, 2015. Van Neste was responsible for developing the resonator device and writing the patent application. Abraham tested and proved dielectric heating

applications of the device through experiments. Hawk, Backs, Hull and Phani characterized the standing wave nature of the resonator device. Thundat and Masliyah provided expert suggestions and proof reading. Parts of this patent form Chapter 5 of this thesis.

Acknowledgments

I would like to express my sincere thanks and appreciation to:

- My supervisor, Professor Thomas Thundat for awakening the researcher in me through his guidance.
- Mr. Artin Afacan who was a positive force, always present to hear me out and give great suggestions as well as technical and moral support.
- Mr. Priyesh Dhandharia for being there to have technical discussions whenever I wanted to and for always giving friendly advice and moral support.
- Dr. Jacob Masliyah for his support and valuable insights about oil sands.
- Dr. Vinay Prasad for his support and guidance.
- Dr. Redford for his teachings about the in situ recovery methods in oil sands.
- Dr. C.W. Van Neste, Mr. J.E. Hawk and Mr. Richard Hull for helping with experiments concerning the resonant autotransformer.
- Dr. Krupal Pal, Dr. Xiaoli Tan, Mr. James Skwarok, Dr. Zeljka for giving technical assistance in characterizing oil sands.
- Institute of Oil Sands Innovation for giving the oil sands samples.
- Dr. Krupal Pal, Mr. Priyesh Dhandharia, Dr. Ankur Goswami, Dr. Naresh Miriyala and Dr. Ravi Gaikwad for being my circle of support through the course of my studies and for continued moral support and friendship.
- Lily Laser for her ever ready to help attitude and great support.
- All fellow members of Professor Thomas Thundat's group and the Canada Excellence Research Chair in Oil Sands Molecular Engineering for financial support.

Finally, I thank my family members for their constant love and support. To my father and mother, I owe the deepest gratitude. I thank you for being my role models and constantly encouraging me to chase my dreams. For instilling values of hard work and integrity and for being there through the darkest times. To my brothers, I thank you for sparing some humour when I needed it and for making me feel that I could fight my demons. To my father and mother in law, I thank you for your constant care, patience and prayers. To my sisters and brother in law, I thank you for your positivity and encouragement. To Samuel and Nicole the bundles of hope, I thank you for making me smile. To all relatives and friends who kept me in their good thoughts and prayers. Most of all,

to Tenny, my soulmate, I thank you for completing this journey with me. All this would have never come true without your dangerous optimism, genuine encouragement and honest love. It is to all of you that I dedicate the fruits of my work.

Finally, it is God Almighty who instilled in me the curiosity and drive to pursue learning and who also saw me through all difficulties. I am ever thankful!

Lastly, this thesis will be in memory of my favourite uncles Late Shibu Joseph Kandarapallil and Late C.T. Jacob Maliekal who passed away during the course of my PhD. R.I.P

Table of Contents

Chapter 1 Introduction	1
1.1 Role of Oil Sands and Heavy Oil in Global Energy Production.....	2
1.2 Challenges of Current Thermal Technologies in Oil Sands.....	2
1.3 Use of Electrical Energy for Heating Oil Sands	4
1.4 Electrical Conduction and Dielectric Relaxation Mechanisms in Oil Sands – The New Research Study.....	6
1.4.1 Approaches to the Research Study.....	6
1.5 Thesis Structure.....	8
1.6 References	10
Chapter 2 Review of Dynamic Electrical Behavior of Oil Sands and Applied Electrical Heating Techniques	14
2.1 Introduction to Electrical Heating.....	14
2.1.1 Background of Ohmic Heating.....	15
2.1.2 Background of Induction Heating	16
2.1.3 Background of Dielectric Heating.....	16
2.2 Application of Electrical Heating to Geological Systems.....	20
2.3 Review of Dynamic Electrical Behaviour of Oil Sands and Applied Electrical Heating Techniques – Numerical Simulation and Modeling, Laboratory and Field Scale Studies	21
2.3.1. Dynamic Electrical Behaviour of Oil Sands – A Heterogeneous Dielectric Mixture. 22	
2.3.1.1 Oil Sands Composition and Microstructural Arrangement	22
2.3.1.2 Electrical Properties and Dominant Electrical Mechanisms in Individual Components of Oil Sands	24
2.3.1.3 Electrical Mechanisms in Heterogeneous Mixtures	25
2.3.1.4 Studies on Electrical Behaviour of Oil Sands.....	27
2.3.2 Electrical Heating Techniques Applied to Oil Sands and Heavy Oil Reservoirs.....	29

2.3.2.1 Ohmic Heating of Oil Reservoir	30
2.3.2.1.1 Indirect Ohmic Heating	30
2.3.2.1.2 Direct Ohmic Heating	32
2.3.2.2. Inductive Heating of Oil Sands Reservoir	53
2.3.2.3. Dielectric Heating of Oil Reservoir	59
2.4 Conclusions & Future Work	73
2.5 References	74
Chapter 3 Conduction and Polarization Mechanisms in Oil Sands	84
3.1 Introduction – Electrical Mechanisms in Oil Sands – A Heterogeneous Dielectric	84
3.2 Theoretical Background of Determination of Conduction and Polarization Mechanisms in Oil Sands	86
3.2.1 Calculation of Electrical Properties from Impedance Spectroscopy Measurements....	86
3.2.2 Determination of Conduction and Polarization Mechanisms in Oil Sands from Electrical Property Variation with Frequency	89
3.2.3 Determination of Bulk Relaxation Mechanisms from Modulus Spectroscopy	91
3.3 Materials and Methods	93
3.4 Results and Discussions	95
3.4.1 Variation of Real and Imaginary Permittivity with Frequency and Composition.....	95
3.4.2 Variation of Loss Tangent with Frequency and Composition.....	96
3.4.3 Variation of Conductivity with Frequency and Composition	98
3.4.4 Modulus Spectroscopy of Oil Sands	100
3.4.5 Variation of Dielectric Constant and Conductivity with Water Concentration as a Function of Frequency.....	101
3.5 Conclusions	102
3.6 References	104
Chapter 4 Temperature based Conduction and Polarization Mechanisms in Oil Sands.....	107

4.1 Introduction	107
4.2 Materials and Methods	108
4.3 Results and Discussions	108
4.3.1 Temperature Based Impedance Spectroscopy of Oil Sands 1	108
4.3.2 Temperature Based Impedance Spectroscopy of Oil Sands 2 to 4.....	113
4.3.3 Temperature Based Impedance Spectroscopy of Oil Sands 5 and 6	116
4.3.4 Impedance Spectroscopy of Oil Sands 1 to 6 on Cooling After Heating.....	118
4.4 Conclusions	119
4.5 References	120
Chapter 5 Characterization of Resonant Autotransformer for Conducting Capacitive Heating of Oil Sands.....	121
5.1 Introduction	121
5.2 Resonant Autotransformer	123
5.3 Load Impedance Based Characterization Studies of Resonant Autotransformer.	126
5.4 Material and Methods.....	126
5.5 Results and Discussions	131
5.5.1 Effect of Varying Dielectric Material.....	131
5.5.1.1 Resonance Frequency (RF).....	131
5.5.1.2. Input Current (IC)	133
5.5.2 Effect of Varying Electrode Spacing.....	135
5.5.2.1 Resonance Frequency (RF).....	135
5.5.2.2 Input Current (IC)	137
5.5.3 Effect of Varying Bottom Electrode Connection	140
5.5.3.1 Resonance Frequency (RF).....	140
5.5.3.2 Input Current (IC)	141

5.5.4. Effect of Changing Oil Sands Capacitance by Varying Area of Electrode	143
5.6 Conclusions	144
5.7 References	144
Chapter 6 Capacitive Heating Studies of Oil Sands Using Resonant Autotransformer	145
6.1 Introduction	145
6.2 Materials and Methods	148
6.3 1D Steady State Heat Transfer Equation with Dielectric Heat Generation in the System	151
6.4 Results and Discussions	154
6.4.1 Heating Profile for Disc Electrode Configuration in Big Oil Sands Capacitor (8.4 pF).....	154
6.4.2. Heating Profile with Disc Electrode Configuration in a Small Oil Sands Capacitor (1.7pF)...	156
6.4.3 Heating Profile with Bullet Electrode Configuration	159
6.5 Conclusions	162
6.6 References	163
Chapter 7 Controlled Capacitive Heating of Oil Sands Based on Its Probed Dynamic Electrical Behaviour	164
7.1 Introduction	164
7.2 Materials and Methods	165
7.3 Results and Discussions	167
7.3.1 Resonance Frequency based Probing and Controlling of Capacitive Heating of Oil Sands.....	167
7.3.1.1 Power Tuned Controlled Capacitive Heating of Oil Sands Having Dominance of Conduction Relaxations and Dipole Polarization	167
7.3.1.2 Frequency Tuned Controlled Capacitive Heating of Oil Sands Having Dominance of Interfacial Polarizations	168

7.3.1.3 Rapid Frequency Tuned Controlled Capacitive Heating of Oil Sands Having Dominance of DC Conduction.....	169
7.3.2. Input Current and Phase Angle Based Probing of Dynamic Variations in Oil Sands Impedance during Capacitive Heating	170
7.3.2.1 Probing of Dynamic Electrical Behaviour of Oil Sands Having Conduction Relaxations and Dipole Polarizations during Capacitive Heating.....	171
7.3.2.2 Probing of Dynamic Electrical Behaviour of Oil Sands Having Interfacial Polarizations during Capacitive Heating.....	174
7.4 Conclusions.....	181
7.5 References.....	182
Chapter 8 Conclusions	183
8.1 Concluding Remarks.....	183
8.1.1 Conduction and Polarization Mechanisms in Oil Sands	183
8.1.2 Capacitive Heating of Oil Sands Using Resonant Autotransformer	184
8.2 Major Contributions.....	186
8.3 Recommendations for Future Research	187
Bibliography	188
Appendix A.....	201
Appendix B.....	204
Appendix C.....	210
Appendix D.....	212

List of Tables

Table 1-1. Comparative account of water, energy consumption, GHG emissions and cost of production in the oil sands industry.....	3
Table 2-1. Direct Ohmic Heating of Oil Reservoirs with Single Vertical Well Electrode with Ground Return –Field Tests.....	35
Table 2-2. Direct Ohmic Heating of Oil Reservoirs using Two Adjacent Well Configuration – Numerical Modeling and Lab Tests.....	41
Table 2-3. Direct Ohmic Heating of Oil Reservoirs using Two Adjacent Well Configuration – Field Tests.....	44
Table 2-4. Direct Ohmic Heating of Oil Reservoirs using Electrical Connection through Tubing and Casing of same well – Numerical Modeling and Lab Tests	47
Table 2-5. Direct Ohmic Heating of Oil Reservoirs using Electrical Connection through Tubing and Casing of same well –Field Tests.....	47
Table 2-6. Ohmic Heating of Oil Reservoirs using Horizontal Wells and ET-DSP process–Field Tests	52
Table 2-7. Induction Heating of Oil Reservoirs –Numerical Simulation, Lab and Field Tests ...	57
Table 2-8. Dielectric Heating of Oil Reservoirs –Field Tests	67
Table 2-9. Dielectric Heating of Oil Reservoirs – Numerical Modeling and Lab Tests	68
Table 5-1. Experimental Methodology for Characterising Load Based Performance of Resonant Autotransformer.....	128
Table 5-2. Capacitance of small and big oil sands capacitor cells.....	130
Table 6-1. Input power and power dissipated as heat in oil sands based on the electric field generated in the oil sands when bottom electrode connection was varied along the resonant autotransformer for big capacitance.....	156
Table 6-2. Tabulation of temperature profile during capacitive heating of oil sands carried out at different input electric field varied by varying the bottom electrode connection along the resonant autotransformer.	156
Table 6-3. Input power and power dissipated as heat in oil sands based on the electric field generated in the oil sands when bottom electrode connection was varied along the resonant autotransformer for small capacitance.....	159

Table 6-4. Tabulation of temperature profile during capacitive heating of oil sands carried out at different input electric field for small capacitance.	159
Table 6-5. Tabulation of input power supplied and heating profile in the oil sands when bullet electrodes were used to carry out capacitive heating.	160
Table 6-6. Tabulation of input power supplied and heating profile in the oil sands when bullet electrodes were used to carry out capacitive heating in the absence of faraday cage	162
Table 7-1. Composition of oil sands used for carrying out re-tuning resonance frequency experiments.	166
Table 7-2. Composition of oil sands used for carrying out experiments for investigating heating by varying bottom electrode connection.	167
Table A-1. Experimental data of three runs carried out for estimating the composition of Oil Sands 1 to 6 using the Dean Stark Extraction Method.	201
Table C-2. Estimation of Electric Field in Big Oil Sands Capacitor based on Spatial Temperature Profile at Steady State Condition.	210
Table C-3. Estimation of Electric Field in Small Oil Sands Capacitor based on Spatial Temperature Profile at Steady State Condition.	211

List of Figures

Figure 2-1. Relationship diagram showing the interdependence of electrical properties of materials with the applied electrical energy in dictating the feasibility/efficiency of electrical heating.....	14
Figure 2-2. Classification of type of electrical heating based on the type of material and the frequency of electrical energy.....	15
Figure 2-3. Different polarization mechanisms in a dielectric material when interacting with electrical energy ⁴	17
Figure 2-4. Depiction of relaxation time τ when a static electric field is switched off.	18
Figure 2-5. Frequency dependence of different polarization mechanisms in homogeneous dielectrics.	19
Figure 2-6. Electrical Resistive Heating for in situ remediation of soil contaminated with organic matter ¹⁵	21
Figure 2-7. Relationship diagram of crucial research components that need to be investigated for efficient electrical heating of oil reservoirs	22
Figure 2-8. Composition of oil sands and electrical properties of each component/phase.....	24
Figure 2-9. Conduction and polarization mechanisms in heterogeneous mixtures consisting of conductive, solid dielectric and polymer like dielectric phases.....	27
Figure 2-10. (a) A typical downhole electrical heating system carrying out indirect ohmic heating (b) Polymer insulated CW cable (c) Mineral Insulated cable adapted from ³⁸	31
Figure 2-11. Schematic of initial configuration of electrothermic heating process applied to reservoir adapted from ⁴⁴	32
Figure 2-12. Schematic of electrothermic heating process patented for oil sands reservoirs adapted from ^{48,52}	36
Figure 2-13. Electrical heating single wellbore configuration adapted from ⁶⁰	45
Figure 2-14. (a) Electrical heating using horizontal and vertical well configuration (b) Electrical heating using a combination of two vertical wells and a horizontal well adapted from ⁶¹	48
Figure 2-15 Field scale illustration of ET-DSP Process.	
http://www.creosoteremediation.com/index.php/etdsp-technology	51
Figure 2-16. Artist's illustration of field scale EM-SAGD adapted from ⁷²	54

Figure 2-17. Triplate electrode configuration (a) fully shielded triplate, (b) triplate line open side equivalent, (c) cylindrical conductor array equivalent adapted from ⁸¹	60
Figure 2-18. Artist’s illustration of radiofrequency heating process in oil sands reservoir ¹⁰⁴	66
Figure 3-1. Conduction and polarization mechanisms that could be found in heterogeneous oil sands.....	84
Figure 3-2. Schematic interpretation of determining conduction and polarization mechanisms in oil sands.	92
Figure 3-3. Composition of different oil sands samples used for this study estimated from Dean-Stark extraction method	93
Figure 3-4. Illustration of impedance spectroscopy experiments carried out for oil sands samples at room temperature.	94
Figure 3-5. (a) Dielectric constant and (b) Dielectric losses of oil sands when swept from 1Hz to 1MHz at room temperature (20°C).....	95
Figure 3-6. Loss tangent ($\tan\delta$) spectroscopy of oil sands at room temperature (20°C), depicting frequencies due to interfacial polarizations / MW relaxations, β relaxations and conduction relaxations.....	97
Figure 3-7. Conductivity spectra of oil sands at room temperature (20°C) depicting electrode polarizations, dc conduction and conduction relaxations.	98
Figure 3-8. Imaginary modulus spectra of oil sands at room temperature (20°C)	101
Figure 3-9. Dielectric constant and conductivity of oil sands as a function of water content at different frequencies.	102
Figure 3-10. Summary of Conduction and Polarization Mechanisms in Oil Sands with Different Composition.....	104
Figure 4-1. Illustration of temperature based transition of oil sands	108
Figure 4-2. (a) Dielectric constant (b) Dielectric losses of Oil Sands 1 when swept from 1Hz to 1MHz as a function of temperature. Inset of (a) and (b) zooms into frequency regime where β relaxations are observed.....	109
Figure 4-3. Conductivity spectra of Oil Sands 1 measured as a function of temperature and fitted with Universal Dielectric Response (UDR) or Jonscher’s Law.	111
Figure 4-4. Modulus spectra of Oil Sands 1 as a function of temperature depicting hopping polarizations and bitumen dipole polarizations.	112

Figure 4-5. Loss tangent of Oil Sands 1 as a function of temperature.....	113
Figure 4-6. (a) Conductivity spectra and (b) Modulus spectra of Oil Sands 2 as a function of temperature	115
Figure 4-7. Loss tangent of Oil Sands 2 as a function of temperature.....	115
Figure 4-8. (a) Conductivity spectra and (b) Modulus spectra of Oil Sands 5 as a function of temperature	116
Figure 4-9. Loss tangent of Oil Sands 5 as a function of temperature.....	117
Figure 4-10. Summary of electrical properties of all six oil sands when cooled down to room temperature after heating to 200 (a) Dielectric Constant (b) Dielectric losses (c) Conductivity (d) Imaginary Modulus (e) Dissipation factor.....	119
Figure 5-1. Block diagram free running oscillator used to carry out industrial RF heating ¹	122
Figure 5-2. Block diagram of 50Ω technology system used for carrying out industrial RF heating ¹	122
Figure 5-3. (a) Picture of resonant autotransformer placed inside a faraday cage in the backdrop. (b) Distributed nature of electric field and magnetic field in the resonant autotransformer. (c) Simulated results of electric and magnetic field magnitudes along turns of the resonant autotranformer.....	125
Figure 5-4, Circuit diagram of resonant autotransformer (a) without load capacitance and (b) with load capacitance.....	126
Figure 5-5. Block diagram of lab scale experimental set up for supplying the required energy to the resonant autotransformer with the capacitance load.	127
Figure 5-6. Schematic illustration of experiment conducted for characterizing working of a resonant autotransformer when connected to a capacitor load.	129
Figure 5-7. Large sized oil sands capacitor cell.....	130
Figure 5-8. Variation of RF for different dielectric materials for a given electrode spacing when bottom electrode is connected at different turn connections.	132
Figure 5-9. Variation of RF for different dielectric materials for a given bottom electrode connection when electrode spacing is varied.....	133
Figure 5-10. Variation of input current with voltage on varying dielectric materials for a given electrode spacing and bottom electrode connection	134

Figure 5-11. Variation of RF for different electrode spacing for a given dielectric materials when bottom electrode is connected at different turn connections.	135
Figure 5-12. Variation of RF for different electrode spacing for a given bottom electrode connection and dielectric material.	136
Figure 5-13. Illustration of reduced spacing between top electrode and ground as the spacing between top and bottom electrode in the capacitor is increased by fixing the bottom electrode and moving the top electrode.....	137
Figure 5-14. Variation of input current with voltage on varying electrode spacing for a given dielectric material and bottom electrode connection	139
Figure 5-15. Variation of RF for different bottom electrode connections for a given dielectric materials for different electrode spacing.....	140
Figure 5-16. Variation of RF for different bottom electrode connections for a given electrode spacing for different dielectric materials.	141
Figure 5-17. Variation of input current with voltage on varying bottom electrode connection for a given dielectric material and electrode spacing	142
Figure 5-18. Variation of resonance frequency and input current with bottom electrode tapping location when two different oil sands capacitor sizes are used.	143
Figure 6-1. A simplified schematic of a dielectric heating system adapted from ¹	145
Figure 6-2. Equivalent circuit diagram of the dielectric heating system adapted from ¹	146
Figure 6-3. (a) Big oil sands capacitor of 8.4 pF made of disc electrodes spaced 6cm apart (b) Small oil sands capacitor of 1.7 pF made of disc electrodes spaced 10cm apart (d)Capacitor made of bullet electrodes spaced 10cm apart	149
Figure 6-4. Schematic illustration of experiment used to carry investigation of capacitive heating pattern in oil sands when heating using resonant autotransformer.	150
Figure 6-5. Depiction of Control Volume across which Heat Transfer model is developed.....	151
Figure 6-6. Heating profile of Oil Sands 4 when capacitive heating was carried out between disc electrodes placed 5cm apart, with bottom electrode connection varied between 29th, 111th and 176th turns	155
Figure 6-7. Heating profile of Oil Sands 4 when capacitive heating was carried out between disc electrodes placed 10cm apart, with bottom electrode connection varied between 29th, 111th and 176th turns	158

Figure 6-8. Heating profile of Oil Sands 4 when capacitive heating was carried out between bullet electrodes placed 10cm apart, with bottom electrode connection varied between 111th and 176th turns	160
Figure 6-9. Heating profile of Oil Sands 4 when capacitive heating was carried out between bullet electrodes placed 10cm apart, with bottom electrode connection varied between 111th and 176th turns in the absence of the faraday cage.	161
Figure 7-1. Capacitive heating data of Oil Sands 1 indicating voltage tuning to increase the heating process.....	168
Figure 7-2. Capacitive heating data of Oil Sands 3 indicating frequency tuning to increase the heating process.....	169
Figure 7-3. Capacitive heating data of Oil Sands 5 indicating more rapid frequency tuning to increase the heating process.....	170
Figure 7-4. Effective permittivity, conductivity and loss tangent of Oil Sands 1 at 20°C	172
Figure 7-5. (a) Capacitive heating results of Oil Sands 1 with input current and phase variations (b) Variation in effective permittivity, conductivity and loss tangent of Oil Sands 1 with temperature at 200 kHz as determined from impedance spectroscopy.....	173
Figure 7-6.(a) Experimental setup used to carry out capacitive heating of bitumen (b) Temperature profile attained during capacitive heating of bitumen.	174
Figure 7-7. Effective permittivity, conductivity and loss tangent of Oil Sands 4 at 20°C	176
Figure 7-8. Loss tangent spectroscopy of Oil Sands 4 at different temperatures	177
Figure 7-9. (a) Capacitive heating results of Oil Sands 4 with input current and phase variations (b) Variation in effective permittivity, conductivity and loss tangent of Oil Sands 4 with temperature at 200 kHz as determined from impedance spectroscopy.....	180
Figure 8-1. Operational strategies for carrying out electrical heating of oil sands based on their dynamic electrical behavior.	187
Figure A-1. Calibrated values of dielectric constant for known components when swept from 1Hz to 1MHz at room temperature (20°C).	202
Figure A-2. Calibrated values of Loss tangent for known components when swept from 1Hz to 1MHz at room temperature.....	202
Figure A-3. Calibrated values of conductivity for known components when swept from 1Hz to 1MHz at room temperature.	203

Figure A-4. Calibrated values of modulus spectra for known components when swept from 1Hz to 1MHz at room temperature.....	203
Figure B-5. Results of 2nd and 3rd runs of temperature based conductivity and modulus spectra of Oil Sands 1.....	204
Figure B-6. Results of 2nd and 3rd runs of temperature based conductivity and modulus spectra of Oil Sands 2.....	205
Figure B-7. Results of 1st, 2nd and 3rd runs of temperature based conductivity and modulus spectra of Oil Sands 3.....	206
Figure B-8. Results of 1st, 2nd and 3rd runs of temperature based conductivity and modulus spectra of Oil Sands 4.....	207
Figure B-9. Results of 2nd and 3rd runs of temperature based conductivity and modulus spectra of Oil Sands 5.....	208
Figure B-10. Results of 1st, 2nd and 3rd runs of temperature based conductivity and modulus spectra of Oil Sands 6.....	209
Figure D-11. Capacitive heating results of Oil Sands 1 with input current and phase variations from repeated experiment.....	212
Figure D-12. Capacitive heating results of Oil Sands 4 with input current and phase variations from repeated experiment.....	213
Figure D-13. Capacitive heating results of Oil Sands 5 requiring rapid frequency tuning from repeated experiment.....	214

Chapter 1 Introduction

Oil controls world economies and so producing oil resources in a process efficient and cost effective manner are crucial objectives of wide-scale research. With increasing economic development, the average greenhouse gas intensity of the global oil supply is expected to increase in the foreseeable future. Thereby, all countries support innovation in the energy sector and the adoption of clean energy technologies to reduce carbon emissions and other environmental impacts associated with energy development. Of the total recoverable oil reserves 46% is found in conventional light crude oil while the remaining 54% is found as heavy oil and bitumen which would inevitably be exploited in the coming years¹. Heavy oil and bitumen are not recoverable in their natural state by ordinary production methods used to pump conventional light crude oil having lower density and viscosity ($>22^{\circ}\text{API}$, 1cP) owing to their high density (10 to 20°API and $<10^{\circ}\text{API}$ respectively) and viscosity (100 cP and 10^{4-7} cP respectively)¹. Enhanced recovery methods utilizing thermal energy or solvent dilution are applied to reduce the viscosity of these oils to make them mobile. The oil sands of Alberta forming the third largest oil reserve in the world, is a heterogeneous mixture of sand, clay and water saturated with dense and highly viscous bitumen. Over the past years, the process of extracting bitumen from this heterogeneous mixture has thrived driven by technology innovation and research. Though evolving technology has played a significant role in better recovery of bitumen, the issues today largely pertain to the elaborate consumption of energy and water in extracting this resource leading to high production costs and some negative environmental impacts. The future calls for technology that can reduce these drawbacks while causing efficient extraction of bitumen. In current operations the thermal energy of steam is harnessed for in situ recovery through different processes like Cyclic Steam Stimulation (CSS) and Steam Assisted Gravity Drainage (SAGD). Apart from issues of water consumption, poor control of steam flow and heat transfer in the reservoir have affected efficient recovery of bitumen and have also resulted in produced water problems in the oil sands industry². As an alternative, few researchers over the years have embarked on researching electrical techniques for heating in situ oil sands²⁻¹². The prospects of implementing this technology, seems bright as electrical energy on being applied to a medium can directly interact with the atoms, molecules and electrons to generate heat resulting in volumetric heating. However, some of the proposed electrical techniques are beset with issues pertaining to discontinuation of heating process on evaporation of water in the reservoir, over heating of electrode surfaces and failure of electrode

systems during the heating process. In order to overcome these challenges and impact successful implementation of electrical heating of oil sands, a good understanding of the dynamic electrical behavior of oil sands as a function of their composition and temperature needs to be attained. This research attempts to address these gaps in the understanding of electrical heating of oil sands with the goal of developing feasible electrical heating in the future.

1.1 Role of Oil Sands and Heavy Oil in Global Energy Production

The total accumulation of heavy oil and bitumen are 3396 and 5505 billion barrels of original oil in place¹. These oil reserves are distributed among 192 heavy oil and 8 bitumen basins with major portion of heavy oil in the Middle East and South America followed by North America. The largest bitumen reservoirs are found in North and South America. Canada and Venezuela together have greater than 35% of the heavy oil and bitumen reserves.

Alberta has the world's third largest oil reserves in the world with 170 billion barrels (bbl) of oil, consisting of 168 billion bbl of bitumen from oil sands and 1.7 billion bbl of conventional crude oil. Oil sands are located in three major areas in northeast Alberta with about 80% of it found in situ at a depth of 75 to 750m while 20% found on the surface above 75m. There are 114 active oil sands projects of which six are producing surface mining projects (three more are under application); the remaining projects use various in-situ recovery methods. The presence of such a vast resource in Alberta has hugely contributed to its economic growth and is expected to generate over 500,000 jobs and \$472 billion as oil sands based royalties and tax revenues in the next 25 years¹³.

1.2 Challenges of Current Thermal Technologies in Oil Sands

The oil sands industry has had to face several environmental and production cost related challenges deeply rooted in processing highly viscous bitumen (10^6 cP at 10°C)¹⁴ found mixed with sand, clay and water in oil sands. This highly viscous nature makes it almost impossible to extract bitumen at lower temperatures or reservoir conditions, unlike crude oil found in other parts of the world. The viscosity of bitumen reduces exponentially as temperature is increased, reducing from 10^6 cP at 10°C to 10 cP at 250°C ¹⁴. Therefore, the extra effort needed to mobilize bitumen in the reservoir is accomplished using thermal recovery techniques utilizing hot/warm water or steam. The thermal energy carriers transfer heat to oil sands through thermal conduction and convection

mechanisms. However, oil recovery factors using these thermal techniques are still low: being about 10% on average for cold heavy oil production, about 25% for cyclic steam stimulation (CSS), and 40 to 60% for steam-assisted gravity drainage (SAGD) ¹⁵.

Although the use of water has been convenient and feasible it has resulted in the production of environmentally hazardous tailing ponds and have also resulted in several produced water treatment problems in addition to many operational inefficiencies. The substantial use of water and energy in the oil sands industry have also contributed to greenhouse gas (GHG) emissions and are reasons for high production cost of bitumen as detailed in Table 1-1. In today’s scenario where the price of oil has fallen severely (\$30 to 50/bbl) it is essential to reduce the cost of producing a barrel (bbl) of bitumen, which stands at an average cost of \$70-90/bbl ¹⁶. This is important for the industry to sustain well in the coming years as the high cost of production is one of the debilitating disadvantages for oil sands industry in comparison to other oil producers. Due to this weakness, Alberta and Canada at large has bared the brunt of several recessions and price volatilities promoted by geopolitical instability in oil producer countries, growing demands and unforeseen global economic events ¹⁷. In light of these issues, the future calls for technology that can reduce cost and such consumption of water and energy for sustainable growth and development of the oil sands industry. As in situ oil sands form 80% of the reserves, it is evident that establishing efficient technology in this sector will be beneficial to Alberta in the coming years ¹⁸.

Table 1-1. Comparative account of water, energy consumption, GHG emissions and cost of production in the oil sands industry.

Parameter	Surface Mining	In Situ Operations
Percentage of total reserve ¹	20%	80%
Water/Steam use ²	3.18 bbl/bbl of bitumen	0.31 bbl/bbl of bitumen
Natural gas use ³	0.5 mcf/bbl of bitumen	1 mcf/bbl of bitumen
GHG Emissions ²	125 kg CO ₂ equivalent/bbl of bitumen which is 8.5% of Canada’s total emissions	
Cost of production ⁴	\$80-90/bbl of bitumen	\$70-80/bbl of bitumen

¹ Alberta Energy Facts and Statistics <http://www.energy.alberta.ca/oilsands/791.asp>

² Canadian Association of Petroleum Producers. 2014. 2014 Progress Report. Page 27 <http://www.capp.ca/~media/capp/customer-portal/publications/255363.pdf> (accessed March 1st 2016)

³ 17

⁴ 16

For in situ extraction methods such as CSS or SAGD, steam-to-oil ratio (SOR) is a measure of the thermal efficiency of the process measuring the average volume of steam needed to produce one barrel of bitumen. A low SOR indicates that steam is more efficiently utilized resulting in reduced capital and operating costs, reduced water use and energy consumption, and lower emissions including GHGs¹⁹. Currently, SOR for in situ extraction process ranges from 2.9 to 3.1 units. However, SAGD projects are presently seeking to achieve a SOR target of 1.8 in their operations¹⁷. In current processes, SAGD tends to be wasteful of steam because of the following reasons:

1. Low initial injectivity of steam leads to poor communication between wells, poor control of injected fluid movement, steam override and poor sweep efficiency², requiring frequent changes to operating regimes making SAGD projects labour intensive.
2. Poor control of steam flow within reservoir to depleted regions or overburden caused by tendency of steam chamber to creep laterally beneath the reservoir cap results in poor thermal efficiency.^{20,21}
3. Production problems include sand production, hot effluent/high water cut production, wellbore scaling and poor recovery rates of bitumen^{22,23}.
4. Production of high water cut in the obtained product results in requirement of produced water treatment which tends to be costly and also results in a host of treatment issues²².
5. The fundamental mechanics of SAGD are still not clearly understood inhibiting rectification of the mentioned operational issues²⁴.
6. These high pressure processes cannot be applied to thin or shallow reservoirs, reservoirs with poor cap rock, fractured reservoirs and high water saturation reservoirs²⁵. Therefore regions between 75m to 200m called the intermediate in situ reservoirs are largely untapped by in situ or mining technologies^{13,26}.

With such reasons it becomes evident that using water based thermal recovery methods is not yet a sustainable technology and newer methods need to be investigated and implemented.

1.3 Use of Electrical Energy for Heating Oil Sands

As an alternative to steam driven thermal processes, few researchers over the years have embarked on electrical techniques for heating in situ oil sands. Electrical energy on being applied to a medium can directly interact with the atoms, molecules and electrons to induce motion mechanisms which result in heat generation within the medium in comparison to heat being

supplied by an external carrier. Therefore, if implemented effectively, localized heating with minimal heat losses (due to avoidance of heat losses from poor control of steam flow in the reservoir) can occur reducing the disadvantages of thermal heat transfer due to energy supplied by another medium. Some of the important advantages of electrical heating technology over thermal based hot water and steam injection methods include:

1. Reduction or elimination of water use.
2. Issues of initial low injectivity of reservoirs faced by steam based processes is not really relevant in electrical heating process.
3. Improved thermal efficiency due to targeted and controlled heating of the reservoir with minimal loss of heat energy, unlike poorly controlled steam based processes, reducing associated GHGs as well as overall cost.
4. More environmentally friendly as compared to other chemical or gas based enhanced oil recovery (EOR) methods as they do not contaminate or alter the geology of the reservoir.
5. Does not generate any solid waste or produce water emulsion treatment problems as seen in steam based extraction methods.
6. Can be applied to thin or shallow reservoirs with the same feasibility as applied to deep and thick reservoirs. It can also be applied to reservoirs with thin cap rock containment.
7. Can be applied effectively to heterogeneous reservoirs with high permeability streaks or fractures, which would have caused steam leakage in steam based processes.

However, even with many advantages as compared to other processes, electrical heating is yet to see the face of commercial success. The underlying scientific premises are sound and relatively simple, and were confirmed by basic experiments performed in the past, particularly in Russia, the USA and Canada ²⁷. While the experiments were encouraging, the overall complexity of the reservoir response to electrical heating was not well understood. This has resulted in inadequate simulation tools which offer under-informed predictions of electrical heating patterns. Also the power supply and electrode well or antenna system were not well designed to suit the reservoir electrical behavior. Moreover the different electrical heating schemes have issues concerning overdependence on water in the oil sands reservoir, overheating of oil sands water near the electrode/antenna surfaces leading to overheating of the electrode surface causing inefficient/non-

uniform and discontinuous heating process following the dynamic changes in the reservoir. For these reasons, this technology is yet to be commercialized.

Understanding the dynamic response of the reservoir to electrical energy involves research about the electrical heat generation mechanisms in oil sands and their variation with increasing temperatures and composition. A clear understanding in this fundamental direction would influence implementation of optimized operational strategies throughout the heating and production cycle as it will directly influence the electrode or antenna sizes, shapes, spacing as well as operating voltage, current and power levels. Moreover they will determine the heating rates, system operating efficiencies and overall electrical energy requirements for an efficient process. Before proceeding towards field trials it would influence implementation of more realistic reservoir simulations and design of efficient electrode/antenna systems for delivering electrical energy to the reservoir.

1.4 Electrical Conduction and Dielectric Relaxation Mechanisms in Oil Sands – The New Research Study

Thus the main objective of this research is to address some or many of the mentioned drawbacks of electrical heating through an integrated understanding of the reasons of electrical heating patterns and behavior of oil sands found in the mutual arrangement of their components and overall composition which changes with temperature. The intention is to fully implement electrical heating technique for extracting bitumen from oil sands so that currently used water based thermal methods can be reduced or eliminated. This would greatly reduce the cost incurred by the oil sands industry and also improve the energy efficiency.

1.4.1 Approaches to the Research Study

The approaches taken in this work to improve technical feasibility of electrical heating of oil sands include understanding its electrical heat generation mechanisms as a function of its composition, temperature, electrical frequency and voltage of application. Six oil sands with increasing water and clay content were investigated for this study. The first study included characterizing the electrical properties of oil sands with electrical frequency, composition and temperature. Impedance spectroscopy was implemented for this study. The goal of this study was to determine the electrical conduction and polarization mechanisms in oil sands and the corresponding energy losses or heat generation due to these mechanisms as a function of their composition, temperature

and frequency of applied electrical energy. The hypothesis was that direct current (dc) conduction mechanisms dominated oil sands having maximum water and clay content, while oil sands with lesser water and clay content would have a dominance of interfacial polarizations and conduction relaxations. Bitumen being a complex hydrocarbon having polar and non-polar components tend to associate strongly to form organized structures throughout the continuous phase of non-polar materials. Thus they can be considered to be like polymers in nature and could also offer dielectric polarizations due to motion of local molecules or side chains or cooperative motion of polymer segments. As temperature of oil sands increases, the loss of water would influence the electrical mechanisms resulting in a convergence of behaviour for all oil sands investigated, irrespective of the initial water and clay content.

The second approach was to study the effect of capacitive heating technique on electrical heat generation in oil sands linked to their dynamic electrical heat generation mechanism. Three oil sands were selected for this study which varied in water and clay content. A resonant radiofrequency generator called the resonant autotransformer was used as the energy source, which served as both an electrical energy applicator and a sensor of the variation of the electrical behaviour of oil sands with heating. While multiple variants of electrical heating techniques such as ohmic heating at 60 Hz²⁸, induction heating at 100 kHz using coils²⁹ and dielectric heating using electromagnetic radiation from antennas from 3 kHz to 300 MHz^{3,25} have been proposed and investigated by other researchers, this study was about using high alternating electric fields for carrying out capacitive or dielectric heating. The hypothesis was that capacitive heating could be the most suitable technique of electrical heat generation in oil sands as they are predominantly dielectrics in nature. The feasibility of capacitive heating was investigated as a function of oil sands volume, electrode geometry, input voltage, oil sands composition and its changing electrical behavior with temperature.

Based on the inferences and conclusions drawn from these two approaches, operational strategies are proposed for the implementation and optimization of suitable electrical heating techniques for different oil sands composition and temperature based changes to it. It is understood from these studies that suiting electrical heating techniques and operational strategies to the conduction and polarization mechanisms in oil sands which vary dynamically as a function of composition and temperature would ensure uniform and continuous heating of oil sands to high temperatures.

1.5 Thesis Structure

This study has been structured as a mix of unpublished and published papers. Chapters 3-7 comprise of published works in scientific journals or conference proceedings.

Chapter 1: This chapter provides the overall introduction to the thesis, which includes some background information and describes the objectives and approach of the thesis.

Chapter 2: This chapter is a comprehensive literature review on electrical heating techniques used to heat oil sands and heavy oil reservoirs based on mathematical models developed and lab and field scale studies conducted. The crucial issues in electrical heating of oil sands have been identified to be overdependence on water in the reservoir resulting in non-uniform heating and discontinuation of heating process once water is exhausted. So also overheating of electrodes and lack of adequate electrode infrastructure as well as inadequate operational strategies have been identified as reasons for unsuccessful implementation of this technology. All these issues have been related to a lack of understanding of the dynamic electrical behavior of oil sands through review of studies on electrical properties of oil sands.

Chapter 3: This chapter describes the conduction and polarization mechanisms in oil sands as a function of their composition and frequency. It was shown that oil sands with least water content (<1%) showed dominance of conduction relaxation mechanisms due to silica sand grains and also showed evidence of bitumen polarizations; oil sands having 1-5% water showed dominance of MW polarizations due to presence of disconnected water forming interfaces between bitumen and sand, which showed relaxation peaks between 1 kHz and 1 MHz; whereas oil sands having >5% water showed dominance of dc conduction mechanism over the scanned frequency range due to the presence of freely connected water channels and fine clay clusters. The results of this chapter are published in the following paper:

Abraham Tinu, Afacan Artin, Dhandharia Priyesh, Thundat Thomas, Conduction and Dielectric Relaxation in Athabasca Oil Sands with Application to Electrical Heating, *Energy & Fuels* 2016, 30 (7), 5630–5642.

Chapter 4: This chapter describes the influence of increasing temperature to the electrical relaxation behaviours of oil sands as a function of composition and frequency. It was observed that from 20 to 120°C all oil sands increased in their conductivity and dielectric constant indicating the

increased motion and vaporization of water. From 120 to 200°C the properties decreased in value converting all oil sands irrespective of their initial water content to behave like low loss dielectrics having a dominance of conduction relaxations and bitumen polarizations. Though bitumen polarizations are thought to be present in all oil sands but is superimposed and hidden due to conduction and polarization mechanisms in water. The results of this chapter are published in:

Abraham Tinu, Afacan Artin, Dhandharia Priyesh, Thundat Thomas, Conduction and Dielectric Relaxation in Athabasca Oil Sands with Application to Electrical Heating, *Energy & Fuels*, 2016, 30 (3), 1987-1996.

Chapter 5: This chapter characterizes the resonant autotransformer that was used for conducting capacitive heating based studies on oil sands. Various capacitor load configurations with varying dielectric materials, electrode spacing and connection of bottom capacitor electrodes to different turns of the coil were tested to find an optimized electrode configuration and connection circuit to the resonant autotransformer for carrying out capacitive heating of oil sands. Findings of this chapter are published partly in the following conference proceeding and patent:

Abraham Tinu, Gaikwad Rohan, Hande Aharnish, Van Neste C. W., Hawk J. E., Phani Arindam, Afacan Artin, Thundat Thomas, In Situ Heating of Oil Sands Using an Electrical Standing Wave Resonance Excitation Approach, *Proceedings of the World Heavy Oil Congress 2015*. 2015, March 24-26; Edmonton, Alberta, Canada.

C.W. Van Neste, Thomas Thundat, J.E. Hawk, Tinu Abraham, Jacob H. Masliyah, Jonathan Backs, Richard Hull, Arindam Phani, Resonant Dielectric Heating, US 2015/0129587 A1, May 14th, 2015.

Chapter 6: This chapter describes results of heating studies when different oil sands capacitor configurations were tested in connection to the resonant autotransformer keeping a common oil sands as dielectric in the capacitor. Flat disk and bullet shaped electrodes were tested. Two different capacitor sizes for flat disk capacitors being 1.7 pF and 8.4 pF were tested. It was observed that 8.4 pF oil sands capacitance resulted in greater temperature rise with a maximum temperature of 150°C obtained. Also bullet shaped electrode configuration considered to replicated cylindrical electrode well configuration showed to depict uniform heating of oil sands for the given

capacitor geometry when high input voltage was applied. The findings of this study are published partly in a scientific journal and partly in a conference proceedings:

Abraham Tinu, Gaikwad Rohan, Hande Aharnish, Van Neste C. W., Hawk J. E., Phani Arindam, Afacan Artin, Thundat Thomas, In Situ Heating of Oil Sands Using an Electrical Standing Wave Resonance Excitation Approach, Proceedings of the World Heavy Oil Congress 2015. 2015, March 24-26; Edmonton, Alberta, Canada.

Abraham Tinu, Van Neste C.W., Afacan Artin, Thundat Thomas, 2016. Dielectric Relaxation-Based Capacitive Heating of Oil Sands in Energy & Fuels, 30 (3), 1987-1996.

Chapter 7: This chapter describes results of controlled capacitive heating of oil sands based on probed variations of its electrical behavior. These studies indicate that it is suitable to conduct ohmic heating on oil sands with >5% water followed by switching to capacitive heating as water content vaporizes. For oil sands with 0.5 to 5% water it is suitable to carry out frequency tuned capacitive heating and for oil sands with <0.5% water power tuned capacitive heating would be a suitable option. The findings of this study are published partly in a scientific journal and partly in a conference proceedings:

Abraham Tinu, Gaikwad Rohan, Hande Aharnish, Van Neste C. W., Hawk J. E., Phani Arindam, Afacan Artin, Thundat Thomas, In Situ Heating of Oil Sands Using an Electrical Standing Wave Resonance Excitation Approach, Proceedings of the World Heavy Oil Congress 2015. 2015, March 24-26; Edmonton, Alberta, Canada.

Abraham Tinu, Van Neste C.W., Afacan Artin, Thundat Thomas, 2016. Dielectric Relaxation-Based Capacitive Heating of Oil Sands in Energy & Fuels, 30 (3), 1987-1996.

Chapter 8: This chapter summarizes the overall conclusions and major contributions and also provides direction for future work.

1.6 References

- (1) Meyer, R.; Attansi, E.; Freeman, P. Heavy oil and natural bitumen resources in geological basins of the world. <http://pubs.usgs.gov/of/2007/1084/> (accessed Jul 1, 2016).
- (2) Hiebert, A. D.; Vermeulen, F. E.; Chute, F. S.; Capjack, C. E. Numerical Simulation

- Results for the Electrical Heating of Athabasca Oil-Sand Formations. *SPE Reserv. Eng.* **1986**, 1 (01), 76–84.
- (3) McPherson, R. G.; Chute, F. S.; Vermeulen, F. E. Recovery of Athabasca Bitumen With the Electromagnetic Flood (Emf) Process. *J. Can. Pet. Technol.* **1985**, 24 (1), 44–51.
 - (4) Vermeulen, F. E.; Chute, F. S. Electromagnetic Techniques in the in-Situ Recovery of Heavy Oils. *J. Microw. Power* **1983**, 18 (1), 15–29.
 - (5) McGee, B. C. W. Electro-Thermal Pilot in the Athabasca Oil Sands: Theory versus Performance. In *Canadian International Petroleum Conference*; 17-19 June 2008, Calgary, Alberta Canada, 2008; Vol. 229, pp 47–54.
 - (6) McGee, B. C. W.; McDonald, C. W.; Little, L. Comparative Proof of Concept Results for Electrothermal Dynamic Stripping Process : Integrating Environmentalism With Bitumen Production. In *International Thermal Operations and Heavy Oil Symposium*; Calgary, 2009; pp 141–145.
 - (7) Yu, C. L.; McGee, B. C. W.; Chute, F. S.; Vermeulen, F. E. Electromagnetic Reservoir Heating with Vertical Well Supply and Horizontal Well Return Electrodes. Patent Number: 5,339,898, 1994.
 - (8) Fisher, S. T.; Fisher, C. B. Induction Heating of Underground Hydrocarbon Deposits. 3,989,107, 1976.
 - (9) Bridges, J.; Taflove, A.; Snow, R. Method for In Situ Heat Processing of Hydrocarbonaceous Formations. 4140180, 1979.
 - (10) Trautman, M.; Macfarlane, B. Experimental and Numerical Simulation Results from a Radio Frequency Heating Test in Native Oil Sands at the North Steepbank Mine. In *World Heavy Oil Congress*; 5-7 March 2014, New Orleans USA; pp 1–14.
 - (11) Francis Eugene Parsche. Electromagnetic Heat Treatment Providing Enhanced Oil Recovery. US 8,701,760 B2.
 - (12) Kinzer, D. E. In Situ Processing of Hydrocarbon Bearing Formations with Variable

- Frequency Automated Capacitive Radio Frequency Dielectric Heating. 7091460B2, 2006.
- (13) Department of Energy. Alberta Energy: Facts and Statistics
<http://www.energy.alberta.ca/oilsands/791.asp> (accessed Apr 6, 2016).
 - (14) Svrcek, W. Y.; Mehrotra, A. K. One Parameter Correlation for Bitumen Viscosity. *Chem. Eng. Res. Des.* **1988**, *66* (4), 323–327.
 - (15) Gates, I.; Wang, J. Evolution of In Situ Oil Sands Recovery Technology: What Happened and What’s New? In *SPE Heavy Oil Conference and Exhibition*; 12–14 December 2011, Kuwait City, Kuwait; pp 1–10.
 - (16) Findlay, J. P. *The Future of the Canadian Oil Sands*; 2016.
 - (17) Betancourt-Torcat, A.; Almansoori, A.; Elkamel, A.; Ricardez-Sandoval, L. Stochastic Modeling of the Oil Sands Operations under Greenhouse Gas Emission Restrictions and Water Management. *Energy and Fuels* **2013**, *27* (9), 5559–5578.
 - (18) Zahabi, A.; Gray, M. R.; Dabros, T. Heterogeneity of Asphaltene Deposits on Gold Surfaces in Organic Phase Using Atomic Force Microscopy. *Energy & Fuels* **2012**, *26* (5), 2891–2898.
 - (19) Holly, C.; Soni, S.; Mader, M.; Toor, J. *Alberta Energy Oil Sands Production Profile 2004-2014*; 2016.
 - (20) Butler, R. M.; Yee, C. T. Progress in the in Situ Recovery of Heavy Oils and Bitumen. *J. Can. Pet. Technol.* **2002**, *41* (1), 31–40.
 - (21) Butler, R. Steam and Gas Push (SAGP). *J. Can. Pet. Technol.* **1999**, *38* (3), 54–61.
 - (22) Deng, X. Recovery Performance and Economics of Steam/Propane Hybrid Process. In *SPE International Thermal Operations and Heavy Oil Symposium*; 1-3 November, 2005, Calgary, Alberta, Canada; pp 1–7.
 - (23) Singhal, A. K.; Ito, Y.; Kasraie, M. Screening and Design Criteria for Steam Assisted Gravity Drainage (SAGD) Projects. In *SPE International Conference on Horizontal Well Technology*; 1-4 November 1998, Calgary, Alberta, Canada; pp 1–7.

- (24) Al-Bahlani, A.-M.; Babadagli, T. SAGD Laboratory Experimental and Numerical Simulation Studies: A Review of Current Status and Future Issues. *J. Pet. Sci. Eng.* **2009**, *68* (3-4), 135–150.
- (25) Pasalic, D.; Vaca, P.; Okoniewski, M.; Diaz-Goano, C. Electromagnetic Heating : A SAGD Alternative Strategy to Exploit Heavy Oil Reservoirs. In *World Heavy Oil Congress*; 24 -26 March, 2015, Edmonton, Alberta, Canada; pp 1–13.
- (26) Flock, D. L.; Tharin, J. Unconventional Methods of Recovery of Bitumen and Related Research Areas Particular to the Oil Sands of Alberta. *J. Can. Pet. Technol.* **1975**, *14* (3), 17–27.
- (27) Mukhametshina, A.; Martynova, E. Electromagnetic Heating of Heavy Oil and Bitumen: A Review of Experimental Studies and Field Applications. *J. Pet. Eng.* **2013**, No. 476519, 1–7.
- (28) McGee, B. C. W.; McDonald, C. W.; Little, L. Electro-Thermal Dynamic Stripping Process. In *The SPE International Thermal Operations and Heavy Oil Symposium*; 20-23 October, 2008, Calgary, Alberta, Canada; pp 1–8.
- (29) Fisher, S. Solid Fossil-Fuel Recovery by Electrical Induction Heating in Situ: A Proposal. *Resour. Recover. Conserv.* **1980**, *4* (4), 363–368.

Chapter 2 Review of Dynamic Electrical Behavior of Oil Sands and Applied Electrical Heating Techniques

2.1 Introduction to Electrical Heating

Electrical heating is the process by which electrical energy is converted to heat energy in a material when a material via its atoms, molecules and electrons either conducts electrical energy or/and store it as polarizations. Both mechanisms result in loss of some amount of electrical energy as heat due to motion and collision of atoms, molecules and electrons during conduction and polarizations. This implies internal heat generation due to electrical heating giving rise to several positive effects, notably uniform heating, higher efficiency, higher temperature as well as better process control if compared with technologies that use external heating sources such as the thermal methods ¹. Different materials depending on whether they are conductors, dielectrics or insulators respond via different motion mechanisms of their electrons, atoms and molecules to generate heat with conductors dominantly conducting electrical energy and dielectrics dominantly storing electrical energy as polarizations. Moving forward, when there is a heterogeneous mixture having a certain proportion of conductors and dielectrics arranged in a specific manner, the resulting conduction and polarization mechanisms in the material becomes a function of the mixture's composition, mutual arrangement of components and temperature. So also, the frequency of electrical energy for a given input power can trigger different motion mechanisms in the given type of heterogeneous material. Therefore it is crucial to understand this complex mechanistic interplay between the nature of electrical energy being supplied and the dynamic electrical mechanisms of the material being exposed to it to carry out an efficient electrical heating process as depicted in the relationship diagram in figure 2-1.

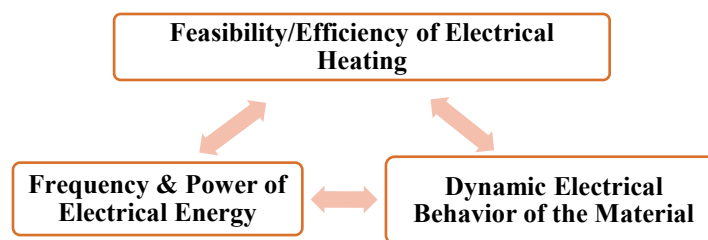


Figure 2-1. Relationship diagram showing the interdependence of electrical properties of materials with the applied electrical energy in dictating the feasibility/efficiency of electrical heating.

Dependent on these parameters, electrical heating of materials is generally categorized into three techniques known as ohmic, inductive and dielectric heating. Classification of these heating techniques via the frequency of electrical energy and the electrical nature of material to be heated is shown in figure 2-2.

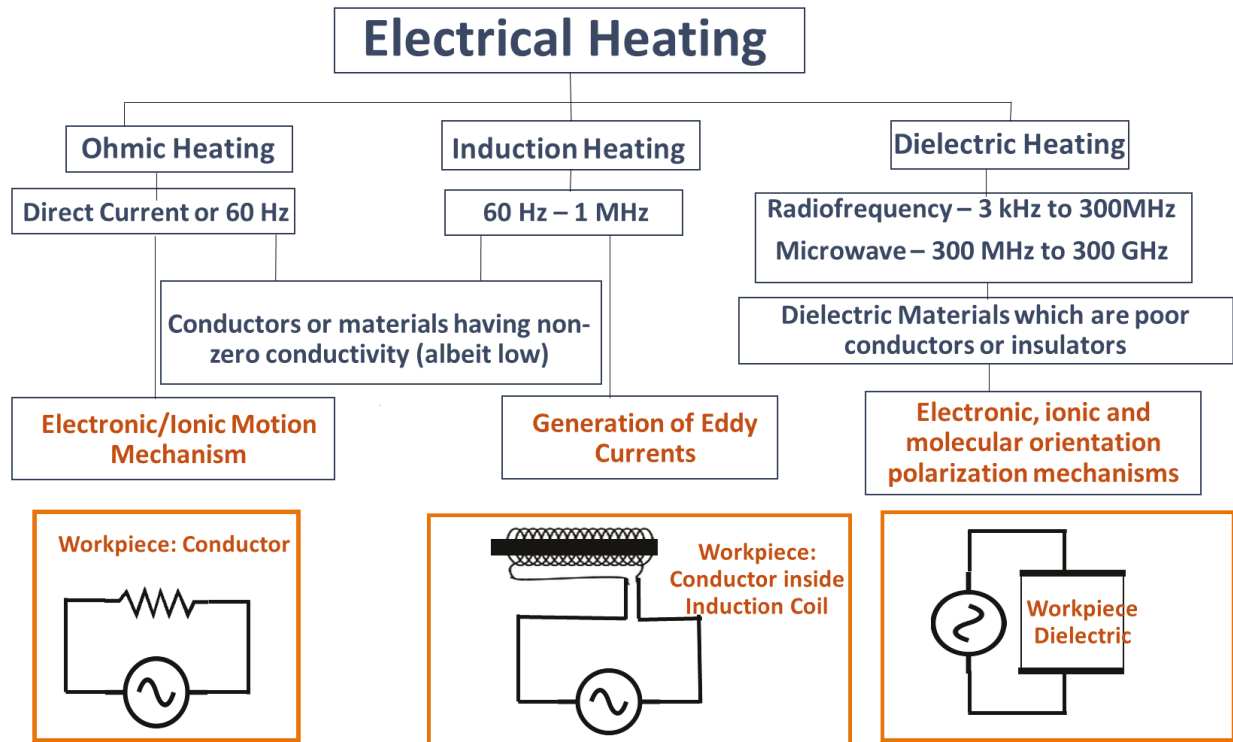


Figure 2-2. Classification of type of electrical heating based on the type of material and the frequency of electrical energy.

2.1.1 Background of Ohmic Heating

James Prescott Joule showed that electricity flowing through a conductor resulted in the generation of heat. He made these findings in 1841 after Georg Ohm published about the Ohm's law in his treatise in 1827². Since then their work has contributed directly to the development of today's applications of ohmic or Joule heating². When direct current (DC) or power frequency of 60 Hz is applied to conductors, current flows through them through motion of free electrons which results in agitation of molecules (or atoms) therein as depicted in figure 2-2. If the material is not a conductor by nature, but has charged species in the form of ions or molecules, they too undergo ohmic heating². An important point is that for ohmic heating to occur, the electrical conductivity must be non-zero. This means that completely nonpolar materials, such as oils, which do not

conduct electricity, cannot be heated ohmically. However, most materials found in nature such as soils, food etc., are aqueous-based, and possess some electrical conductivity (albeit low), and can therefore be heated ohmically². This type of heating is also called resistance or Joule heating.

2.1.2 Background of Induction Heating

The second type of heating also called induction heating is carried out between 60 Hz and 1 MHz on conductors as depicted in figure 2-2. Induction heating is a non-contact heating process. The first induction phenomenon was observed by Michael Faraday in the middle of 1800s when the effect that caused the heating of transformer and motor windings was considered undesirable. The first constructive use of induction occurred in 1916 when it was used to melt metals³. Induction heaters are used to provide alternating electric current to an electric coil (the induction coil) which becomes the electrical source that induces an electrical current into the metal part to be heated. The alternating current (ac) in an induction coil has an invisible magnetic force field around it. When the induction coil is placed next to or around a workpiece, the force field induces an equal and opposing electric current in the workpiece, with the workpiece then heating due to the resistance to the flow of this induced electric current. The induced currents are sometimes referred to as eddy-currents, with the highest intensity current being produced within the area of the intense magnetic fields³. Induction heating, like ohmic heating also requires that the conductivity of the material be non-zero.

2.1.3 Background of Dielectric Heating

Contrary to these methods, dielectric heating is suitable to heat dielectric materials which have electrons, ions, molecules or atoms that can be displaced or in other words polarized by an applied electric field. A dielectric material is thereby a poor conductor of electricity, but a supporter of electrostatic fields in the form of polarizations. Polarizations arise whenever charges in a material are somewhat displaced with respect to one another under the influence of an electric field. The displacement is also called dipole moment μ . Therefore polarization P can also be termed as the sum of all dipole moments contained in a given volume V of the material as is given below:

$$P = \frac{\sum \mu}{V} \quad (1)$$

When a static electric field is applied to a homogenous dielectric material, the total polarization in it arise from four sources of charge displacement or dipole moments caused due to electronic, ionic/atomic, orientational and space charge polarization as shown in figure 2-3.

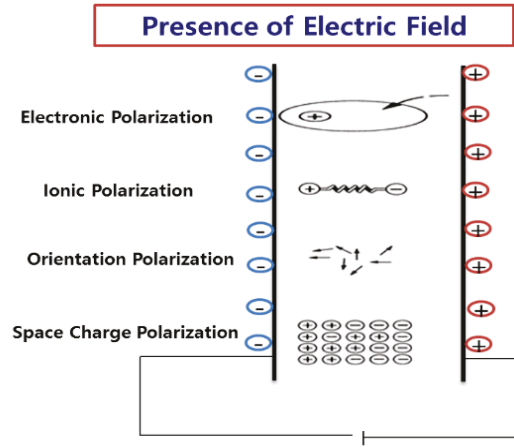


Figure 2-3. Different polarization mechanisms in a dielectric material when interacting with electrical energy ⁴.

One process common to all homogeneous dielectrics is electron polarization (P_e) or the shift of centre of gravity of a negative electron cloud in relation to the positive atom nucleus in the electric field. The second mechanism is the displacement of positive and negative ion in relation to one another called ionic or atomic polarization(P_i). The third kind of polarization is associated with the presence of permanent electric dipoles which exist even in the absence of an electric field. When the electric field is applied, the electric dipoles tend to orient in the direction of the electric field and hence result in orientation polarization(P_d). The final source of polarization is mobile charges which are present because they are impeded by interfaces or also because they are not supplied at an electrode or discharged at an electrode resulting in space charge polarization(P_s). The algebraic sum of the aforementioned polarizations results in total polarization (P) given as:

$$P = P_e + P_i + P_d + P_s \quad (2)$$

When a static electric field is applied, the total polarizations occurring in the dielectric material is related to the dielectric constant as shown:

$$P = \epsilon_0(\epsilon' - 1)E \quad (3)$$

Where ϵ_0 is permittivity of free space, ϵ' is dielectric constant and E is the applied electric field. In an ideal case, the electric charge adjusts itself or polarizes instantaneously to any change in voltage. In practice, however there is an inertia to charge movement that shows up as relaxation time for charge transport. To explain this better, when a static electric field is switched off, the polarized charge in the material will only overcome its displacement by some interactions involving collisions and friction with other charges in the medium. Therefore it will take a characteristic time dependent roughly on the time between collisions to follow the changes in the electric field. The average time taken for the given polarization to catch up with the changing electric field is therefore called its relaxation time τ as shown in figure 2-4.

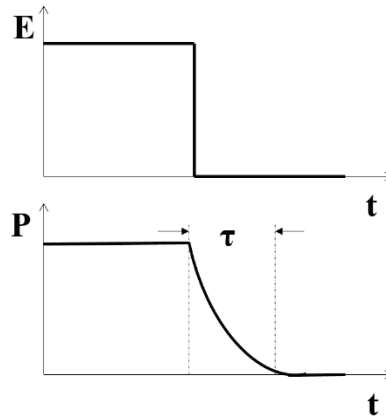


Figure 2-4. Depiction of relaxation time τ when a static electric field is switched off.

When instead of a static or direct current (dc) electric field, an alternating current (ac) electric field switching at a certain electrical frequency is applied, the polarizations respond differently based on their inertia or collision effects. Different polarization mechanisms will have a varying time response capability to an applied field frequency as shown in figure 2-5. Electronic displacement responds rapidly to the field reversals, and no lag of the polarization contribution occurs up to 10^{17} Hz which lies in the visible region of the electromagnetic spectrum. As is expected, ions, which are larger and must shift within the crystal structure, are less mobile, and have a less rapid response. Therefore ionic or atomic polarization are able to follow electric fields alternating frequencies up to the infrared region of the spectrum lying around 10^{13} Hz. Orientation polarization occurs at frequencies up to 10^9 Hz and interfacial or space charge polarizations have relaxation times at much lower frequencies up to 10^7 Hz⁵. The peaks which occur near limiting frequency for ionic

and electronic polarization are due to the resonance points where the applied frequency equals the natural frequency of the material as shown in figure 2-5.

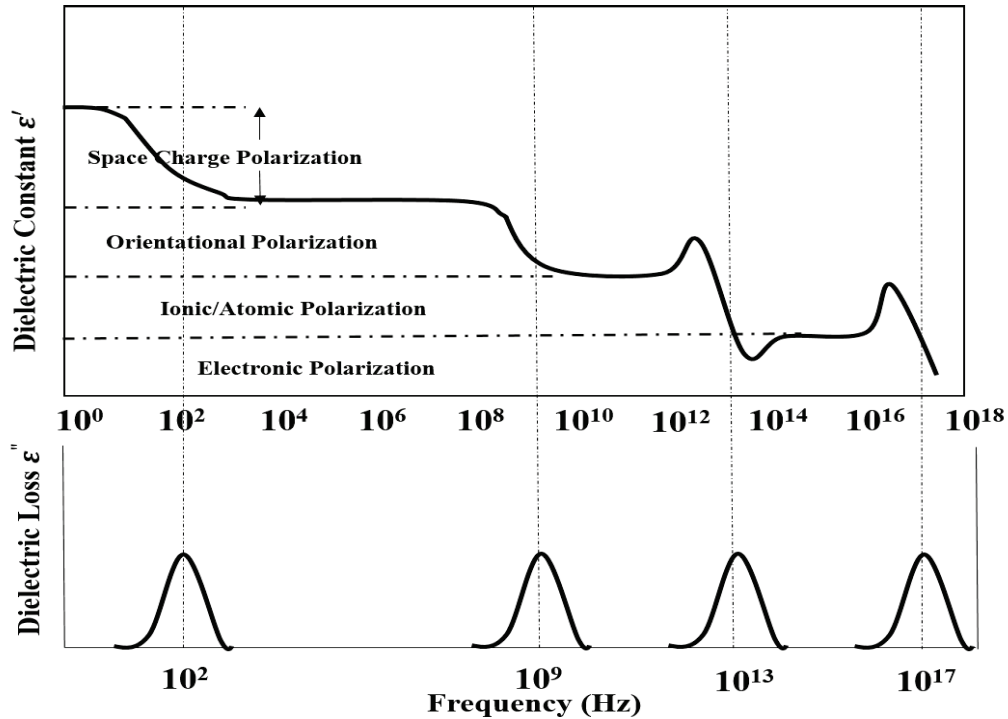


Figure 2-5. Frequency dependence of different polarization mechanisms in homogeneous dielectrics.

An efficient dielectric supports a varying charge with minimal dissipation of energy in the form of heat. However, some amount of heat gets dissipated when the polarization process tries to overcome the inertia while catching up with the alternating electric field. The heat loss contribution is maximized at a frequency where the applied field has the same period of the relaxation process. Simply put, the losses are small when the relaxation time and the period of the applied field differ greatly and especially high around the relaxation or resonance frequencies of the polarisation mechanisms.

The method of dielectric heating saw its first beginnings in the 1940s when the effect of frequency on materials became more noticeable with the advent of radio and then radar, where progressively higher frequencies were used ⁶⁻¹¹. The electric cables which are insulating or dielectric materials used for separating electrical conductors, performed well at 50 Hz but were found to heat up when

the cables were used to transmit power at higher frequencies. In the cable making industry this gave rise to the term dielectric loss factor which denotes heat lost in the dielectric materials. From there on the cable makers 'loss' became the dielectric heating industry's gain ¹¹. Over the years, dielectric heating has made its way into several industrial heating applications most popular of which is food processing ¹². Dielectric heating are usually carried out at high frequencies such as radio frequencies covering 3 kHz to 300 MHz and microwaves covering 300 MHz to 300 GHz ¹². It can further be classified into capacitive and radiative dielectric heating with the former used in frequency range of 100 kHz to 100 MHz and the latter used in the frequency range of 100MHz to 100GHz ¹³.

2.2 Application of Electrical Heating to Geological Systems

Electrical heating has been considered for application in two main geological systems; decontamination of soils contaminated with organic content and for enhanced oil recovery from heavy oil and oil sands reservoirs. Ohmic heating is widely used in in situ soil remediation for decontaminating organic material leaked into soils ¹⁴ by the process called Electrical Resistance Heating (ERH). Electric current is passed through a targeted soil volume between sub-surface electrode elements as shown in figure 2-6 ¹⁵. The resistance to current flow that exists in the soil causes the formation to heat causing an increase in temperature until boiling point of water is reached. Beyond this temperature further energy input causes a phase change, forming steam and removing volatile components ¹⁶. There are predominantly two electrical load arrangements for ERH; three-phase heating and six-phase heating. Three-phase heating consists of electrodes in a repeating triangular or delta pattern. Adjacent electrodes are of a different electrical phase so electricity conducts between them. Six-phase heating consists of six electrodes in a hexagonal pattern with a neutral electrode in the center of the array.

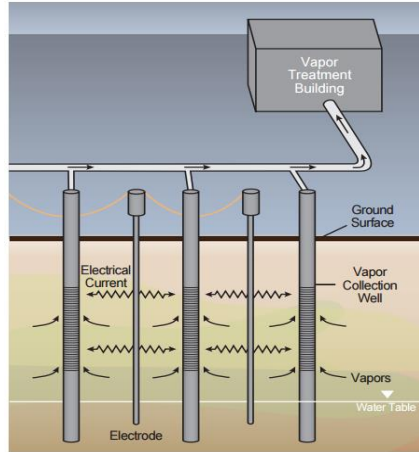


Figure 2-6. Electrical Resistive Heating for in situ remediation of soil contaminated with organic matter¹⁵.

Alongside these applications, it was proposed early on that electrical heating can be carried out as an enhanced oil recovery technique for heavy and extra heavy oil reservoirs containing bitumen. The earliest patent in this field was by Richey in 1956 who proposed the design to transfer electromagnetic waves to well bore from the surface through coaxial system of internal and external tubing and casing¹⁷. Since then, several lab and field scale studies have been carried out which have implemented ohmic, inductive and dielectric methods for heavy oil and oil sands reservoirs. However, full scale commercialization of such electrical heating techniques for oil sands are still unaccomplished.

The upcoming sections are an attempt at focused literature review for determining factors that have inhibited electrical heating from becoming a fully operational enhanced oil recovery technique particularly in the case of oil sands. It is an attempt to outline the work done so far by other researchers and companies in understanding and implementing electrical heating of oil sands at lab and field scales. Integrated understanding of the properties and electrical heating methodology will highlight the crucial gaps in the current understanding of electrical heating of oil sands and thereby strengthen the motive of my thesis in contributing to its future implementation.

2.3 Review of Dynamic Electrical Behaviour of Oil Sands and Applied Electrical Heating Techniques – Numerical Simulation and Modeling, Laboratory and Field Scale Studies

It is well understood that electrical heating is an interactive processes whereby the electrical behaviour of the medium being heated has a crucial role to play in dictating the efficiency of the heating process. Therefore the starting point of fundamental research on this topic would be to

identify gaps in the understanding of the electrical behaviour of oil sands in its entirety covering aspects of dynamic variations with composition, temperature, frequency and power. A good understanding in this direction would dictate the electrode or antenna sizes, shapes and configuration and will also dictate optimum operating strategies concerning operating frequency and power levels during the dynamic heating process. Together a thorough understanding of all three factors will lead way to development of fully feasible and efficient electrical heating process as shown in the relation diagram in figure 2-7.

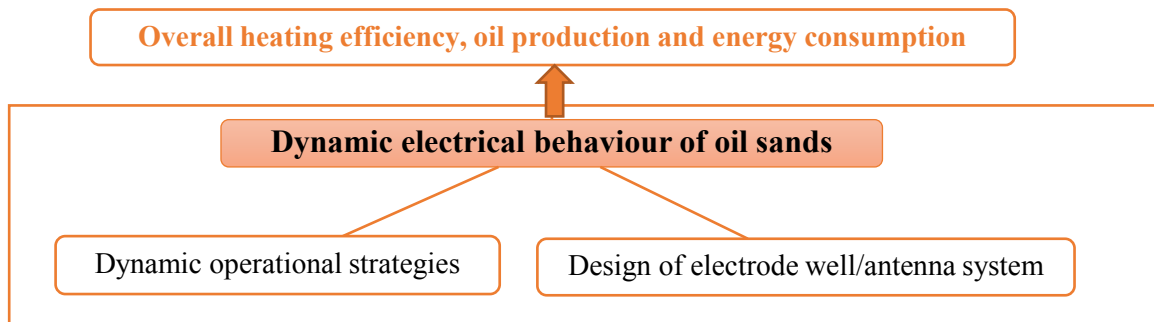


Figure 2-7. Relationship diagram of crucial research components that need to be investigated for efficient electrical heating of oil reservoirs

The first part of the literature analysis will delve into findings of the dynamic electrical behaviour of oil sands. The second part of the study will discuss ohmic, inductive and dielectric heating methods studied for heavy oil and oil sands reservoirs with respect to the findings of numerical simulations, lab and field scale studies. The review helps in identifying gaps in the current understanding of the dynamic electrical behaviour of oil sands is discussed in section 2.3.1 and in determining crucial reasons for non-commercialization of the electrical heating technique as given in section 2.3.2. This review helps in addressing the identified gaps for feasible implementation of electrical heating of oil sands in the future.

2.3.1. Dynamic Electrical Behaviour of Oil Sands – A Heterogeneous Dielectric Mixture

2.3.1.1 Oil Sands Composition and Microstructural Arrangement

Oil sands typically is a heterogeneous mixture consisting of coarse sand grains ($> 44 \mu\text{m}$) of quartz minerals, fine mineral solids ($< 44 \mu\text{m}$) comprising clays ($< 5 \mu\text{m}$), formation water with electrolytes as well as bitumen¹⁸. The mineral solids constitute the major component of oils sands approximating 80 to 90% and are mostly solid dielectrics in nature. Bitumen content can vary

widely between 7 to 16% by weight and is a polymer like organic material that could be polarized in response to an applied electric field ¹⁹. Water content in oil sands can vary from nearly zero in weathered ores to as high as 7% by weight and are considered as the conductive components in this heterogeneous disordered system. The indigenous formation water contains a variety of electrolytes including Na⁺, Ca²⁺, Mg²⁺, Cl⁻, K⁺, SO₄²⁻ and HCO₃³⁻ ions ¹⁸. Clay minerals being a major component of fines are dominantly kaolinite, illite with small amounts of montmorillonite. The electrical categorization of individual components of oil sands is given in figure 2-8. Among the different structural models proposed for oil sands regarding the mutual arrangement of solid particles, water and bitumen, Takamura's model ²⁰ is most widely accepted as depicted in figure 2-8. Adapting from earlier models, this model proposes that the coarse sand grains are hydrophilic in nature with water serving as an interface between the sand grains and bitumen. In rich grade oil sands, water forms pendular connections at grain to grain contact points and are also present as a roughly 10-15 nm thick film which covers the sand surfaces. This water layer is stable because of the double layer repulsive forces acting between the sand and bitumen surfaces ²⁰. In some cases, the sand surfaces are covered by clay minerals precipitated on them. Thus, the thin layer water films also cover clay minerals in the oil sands. In poor grade oil sands, in addition to the above mentioned arrangement, clusters of fine particles exist within the framework formed by coarse sand grains. These clusters of fine particles are saturated with water. Oil sands having higher fines content are thereby also known to have higher water content ^{18,20}.

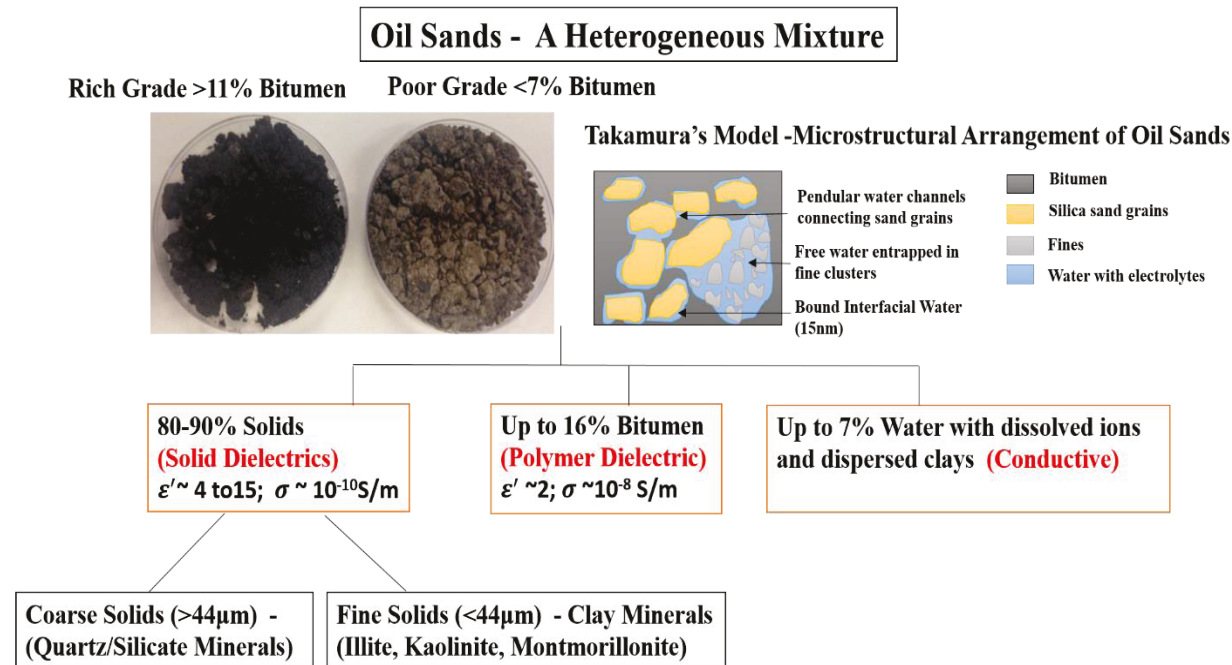


Figure 2-8. Composition of oil sands and electrical properties of each component/phase.

2.3.1.2 Electrical Properties and Dominant Electrical Mechanisms in Individual Components of Oil Sands

The response of oil sands to electrical excitation is expressed in terms of its ability to store electrical energy as polarizations termed as its dielectric constant or relative permittivity (ϵ') and in terms of its ability to conduct electrical energy termed as electrical conductivity (σ). Knowledge of these electrical properties is crucial to the design and optimization of any electrical heating scheme. Dissecting the electrical properties of the individual components of oil sands it is understood that quartz minerals are known to be solid dielectric materials ($\epsilon' \sim 4 \text{ to } 15; \sigma \sim 10^{-10} \text{ S/m}$), and these properties are independent of frequency below GHz in the absence of any water²¹. Distilled water devoid of any ions is also an insulating dielectric material ($\epsilon' = 80; \sigma \sim 10^{-6} \text{ S/m}$) having electrical properties that are strongly temperature dependent but independent of frequency below several GHz²¹. However adding salt to water dramatically increases its conductivity (σ) while barely altering its dielectric constant or relative permittivity (ϵ')²². Interestingly, it is known that the addition of small quantities of salt water to insulating dry silicate minerals dramatically increases both conductivity and permittivity of the combined system as frequencies are reduced below GHz²³⁻²⁵. The presence of charged clay particles in salt water further enhances the relative permittivity and conductivity values at frequencies below GHz^{21,26-29}. Bitumen being oil can be

considered as polymer like dielectric and is known to have a low dielectric permittivity ($\epsilon' \sim 2$) and low electrical conductivity ($\sigma \sim 10^{-8}$ S/m), which stays constant in the kHz to GHz frequency range³⁰. However, its relative permittivity increases significantly at frequencies lower than kHz attributed to the presence of polar asphaltenes in non-polar maltenes. The individual components based electrical properties of oil sands is depicted in figure 2-8.

2.3.1.3 Electrical Mechanisms in Heterogeneous Mixtures

Heterogeneous mixtures tend to have a combination of conductive and dielectric components. While individual components/phases have their own unique conduction and polarization mechanisms, the differences in the electrical properties of the individual phases also give rise to interfacial polarizations; the build-up of space charges near the interfaces between the various phases³¹ as shown in figure 2-9. Thus, heterogeneous media such as oil sands which have been discussed to have conductive and dielectric phases in section 2.3.1.2 present an interesting class of materials for dielectric research. Solid dielectrics such as quartz minerals are heterogeneous polycrystalline solids. In such dielectrics, localized charges such as ions or electrons can hop from one site to the neighboring sites creating hopping polarization which results in a dispersion in the conductivity spectra also called conduction relaxations (Kao 2004). Polymer dielectrics such as bitumen can undergo several relaxations associated with glass transitions, segmental mobility of polar groups and crystallization process which have signatures in the Hz to MHz frequency range and have certain temperature dependent trends (Kremer & Schönhal 2003; Psarras et al. 2002). The presence of the conductive water in oil sands depending on its concentration can contribute to dc conduction mechanism. At low frequencies between mHz and Hz, electrochemical polarizations arising due to chemical reaction mechanisms from oxidation, reduction reactions between water and metallic minerals, ion-exchange reactions commonly involving negatively charged clay in ionic water as well as clay-organic material reactions are discussed to be the reasons for high dielectric property values of heterogeneous soils which are comparable to oil sands (Lesmes & Friedman 2005; Chelidze et al. 1999; Olhoeft 1985; Revil et al. 2013). Having understood the general electrical properties of individual oil sands components which seem to be trivially low, it is interesting to note that when these components are present as a heterogeneous mixture, they result in significantly large values of dielectric constant ($\epsilon' \sim 10^6$) at low frequencies and are frequency dependent below GHz^{32,33}. Thus the anomalous behaviour could be governed mainly by polarizations occurring at its solid-liquid and liquid-liquid interfaces. Interfacial polarizations

considered as a case of space charge polarizations usually occurs at frequencies lower than the time scales typical of dipolar polarizations. Moreover the contribution of interfacial polarization to the dielectric properties of a material is often much larger than the dipolar contributions ³¹. Between Hz and MHz interfacial polarizations occur due to migration of free charges or ions to grain boundaries, particle edges or phase boundaries and are also called Maxwell-Wagner (MW) polarizations ³¹. Maxwell and Wagner derived a mean-field theory for materials containing dispersed dielectric spheres in a dielectric medium ³¹. Sillars extended the model to a suspension of ellipsoid particles eventually resulting in the Maxwell-Wagner-Sillars theory ^{23,31}. This model however considered a low volume of filler concentration (<20%)³¹. Bruggeman ³⁴ and Hanai ³⁵ extended the model for higher filler concentration using a differential increment approach considering dynamic fields and conducting components and developed a comprehensive theory for estimating the complex dielectric constant and conductivity of concentrated suspensions termed as Maxwell-Wagner-Bruggeman-Hanai (MWBH) model ²³. This model which takes into account bulk properties, shape and partial volume of components is shown to accurately predict interfacial polarizations for multi component heterogeneous materials such as geological rocks and soils for frequencies greater than 10 MHz ²³. However it is not suitable at lower frequencies because it doesn't consider the surface contribution to polarization as well as spatial distribution and aggregation of inclusions ^{23,26}.

In lieu of this understanding, heterogeneous mixtures such as oil sands can result in electrochemical polarizations, interfacial or MW polarizations as well as relaxations associated with polymer dielectrics having certain crucial frequency ranges where energy losses due to these relaxations are maximum as shown in figure 2-9. Furthermore, dc conduction as well as conduction relaxations can also be present in such mixtures ^{23,31}.

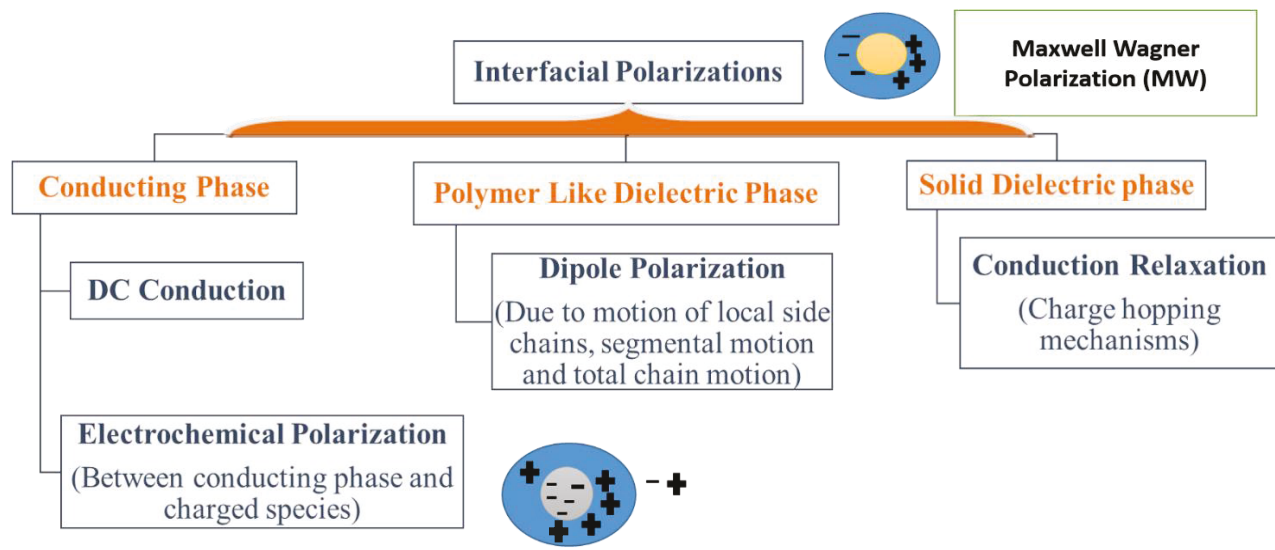


Figure 2-9. Conduction and polarization mechanisms in heterogeneous mixtures consisting of conductive, solid dielectric and polymer like dielectric phases.

2.3.1.4 Studies on Electrical Behaviour of Oil Sands

While a number of logging tools and other methods permit a direct in situ determination of the electrical parameters, the bulk of available data on oil sands have been obtained from measurements on samples reconstituted from mined oil sands and reconstituted under conditions of temperature, pressure and moisture content intended to represent the formation as closely as possible³⁶. Measurements on such samples may typically vary up to 20% from the original value at reservoir, attributed to the inherent differences in the reconstituted pore geometry from sample to sample³⁶. However, the mean values of measurements of many such samples have been assumed to characterize a volume of the formation much larger than an individual sample.

The studies that have been carried out for investigating the electrical behaviour of oil sands have mainly focused on estimating the electrical properties such as dielectric constant (ϵ') electrical conductivity (σ) and loss tangent ($\tan\delta$) of different grades of oil sands as a function of frequency, moisture and temperature. Chute et al.³² showed frequency dependence of ϵ' and σ over the frequency range 60 Hz to 1 GHz for Athabasca oil sands samples reconstituted from mined sand. They showed that for all oil sands the effective conductivity varies slowly with frequency and is virtually constant up to a frequency of $10^{6\text{ to }7}$ Hz. The magnitude of σ ranges from $10^{-1\text{ to }-4}$ S/m increasing with increasing moisture content. Above 10^7 Hz there is a substantial linear

increase in σ with frequency. In the case of ϵ' opposite observation with frequency is true. At frequencies below 10^3 to 4 Hz, ϵ' increases approximately linearly with decreasing frequency with values in excess of 10^5 obtained. At higher frequencies, ϵ' asymptotically approaches a constant value that depends on moisture content which rarely exceeds values above 5. They also studied these properties for dried samples and found that σ varies approximately linearly with frequency over the entire frequency range above 10^3 Hz which suggested the departure of dried oil sands samples from a linear relationship may be due to presence of small amount of adsorbed water forming interconnected paths through the supposedly dry oil sands sample or due to a significant contribution to the low frequency conductivity from mineral and clay matter in the sample. The ϵ' rarely exceeded approximately 10 at low frequencies for dried samples and is of the order of 3 at microwave frequencies which is comparable to the values of host rock and bitumen.

Temperature based studies indicate that at temperatures less than 120°C , sample conductivities increase approximately linearly with increasing temperature that is virtually the same for all samples independent of moisture and bitumen content. In this temperature range the increase in conductivity was explained to be due to rapid decrease in pore water viscosity and associated increase in ionic mobilities. At temperatures above 100 to 125°C , the conductivity at a frequency of 60 Hz was observed to increase at a slower rate than at lower temperatures. Above 200°C the conductivity showed to decrease. Hiebert et al.³⁷ concluded that complex hydrothermal reactions in the clay water bitumen system at higher temperatures were responsible for the observed variations in sample conductivities above 125°C . He also showed that when the oil sands samples were held at fixed temperatures in excess of 100°C for extended periods of time, the electrical conductivity decreased significantly.

Chute et al.³² showed that at frequencies above 10^6 Hz, ϵ' varied only slightly with temperature up to 150°C , reasoned to be due to the fact that polarization mechanisms being molecular, ionic or electronic were not significantly temperature dependent. At frequencies lower than 10^6 Hz, where interfacial effects contribute more strongly to the effective dielectric constant, substantial temperature dependence could be expected especially from high moisture content sample. Das et al.³³ observed that even with very low moisture content oil sands samples the dielectric constant varied dramatically with temperature at low frequencies. They showed that at frequencies below 50 kHz, ϵ' showed increasing temperature sensitivity and at 200 Hz was observed to increase in a

sharply nonlinear manner at temperatures above 120°C. The anomalous behaviour observed at 400°C was attributed to the creation of mobile charges due to thermal decomposition and fragmentation of the oil sands bitumen.

Even though these electrical property investigations for oil sands touched on the presence of polarization mechanisms to reason some of the property variations they didn't go deeper into the subject matter to identify crucial frequency domains where relaxations due to them could be dominant. Also depending on the water content and temperature, the variation of these polarization mechanisms as well as the interplay between conduction and interfacial polarization mechanisms needs to be understood to determine suitable electrical heating methods for carrying out optimized heating in sync with the dynamic electrical behaviour of oil sands. Having gained only an understanding of the electrical properties would not be sufficient enough to carry out an energy efficient and feasible electrical heating as will be understood in the next section. A gap in the understanding of the dynamic electrical behaviour of such a heterogeneous oil sands mixture has resulted in inadequate operational strategies which have resulted in discontinuation of the heating process at higher temperatures due to overdependence on water in the reservoir, excessive heating near the electrodes, non-uniform heating of the reservoir and failure of electrode/antenna equipment which will be highlighted in the next section.

2.3.2 Electrical Heating Techniques Applied to Oil Sands and Heavy Oil Reservoirs

All three methods of electrical heating for oil reservoirs namely, ohmic, inductive and dielectric heating have been proposed and investigated since the 1950s for different aspects via lab experiments, numerical simulation and modeling and field scale executions. Yet, there isn't a fully commercialised electrical heating based oil sands extraction unit today and it is important to understand the reasons for this in order to affect a change in the status quo. The following section discusses the critical gaps in implementation of a reliable electrical heating method for oil sands. Each type of heating method is investigated for its history of development, lab and field scale implementation and the mathematical models developed. Through this study, importance is drawn to the main findings which support electrical heating as a feasible technology and at the same time research gaps inhibiting commercial success are discussed.

2.3.2.1 Ohmic Heating of Oil Reservoir

2.3.2.1.1 Indirect Ohmic Heating

Indirect ohmic heating of downhole reservoirs makes use of an electrical heater installed downhole in the form of polymer insulated or mineral insulated (MI) cables in the production tubing, which gets heated resistively and thereby transfers the heat to the reservoir through thermal conduction or convection³⁸. A typical downhole electrical heating system is depicted in figure 2-10(a). In this system the major components would include the electric heater, thermocouple, a means to affix the heater to the production tube, a well head penetration for the heater to be brought to the topside and a control/power panel and transformer. The earliest downhole electrical heating technology was self-regulating which eventually transitioned to polymer insulated Constant Wattage (CW) technology³⁸. The cable used consisted of three insulated conductors running parallel to each other. The conductors were insulated and had a metal braid, polymer jacket and an overall armor as shown in figure 2-10(b). A voltage applied across the conductor caused the current to flow generating heat³⁸. Mineral Insulated (MI) cables consist of one or two conductors embedded in a magnesium oxide insulation enclosed in a metal sheath as shown in figure 2-10(c). These cables are known to have a better heat output capability as compared to the CW cables³⁸. The latest developments in MI cables have enabled the implementation of a medium voltage (4160 V) heater system. The heater technology can produce 1000 W/m and have a length of 1000m³⁹. Use of indirect ohmic heating has been widely implemented today for various down hole applications such as flow assurance, paraffin buildup, hydrate elimination, viscosity reduction and in situ upgrading⁴⁰. The earliest application of this method of heating was reported before 1969 in USSR and USA with more than hundred wells being stimulated electrically. This indirect ohmic heating technology provided an effective solution for wells with heavy crude as well as low temperature wax, paraffin and hydrate issues, but this was eventually limited by the amount of thermal power density that this type of cable was able to produce³⁸. It was observed that obtaining oil and gas production through indirect ohmic heating was similar to steam stimulated volumes but had issues of significant electrical power requirements. It was predicted that a gigawatts of energy was required for producing 200,000 barrels per day. The highest power and temperature application of downhole electrical heater application is the Shell Oil developed “In situ Conversion Process” for oil shale and the “In situ Upgrading Process” for heavy oil. This technology can be thought of as

a virtual refinery in the ground. The most recent production pilot produced over 1800 barrels equivalent of oil ⁴⁰. Post coring confirmed the liquid recovery efficiency to be above 60%.

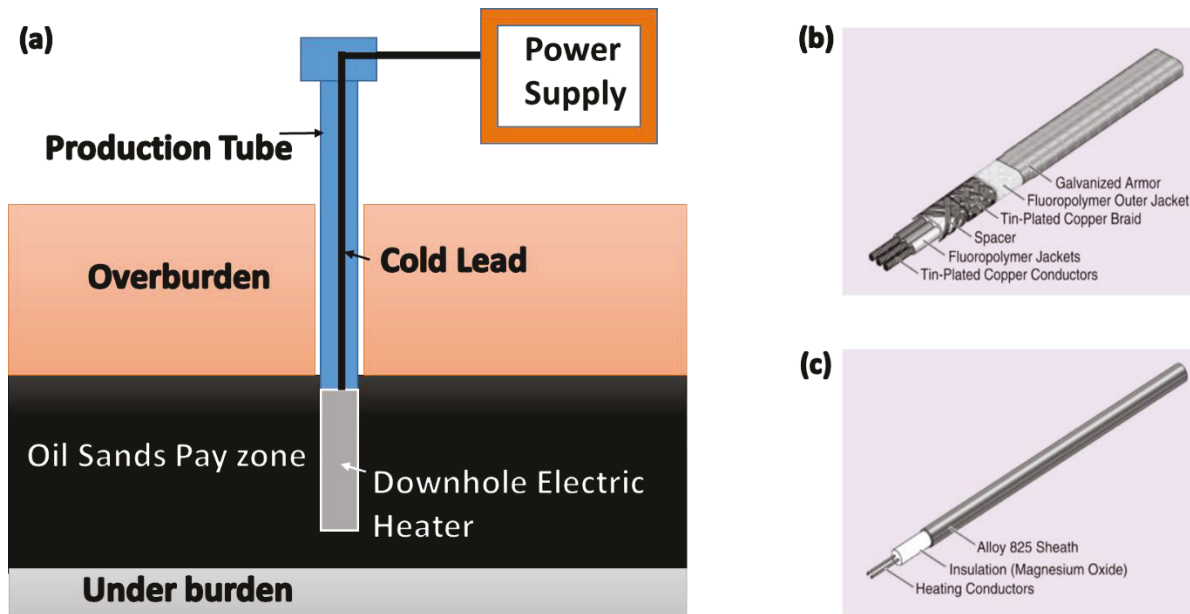


Figure 2-10. (a) A typical downhole electrical heating system carrying out indirect ohmic heating (b) Polymer insulated CW cable (c) Mineral Insulated cable adapted from ³⁸.

There are however several inherent challenges with using downhole electrical heaters. To increase the production flow, a relative amount of heat would have to be applied into the immediate area of the reservoir, so in effect the heat itself would need to be concentrated toward a relatively small area of the total production tube length which is in the pay zone area of the reservoir. Also since the production tube has very small diameter, large amount of heat would have to be applied through minimum passes or the diameter of the cables should be small enough to allow multiple passes to be installed. Finally, the technology needs to be rugged enough to withstand the tubing and long term wellbore conditions. There are significant chemical reactions that interact with the electrical heater systems. These reactions can vary from actual breakdown of molecules to simple viscosity reduction. The former processes involve cracking and in situ hydrogenation of molecules. Main difference between the two processes is the average temperature of the reservoir to obtain the objective product. With thermal cracking and hydrogenation the temperatures must be hot enough to result in thermal cracking. This requires substantial power along the heater on the order of 1000-1300 Watt/m ^{40,41}. The average reservoir temperature would be on the order of 150°C. Viscosity

reduction can be obtained at lower average powers but to accelerate the process the power required is not that different (820-1150 Watts/m). The average reservoir temperature might be on the order of 120°C^{40,41}. Thus downhole electrical heaters provides the ability for precise targeting of heat and capabilities that range from oil viscosity reduction to in situ upgrading of heavy hydrocarbons. In this sense, indirect electrical heating is quite flexible and tailorable to a variety of reservoir scenarios. Research however is ongoing to increase operating voltages of mineral insulated cables. Also temperature source heaters are being developed to mitigate issues with variable thermal diffusivity in the near well bore region.

2.3.2.1.2 Direct Ohmic Heating

Direct ohmic heating of oil reservoirs as an enhanced oil recovery technique was christened as Electrothermic process in the early 1970s⁴² due to an electrode well technology invented by Electrothermic Co. of Texas. The technique consisted of the application of electric current into an oil reservoir through a specially designed electrode⁴³. The string of tubing insulated by fibre glass was connected to the exposed metal electrode inserted into an oil bearing formation. A source of electrical power was connected between the tubing and an infinite remote ground return electrode as shown in figure 2-11. Current flowed from the resistance of the steel tubing to the electrode and then through the formation returning through an infinite conductor the earth.

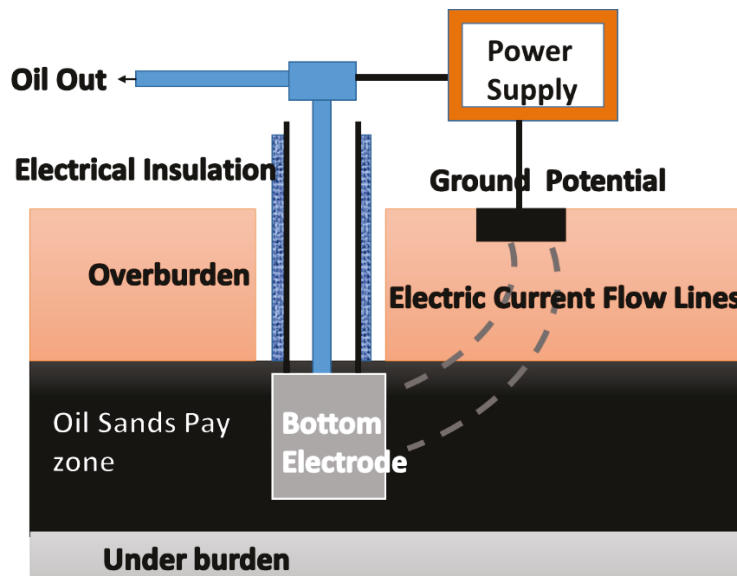


Figure 2-11. Schematic of initial configuration of electrothermic heating process applied to reservoir adapted from⁴⁴.

The wells were usually 1000 m deep and an input energy of 480 V and 60 Hz was applied to carry out heating⁴³. For such cases the resistance of the earth was calculated to be 1.6Ω from considering the conductivity of oil reservoirs in salt water wet sand formation to be 0.02 S/m. Using this method 85% of the total heating takes place within a considerable distance spanning 15 m around the well, heating to temperatures up to 90 to 120°C unless higher temperatures were needed. The earliest studies predicted that the overall recovery efficiency of such a process would be 20 to 25% and the cost of producing would be \$ 1.25/bbl of heavy oil. The cost could increase or decrease depending on the temperature needed to reduce viscosity⁴³. The successful aspect of the technology was the development of successful design and completion of downhole electrode system for high current, high power application. The electrodes used could typically handle several hundred amperes at a few hundred volts for a single well power levels of up to 200 kW.

Field trials of Electrothermic systems were demonstrated as early as 1969 in a heavy oil reservoir in Texas^{45,46}. It was reported that the production of four wells with heavy oil had increased from 1bbl/day to an impressive average of 20 bbl/d on attaining a temperature of 120°. This attracted investigators and a number of variants of the process were patented in the 1970s⁴⁷⁻⁵⁰. Following which electrothermic systems were implemented in several field trials in asphalt and paraffin based crude oil reservoirs in Texas, Utah, Mexico and Oklahoma. These field trials demonstrated increase in oil production as compared to thermal flooding (steam and hot water) processes and additional wells were planned for most of these operations. The oil produced by Electrothermic heating was also proportional to the watts of energy supplied to the electrode system and in some cases also resulted in casing failure due to corrosion⁴³. The same electrode configuration was also applied to three wells in Lloydminster area heavy oil formations⁵¹. The energy flow was into the reservoir and up through the overburden to surface ground wells to complete the circuit. A positive production response was obtained through the application of ohmic heating to two of these wells while the third well was shut down due to sanding problems and eventual failure of casing insulation. Even though the other two wells indicated a quick response to heating even at low power input levels, long term heating couldn't take place due to issues with the electrical delivery systems as well as casing insulation failure that resulted in short term heating. The electrical data also showed that the impedance of the reservoir indicated by the power drawn into the reservoir varied with time indicating that the variation in reservoir properties affected the overall impedance and performance of electrical heating. The authors suggested that long term economic potential of

the process cannot be realized without long term heating. They also reported that the mechanical problems related to casing insulation failure made long term heating doubtful. To overcome this drawback they proposed that cable delivery systems could be more suitable. Results of field trials using the mentioned electrode configuration are tabulated in table 2-1.

Table 2-1. Direct Ohmic Heating of Oil Reservoirs with Single Vertical Well Electrode with Ground Return –Field Tests

Year	Reference	Region	Type of Reservoir	Input Electrical Energy	Temperature Attained and Oil Recovered	Production Problems
1969	^{45,46}	Little Tom Field, Texas (4 electrode wells)	Heavy Oil (8-12°API)	60 Hz	120°C Increase from 1bbl/day to 20 bbl/day	
1979	⁴³	North Texas	Heavy Oil	60 Hz 480V	Increase from 10 bbl/day to 16 bbl/day for 20 months	
1979	⁴³	Southwest Texas (1000m deep well)	Asphalt base crude (11°API)	60 Hz, 150 kW initially followed by 12 kW	Increase from 0 bbl/day to 76 bbl/day at 150 kW and 10 bbl/day at 12 kW with continuous production continuing for 11 years	
1979	⁴³	West Texas (1300m deep well)	Paraffin base crude (39°API)	60 Hz	Increase from 5 bbl/day to 45 bbl/day and later settled to 24 bbl/day for 70 days operation	Casing failure up hole due to H ₂ S corrosion
1979	⁴³	Eastern Utah (900m deep well)	Paraffinic and Asphalt base crude combined(22°API)	60 Hz, 60 kW	Increase from 4 bbl/day to 50 bbl/day for seven months operation	
1979	⁴³	Mexico (500m deep well)	Asphalt base crude (19°API)	60 Hz	Increase from 6 bbl/day to 283 bbl/day for 35 days. Final production was at 65 bbl/day	Water coning
1979	⁴³	South Central Oklahoma (2400m deep well)	Asphalt base crude (11°API)	60 Hz, 56.5 kW initially followed by 100 kW	Increase from 20 bbl/day to 50 bbl/day for six months of operation for initial power. Later increased to 80 bbl/day for 100 kW.	Sand production
1989	⁵¹	Sparky Formation, Lloydminster (3 wells)	Northminster Heavy Oil (13.7°API)	60 Hz, Initially 20 kW with 4 hour pulsing spikes of 30 kW twice daily. Power gradually increased to kW	Increase from 62 bbl/day to 125 bbl/day for three weeks operation.	Failure of casing insulation
			Lashburn Heavy Oil (11.4°API)	60 Hz, 13-18kW	Erratic production averaging around 31 bbl/day for two months operation.	Failure of electrical delivery system.

The next electrode well configuration considered was adapted from the electric heating model patented by Kern ⁴⁸. According to this patented process, AC current is sent down a wellbore, through the formation and back up an adjacent well. Formation brine provides the conductive medium in most of the formation. A schematic is given in figure 2-12.

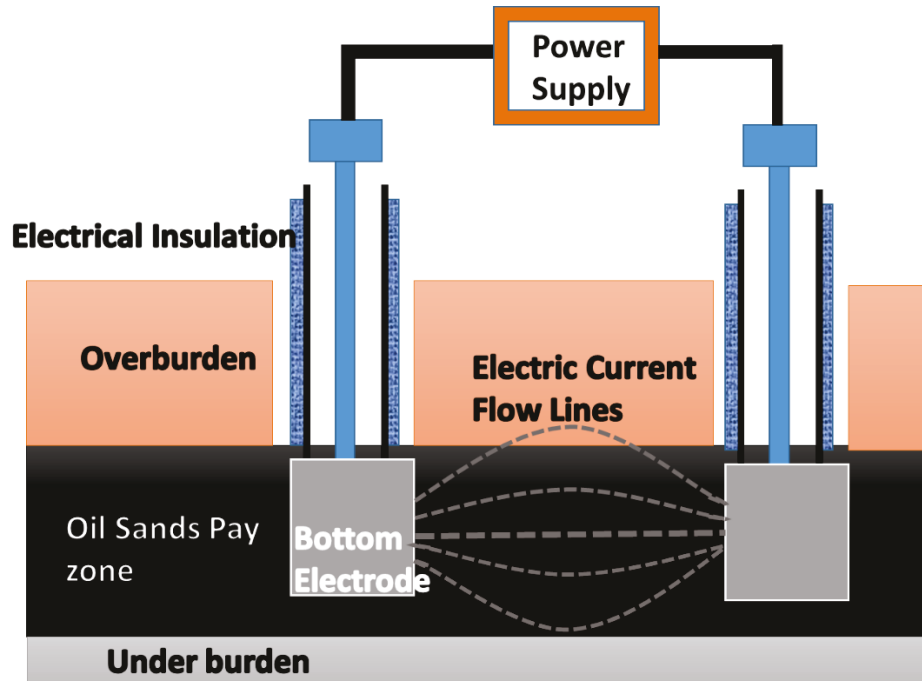


Figure 2-12. Schematic of electrothermic heating process patented for oil sands reservoirs adapted from^{48,52}.

To prevent flow of electricity to overburden, casing above the electrode was electrically insulated. The tubing would be externally insulated or it would be equipped with non-conductive centralizers and installed with an insulating fluid in the casing tubing annulus. Several studies pertaining to numerical modeling were carried out for this configuration. It was El-Feky ⁵³ who carried out the first academic research on direct ohmic heating of oil reservoirs using such an electrode configuration. He developed and tested numerical model that was based on implicit pressure and explicit saturation formulation over a 2D rectangular grid. Experimental data came from a laboratory model consisting of a five-spot graphite electrode pattern. This physical model was packed with sand pack consisting of silica sand, saturated with brine at a concentration of 75,000 ppm of NaCl. The resistivity of the sand pack was considered to be 3.12 Ωm . Temperature and voltage were measured and showed to validate the results from the developed numerical model.

The earliest implementation of direct ohmic heating on real oil sands through lab scale experiments were carried out in 1977⁵⁴. Electric energy at 60 Hz and from one to thousand volts were passed through a quantity of oil sands positioned below a water column between two electrodes. Results showed that bitumen separated from the tar sands and floated at the surface of the water leaving the sand behind. Though this experiment did not indicate direct ohmic heating of an oil sands reservoir, it certainly paved a positive move in the direction of implementing electrical heating of oil sands.

A two-part numerical simulation for in situ electric heating of Athabasca oil sands reservoirs was proposed by Todd and Howell⁵⁵. The first part of their simulation consisted of a 2D radial electrothermic model to calculate current flow and heating around a wellbore. The second part used this information to determine 3D distribution of voltage, heat, pressure and oil production rate. The radial model developed indicated high heating temperatures near the wellbore which dropped exponentially with increasing distance from it. The resistivity of the oil sands investigated were from 23 to 200 Ωm and showed that the energy dissipated were the same irrespective of the resistivity as the voltage could be raised accordingly. The radial model results also showed that a larger effective electrode radius would permit more rapid heating of oil sands, well cooling in the electrode region would prevent vaporization of connate water. The 3D model developed also indicated that increased electrode radius resulted in increased heating in the mid region of the well pair, and increased well spacing allowed a much larger volume to be electrically heated, which in turn increased the energy demand to effect a given flow rate.

Harvey et. al. carried out investigations for selective heating of reservoirs which cannot be readily contacted by injected fluids by combining electrical heating with water flooding⁵⁶ using previously developed 2D simulation model⁵³. The developed simulation model was validated by lab scale experiments and was used to predict heating patterns in hypothetical field cases. First technique proposed was to establish a path of current flow between electrodes installed in injection wells, using alternate polarity of adjacent wells. This arrangement allowed current to flow from injection well to injection well, passing through the region that would not normally be swept by injected fluid. In order to reduce heating near the electrodes, water injected while heating should be less resistive than formation water. The second technique involved the injection of a slug of either fresh water or saline water prior to electric heating. Under favourable reservoir conditions, the salinity of this water can be selected so that most of the heating will occur in those portions of

the reservoir that were not invaded by the injected water. The studies concluded that selective electric heating will increase oil recovery from a layered reservoir. The injection of a resistive fluid prior to heating will tend to concentrate the heating effects in low permeability zones which would otherwise be largely bypassed by injected fluids. The electric power requirements in this study were however very high and preliminary calculations suggest that the process could be designed to operate at a lower wattage.

Electric Preheat Steam Drive (EPSD) process was proposed to have great promise for in situ recovery of bitumen from the moist sands of the Athabasca region ³⁶. It involved completing an array of vertical wells into the formation some of which act solely as electrodes while the remainder are completed for dual service as either electrodes/steam injectors or as electrodes/producers. The rate of power dissipation is controlled so that pore water is not vaporised and a conductive path through the formation is maintained. On heating for weeks or months, the viscosity of bitumen would be reduced between injector and producer wells to the point that it can be displaced by injection of steam. Electrical energy is thus used to supply only a fraction of the thermal energy requirement of for the recovery process. Numerical simulation was carried out for a pattern where the wells were arranged in rows spaced so that every fourth electrode well also serves as either an injector or producer in a 7 spot production pattern. At the end of an 18 month preheating period at a current level of 400 A per well, the temperature in the rich oil sands midway between wells in adjacent rows can be increased from 15 to 50°C. Simulations indicated that approximately 70% of the original oil in place could be recovered before steam breakthrough to the producers, at an overall oil/steam ration of 0.44.

A version of EPSD was successfully tested on a small scale by Towson ^{36,57}. He reported progress on an electrical heating pilot plant operated by Petro-Canada. The pilot consisted of four electrode wells spaced 30 m apart and eight observation wells. Electric pre-heating was maintained for about 1 year beginning in April 1981; then a steam- injection phase was begun. Peak temperatures of 100°C were obtained and average temperatures of 65°C was attained by the end of the electrical heating phase. An economic evaluation of the EPSD process was also carried out in 1984 to estimate the average cost of production to be \$20/bbl of bitumen produced.

Carrying on from the work of numerically modeling selective heating of oil reservoirs ⁵⁶, a fully implicit 3D reservoir numerical simulator was developed ⁵⁸. The simulator tried to overcome some of the deficiencies of the previous attempts by including sufficient physics related to vaporization

of connate water and movement of saline concentration within the reservoir. The dependence of conductance on temperature, water saturation and salt concentration was rigorously modeled. Validation of the model was accomplished using two approaches. First, the model results were compared with the experimental data of El-Feky. Next, an analytical solution was used in the evaluation of model calculation. In both cases the comparisons were excellent. The model was further applied to general well and electrode geometries to allow for any possible configuration including horizontal wells and conductive fractures. Near well phenomena was better analysed using a curvilinear grid which accounted for both near well as well as pattern phenomena. An option for efficient solution for multiphase alternating current case was also included.

Hiebert et al. ³⁷ listed some disadvantages of ohmic heating stating that it could be more costly than same amount of steam energy. Also electrically insulating all or part of the tubing, casing, and well head is necessary to protect the operating personnel and to prevent short circuits. They developed a numerical simulator named MEGAERA to study the process of electrically heating of oil sands reservoirs consisting of several layers with different electrical resistivities. The simulator was used to study the effects of electrode placement on the final temperature contours resulting from electrically heating realistic reservoirs. Their 2D simulations showed that using conducting adjacent formations as extended electrodes permitted relatively uniform electrical heating of an oil sands formation with a well spacing of 50 to 75m. Uniform heating becomes much more difficult for these reservoirs where the rich oil sands layer rests directly on a relatively poorly conducting limestone layer. If an existing well is adapted to electrical heating process, it would have to be recompleted to insulate both the tubing and the section of casing containing the electrode from the rest of the casing and almost all electrical heating would occur immediately next to the wellbore. They also concluded that the area that needed maximum development was well completion technology in order to reduce well bore electrical losses. Another 2-D simulator was developed to study electrical resistance heating based oil production rate which showed that four parameters such as initial oil viscosity, formation thickness, drainage radius and induced temperature change accounted for the variations in production rate ⁵⁹.

In 1987-88 a field test was conducted on a single well by Petrobras in the Rio Panon reservoir which resulted in the increase of oil production rate from 1 to 6 bbl/day at a power level of 20 kW which further increased to 12 bbl/day as the power was increased to 40 kW. It was suggested that the heating had removed the visco-skin, but the test was later terminated due to voltage control

problems^{45,46}. Pizarro et al. also carried out 2D numerical simulation to simulate the electrical resistive heating method for this field test. Field test data from Rio Panon were matched well by this numerical simulations and it was predicted by these simulations that for a 1500 day operation, 86% increase in the accumulated production could be attained. The simulations also showed that the heating effect is usually concentrated near the well region. At a distance of 30m, the temperature increase is less than 2°C after 5 years of heating. For this reason, this method was proposed to be suitable for well stimulation rather than a holistic heating method. Table 2-2 lists the results of numerical modeling and lab scale studies carried out using the adjacent vertical well configuration whereas table 2-3 lists the field scale implementation of this heating scheme.

Table 2-2. Direct Ohmic Heating of Oil Reservoirs using Two Adjacent Well Configuration – Numerical Modeling and Lab Tests

Year	Reference	Type of Study	Oil Sample Specifications	Electrode Configuration	Input Electrical Energy	Parameters modeled/measured	Results
1977	⁵³	Numerical Modeling in a 2D rectangular grid with experimental validation in a 5 spot electron pattern model (30 x 10 x 42 x 1.6 inches).	Sand pack made of 70-100 mesh silica sand, 100% saturated with brine solution of 75,000ppm NaCl concentration.	5 electrodes in injection wells and a production well	60 Hz, 110 V	Voltage, current and temperature profile	Developed 2D numerical model based on implicit pressure and explicit saturation validated by experimental data.
1977	⁵⁴	Lab experiment of electrical heating based separation of bitumen from oil sands	Oil Sands (13.4% Bitumen, 1.1% Water, 85.5% solids)	Flat circular parallel electrodes	60 Hz, 1-1000V	Bitumen froth yield from electrical separation process	Bitumen froth yield consisted of 56% bitumen, 15% solids.
1978	⁵⁵	Numerical simulation of near well bore heating carried out in two parts. First part was development of electrothermic radial model, solution of which was used for the development of 3D model which was the second part.	Oil sands ($\rho=23$ to $200\Omega\text{m}$)	Electrode Radius is 5 ft, 10 ft and spacing at 75 ft and 100 ft	60 Hz, 16.6 kW/ft.	Voltage, current and temperature profile in radial model and temperature and oil production in 3D model.	High temperature near well bore falling exponentially with distance. Total energy dissipated in the formation with different initial resistivities is the same as voltage can be increased accordingly. Larger the electrode more evenly heated is the sand body. Well bore cooling desired. Temperature to be below steam saturation temperature while applying current. Increased well spacing produces a much larger volume to be electrically heated which increases the energy demand to effect a given flow rate of oil.

Year	Reference	Type of Study	Oil Sample Specifications	Electrode Configuration	Input Electrical Energy	Parameters modeled/measured	Results
1979	⁵⁶	2D mathematical model validated by lab experiment ⁵³ and used for prediction of hypothetical field results for carrying out selective heating of reservoir using electrical heating and water flood. Two cases considered were injection of brine with electrical heating and injection of water prior to electrical heating so that selective permeability zones having lower resistivity could be electrically heating	Lab experiment same as ⁵³ with oil and water saturation at 86% and 14% and 200,000 ppm NaCl water injected for 14 minutes before electrical heating	5 electrodes in an injection wells and a production well for lab experiment and hypothetical field case.	60 Hz, 110 V	Electric potential, temperature profile, cumulative oil production	Oil recovery with selective heating was 13% higher than with water flooding. Injection of a resistive fluid prior to heating will tend to concentrate the heating effects in low permeability zones which would otherwise be largely bypassed by injected fluids.
			Field Case 1 same as above	Electrode spacing at 450 ft.	60 Hz, 1000V for 42 days		Process predicted to increase oil production by 55,581 stock barrels.
			Field case 2 same as above but having different permeability layers with low salinity water (1000 ppm) injected into reservoir.	Electrode spacing at 500 ft.	60 Hz, 2000 V for 11 days and then reduced to 1250 V for 17 days		Process predicted to increased temperature of less permeable zone as compared to that of more permeable zone.
	³⁶	Numerical simulation of EPSD at reservoir scale using a 7-spot electrode well pattern	Rich grade oil sands	Electrode spacing at 25m vertically and 87m horizontally with	60 Hz, 400A per well	Temperature profile, recovery efficiency, oil to steam ratio	Temperature rose from 15 to 50°C with 70% recovery before steam breakthrough and 0.44 oil/steam ratio.
1982	⁵⁸	3D reservoir numerical simulation. To develop a fully implicit model to include connate water vaporization and movement of saline concentration. Dependence of conductance on temperature, water saturation and salt	2 moderately viscous oils (245cP, 17°API) and (1930cP, 13°API)	40 acre pattern model on conventional well completion scheme	60 Hz 110 V	Oil production rate and water oil ratio	Electrical heating is better used as a stimulation and rate acceleration procedure than an enhanced oil recovery.
			Conductive fracture	Conductive fracture 50 ft in length was used in 40 acre five spot pattern	60 Hz, 500 KW	Oil production rate and water oil ratio	Three times the volume of oil delivered as compared to waterflood only case. Linear heating of reservoir not enough to substantially affect fractional flow.

Year	Reference	Type of Study	Oil Sample Specifications	Electrode Configuration	Input Electrical Energy	Parameters modeled/measured	Results
		concentration was also considered. Curvilinear grid was considered to better analyse near well phenomena and multiphase alternating current case was included.		Horizontal well electrodes 2000 ft in length in 15 acre pattern	60 Hz, 125 kW and 250 kW	Oil production rate	For both power levels, oil breakthrough time was considered to be 8-10 years compared to 2 years for waterflood process.
				80 acre, nine spot pattern with 3 producer wells subject to different power sources.	60 Hz, 200 kW and 400 kW.	Heating rate	The increased power results in a reduction in oil production rate for the DC case and an increase for the multiphase power case. Excess heat builds up in the well for high power case.
1986	³⁷	Numerical Simulation using 2D simulator MEGAERA. Study the effects of electrode placement on the final temperature contours resulting from electrically heating realistic reservoirs.	Multilayer model of oil sands, water, shale and limestone with outer radius of the simulation volume set at 26m with electrode height as 15m	1 electrode per well in a 5 spot pattern	60 Hz 300 kW	Temperature profile	Using conducting adjacent formations as extended electrodes permits uniform electrical heating of an oil-sand formation with a well spacing of 50 to 75 m. If the electrical heating process is applied to an existing well with a small-diameter casing (18 cm or less), where the electrode is completed in the middle of the reservoir and no extended electrodes are jet-cut into the formation, almost all the electrical heating will occur immediately next to the wellbore. The area that needs the most development is the well-completion technology.
				2 electrodes per well in a seven spot pattern.	60 Hz 410 kW		
				Staggered, parallel, horizontal electrode wells.	60 Hz 13 kW/m		

Year	Reference	Type of Study	Oil Sample Specifications	Electrode Configuration	Input Electrical Energy	Parameters modeled/measured	Results
1988	⁵⁹	2D Numerical Simulation. Study to determine method of estimating steady state stimulated production.	Oil viscosity varied from 10 to 300 cP	Electrode height from 5 to 500 ft, radius from 118 to 745 ft	60 Hz	Steady state oil flow rate dependent on variation of physical parameters	Production rate was most affected by initial oil viscosity, formation thickness, drainage radius and induced temperature change.
990	⁴⁵	2D numerical simulation of electrical resistive heating validated by analytical method and Rio Panon field test results.	Heavy oil (2452 cP)	Same as Rio Panon Field case	60 Hz, 20 kW initially and 40 kW later	Oil production, power consumption, temperature rise	Field test data matched reasonably well and it was predicted that for a 1500 day operation 86% increase in accumulated production would be achieved.

Table 2-3. Direct Ohmic Heating of Oil Reservoirs using Two Adjacent Well Configuration –Field Tests

Year	Reference	Region	Type of Reservoir	Input Electrical Energy	Temperature Attained and Oil Recovered	Production Problems
1981	^{36,57}	Stoney Mountain Canada (Four electrode wells of 15m length and spaced 30 m apart)	Oil Sands	60 Hz, 550 A, 450 to 680 kW	Peak temperature of 100°C and average temperature of 65°C after 296 days of heating	Cooling fluid needed to be circulated to keep the casing temperature within structurally safe limits.
1987-88	⁴⁶	Rio Panon, Brazil (300 m deep well)	Heavy oil (15°API, 2250 cP)	60 Hz, 20 kW initially followed by 40kW	Increased from 1 to 6 bbl/day for 70 days of operation for initial power which was later increased to 12 bbl/day for higher power.	Voltage control problems

A third type of electrode well configuration was considered where the electrode assembly consisted of a bare casing pipe with fiberglass electrical isolation joints attached to the ends. The current return or ground was the casing string above the fiberglass insulation. Current leaving the power supply was conducted down the power delivery system to the electrode assembly which was in electrical contact with the reservoir formation. From the electrode, the current would flow through the reservoir and return to the power supply up the casing. The connate water in the reservoir was considered as the current carrier and the resistance heating element. Heat is exchanged with the oil in contact with the connate water. An adapted figure of the electrical heating single wellbore configuration is shown in figure 2-13⁶⁰. All downhole equipment were contained within a single equipment within a single wellbore. The power supply was capable of delivering up to 300 kW of power and the power delivery system consisted of tubing, cables or a combination of both.

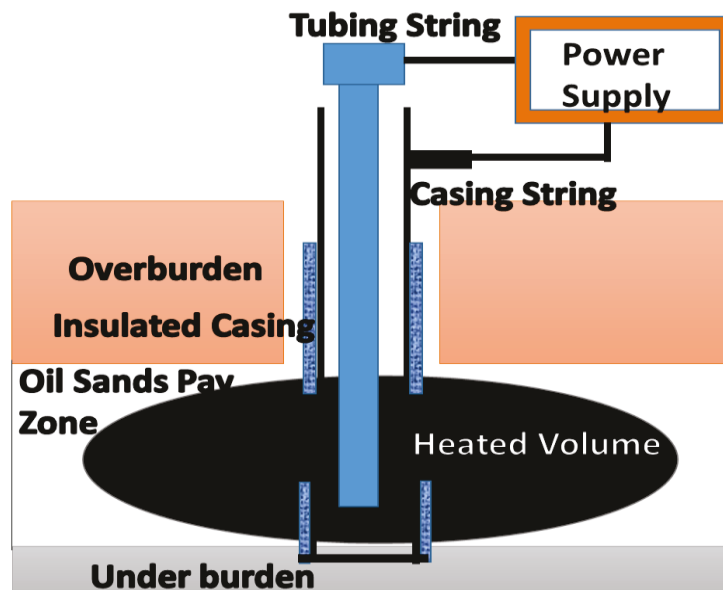


Figure 2-13. Electrical heating single wellbore configuration adapted from⁶⁰.

A stimulation test using the above described technique was conducted on a single oil production well in Schoonebeek reservoir in the Netherlands⁴⁶. Prior to electrical stimulation, the oil production rate was 82 bbl/day at a water cut of 35%. As the surface power dissipated was increased above 60 kW, the oil production rate increased abruptly to 190 bbl/day with a bottom hole temperature in the range of 54 to 60°C. In the single well electrical heating process a low frequency electric current flows radially from the electrode a few meters into the formation and

then begins to bend vertically towards the return electrode which is usually the casing. The electric power causes ohmic heating and the dissipated power density decreases as the inverse square of the radius from the electrode. Thus at a steady state, the excess temperature over ambient decreases as the logarithm of the radius. The productivity increase by electrical heating was predicted to be because of removal of thermal adaptable skin effects called visco-skin and the reduction of the oil viscosity and the reduction of the oil viscosity in the vicinity of the wellbore. Vinsome et al.,⁶⁰ described the use of electrical heating to remove visco-skin and modified a 3D numerical simulator called TETRAD to predict fluid rates, and temperature distribution in the reservoir and on the electrode during electrical resistance heating. Voltage-current relationship were obtained to design power supplies and operational criteria such as input power requirements as a function of flow rate and reservoir heterogeneity were determined. The simulator was validated against analytical calculations and field data. It includes treatment of the electrical conductivity as a function of temperature, salinity and saturation. It has been used to design several electrode completions and assist in developing operating strategies for field implementation of the electrical heating process. Table 2-4 lists the results of numerical modeling and lab scale studies carried out using electrode connection through tubing and casing of same well whereas table 2-5 lists the field scale implementation of this heating scheme.

Table 2-4. Direct Ohmic Heating of Oil Reservoirs using Electrical Connection through Tubing and Casing of same well – Numerical Modeling and Lab Tests

Year	Reference	Type of Study	Oil Sample Specifications	Electrode Configuration	Input Electrical Energy	Parameters modeled/measured	Results
1994	⁶⁰	Reservoir Simulation by TETRAD and validated with actual field data and semi analytical model by enabling simulator to include treatment of electrical properties of reservoir	Paraffin base crude (39°API)	Single vertical well Electrode with ground return	Analytical Model 60 Hz, Field Case 60 Hz, initially 5 kW and later 30 kW	Temperature and production rate	Developed model was well validated by analytical method and field case.

Table 2-5. Direct Ohmic Heating of Oil Reservoirs using Electrical Connection through Tubing and Casing of same well –Field Tests

Year	Reference	Region	Type of Reservoir	Input Electrical Energy	Temperature Attained and Oil Recovered	Production Problems
1989	⁴⁶	Schoonebeek, Netherlands	Conventional Oil (27°API ,160 cP)	60 Hz, 60kW	Temperature increased to 54-60°C and oil production increased from 82 bbl/day to 190 bbl/day	

In order to suit electrical heating process to existing SAGD horizontal wells, McGee⁶¹ carried out field tests in the Lloydminster heavy oil area for electrically heating a horizontal well with vertical wells which could be considered as the fourth type of electrode configuration. Horizontal wells typically 500 m in length and longer are common in the exploitation of heavy oil reservoirs around the world. These offer prospects of improved performance over vertical wells, primarily due to larger contact area between the formation and the wellbore. The most significant production challenge was the integration of the electrical heating system into the existing production system without compromising the production capability of the well. In vertical wells, the fluid level above the perforations increased with the electrical heating, indicating productivity improvement in the wells. Long term production could not be achieved because of sand and possibly pump problems. The horizontal well however did not show a production response and also showed only a small temperature response. The project was a technical success in that the electrical current from two vertical wells was returned to the power units via the horizontal well and a thermal response was observed at all wells. The configuration is shown in figure 2-14.

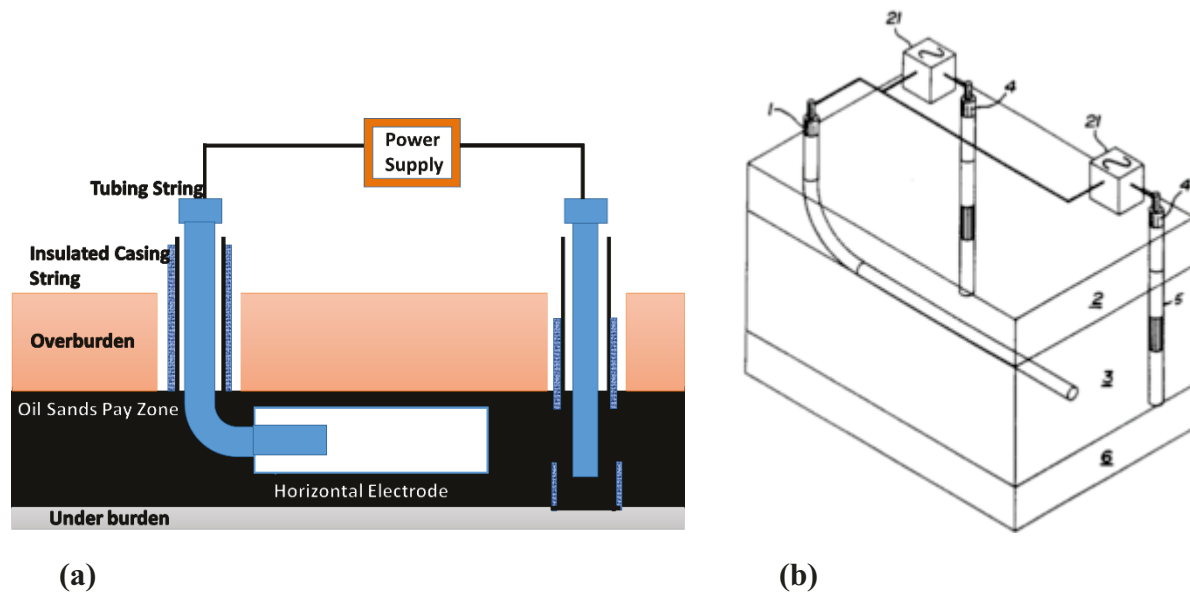


Figure 2-14. (a) Electrical heating using horizontal and vertical well configuration (b) Electrical heating using a combination of two vertical wells and a horizontal well adapted from⁶¹.

Low frequency direct ohmic heating methods that have been proposed so far have the common limitation of being able to transfer heat uniformly and hence efficiently through the oil sands. This is largely a result of the inherent geometry of current flow emanating from an electrode whereby

the current densities and heating rates are highest locally and the water in the immediate vicinity of the electrode vaporizes. Therefore the continuous water path which is the electrical circuit between the electrodes and oil sands is broken. Therefore, these processes require cooling around the electrode that removes the heat to prevent vaporization so that electrical contact is maintained. McGee⁶² came up with the Electro-Thermal Dynamic Stripping Process (ET-DSP) as can be seen in figure 2-15 which was designed so that energy is not remove from the system but rather transferred to the oil sands. In this process electrical heating is coupled with heat transfer by convection, achieved by injecting recycled water at relatively low rate (1m³/day per electrode) into the ends of the electrodes where the power density is greatest. Voltage and phase distribution control between individual electrodes were controlled so that the current may be uniformly applied independently of variable lithology. Water was injected into the ends of the electrodes deliberately so that the current can flow more uniformly through the entire surface of the electrode into the soil and thus prevent boiling off of the water phase necessary for maintaining current flow in the oil sands. The geometric position of the electrode and extraction wells were stationed in such a manner that it maximize recovery of the heated bitumen and minimize dead zones. The recovery factor from ET-DSP process was comparable to a good SAGD project. The large number of well locations needed however to implement this process may limit the depth of the formation where these processes are economical. The application of ET-DSP was further demonstrated at pilot scale test and showed to have favourable energy intensity of production compared favorably to alternative thermal bitumen extraction techniques. The production of bitumen was achieved with reduced greenhouse gas emissions as compared to other thermal methods with trace amounts of sand and no emulsions. A limiting feature of this process was the large number of electrode and extraction wells needed to implement the process. The electrodes were spaced approximately 16 m apart resulting in as many as 18 electrodes and 8 extraction wells per acre. A review summary of the field trials as well as the numerical simulation and lab scale experiments carried out for direct ohmic heating are given in Table 2-6.

In order to gauge the energy efficiency of in situ direct ohmic heating of subsurface oil reservoirs, it was essential to know the percentage of power supplied to the wellhead which actually heated the formation. It was understood that the use of alternating current (ac) could lead to a significant increase in transmission power loss in the presence of steel tubular goods, primarily because of magnetic hysteresis and eddy current losses. Newbold and Perkins⁵² carried out lab scale

experiments to determine transmission losses in complex well-bore systems for the same configuration as shown in figure 4 . Methods were developed to determine power loss when copper cables were used to conduct power down hole and when steel pipe was used as a conductor. The method was further used to calculate power losses in a field scale shallow well and validated with measured values.

In a review study done by Vermeulen ⁶³ they summarized the findings by previous researchers in stating that when ohmic heating of reservoirs was carried out, significant stimulated production rates were attained, but long term heating could not be achieved due to short comings in operational strategies and failures in the oil production system. In such a heating method, power must be controlled so that the formation temperature is kept below the boiling point of water otherwise the water will vaporize and electrical continuity would be lost. The production rate and operational requirements that are unique for each well determine the power for the well. Fluids flow towards the well and increase in temperature because of the high rate of conversion of electrical energy to heat in the near wellbore region. As the flow rate increases, more electrical energy is required to compensate for increased rate of energy withdrawal. Too much power can result in excessive temperatures and may damage the electrode assembly. Their studies indicated that electrical wellbore stimulation is continuously evolving and commercialization of the technology will likely take place in the not too distant future. Field pilot tests of electrical wellbore stimulation indicate the remaining technical challenges are with operational and mechanical issues. Table 2-6 gives details of the ET-DSP process as well as the horizontal and vertical well based electrical heating of oil sands.

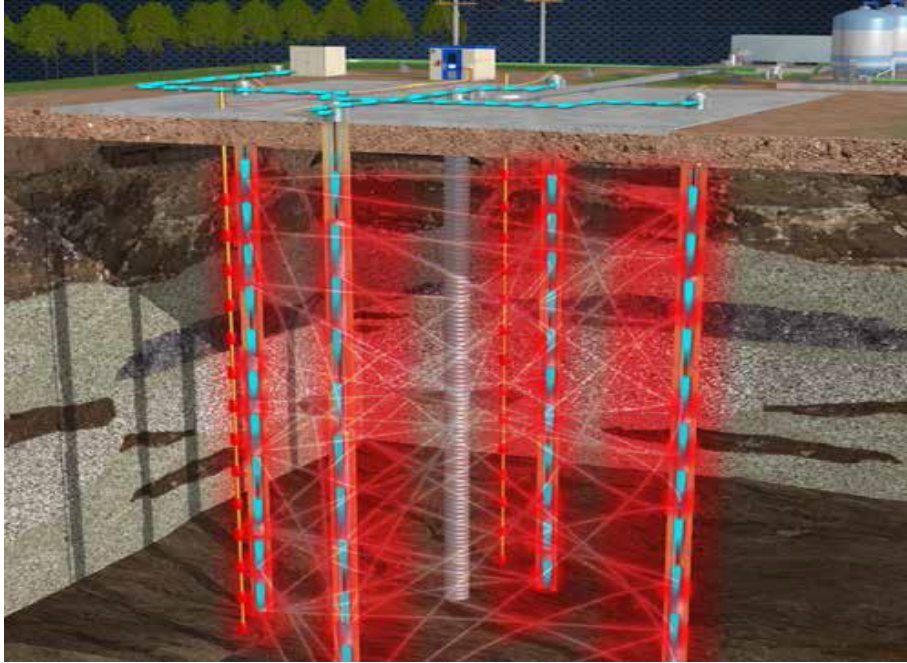


Figure 2-15 Field scale illustration of ET-DSP Process.
<http://www.creosoteremediation.com/index.php/etdsp-technology>

Based on all the studies carried out via direct ohmic heating it can be concluded that heating the reservoir at 60 Hz frequency has not really proved useful because of the following reasons:

1. Over dependence on water in the reservoir to initiate and continue the heating process resulting in non-uniform heating of the reservoir due to absence of continuous water channels.
2. Over-heating of water at electrode surfaces and generation of hot spots in these regions leading to failure of electrode equipment and discontinuation of the heating process.
3. Underdeveloped electrode systems which fail due to sanding problems and production issues.

Table 2-6. Ohmic Heating of Oil Reservoirs using Horizontal Wells and ET-DSP process–Field Tests

Year	Reference	Region	Type of Reservoir	Input Electrical Energy	Temperature Attained and Oil Recovered	Production Problems
1999	⁶¹	Lloydminster, Frog lake lease. 1 horizontal well and 2 vertical wells.	Heavy oil (10-14°API)	60 Hz, 25 kW	Production increased from 2 to 4 times the primary production from vertical wells. No production response and a small temperature response at horizontal well.	Sanding problems and premature equipment failure.
2007	⁶⁴	ET-DSP process 9 electrode well locations each completed with 3 electrodes and 4 extraction wells	Oil sands (Bitumen 10 °API)	60 Hz, 30 kW/electrode	45°C at 10m distance and 95 °C near electrodes. 75% recovery from oil wells with a total of 2200 bbl of bitumen produced through the total test period	Failure of electrode wells

2.3.2.2. Inductive Heating of Oil Sands Reservoir

Induction heating as a method of heating oil reservoirs was first patented by Fisher et al. in 1976^{65,66}. The proposed method of induction heating was to drill shafts and tunnels from the surface to form a series of adjacent loops surrounding parts of the fossil fuel deposit⁶⁷. In each of these passages a conductor would be placed forming a complete loop. A large alternating current passed through a group of these loops sets up electric and magnetic fields in the deposits. These fields heat the deposit by inducing displacement and eddy currents in it. In the same period Chute et al.⁶⁸ investigated induction heating of low loss materials such as wood, concrete and different grades of Athabasca oil sands through theoretical calculations and experimental verification. Their studies showed that efficient and uniform heating of low loss cores at low frequencies is possible even though the eddy current heating usually associated with an induction coil is negligible in these cases. Their studies showed that sheath helix model configuration could be used to approximate the fields of a coil wound on a core of lossy material. The resulting heating is shown to be uniform over the core, except for an end effect and to be orders of magnitude more efficient than eddy current heating alone. Further studies of induction coils buried in and in direct contact with a fossil fuel formation were examined analytically and experimentally using scaled physical models⁶⁹. Both approaches considered indicate that dominant electric field generated in the formation generated displacement currents which caused heating of the formation. They also concluded that there was no evidence that eddy currents produced significant heating and that traditional approaches used in common induction heating of metallic objects cannot be used in this case. The studies concluded that for the induction heating configuration proposed by Fisher^{65,67} heating of the formation would predominantly take place near the feed terminals while little heating would occur elsewhere in the formation. Also, higher frequencies of the order of 10 kHz as compared to 60 Hz could lead to more acceptable efficiencies. The double loop configuration proposed by Fisher⁶⁵ was also analysed for its design and it was suggested that when the mutual coupling between the adjacent loops was small, each loop would act as a short circuited transmission line. Based on all these reasons these studies concluded that induction heating would not be technically feasible for heating oil reservoirs.

A system utilizing electrical induction principles to heat selected zones in oil wells called the Triflux system was developed, tested and commercialized a few years later⁷⁰. The system was used for stimulation of heavy oil production through heating of near well bore regions, elimination

of skin resistance and improvement of pumping efficiency. The Triflux system consisted of a power inductor assembly electrically connected to a surface mounted power conditioning unit and power supply by a power cable. The inductor assembly consisted of an array of coils connected in a way to produce the electromagnetic effects. Alternating current is conducted through the coils of the inductor generating magnetic flux necessary to induce current in the steel walls of the well's production casing or liner thereby producing heat by a combination of ohmic and hysteresis loss. The Triflux system mitigates problems of insulation thermal degradation because the heating occurs in the steel walls of the well away from physical contact with the highest temperature regions. Field test results showed that heating by this method resulted in increase in production rates to 80 bbl/day for short periods and to more than 40 bbl/day for long periods with power input levels not exceeding 13 kW.

Inductive heating method was further revived in 2008⁷¹ by carrying out 3D reservoir simulation of thick, thin and shallow reservoirs when induction heating is integrated with SAGD. In order to test the simulation results a sandbox test in the scale of 1: 1000 was conducted with an inductive heating circuit installed in the box filled with sand and salt water solution with inductive heating carried out 200 kHz and 7.2 kW and observed that experimental results match simulation results in temperature values. From these experimental validation the simulation was used to evaluate the feasibility of electromagnetic SAGD i.e EM-SAGD for thin, thick and shallow reservoirs. It was concluded that enhanced bitumen recovery could be obtained by this method and the initial heating phase can be optimized serving for an early production. An artist illustration of field scale implementation of EM SAGD is given in figure 2-16.

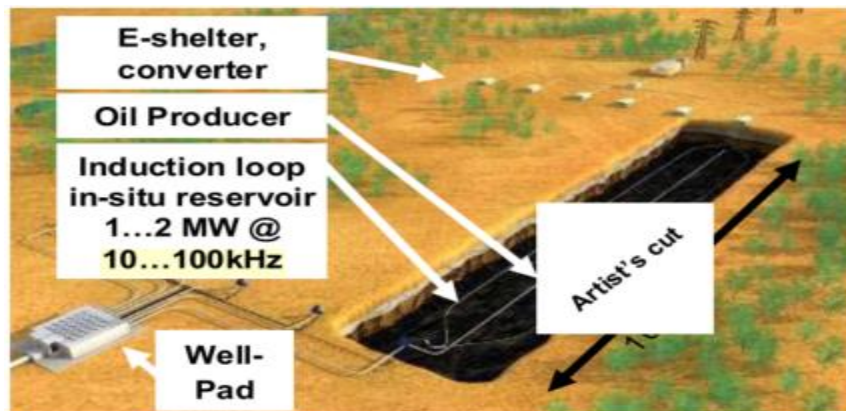


Figure 2-16. Artist's illustration of field scale EM-SAGD adapted from⁷²

After a successful laboratory test and lab scale simulation, Siemens continued with a series of field tests in conductive subsurface layers (no hydrocarbons) ⁷². No steam was applied to the tests and the tests were run under down scaled field conditions. The successful correlation of simulation and practically obtained results for the specific ground and measured temperature rise led to proceed to next scale up step of conducting the test on actual oil sands reservoir. The conclusions drawn from the pilot studies were that inductive heating would be more feasible than other electrical heating methods. Applying horizontal drilling, a horizontal inductor loop is pulled into the reservoir, equal to the length of today's SAGD well pairs. This allows a micro invasive footprint for the overall installation. It is designed to heat bulk reservoir with a penetration depth of up to 100m into the reservoir. The penetration depth is a result of basic engineering and can be adapted to the specific reservoir. It does not rely on thermal conduction throughout the reservoir; instead, eddy currents are generated in the bulk of the reservoir where they trigger heat production. Sufficient power in order of 1 to 4 kW per meter cross section can be delivered into the reservoir, giving an acceptable ramp up. It is not limited to the depth of the reservoir, since vertical losses are avoided significantly. Siemens has investigated over 100 reservoir cases with STARS simulation coupled with inductive heating. In summary, most cases promise at least a 20% additional business value. Poor SAGD cases with high SOR could be turned into highly profitable business; good SAGD cases can be further improved.

Siemens further carried out numerical simulation study of induction heating assisted heavy oil recovery ⁷³. The study was focused on the recovery drive mechanism and the influence of the reservoir and the operating parameters on the production. A 2D pay zone completely surrounded by impermeable barriers and two horizontal SAGD – like well pairs, a pair of producer (lower well) and inductor (upper one) were considered for the study. Different well constraint cases and the sensitivity to fluid and reservoir properties (pay zone thickness, depth of a reservoir, distance between wells and electrical conductivity contrast between pay zone. The results showed that operating pressure plays a significant role for the production. It defines the water boiling temperature and controls underground steam generation and consequently the drive mechanism. Steam transfers the heat from the one part of reservoir to the other as well as displaces the heated bitumen to producer by gravity drainage. For most cases the distance between inductor and producer of 10 m gives higher production rates than 5 m. The conductivity contrast between pay zone and over/under burden hasn't a significant influence on the production rate and energy

efficiency for most cases. Deep reservoirs has a higher production rate in the beginning due to the higher pressure difference between reservoir and producers, and then the shallow reservoir has a higher production due to the steam generation at lower boiling temperature. The recovery from the shallow reservoir can be limited by low boiling temperature and high corresponding viscosity of bitumen. In some cases the oil from thin reservoirs is produced much faster than from thick reservoir, but the amount of oil in thin reservoir is much lower and the efficiency of the process is the same or even less than in case of the thick formation. High initial water saturation in some cases has an advantage for recovery, but has no advantages in terms of energy efficiency. Gas or water injection or increase in power of the inductors is desirable to improve the production performance of oil sands. For heavy oils inductive heating technology may be applied without additional measures. The history of development and the experimental results for induction heating of oil reservoirs are given in Table 2-7.

Even though the studies carried out for induction heating showed promise in replacing SAGD technology it could have the following disadvantages:

1. It is again an indirect process of heating depending on presence of water saturation in the reservoir to carry out the heating process.
2. Also regions around the current loop would be most heated as compared to the inner regions of the reservoir resulting in uneven heating.
3. Finally it is technologically hard to develop a SAGD loop in the field which makes the practical implementation of this technology not very promising.

Table 2-7. Induction Heating of Oil Reservoirs –Numerical Simulation, Lab and Field Tests

Year	Reference	Type of Study	Subject of Study	Parameters modeled/measured	Oil Sample Specifications	Input Electrical Energy	Electrode Configuration	Results
1978	⁷⁴	Design proposal & theoretical calculations for induction heating of fossil fuel reservoirs	Induction loop design and theoretical calculations for field scale implementation	Evaluated parameters of induction loop design for proposed installation at field scale	Fossil fuels such as gas, oil and coal, oil sands and oil shale	50 Hz	Double loop electrical coil drilled into a shaft and tunnel in the reservoir	Computed design parameters of a toroidal coil.
1980	^{67,75}	Feasibility study of carrying out induction heating	Evaluation of technical and economic feasibility	Energy consumed and cost incurred in carrying out induction heating	Fossil fuels such as gas, oil and coal, oil sands and oil shale	500 Hz	Double loop electrical coil drilled into a shaft and tunnel in the reservoir	Rendered economically and technically feasible
1981	⁶⁸	Theoretical calculations with lab scale experiments	Feasibility of solenoid coil to carry out induction heating on low loss dielectric materials	Conductivity of material and temperature as a function of the distance from the coil	Wood, concrete, Athabasca Oil Sands	300 kHz to 35 MHz, 300 W	Solenoid coil wound around a low loss core material	Sheath helix model suitable for approximating fields of a coil. Heating shown to be uniform over the core.
1985	⁶⁹	Analytical model and lab scale experiment	Feasibility of double loop induction coil in heating oil sands	Temperature distribution of material heated inductively	Oil Sands	1.61 MHz at several hundred watts	Coil wound in a rectangular fashion with 20 uniformly spaced turns	Formation overheated near the ends of the coil while heating in the centre of the coil was uniform
1998	⁷⁰	Field scale studies	Mechanical and design considerations of triflux system for inductively heating oil wells	Oil production rate and temperature attained downhole	Heavy oil (10° API)	13kW	Induction coil assembly is placed in oil wells in the production zone	Oil production increasing to rates as high as 80 BPD for short periods and to more than 40 BPD for long period

Year	Reference	Type of Study	Subject of Study	Parameters modeled/measured	Oil Sample Specifications	Input Electrical Energy	Electrode Configuration	Results
								with temperatures as high as 150°C
2008	⁷¹	Numerical simulation and lab scale experiment	Feasibility of combining induction heating with SAGD thick thin and shallow reservoirs	Power and temperature distribution	Oil Sands	200 kHz	Inductive loop in the sandbox test with a mix of sand and salt water solution	Simulations and sandbox tests show that the method is feasible.
2011	⁷²	Reservoir simulation and pilot scale test	100 reservoir cases with STAR Stimulation	Temperature distribution	Oil Sands	1 to 4 kW	Inductive loop with SAGD	
2013	⁷³	Reservoir simulation	Investigation of recovery drive mechanism and influence of reservoir and operating parameters on the production	Effect of payzone thickness, depth of reservoir, distance between wells and electrical conductivity contrast are evaluated	Heavy Oil	10 to 200 kHz		

2.3.2.3. Dielectric Heating of Oil Reservoir

The earliest documentation in the use of higher frequency electromagnetic energy for enhanced oil recovery was a patent by Ritchey in 1956 where in a well design was proposed to heat oil reservoirs by applying radiation heating ⁷⁶. The design of the well was to transfer electromagnetic waves above 15 kHz to well bore from the surface through coaxial system of internal tubing and external casing very similar to figure 2-13. Another patent was filed later for using high frequency energy in the microwave region for heating oil reservoirs ⁷⁷. It involved use of magnetrons positioned within the well bore to generate microwave radiation as well as utilization of carbon tetrachloride to provide a lower loss transmission path between said radiation means and the reservoir.

In Russia, field tests of radio frequency (RF) electromagnetic (EM) heating of near-wellbore zone were first launched in 1969 in Ishimbayskoye oil field in Bashkortostan and continued in the Yultimirovskoye Bitumen Field in Tatarstan ⁷⁸. The source of high-frequency electromagnetic energy was a generator providing an optimum oscillation output power of 63 kW at a frequency of 13.56MHz was used in Ishimbayskoye oil field. The data indicates a temperature increase of 40°C within 5 days of continuous treatment. This test justified the technical feasibility of heating a well's bottom-hole zone by RF-EM radiation. In the Yultimirovskoye bitumen field two wells spaced 5 meters apart were studied. Input power was increased from 20 kW to 60 kW which caused the temperature to increase to 310°C in 6 days. One of the problems faced was that the fluoroplastic collars that centered the tubing in the well melted as their maximum operating temperature was 299°C). As a result, a short circuit between the casing and tubing occurred and the RF-EM unit broke and was disabled. Before this disruption, the RF-EM installation worked steadily throughout the field experiment. Five of the wells of the Mordovo-Karmalskaya bitumen deposit underwent RF-EM treatment operations to heat a significant volume of the bottom-hole zone to a temperature that permitted the initiation of in-situ combustion (fire-flooding) during the injection of an oxidizer (air). The RF-EM energy was transmitted from a generator through the well to an in-well radiator; the bottom-hole zone was heated with simultaneous injection of air till hydrocarbon combustion occurred. The method suggests initial RF-EM treatment of the bottom-hole zone for a period of 30-70 hours at 20-40 kW to attain temperatures of 120-150°C.

The earliest research work carried out on mathematically modeling was radial distribution of temperature around a dipole antenna placed in a reservoir rock formation of absorption coefficient 0.000792/cm as well as the resulting flow rate based on increasing input power (5 to 320 kW) and

frequency (60 Hz to 20 GHz)⁷⁹. The results showed that flow rate can be expected to double within four weeks of radiation heating. Also at a modest power input of 20kW, 50% to 300% rate increase may be possible depending on the power absorption coefficient.

Researchers in IIT Research Institute conceived a radio frequency based dielectric heating technique for extraction of oil from shale, tar sands and other hydrocarbonaceous deposits which was granted a patent after initial lab confirmation^{80,81}. The technique made use of a transmission line approach for dielectric heating using special electrode pattern inserted into bore holes in the target resource. The electrode array arranged in a basic triplate line configuration was predicted to offer nearly uniform volumetric heating of the resource enclosed in the array. Theoretical analysis predicted that the enclosed electric fields are essentially uniform except near and beyond the edges of the inner electrode. Also when the excitation arrangement was such that the RF voltage was connected to the centre row of electrodes with the outer row being maintained at ground potential and by maintaining the proper line geometry, virtually all the RF energy could be contained within the precise volume of the triplate line with essentially no RF heating of adjacent material⁸². Such a configuration would thus prevent leakage fields. The electrode arrangement is depicted below in figure 2-13.

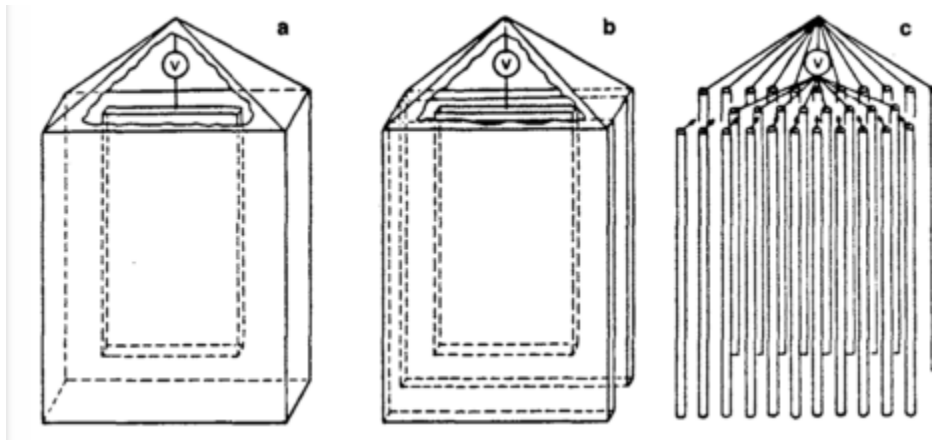


Figure 2-17. Triplate electrode configuration (a) fully shielded triplate, (b) triplate line open side equivalent, (c) cylindrical conductor array equivalent adapted from⁸¹.

Lab experiments on core samples obtained from Utah tar sands were conducted to establish technical feasibility of this method. RF heating using the triplate electrode arrangement was carried out on 300 kg of Asphalt Ridge oil sands and it was heated to 150°C. Sodium orthosilicate surfactant solution was heated and injected as a fluid replacement technique to recover bitumen. About 84% of the total bitumen in the tar sands as recovered using this method, however it was

reported in the paper that using large quantities of heated surfactant solution would prove to be expensive as opposed to gravity drive with or without autogenously developed gas pressure⁸³. Field experiments were carried out on 25 m³ of the tar sands volume with electrode holes drilled 6 m into the deposit. RF input power varied between 40 and 75 kW and average deposit temperatures of about 120 and 200°C were achieved. Tar sands initially behaved like high loss materials when water was present, however as temperature increases, loss tangent decreases to a value of less than 0.1 as moisture is evaporated. To accommodate for the changes in the power absorption properties of the deposit, the frequency of applied RF power was changed from an initial value of 2.3 MHz to 13.56 MHz. Temperature measurements during heating indicated that heating was uniform and in good agreement with earlier computer predictions. The total bitumen recovered from the experiment was about 336 gallons or 35% recovery at the end of 20 days of operation which indicated that 60 to 70 % of the total bitumen could be recovered in 6 months which were encouraging results.

McPerson⁸⁴ conceptualised an electromagnetic flood (EMF) process and developed a first order numerical model to examine it. They proposed installing horizontal wells attached to high frequency power source which would generate electromagnetic wave travelling from the source horizontally into the payzone area. Athabasca oil sands were considered as the sample medium and energy input was 250 kHz and 2MW. The power was applied to payzone section by a series of upper and lower electrode well pairs having a vertical separation of 20 m, with the length of the well, being 100 m long. Similarly five electrode well pairs were modeled. After approximately 6 months it was seen that the production per electrode well pair was risen to about 70 bbls/day. By the end of 2 years the production increased to 200 bbls/day.

Fanchi⁸⁵ performed numerical simulation of reservoir heating using EM irradiation as a heating stimulation tool to assess the feasibility of the method for both sandstone and carbonate reservoirs. In the design of simulation, the properties of radiofrequency generator and waveguide, and electrical conductivity of reservoir fluid and reservoir depths were considered. He concluded that EM power attenuates exponentially in a linear, homogeneous, dielectric medium. The developed algorithm of the simulation worked nicely for hypothetical reservoirs such as oil-bearing sandstone reservoir with connate water and oil-bearing carbonate reservoir. The results of sandstone and carbonate reservoirs showed similar behavior, i.e., with an increase in electrical conductivity, the near-wellbore temperature increases. He noted that EM energy was absorbed by few feet of

wellbore even at low electrical conductivity. He also reported that algorithm results are especially sensitive to input data such as electrical conductivity, water saturation, and relative electric permittivity. Finally, he concluded that EM heating process appears to be most applicable as either a well stimulation technique or a mobility enhancing process.

Kasevich et al. ⁸⁶ studied the heating characteristics of diatomaceous earth using different input powers at 50.55 MHz and 1 kW, as well as at 144 MHz and 200 W. Temperature rose to 150°C. An in situ borehole RF Antenna at a depth of 620 ft was implemented at Texaco oil recovery site in Bakersfield California at pilot scale in a heavy oil reservoir. Input power was supplied at 13.56 MHz and 25 kW. The temperature rise was observed to be 120°C in 40 hours of heating.

Attempts of carrying out electromagnetic heating on tar sands of Ugnu in Alaska were also conducted in 1991 ⁸⁷. One of the issue in using thermal methods in this region was the presence of a large permafrost region which reduced effective heat conduction through the tar sands. Using electromagnetic heating using downhole horizontal wells were studied for more efficient heating. Numerical simulations showed that 40% of the oil in place could be recovered using EM heating through horizontal wells. Also, with 50% increase of electrical power the oil production would increase by 125%.

Chakma and Jha ⁸⁸ presented a study on EM heating of scaled thin heavy oil reservoir pay zones. They also studied the combination of EM heating and gas injection with horizontal wells and reported that higher EM frequencies provide faster heating rate and can overcome problems associated with the discontinuity of the media through which EM waves must propagate. They stated that heat loss can be minimized with the use of higher frequencies and it is not necessary to heat the entire pay zone for moderately heavy oil reservoirs (less than 1000 mPa.s). The frequency of the EM source affected, i.e., for 5 MHz, 10 MHz, and 20 MHz frequencies, the overall recovery went up to 29%, 32%, and 37% of the original oil in place (OOIP), respectively. They observed oil recoveries as high as 45% of OOIP using EM heating and gas injection compared to primary recovery rates of less than 5%.

Downhole electrical heating in Venezuela fields was simulated for possible application of this method. Ovalles et al. ⁸⁹ carried out a case study on downhole dielectric heating for three conceptual reservoirs in Venezuela with three kinds of crude oils [medium (24°API), heavy (11°API) and extra-heavy crude oil (7.7°API)]. They reported that radiofrequency can recover 86% oil when the reservoir is heated with 140 MHz radiofrequency at 50 kW over 10 years of

period. Gasbarri et al. ⁹⁰ also studied the effect of electrical heating of bottom-hole on production and recovery factor of extra-heavy Orinoco Oil Belt reservoirs. They carried out numerical simulations and analysis of influential parameters of horizontal wells with different crude oils of 8.1, 10, 12, and 15°API gravity. On the basis of the simulation results, they concluded that EM heating process can increase the oil recovery rate up to 60%.

Carrizales et al. ⁹¹ developed a model for single-phase flow to calculate the temperature distribution and the productivity improvement when an EM heating source such as an antenna is placed in a well. Both counter and co-current flow with respect to fluid flow and EM energy flow were considered. Their studies concluded that co-current flow results in better productivity of oil as compared to counter current flow and their findings also suggest that EM heating is better than resistive heating. Later on, they developed a multiphase, two dimensional radial model that describes the three phase flow of water, oil and steam and heat flow in a reservoir ⁹². A single well was used to locate the EM source and also to produce oil. They used Lagrange-quadratic finite elements in the environment provided by COMSOL Multiphysics software and applied the model on different reservoir types to simulate EM heating method. The simulation results showed that, after 3 years heating, oil recovery by EM heating reached 18% whereas only 2% recovery was obtained by cyclic steam stimulation. Lastly, simulations were carried out for an extra heavy oil reservoir with an initial viscosity of 12,115 cP and 7°API gravity at 100°F. For this type of extra heavy oil reservoir, EM heating produced more than 63% of cumulative oil compared to cyclic steam stimulation confirming that EM heating gives better results than the other conventional heating processes. They also reported that energy consumption is very small in the EM heating process.

Comparative studies were also performed for steam injection methods other than SAGD and EM heating methods. To present a comparative overview of these two methods Das ⁹³ studied the EM heating in viscous oil reservoir. He described the advantages and disadvantages of EM heating over steam injection and reported that heat penetration is less in the case of EM heating over steam-based heating, and that volumetric sweep efficiency can be improved by EM heating in the low permeability area whereas fluid displacement technique might not be effective. He also carried out simulation of EM heating for viscous oil reservoir using CMG STARS thermal simulator and concluded that most heating takes place near the electrode area.

Hascakir et al. ^{94,95} performed experimental and numerical studies to measure the upgrading capability of electrical heating in the presence of iron-micro-particles. Their retort experiments showed that the viscosities of two different crude oils can be reduced 86% and 63% after addition of 0.5% iron powder. They used these results to construct a field scale model and defined the economic limits of the process. Hascakir et al. ⁹⁶ also conducted microwave experiments with three crude oil samples in a sand pack. Results indicated that 60% water saturation generates more temperature than 40% and 20% cases. They reported that higher initial water saturation shows higher recovery by microwave heating. They also examined the effect of initial wettability of the sample on oil recovery by EM heating method and showed that water wet and mixed wet systems give better results than oil wet system. Effect of heating time on oil production was also tested in this work. It was observed that with increasing heating time oil production also increases and high porosity and permeability also enhance the oil recovery.

Davletbaev et al. ⁷⁸ discussed the improvement of recovery efficiency of heavy oil/bitumen by radiofrequency and EM heating methods. They analysed the mechanism and dynamics of the radiofrequency and EM heating for several field scale applications in Russia. According to their simulation results, bottom-hole temperature and heat/mass transfer effects in reservoir can be controlled by setting output performance of RF generator and by the difference between bottom-hole and reservoir pressure. Mathematical model results showed that higher water cuts (>30%) are possible with electric heating. It was also reported that paraffin deposition can be controlled as RF-EM energy was lost along the wellbore during heating.

Godard et al. ⁹⁷ discussed development of a downhole Radio Frequency generator composed of triodes. An antenna was added to form a complete assembly. The optimization of this device concerned the impedance adaptation between generator and the antenna and the impedance of the antenna depended on the electrical characteristics of the reservoir which is in turn dependent on the water. Their studies developed solution to keep an optimum conversion ratio from high frequency electrical energy to heat.

Peraser et al., ⁹⁸ carried out computational modelling to investigate the effect of EM power levels and frequency on heat penetration into reservoir as well as its temperature and oil production for heavy oil reservoirs in Alaska. An axisymmetric 2-D model was built and the results showed that with the use of EM heating, the oil production rate can be increased to more than 200%. Since it is a continuous process as opposed to CSS, oil production can be continuous without the need to

shut in the well. Also for the same amount of input energy, EM heating recovers more oil than CSS.

Bogdanov et al.⁹⁹ carried out computation modelling to determine the application of optimal frequency conditions including a known range of initial and operational conditions and oil viscosities typical for making heavy oil mobile. Making use of the vertical antenna model the model study was begun with the determination of minimal energy loss at initial conditions i.e. optimal frequency. The results showed that initial optimal frequency for vertical antenna lies within the interval of 53 to 61 MHz which is practically independent of antenna position.

A consortium of Harris Corporation, Nexen Energy ULC, Suncor Energy, Inc., Devon Canada Corporation, and Alberta's Climate Change and Emissions Management Corporation (CCEMC) are developing Effective Solvent Extraction Incorporating Electro-magnetic Heating (ESEIEH™)^{100,101}. The ESEIEH process integrates electromagnetic heating with solvents to reduce energy consumption and to eliminate the need for added water (steam) when compared to SAGD. Further to the operational benefits are the reduction of surface facilities and the option to economically export undiluted bitumen without the added cost of diluent recovery units. Utilizing Harris' Coupled Electromagnetic Reservoir Simulator (CEMRS), the ESEIEH process is first simulated as a single well pair as can be seen in figure 2-18. Applying a field scheduling tool, the resulting reservoir run is then duplicated in time until sufficient wells are in place to establish a sustained field level oil production rate of 10,000 bpd. The technology, which began development in 2010 and recently commenced the second technical demonstration phase in July 2015 is expected to be economically viable in a sustained sub-\$60 WTI (USD) oil price environment.

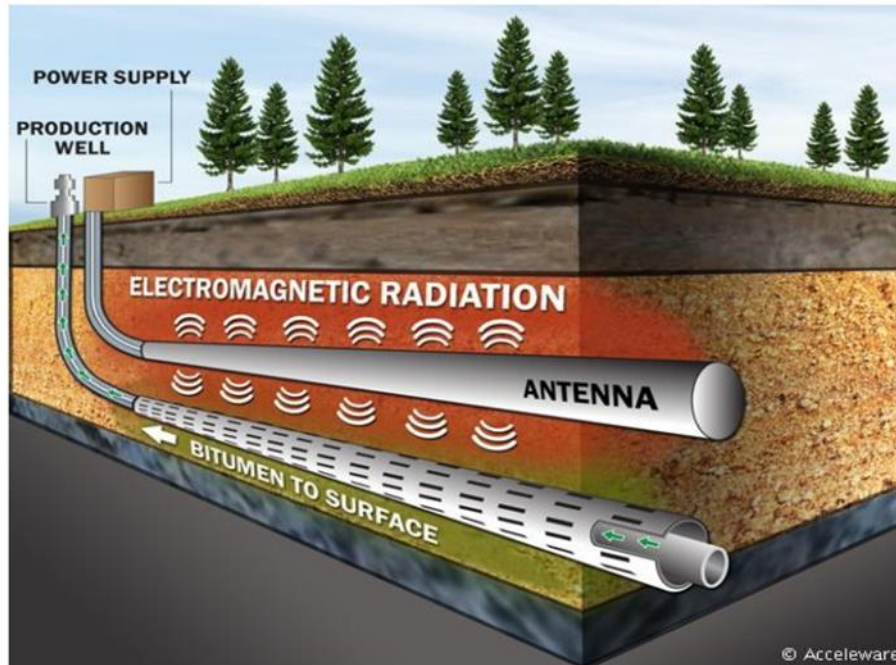


Figure 2-18. Artist's illustration of radiofrequency heating process in oil sands reservoir¹⁰⁴.

Based on all the studies carried out via dielectric heating it can be concluded that heating the reservoir at radio frequency has shown promising results however has had some drawbacks due to the following reasons:

1. Exponential decay of heating away from the antenna surface.
2. Discontinuation of heating process as the properties of oil sands change after certain temperatures are attained, requiring operational strategies which could help in continuing the heating process following the changes.
3. Requirement of adequate simulation models which have considered the dynamic electrical behaviour of the reservoir.

Table 2-8. Dielectric Heating of Oil Reservoirs –Field Tests

Year	Reference	Region	Type of Reservoir	Input Electrical Energy	Electrode Configuration	Temperature Attained and Oil Recovered	Production Problems
1969	¹⁰²	Ishimbayneft	Heavy Oil	63 kW at 13.56 MHz	RF coaxial Cable in a production well	Increase of 40°C within 5 days of continuous treatment.	
1969	¹⁰²	Yultimirovskoye	Bitumen	20 kW, 30 kW and 60 kW	RF heating between two wells spaced 5 m apart	310°C obtained within 6 days of operation	Melting of fluorplatic collar
1969	¹⁰²	Mordovo-Karmal'skaya	Bitumen	20-40 kW followed by in situ combustion	5 wells exposed to RF EM heating	120 to 150 °C	
1981	⁸³	Asphalt Ridge, Utah	Tar Sands	40 and 75 kW, 2.3 MHz to 13.56 MHz	Triplate electrode configuration	120°C initially and later 200°C. 336 gallons in 20 days indicating 35% recovery which meant 60 to 70% recovery in 6 months.	Inadequate roof support for electrode arrangement
1992	⁸⁶	Bakersfield, California	Heavy Oil	13.56 MHz, 25 kW	RF Antenna	120°C in 40 hours	Required proper design of equipment for suitable down hole operation
2012	¹⁰³	North Steepbank Mine, Alberta	Rich grade oil sands	6.78 Hz, Initial power 28 kW, then 49 kW and later lowered to 12 kW	Antenna inserted into a horizontal well bore	Maximum formation temperature observed was 127°C observed 1m below the antenna	

Table 2-9. Dielectric Heating of Oil Reservoirs – Numerical Modeling and Lab Tests

Year	Reference	Type of Study	Subject of Study	Oil Sample Specifications	Input Electrical Energy	Electrode Configuration	Parameters modeled/measured	Results
1976	⁷⁹	Mathematical Modeling	2D Wellbore Radial model	Reservoir rock with absorption coefficient .000792/cm	60 Hz to 20 GHz, 5 to 320 kW	Dipole Antenna	Flow rate and temperature distribution as a function of input power	Flow rate can be expected to double within four weeks of radiation heating. Also at a modest power input of 50% to 300% rate increase may be possible depending on the power absorption coefficient.
1986	⁸³	Lab Test	Gravity drainage based recovery with and without gas pressure	Asphalt Ridge Tar Sands	Thermal Energy via conduction	Steel reactor 4.75 cm diameter and 30 to 150 cm length	Temperature rise, recovery rate	50 % bitumen recovered when temperature maintained at 150°C for 4 months, under nitrogen pressure of 70 kPa
			Autogenously developed gas drive to bitumen recovery		Thermal energy via conduction	Steel reactor 4.75 cm diameter and 30 to 150 cm length		Recovery of bitumen started at 175°C but the rate of recovery increased significantly beyond 250 °C
			Triplate electrode based RF heating with surfactant based solution drive for bitumen recovery		RF energy with surfactant solution drive	300 kg oil sands packed into 90 cm stainless steel reactor	84 % recovery observed when temperature was increased to 150°C	
1985	⁸⁴	Numerical Modelling	Conceptualized design of electromagnetic flood process and development of first order numerical model	Athabasca oil sands (1.6% water with 13.4% bitumen)	250 kHz, 2 MW	Five pairs of horizontal 100 m long upper and lower electrode pairs separated at 20 m by payzone	Temperature rise and recovery rate	70 bbl/day in 6 months and 200 bbl/day in 2 years

Year	Reference	Type of Study	Subject of Study	Oil Sample Specifications	Input Electrical Energy	Electrode Configuration	Parameters modeled/measured	Results
1990	⁸⁵	Numerical Modelling	Temperature distribution around well during electromagnetic irradiation by wells	Oil bearing sandstones and oil bearing carbonate reservoirs	0.3 to 2 GHz, 30 to 60 kW		Power attenuation and temperature distribution	Algorithm developed EM irradiation in sandstone and carbonate reservoir. Algorithm was sensitive to input data such as electrical conductivity, water saturation and electrical permittivity.
1991	⁸⁷	Numerical modelling	Recovery rate increase with power input when EM heating is carried out using horizontal wells	Ugnu Tar Sands	12 kW/m	Horizontal wells 300 m long and 22 cm diameter	Recovery rate	40% of the oil in place could be recovered. With 50% increase of electrical power the oil production would increase by 125%.
1994	⁸⁶	Lab Test	Temperature Rise at different input power	Diatomaceous Earth	50.55 MHz, 1 kW and 144 MHz and 200 W	Electric monopole antenna in a 55 gallon drum of sample	Temperature rise	Temperature rose to 150°C
1999	⁸⁸	Lab Test	Recovery of oil from thin reservoirs using EM Heating and gas injection	Heavy Oil (1000 mPa.s)	5 MHz, 10 MHz, and 20 MHz	Horizontal electrodes 100 mm long placed in a 20 by 20 by 10 cm box	Recovery rate	Overall recovery went up to 29%, 32%, and 37% corresponding to 5 MHz, 10 MHz, and 20 MHz frequencies
2002	⁸⁹	Numerical Simulation with experimental validation	Dielectric Heating based oil recovery of Venezuelan reservoirs	Medium (24°API), heavy (11°API) and extra-heavy crude oil (7.7°API)	140 MHz, 50 kW	300 ml diameter and 10 cm long cylindrical flask irradiated with microwave energy	Recovery of oil	86% recovery over a 10 year period
2008	⁹¹	Mathematical Modelling	Counter current and	Heavy Oil (11°API)	140 MHz, 915 MHz, 20 kW, 63 kW,	Antenna and Producer in the same well in	Temperature distribution and	Co-current flow gives better production rate than counter current flow. EM heating is

Year	Reference	Type of Study	Subject of Study	Oil Sample Specifications	Input Electrical Energy	Electrode Configuration	Parameters modeled/measured	Results
			co-current EM Heating		150 kW	counter current configuration and antenna and producer in adjacent wells in co-current configuration	Productivity improvement	more efficient than resistive heating
2008	⁹³	Numerical Simulation	Electromagnetic heating of few viscous oil reservoirs	Viscous oil (3500 cP at reservoir condition)		Reservoir 1800ft long, 575 ft wide and 29ft thick with a pair of 1500ft long horizontal wells placed near the two edges at a distance of 500ft from each other. These	Temperature and production rate	100 bpd after 3 years of heating and temperature reached to 90 to 100°C
2008	⁹⁴	Lab scale experiment and numerical simulation	Electrical heating of oil shale by enhancing conductivity using iron powders	Oil Shale	1000W	Stainless steel cylinder 10 cm in diameter and 20 cm in height wrapped with a band heater	Temperature and Oil Production rate	Viscosities of two different crude oils can be reduced 86% and 63% after addition of 0.5% iron powder.
2009	⁹⁶	Lab scale experiment	Effect of microwave for oil production and temperature rise	Heavy Oil (9.5°API, 12°API, and 18°API)	2.45 GHz, 1400 W	Graphite core holder 5.2 cm diameter and 8.5 cm height	Recovery rate and temperature increase	Up to 80% oil recovery depending on rock properties and temperature rose to 170°C
2010	⁹²	Numerical simulation	Development of 2D multiphase radial model for EM heating of thin pay zones, low	Extra Heavy Oil (7°API)	915 MHz, 70 kW	Cylindrical grid (50x1x32) with an injector/producer located in the center	Recovery rate	Oil recovery by EM heating reached 18% in 3 years as compared to 2% recovery obtained by cyclic steam stimulation. Also energy consumption is low as compared to CSS.

Year	Reference	Type of Study	Subject of Study	Oil Sample Specifications	Input Electrical Energy	Electrode Configuration	Parameters modeled/measured	Results
			permeability and extra heavy oil reservoirs					
2010	⁷⁸	Numerical Simulation	2D modelling of RF –EM Heating of heavy oil	Heavy oil of different viscosities	40 kW and 60 kW	RF heating system through a well bore	Temperature distributions	Bottom-hole temperature and heat/mass transfer effects in the reservoir can be controlled by setting the output performance of the RF generator and by the difference between the reservoir and bottom-hole pressure.
2011	⁹⁷	Numerical Simulation	Conceptual design and simulation of a downhole RF heater	Sand water mixture	10 MHz, 100 kW	Antenna based RF heating	Electric field and temperature distribution	The electrical aspects and constraints were well identified for a downhole compact integrated dielectric heating device.
2011	⁹⁰	Numerical Simulation	Dielectric heating of oil	Heavy oil (8.1, 10, 12 and 15°API)		Horizontal well in reservoir which is 4000 ft in length and breadth.	Pressures, temperatures, viscosities, production rate, gas-oil ratio.	Oil recovery rate increases to 60%
2013	⁹⁸	Computational modeling	2D Radial well model of electromagnetic heating of oil reservoirs	Alaskan Heavy Oil	140 MHz to 2450 MHz, 70 KW	Antenna based heating	EM power levels and frequency on heat penetration into reservoir, temperature and oil production	Heavy oil production rates increased by 200% using only moderate power levels and continuous oil production could be sustained without any need to shut the well for heat dissipation.
2014	⁹⁹	Computational modeling	2D axisymmetric and 3D coupled model between	Heavy Oil	4 to 78 MHz, 300 kW	Two antennas vertically positioned	Influence of well pattern, spacing and orientation on the efficiency and	Initial optimal frequency for vertical antenna lies within the interval of 53 to 61 MHz which is

Year	Reference	Type of Study	Subject of Study	Oil Sample Specifications	Input Electrical Energy	Electrode Configuration	Parameters modeled/measured	Results
			dedicated reservoir and multi-physics simulators				application limits of oil production	practically independent of antenna position.
2012	¹⁰³	Reservoir simulation using CEMRS and validating with field test		Rich Grade oil sands	6.78 MHz, 49 kW for 60 days	Antenna inserted into a horizontal well.	Temperature profile	Maximum temperature was 130°C at radius 2.5 m and 35°C at radius 5m respectively. Heating above the initial formation temperature extended to a radial distance of 7m in this time period. Predicted that temperature distributions would be best if separation between injector and producer would be 5m.
2015	¹⁰⁴	Reservoir simulation using AxHeat software		Oil Sands	10 kHz to 100 MHz,	Two horizontal wells. 800m antenna, 5m above producer well.	Temperature profile, oil production rate, energy consumption	Energy consumption is 4 GJ/m ³ as compared to 9 GJ/m ³ for SAGD.
					20 MW	Single horizontal well		60% recovery achieved in 2 years. Energy/oil ratio is 20

2.4 Conclusions & Future Work

While electrical heating has several overriding advantages over thermal methods it also has certain operational disadvantages of its own. Some of which being, uneven distribution of electrical energy in the targeted regions of the reservoir due to reduction of electromagnetic radiation intensity from the electrode/antenna in high frequency radiation heating ¹⁰⁴; over dependence on water in the reservoir for low frequency ohmic heating ¹⁰⁵; excessive heating at electrode/antenna surfaces for both high and low frequency heating processes as well as trouble keeping up with the dynamic heating process often leading to overheating and equipment failure ³⁶. For perfecting the art of carrying out volumetric heating of oil sands it is essential that the electrical energy be evenly distributed in the reservoir in the region between the electrodes so that all portions heat up to the same temperatures uniformly. Thus it is essential to adjust the input power and the frequency of electrical energy such that maximum heat generation occurs in the reservoir and water is not the only heat generating source. Bitumen being the major component of oil sands and also the product of interest should interact with the electrical energy and be one of the reasons of volumetric heat generation apart from water.

All of these issues arise from a lack of understanding of the electrical heat generation mechanisms in oil sands and the dynamic nature of their variation with increasing temperatures in the reservoir. Previous studies in this direction determined complex permittivity, conductivity and loss tangent of oil sands as a function of temperature and composition ^{32,33}. A clear understanding in this fundamental direction would influence implementation of optimized operational strategies throughout the heating and production cycle for an efficient process. It would influence implementation of more realistic reservoir simulations and design of efficient electrode/antenna systems for delivering electrical energy to the reservoir.

Thus the main objective of this research is to address some or many of the mentioned drawbacks of the current process through an integrated understanding of the reasons of electrical heating patterns and behavior of oil sands found in the mutual arrangement of their components and overall composition which changes with temperature. This would help in shedding light on the operational strategies that could be undertaken to reduce the issues concerning overdependence on water, overheating of electrode/antenna surfaces and facilitation of continuous heating process following the dynamic changes in the reservoir to make electrical heating an efficient reality. The intention

is to fully implement electrical heating technique for extracting bitumen from oil sands so that currently used water based thermal methods can be reduced or eliminated.

2.5 References

- (1) Lupi, S.; Forzan, M.; Aliferov, A. *Induction and Direct Resistance Heating: Theory and Numerical Modeling*; Springer, 2015.
- (2) Sastry, S. K. Overview of Ohmic Heating. In *Ohmic Heating in Food processing*; Ramaswamy, H. S., Marcotte, M., Sastry, S., Abdelrahim, K., Eds.; CRC Press, Taylor & Francis Group, 2014.
- (3) Haimbaugh, R. E. Theory of Heating by Induction. In *Practical Induction Heat Treating*; ASM International, 2001; pp 5–18.
- (4) Foll, H. Electronic Materials http://www.tf.uni-kiel.de/matwis/amat/elmat_en/index.html (accessed Jul 1, 2016).
- (5) Williams, G.; Thomas, D. K. Phenomenological and Molecular Theories of Dielectric and Electrical Relaxation of Materials. *Novocontrol Appl. Note Dielectr.* **1998**, *3*, 1–29.
- (6) Grinstead, L. Dielectric Heating by the Radio Frequency Method. *J. Br. Inst. Radio Eng.* **1945**, 128–145.
- (7) Dakin, T. W.; Auxier, R. . Dielectric Heating – Application of Dielectric Measurements to Cellulose and Cellulose Filled Phenolic Laminating Materials. *Ind. Eng. Chem.* **1945**, *37* (3), 268–275.
- (8) Scott, G. W. The Role of Frequency in Industrial Dielectric Heating. *Electr. Eng.* **1945**, *64* (8), 558–562.
- (9) Pinder, K. Induction and Dielectric Heating. *Electr. Eng.* **1947**, *66* (2), 149–160.
- (10) Duryee, L. M. Some Economic Aspects of Radio-Frequency Heating. *Trans. Am. Inst. Electr. Eng.* **1948**, *67* (1), 105–112.
- (11) Hulls, P.; Shute, R. Dielectric Heating in Industry Application of Radio Frequency and Microwaves. *IEE Proc. A - Phys. Sci. Meas. Instrumentation, Manag. Educ. - Rev.* **1981**,

128 (9), 583–588.

- (12) B.Awuah, G.; Ramaswamy, H. S.; Tang, J. *Radio-Frequency Heating in Food Processing, Principals and Applications*; CRC Press, Taylor & Francis Group, 2015.
- (13) Zhao, Y.; Park, J. A. E. W.; Wells, J. H. Using Capacitive (Radio Frequency) Dielectric Heating in Food Processing and Preservation - A Review. *J. Food Process Eng.* **1999**, 23 (860), 25–55.
- (14) Bientinesi, M.; Scali, C.; Petarca, L. Radio Frequency Heating for Oil Recovery and Soil Remediation. *IFAC-PapersOnLine* **2015**, 48 (8), 1198–1203.
- (15) Environmental Protection Agency (EPA). *A Citizen 's Guide to In Situ Thermal Treatment*; 2012.
- (16) Environmental Protection Agency (EPA). *Engineering Paper: In Situ Thermal Treatment Technologies: Lessons Learned*; 2014.
- (17) Bera, A.; Babadagli, T. Status of Electromagnetic Heating for Enhanced Heavy Oil/bitumen Recovery and Future Prospects: A Review. *Appl. Energy* **2015**, 151, 206–226.
- (18) Masliyah, J.; Czarnecki, J.; Xu, Z. Physical and Chemical Properties of Oil Sands. In *Handbook on Theory and Practice of Bitumen Recovery from Athabasca Oil Sands. Vol. 1: Theoretical Basis.*; Kingsley Knowledge Publishing, 2011.
- (19) Masson, J. F.; Polomark, G. M. Bitumen Microstructure by Modulated Differential Scanning Calorimetry. *Thermochim. Acta* **2001**, 374 (2), 105–114.
- (20) Takamura, K. Microscopic Structure of Athabasca Oil Sand. *Can. J. Chem. Eng.* **1982**, 60, 538–545.
- (21) Lesmes, D. P.; Friedman, S. P. Relationships between the Electrical and Hydrogeological Properties of Rocks and Soils: In *Hydrogeophysics*; Springer, 2005; pp 87–128.
- (22) Lesmes, D. P.; Morgan, F. D. Dielectric Spectroscopy of Sedimentary Rocks. *J. Geophys. Res.* **2001**, 106 (B7), 13329.

- (23) Chelidze, T. L.; Gueguen, Y. Electrical Spectroscopy of Porous Rocks: A review—I. Theoretical Models. *Geophys. J. Int.* **1999**, *137* (1), 1–15.
- (24) Levitskaya, T. M.; Sternberg, B. K. Polarization Processes in Rocks: 1. Complex Dielectric Permittivity Method. *Radio Sci.* **1996**, *31* (4), 781.
- (25) Olhoeft, G. R. Electrical Properties of Rocks. *Phys. Chem. Rocks Miner.* **1976**, 262–278.
- (26) Chelidze, T. L.; Gueguen, Y.; Ruffet, C. Electrical Spectroscopy of Porous Rocks: A review—II. Experimental Results and Interpretation. *Geophys. J. Int.* **1999**, *137* (1), 16–34.
- (27) Olhoeft, G. R. Low-frequency Electrical Properties. *Geophysics* **1985**, *50* (12), 2492–2503.
- (28) Revil, A.; Eppehimer, J. D.; Skold, M.; Karaoulis, M.; Godinez, L.; Prasad, M. Low-Frequency Complex Conductivity of Sandy and Clayey Materials. *J. Colloid Interface Sci.* **2013**, *398* (November 2015), 193–209.
- (29) Sen, P. N.; Chew, W. C. The Frequency Dependent Dielectric and Conductivity Response of Sedimentary Rocks. *J. Microw. Power* **1983**, *18* (1), 97.
- (30) Goual, L. Impedance Spectroscopy of Petroleum Fluids at Low Frequency Impedance Spectroscopy of Petroleum Fluids at Low Frequency. *Energy & Fuels* **2009**, *23* (4), 2090–2094.
- (31) Kremer, F.; Schönhals, A. Analysis of Dielectric Spectra. In *Broadband Dielectric Spectroscopy*; Springer-Verlag Berlin Heidelberg New York, 2003.
- (32) Chute, F. S.; Vermeulen, F. E.; Cervenán, M. R.; McVea, F. J. Electrical Properties of Athabasca Oil Sands. *Can. J. Earth Sci.* **1979**, *16* (10), 2009–2021.
- (33) Das, M.; Thapar, R.; Rajeshwar, K.; DuBow, J. Thermophysical Characterization of Oil Sands: 3. Electrical Properties. *Can. J. Earth Sci.* **1981**, *18* (4), 742–750.
- (34) Bruggeman, V. D. A. G. Calculation of Various Physics Constants in Heterogenous Substances I Dielectricity Constants and Conductivity of Mixed Bodies from Isotropic

- Substances. *Ann. Phys.* **1935**, 24 (7), 636–664.
- (35) Hanai, T.; Koizumi, N.; Goto, R. Dielectric Constant of Emulsions. *Bulletin of the Institute for Chemical Research, Kyoto University*. 1962, pp 240–271.
- (36) Chute, F. S.; Vermeulen, F. E. Electrical Heating of Reservoirs. In *AOSTRA Technical Handbook on Oil Sands, Bitumen and Heavy Oils*; Hepler, L. G., Hsi, C., Eds.; Alberta Oil Sands Technology and Research Authority, 1991; pp 337–373.
- (37) Hiebert, A. D.; Vermeulen, F. E.; Chute, F. S.; Capjack, C. E. Numerical Simulation Results for the Electrical Heating of Athabasca Oil-Sand Formations. *SPE Reserv. Eng.* **1986**, 1 (01), 76–84.
- (38) Mcqueen, B. Y. G.; Parman, D.; Williams, H. A Case Study of Enhanced Oil Recovery of Shallow Wells. *Tyco Thermal Controls IEEE Industry Applications Magazine*. 2012, pp 18–25.
- (39) Sandberg, C. Benefits of Heating Heavy Oil with Medium-Voltage Mineral Insulated Cables. *Oil & Gas Engineering*. 2015, pp 8–9.
- (40) Hale, A.; Sandberg, C.; Kovsky, A. History and Application of Resistance Electrical Heating in Downhole Oil Field Applications. In *SPE Western Regional & AAPG Pacific Section Meeting 2013 Joint Technical Conference*; 19-25 April 2015, Monterey California, USA; pp 1–10.
- (41) Sandberg, C.; Thomas, K.; Hale, A. Advances in Electrical Heating Technology for Heavy Oil Production. In *SPE Heavy Oil Conference*; 10-12 June 2014, Alberta Canada; pp 1–6.
- (42) Flock, D. L.; Tharin, J. Unconventional Methods of Recovery of Bitumen and Related Research Areas Particular to the Oil Sands of Alberta. *J. Can. Pet. Technol.* **1975**, 14 (3), 17–27.
- (43) Gill, H. The Electrothermic System for Enhancing Oil Recovery. In *First International Conference on the Future of Heavy Crude and Tar Sands*; New York City: McGraw-Hill Book Co. Inc., 1979; pp 469–473.

- (44) SPE International. Electromagnetic heating of oil
http://petrowiki.org/Electromagnetic_heating_of_oil#cite_note-r4-4 (accessed Jun 1, 2016).
- (45) Pizarro, J. O. S.; Trevisan, O. V. Electric Heating of Oil Reservoirs. Numerical Simulation and Field Test Results. *J. Pet. Technol.* **1990**, 1320–1326.
- (46) Rice, S. A.; Kok, A. L.; Neate, C. J. A Test of the Electric Heating Process As a Means of Stimulating the Productivity of an Oil Well in the Schoonebeek Field. *Pet. Soc. CIM* **1992**, *4*, 1–16.
- (47) Crowson, F. L.; Gill, W. G. Method and Apparatus for Secondary Recovery of Oil. US3605888, 1971.
- (48) Kern, L. R. Method of Producing Bitumen from a Subterranean Tar Sand Formation. US3,848,671, 1974.
- (49) Hagedorn, A. R. Oil Recovery by Combination Steam Stimulation and Electrical Heating. US3,946,809, 1976.
- (50) Pritchett, W. C. Method Ad Apparatus for Producing Fluid by Varying Current Flow Through Subterranean Source Formation. US3,948,319, 1976.
- (51) Davison, R. J. Electromagnetic Stimulation of Lloydminster Heavy Oil Reservoirs: Field Test Results. *J. Can. Pet. Technol.* **1995**, *34* (1), 15–24.
- (52) Newbold, F. R.; Perkins, T. K. Wellbore Transmission of Electrical Power. *J. Can. Pet. Technol.* **1978**, *3* (3), 39–53.
- (53) El-Feky, S. A. Theoretical and Experimental Investigation of Oil Recovery by the Electrothermic Technique, University of Missouri, Rolla, 1977.
- (54) Vermeulen, F. E.; Chute, F. S. Electrical Extraction of Oil From Tar Sand. *IEEE Trans. Ind. Appl.* **1977**, *IA-13* (6), 604–607.
- (55) Todd, J. C.; Howell, E. P. Numerical Simulation Of In-Situ Electrical Heating To Increase Oil Mobility. *J. Can. Pet. Technol.* **1978**, *2* (1), 31–41.

- (56) Harvey, A. H.; Arnold, M. D.; El-Feky, S. A. Selective Electric Reservoir Heating. *J. Can. Pet. Technol.* **1979**, *18* (3), 47–57.
- (57) Towson, D. The Electric Preheat Recovery Process. In *Second International Conference on Heavy Crude and Tar Sand*; 7-17th February, 1982, Caracas, Venezuela, 1982; pp 1–10.
- (58) Killough, J. E.; Gonzalez, J. A. A Fully-Implicit Model for Electrically Enhanced Oil Recovery. In *61st Annual Technical Conference and Exhibition of the Society of Petroleum Engineers*; 5-8 October, 1986, New Orleans, USA, 1986; pp 1–16.
- (59) Wattenbarger, R. A.; McDougal, F. W. Oil Production Response To In Situ Electrical Resistance Heating (Erh). *J. Can. Pet. Technol.* **1988**, *6* (3), 45–50.
- (60) Vinsome, K.; McGee, B.; Vermeulen, F.; Chute, F. Electrical Heating. *J. Can. Pet. Technol.* **1994**, *33* (4), 29–36.
- (61) McGee, B. C. W.; Vermeulen, F. E.; Yu, L. Field Test of Electrical Heating with Horizontal and Vertical Wells. *J. Can. Pet. Technol.* **1999**, *38* (3), 46–53.
- (62) McGee, B. C. W.; Vermeulen, F. E. The Mechanisms of Electrical Heating for the Recovery of Bitumen from Oil Sands. *J. Can. Pet. Technol.* **2007**, *46* (1), 28–34.
- (63) Vermeulen, F. E.; McGee, B. C. W. In Situ Electromagnetic Heating for Hydrocarbon Recovery and Environmental Remediation. *J. Can. Pet. Technol.* **2000**, *39* (8), 25–30.
- (64) McGee, B. C. W. Electro-Thermal Pilot in the Athabasca Oil Sands: Theory versus Performance. In *Canadian International Petroleum Conference*; 17-19 June 2008, Calgary, Alberta Canada, 2008; Vol. 229, pp 47–54.
- (65) Fisher, S. T.; Fisher, C. B. Induction Heating of Underground Hydrocarbon Deposits. 3,989,107, 1976.
- (66) Fisher, S. T.; Fisher, C. B. Method for Induction Heating of Underground Hydrocarbon Deposits Using a Quasi Toroidal Conductor Envelope. 4,008,761, 1977.
- (67) Fisher, S. T. Processing of Solid Fossil-Fuel Deposits by Electrical Induction Heating.

- IEEE Trans. Ind. Electron. Control Instrum.* **1980**, IECI-27 (1), 19–26.
- (68) Chute, B. F. S. On the Electromagnetic Heating of Low Loss Materials Using Induction Coils. *Can. Electr. Eng. J.* **1981**, 6 (1), 20–28.
- (69) Vermeulen, F. E.; Chute, F. S. The Induction Heating of Fossil Fuels in-Situ by Electric and Magnetic Fields. *Can. Electr. Eng. J.* **1985**, 10 (4), 147–151.
- (70) Spencer, H. L.; Isted, R. E. Electrical Induction Heating of Heavy Oil Wells Using the Triflux System. 1998, pp 1–6.
- (71) Koolman, M.; Huber, N.; Diehl, D.; Wacker, B. Electromagnetic Heating Method To Improve Steam Assisted Gravity Drainage. In *SPE International Thermal Operations and Heavy Oil Symposium*; 20–23 October 2008, Calgary, Alberta, Canada, 2008; pp 1–12.
- (72) Wacker, B.; Helget, A.; Torlak, M.; Karmeileopardus, D.; Trautmann, B. Electromagnetic Heating for In-Situ Production of Heavy Oil and Bitumen Reservoirs. In *Canadian Unconventional Resources Conference*; 15–17 November 2011, Calgary, Alberta, Canada; pp 1–14.
- (73) Mustafina, D.; Koch, A.; Danov, V.; Sotskiy, S.; Ag, S. Mechanism of Heavy Oil Recovery Driven by Electromagnetic Inductive Heating. In *SPE Heavy Oil Conference Canada*; 11–13 June 2013, Calgary, Alberta, Canada, 2013; pp 1–9.
- (74) Fisher, S. T. Electrical Induction Heating for the Processing of Fossil Fuels. *Electron. Power* **1978**, 527–530.
- (75) Fisher, S. T. Solid Fossil Fuel Recovery by Electrical Induction Heating in Situ: A Proposal. *Resour. Recover. Conserv.* **1980**, 4, 363–368.
- (76) Ritchey, H. W. Radiation Heating. 2757738, 1956.
- (77) Haagensen, D. B. Sub-Surface Heating System. 3104711, 1963.
- (78) Davletbaev, A.; Kovaleva, L.; Babadagli, T. Heavy Oil and Bitumen Recovery Using Radiofrequency Electromagnetic Irradiation and Electrical Heating : Theoretical Analysis and Field Scale Observations. In *Canadian Unconventional Resources & International*

- Petroleum Conference*; 19–21 October 2010, Calgary, Alberta, Canada; pp 1–14.
- (79) Abernethy, E. R. Production Increase of Heavy Oils by Electromagnetic Heating. *J. Can. Pet. Technol.* **1976**, 3 (12), 91–97.
- (80) Bridges, J.; Taflove, A.; Snow, R. Method for In Situ Heat Processing of Hydrocarbonaceous Formations. 4140180, 1979.
- (81) Bridges, J.; Stresty, G.; Taflove, A.; Snow, R. Radio-Frequency Heating to Recover Oil from Utah Tar Sands. In *First Intl. Conference on the Future of Heavy Crude and Tar Sands*; New York City: McGraw-Hill Book Co. Inc., 1979; pp 396–409.
- (82) Carlson, R. D.; Blase, E. F.; Mclendon, T. R. *Development of the IIT Research Institute RF Heating Process for In Situ Oil Shale Tar Sand Fuel Extraction - An Overview*; 1981.
- (83) Sresty, G.; Dev, H.; Snow, R.; Bridges, J. Recovery of Bitumen From Tar Sand Deposits With the Radio Frequency Process. *SPE Reserv. Eng.* **1986**, 1 (1), 85–94.
- (84) McPherson, R. G.; Chute, F. S.; Vermeulen, F. E. Recovery of Athabasca Bitumen With the Electromagnetic Flood (Emf) Process. *J. Can. Pet. Technol.* **1985**, 24 (1), 44–51.
- (85) Fanchi, J. R. Feasibility of Reservoir Heating by Electromagnetic Irradiation. In *65th Annual Technical Conference and Exhibition of the Society of Petroleum Engineers*; 23-26 September, 1990, New Orleans, USA, 1990; pp 1–12.
- (86) Kasevich, R. S.; Price, S. L.; Faust, D. L.; Fontaine, M. F. Pilot Testing of a Radio Frequency Heating System for Enhanced Oil Recovery from Diatomaceous Earth. In *SPE 69th Annual Technical Conference and Exhibition*; 25-28 September 1994, New Orleans, USA, 1994; pp 105–119.
- (87) Wadadar, S. S.; Islam, M. R. Numerical Simulation of Electromagnetic Heating of Alaskan Tar Sands Using Horizontal Wells. *Pet. Soc. CIM AOSTRA* **1991**, 35, 1–14.
- (88) K. N. Jha, A. Chakma. Heavy-Oil Recovery from Thin Pay Zones by Electromagnetic Heating. *Energy Sources* **1999**, 21 (1-2), 63–73.
- (89) Ovalles, C.; Fonseca, A.; Lara, A.; Alvarado, V.; Urrecheaga, K.; Ranson, A.; Mendoza,

- H. Opportunities of Downhole Dielectric Heating in Venezuela: Three Case Studies Involving Medium Heavy and Extra-Heavy Crude Oil Reservoirs. In *SPE International Thermal Operations and Heavy Oil Symposium and International Horizontal Well Technology Conference held*; 4–7 November 2002, Calgary, Alberta, Canada; pp 1–10.
- (90) Gasbarri, S.; Diaz, A.; Guzman, M. Evaluation Of Electric Heating On Recovery Factors In Extra Heavy Oil Reservoirs Low-Medium Frequency Current Low Frequency Current High Frequency Current Resistive Inductive Microwave Ohmic Radio Frequency. In *SPE Heavy Oil Conference and Exhibition*; 12–14 December 2011, Kuwait City, Kuwait; pp 1–17.
- (91) Carrizales, M. a; Lake, L. W.; Johns, R. T. Production Improvement of Heavy-Oil Recovery by Using Electromagnetic Heating. In *SPE Annual Technical Conference and Exhibition*; 21–24 September 2008, Denver, Colorado, USA; pp 1–16.
- (92) Carrizales, M. A.; Lake, L. W.; Johns, R. T. Multiphase Fluid Flow Simulation of Heavy Oil Recovery by Electromagnetic Heating. In *SPE Improved Oil Recovery Symposium*; 24–28 April 2010, Tulsa, Oklahoma, USA; pp 568–580.
- (93) Das, S. Electro-Magnetic Heating in Viscous Oil Reservoir. In *SPE International Thermal Operations and Heavy Oil Symposium*; 20–23 October 2008, Calgary, Alberta, Canada; pp 1–11.
- (94) Hascakir, B.; Babadagli, T.; Akin, S. Experimental and Numerical Simulation of Oil Recovery from Oil Shales by Electrical Heating. *Energy & Fuels* **2008**, 22 (11), 3976–3985.
- (95) Hascakir, B.; Babadagli, T.; Akin, S. Field-Scale Analysis of Heavy-Oil Recovery by Electrical Heating. In *International Thermal Operations and Heavy Oil Symposium*; 20–23 October 2008, Calgary, Alberta, Canada; pp 131–142.
- (96) Hascakir, B.; Acar, C.; Akin, S. Microwave-Assisted Heavy Oil Production: An Experimental Approach. *Energy & Fuels* **2009**, 23 (18), 6033–6039.
- (97) Godard, A.; Rey-Bethbeder, F. Radio Frequency Heating , Oil Sand Recovery

- Improvement. In *SPE Heavy Oil Conference and Exhibition*; 12–14 December 2011, Kuwait City, Kuwait; pp 1–8.
- (98) Peraser, V.; Patil, S. L.; Khataniar, S.; Dandekar, A. Y.; Sonwalkar, V. S. Evaluation of Electromagnetic Heating for Heavy Oil Recovery From Alaskan Reservoirs. In *SPE Western Regional Meeting*; 19–23 March 2012, Bakersfield, California, USA; pp 1–15.
- (99) Bogdanov, I.; Cambon, S.; Prinet, C.; Total, S. A. Analysis of Heavy Oil Production by Radio-Frequency Heating. In *SPE International Heavy Oil Conference and Exhibition*; Society of Petroleum Engineers: 8-10 December 2014, Magaf, Kuwait; pp 1–13.
- (100) Trautman, M.; Ehresman, D. T.; Edmunds, N.; Taylor, G.; Cimolai, M. Effective Solvent Extraction System Incorporating Electromagnetic Heating. US 2012/0118565 A1, 2012.
- (101) Wise, S.; Patterson, C. Reducing Supply Cost With EseehTM Pronounced Easy. In *SPE Canada Heavy Oil Technical Conference held*; Society of Petroleum Engineers: 7–9 June 2016, Calgary, Alberta, Canada; pp 1–12.
- (102) Davletbaev, A.; Kovaleva, L.; Babadagli, T. Mathematical Modeling and Field Application of Heavy Oil Recovery by Radio-Frequency Electromagnetic Stimulation. *J. Pet. Sci. Eng.* **2011**, 78 (3-4), 646–653.
- (103) Trautman, M.; Macfarlane, B. Experimental and Numerical Simulation Results from a Radio Frequency Heating Test in Native Oil Sands at the North Steepbank Mine. In *World Heavy Oil Congress*; 5-7 March 2014, New Orleans USA; pp 1–14.
- (104) Pasalic, D.; Vaca, P.; Okoniewski, M.; Diaz-Goano, C. Electromagnetic Heating : A SAGD Alternative Strategy to Exploit Heavy Oil Reservoirs. In *World Heavy Oil Congress*; 24 -26 March, 2015, Edmonton, Alberta, Canada; pp 1–13.
- (105) McGee, B. C. W.; McDonald, C. W.; Little, L. Electro-Thermal Dynamic Stripping Process. In *The SPE International Thermal Operations and Heavy Oil Symposium*; 20-23 October, 2008, Calgary, Alberta, Canada; pp 1–8.

Chapter 3 Conduction and Polarization Mechanisms in Oil Sands

3.1 Introduction – Electrical Mechanisms in Oil Sands – A Heterogeneous Dielectric

Developing adequate knowledge and understanding about the dynamic electrical behavior of oil sands is crucial for developing accurate simulations and for thereby implementing feasible electrical heating operations in the reservoir. It is also crucial for the design of downhole electrode well equipments needed to carry out electrical heating. Such an assessment, requires that the investigation of the electrical behavior of oil sands be carried out by considering it to be a heterogeneous media wherein different conducting and dielectric phases interact in specific ways to give rise to unique heat generation mechanisms as discussed in figure 2-9 in section 2.3.1.3 of chapter 2. Oil sands discussed to have a conductive phase (from water with dissolved ions and dispersed clays), solid dielectric phase (from quartz minerals) and polymer like dielectric phase (from bitumen) can have conduction and polarization mechanisms as shown in figure 3-1.

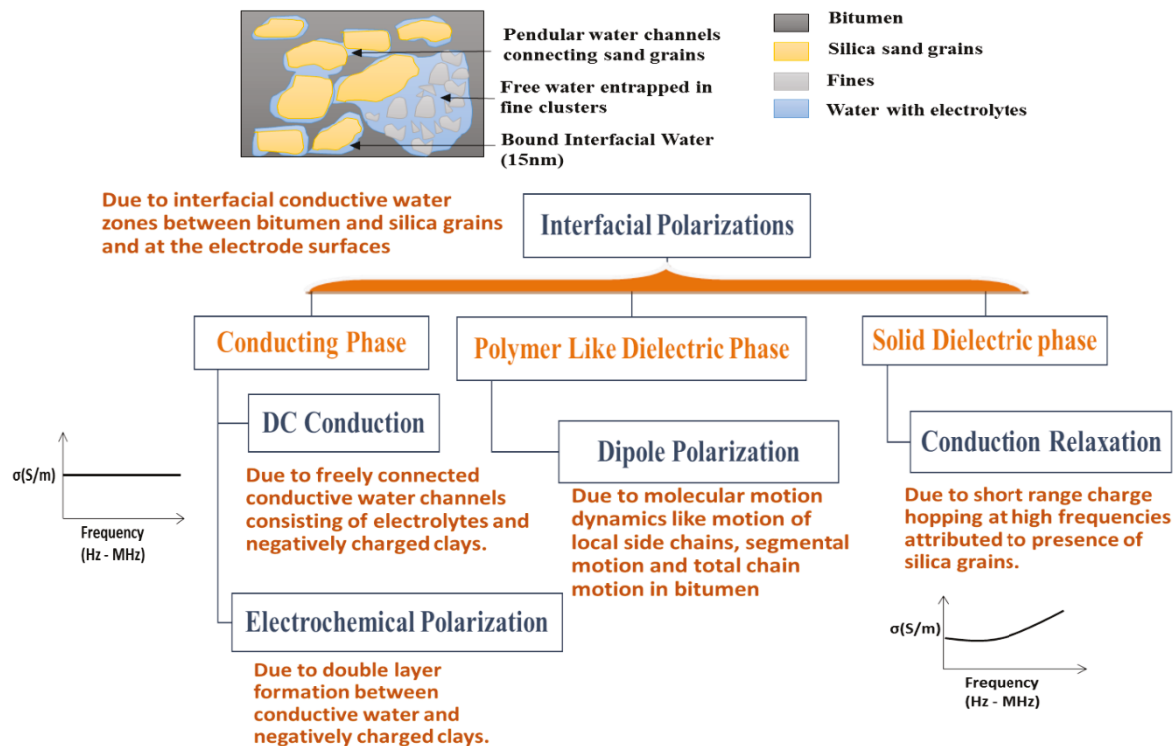


Figure 3-1. Conduction and polarization mechanisms that could be found in heterogeneous oil sands.

Considering the role of conductive water phase, it is important to realize that water can contribute to both conduction and polarization mechanism in oil sands. When water is present in high concentrations such as in the case of poor grade oil sands, it can be expected that water be present as free water channels having fine clusters as depicted from Takamura's microstructural model. In such cases, electrical energy supplied to the oil sands can be expected to be conducted through the freely connected water channels resulting in a dominance of dc conduction mechanism in the oil sands. If the concentration of water is low such as in the case of medium and rich grade oil sands, it can be expected to be presented as isolated zones with some pendular connections between adjacent silica grains. In such cases water is therefore mainly present at interfaces between bitumen and silica grains and thereby have the ability to store the electrical energy in the form of interfacial polarizations. In such heterogeneous media the difference in conductivity of phases give rise to interfacial polarizations from the build-up of space charges near the interfaces between the various phases¹. The relaxations due to such polarizations occur at frequencies lower than the time scales typical of dipolar polarizations. Also the magnitude of dielectric loss associated with interfacial polarizations is often much larger than dipolar contributions. Irrespective of the concentration of water, in the case where a charged phase such as clay having negative charge is dispersed in it, electrochemical double layer polarizations may occur at frequencies lower than interfacial polarization frequencies between mHz and Hz². Also, the presence of polymer like dielectrics such as bitumen in the medium can lead to motional processes which result in dipole fluctuations occurring at different frequencies¹. Such motional processes can be localized fluctuations within a backbone segment or local fluctuations of short side chain or segmental motion at longer time scales. On a more extended length scale, the translational motion of the entire polymer chain may occur. The presence of quartz or silicate minerals which are polycrystalline species, charge hopping polarizations can result in conduction relaxations resulting in a dispersion in the conductivity spectra as shown in figure 3-1. Therefore when electrical energy is applied to such a heterogeneous oil sands media, one or more mechanisms can contribute to the heat generation and electrical heating pattern, depending on the composition. Therefore it can be hypothesized that contributions due to dc conduction, interfacial polarizations and dielectric polarizations could show up at frequencies lower than dipolar polarizations as shown in figure 3-1, in addition to dipolar, atomic and electronic polarizations at higher frequencies as explained in figure 2-4 of Chapter 2. These mechanisms result in energy conduction, storage and dissipation in the

heterogeneous media. Due to the composition and mutual arrangement of components, the conduction and polarization mechanisms can vary widely in different grades of oil sands. These mechanisms also get altered as temperature affects the inherent composition and mutual arrangement.

With these predictions about the electrical behaviour of heterogeneous media such as oil sands this study is carried out to observe conduction and polarization mechanisms in them as a function of their composition and mutual arrangement of the components with variation of electrical frequency between 1 Hz and 1 MHz. Very low frequencies between 1 mHz and 1 Hz where electrochemical polarizations can be investigated are not considered in this study, because these low frequencies are not usually used for electrical heating purposes. Investigating between 1 Hz and 1 MHz helps in determining the dominant electrical conduction and polarization mechanisms that lead to electrical heat generation in a given type of oil sands. Determining relaxation frequencies due to polarization mechanisms and relevance of dc conduction in these different moisture content oil sands is essential to carry out efficient frequency based electrical heating and this study is an attempt to contribute to this abyss in literature with the goal of perpetrating electrical heating for efficient recovery of bitumen from oil sands.

3.2 Theoretical Background of Determination of Conduction and Polarization Mechanisms in Oil Sands.

3.2.1 Calculation of Electrical Properties from Impedance Spectroscopy Measurements

The impedance analyzer is utilized to measure impedance and hence the electrical properties of heterogeneous oil sands. This information obtained from impedance spectroscopy is further used to determine conduction and polarization mechanisms in them. The impedance analyzer measures the total impedance (Z) and phase (φ) response from the sample when an alternating voltage (V) is supplied to it, causing a current (I) to flow through the sample. The impedance (Z) is a complex sum of real (Z') and imaginary (Z'') components given by $Z = Z' + j Z''$ in which (Z') is indicative of the electrical energy lost and (Z'') is indicative of the electrical energy stored. The the real and imaginary parts can be calculated from the modulus of total impedance and phase angle as given below in equations (2) and (3):

$$|Z| = \sqrt{(Z')^2 + (Z'')^2} \quad (2)$$

$$\varphi = \tan^{-1} \left(\frac{(Z'')}{Z'} \right) \quad (3)$$

The electrical energy stored and lost can in turn be discussed in terms of material properties such as effective relative permittivity (ϵ_{eff}) and effective conductivity (σ_{eff}) respectively. The effective properties of a sample are determined equating the response of the sample to a parallel circuit consisting of a resistor (R_p) in parallel with a capacitor (C_p). In parallel mode the complex admittance (Y) is measured and is given as:

$$Y = G_p + jB_p = \frac{1}{Z} = \frac{1}{Z' + jZ''} \quad (4)$$

Where, ($G_p = \frac{1}{R_p}$) is conductance and ($B_p = \omega C_p$) is susceptance. Simplifying:

$$Y = G_p + jB_p = \frac{Z'}{|Z|^2} - j \frac{Z''}{|Z|^2} \quad (5)$$

From the above equations, the effective parameters can be found as follows:

$$\epsilon_{\text{eff}} = - \frac{Z''}{|Z|^2 \omega C_0} \quad (6)$$

$$\sigma_{\text{eff}} = \frac{Z' \times 2\pi l}{|Z|^2 \ln(b/a)} \quad (7)$$

Where:

$\omega = 2\pi f$ where f is frequency in (Hz)

$C_0 = \frac{\epsilon_0 \ln(b/a)}{2\pi l}$ is capacitance of empty coaxial capacitor having length (l), outer diameter (b) and inner diameter (a) and (ϵ_0) is permittivity of free space given as 8.85×10^{-12} F/m.

Rather than referring to two effective parameters, the response of a material can be described with a single, but complex parameter that represents both energy storage and energy loss. There are two equally valid ways to do this in terms of total complex dielectric permittivity (ϵ_T) or in terms of total complex conductivity (σ_T). These are given as:

$$\epsilon_T = \epsilon'_T - j\epsilon''_T \quad (8)$$

$$\sigma_T = \sigma'_T - j\sigma''_T \quad (9)$$

It is important to emphasize that (ϵ_T) and (σ_T) contain the same information and are simply two ways of expressing what is measured and are related as follows:

$$\epsilon_T = \frac{\sigma_T}{j\epsilon_0\omega} \quad (10)$$

The effective storage and loss of electrical energy in the sample can be traced to fundamental mechanisms rooted in polarizations and charge conduction. Both these mechanisms can result in energy storage and energy losses. Energy storage can be due to both dielectric polarization and faradaic diffusion which is due to space charge polarizations resulting in interfacial polarizations and conduction relaxations in our case. Energy loss can be due to both polarization lag and ohmic conduction. This emphasizes the point that there is more than dielectric polarization contributing to what we measure as the effective permittivity or stored energy in the system and there is more than ohmic conduction contributing to what we measure as effective conductivity or energy loss in the system. These energy storage and loss mechanisms can in turn be correlated to the effective energy storage and loss parameters as follows:

$$\epsilon_{eff} = \epsilon'_T = \frac{\sigma''_T}{\epsilon_0\omega} = \text{Dielectric Polarization} + \text{Faradaic Diffusion} \quad (11)$$

$$\sigma_{eff} = \sigma'_T = \omega\epsilon_0\epsilon''_T = \text{Polarization Lag} + \text{Ohmic Conduction} \quad (12)$$

The relative importance of ε_{eff} and σ_{eff} in describing the response of the material to an applied electric field is given by loss tangent $\tan\delta$. It is an overall measure of the heat generated in oil sands and is defined as:

$$\tan\delta = \frac{\sigma_{eff}}{\omega\varepsilon_0\varepsilon_{eff}} \quad (13)$$

Application of an alternating electric field on heterogeneous media such as oil sands can result in microscopic fluctuation of molecular dipoles in polymer like bitumen and propagation of mobile charge carriers by translational diffusion of electrons, holes or ions present in all components of the complex media ¹. Additionally, depending on the arrangement of conductive and dielectric phases in the media, the translational diffusion of mobile charge carriers can also result in polarization effects due to separation of charges at interfaces either at inner dielectric boundaries called interfacial polarizations and/or at external electrodes contacting the sample resulting in electrode or space charge polarizations ¹. By conducting impedance spectroscopy we measured ε_{eff} and σ_{eff} properties and studied their variation with respect to frequency. In order to get insights about the conduction, interfacial polarizations as well as dipole polarization mechanisms in oil sands, it is useful to study the manner in which the calculated electrical properties vary with frequency. The following section discusses graphical observations that indicate the presence of relevant electrical mechanisms applicable to heterogeneous media such as oil sands.

3.2.2 Determination of Conduction and Polarization Mechanisms in Oil Sands from Electrical Property Variation with Frequency.

Heterogeneous media such as oil sands depict a dispersion of conductivity and permittivity with frequency as explained in figure 3-2. Depending on the concentration of conducting components being mostly pore water with dissolved ions and dispersed clays, ohmic/dc or non-ohmic conduction can be observed in such heterogeneous mixtures. When the concentration of conductive water is high where there are more connected pore water channels through pendular connections between sand grains and water entrapped in fine clusters, ohmic or dc conduction is the dominant mechanism. It occurs due to ionic conduction through these pore fluids, surface conduction associated with excess charges in the electrical double layer at the solid-fluid interfaces as well as through electronic conduction ³. While investigating the electrical behaviour of heterogeneous materials such as oil sands, the presence of a dominant dc conduction mechanism

is considered when the conductivity versus frequency looks like the graph in figure 3-2(a) ¹. When the concentration of conducting water channels is less, such that the water is mostly limited to 10-15 nm interfacial bound water between bitumen and silica grains or as isolated pendular connections between sand grains, the ohmic or dc conduction mechanism is accompanied by non-ohmic ac conduction with the presence of a conduction relaxation arising from silica grains at low frequencies as shown in figure 3-2(b) ¹. This non-ohmic conductivity dispersion is observed because at low frequencies ions get more time to drift over large distances and when limited by isolated conducting regions the mean displacement of ions is reduced resulting in localized back and forth motion in conductive phases only at high frequencies ⁴. Arising from ion diffusion transport are polarizations due to charge separations at mesoscopic interfaces and macroscopic electrode boundaries. These are generally depicted together in the graph of real and imaginary part of permittivity versus frequency as shown by sections (1) and (2) in graph of figure 3-2(c) ^{1,5,6} where (1) represents electrode polarization and (2) represents interfacial polarizations. The effect of electrode polarization can be excluded to some degree by subtraction of 45° low frequency slope from the observed data to obtain just the effect of interfacial polarizations ⁵. Thus charge separation based polarizations can occur either due to diffusive and sub-diffusive motions of ions and in turn are dependent on the concentration of the conducting phase which allow charges to migrate and accumulate at interfaces between components with dissimilar electrical properties ^{3,5,7-13}. Maxwell and Wagner derived a mean-field theory for materials containing dispersed dielectric spheres in a dielectric medium ¹. In this study we consider frequencies up to 1 MHz and have not attempted to fit any specific model to explain interfacial polarizations. Therefore, we will refer to interfacial polarizations in a general manner as Maxwell-Wagner (MW) polarizations. The polarizations of the electrical double layer called electrochemical polarizations caused due to the presence of negatively charged clays in ionic water play a dominant role at frequencies less than 1Hz and thus show up as high values of dielectric permittivity at these frequencies ^{3,7,10,12}. Considering dispersions due to polarization mechanisms arising from rotational diffusion, single components display dipolar polarization dispersions in the frequency range between 1kHz and 1GHz ¹³. When the earth materials are covered with hydrocarbons such as oils and bitumen in the case of oil sands, they can be treated as polymer systems which can undergo several relaxations associated with glass transitions, segmental mobility of polar groups and crystallization process which have signatures in the Hz to MHz frequency range and have certain temperature dependent trends ^{13,14}.

In such figures by convention, dielectric relaxation are characterized by a peak in the imaginary part of permittivity and a step like decrease in the real part as shown in figure 3-2(d) ¹.

3.2.3 Determination of Bulk Relaxation Mechanisms from Modulus Spectroscopy

Electrode polarization and interfacial polarization effects are commonly eliminated from the study of bulk conduction, and dielectric relaxations by studying electric modulus formalism ^{15,16} which is defined as the inverse quantity of complex permittivity by the following equation (13). The use of electric modulus offer some advantages in interpreting bulk relaxation processes since by its definition, variation of large values of permittivity and conductivity at low frequencies are minimized ¹⁷.

$$M = \left(\frac{1}{\epsilon_T} \right) = M' + jM'' \quad (14)$$

Where:

$$M' = \frac{\epsilon_T'}{\epsilon_T'^2 + \epsilon_T''^2} \quad (15)$$

$$M'' = \frac{\epsilon_T''}{\epsilon_T'^2 + \epsilon_T''^2} \quad (16)$$

Where M' is the real and M'' the imaginary part of electric modulus.

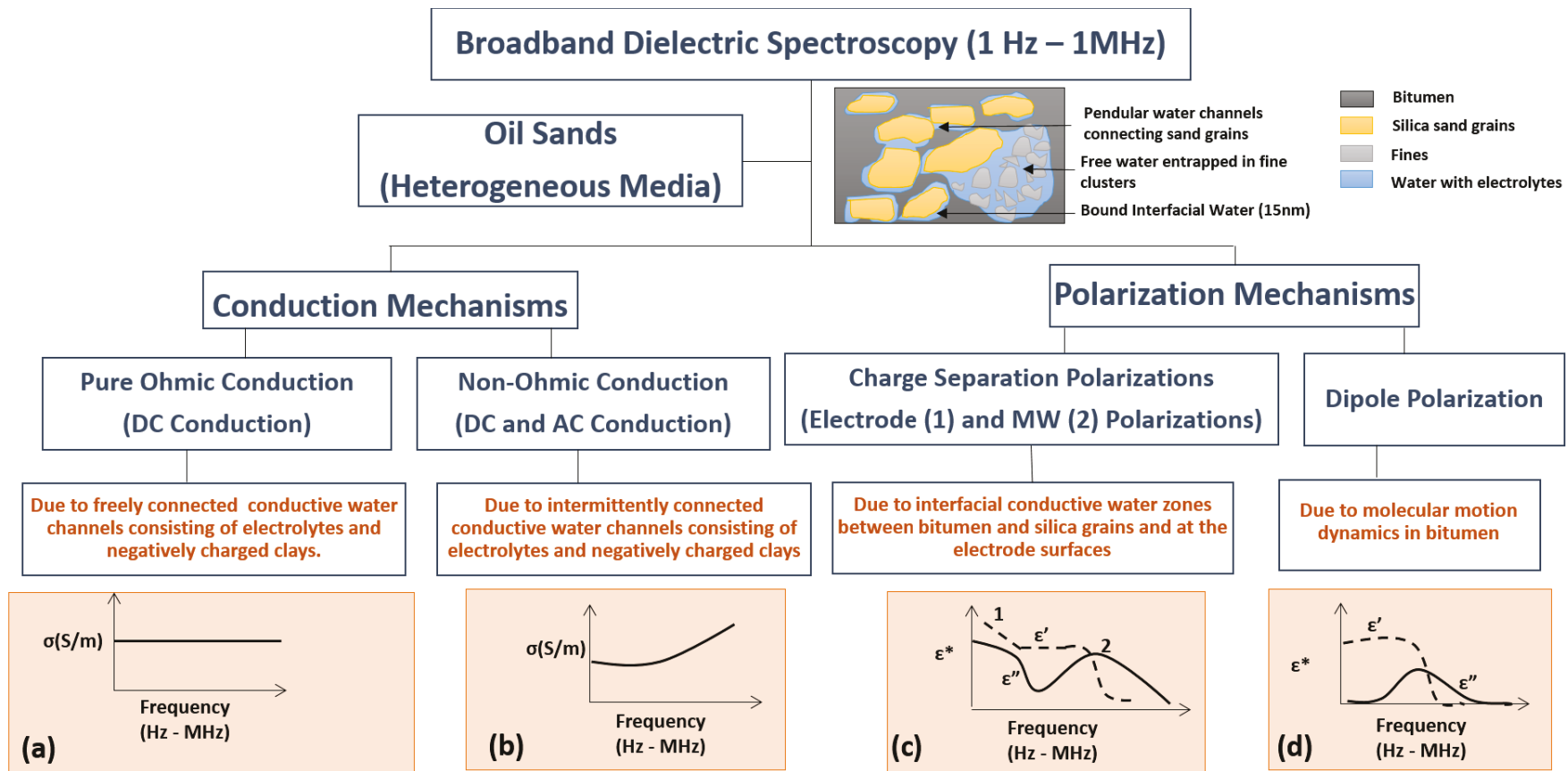


Figure 3-2. Schematic interpretation of determining conduction and polarization mechanisms in oil sands.

3.3 Materials and Methods

Six oil sands with increasing water and clay content were investigated for this study. The study included characterizing the electrical properties of oil sands with electrical frequency and composition. Impedance spectroscopy was implemented for this study. The six selected oil sands samples having different water and fine content are shown in figure 3-3. The composition of oil sands was determined using Dean–Stark extraction method, the working protocol of which can be found in studies conducted by Chute et al.¹⁸. The Oil Sands 1 sample has the least water and fines content, where the Oil Sands 6 sample has the most water and fines content. Solids obtained from the Dean–Stark extraction process were dried and dry-sieved using Mesh 425 to obtain a fines content less than 44 μm . Oil Sands 1–5 can be categorized as rich grade, having bitumen between 11 and 13%, whereas Oil Sands 6 had the least amount of bitumen, 3.8%, indicating it to be poor grade¹⁹. Three repetitions of the Dean–Stark extraction process were conducted, and the average percentage composition of components is plotted in figure 3-3. The error bars indicate standard deviation observed between three different runs for each set of experiments. Table A-1 of Appendix A lists the experimental data of three runs of Dean-Stark extraction carried out for all 6 oil sands. Fines content was estimated from wet sieving method.

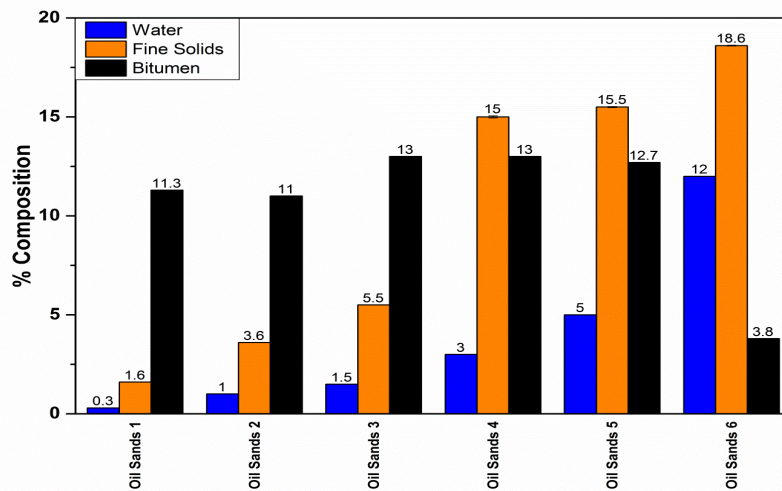


Figure 3-3. Composition of different oil sands samples used for this study estimated from Dean-Stark extraction method

Impedance spectroscopy studies were performed on all the given oil sands samples to determine their complex impedance behavior from which conduction and polarization mechanisms could be

inferred. A Gamry Potentiostat/ Galvanostat/ZRA Reference 30000 instrument was used for this study. A coaxial cylindrical test fixture as shown in figure 3-4 is used to house the oil sands for this study. The test fixture was made of copper electrodes having the following dimensions: 5 cm length, 3 cm hollow outer electrode diameter, 1.5 cm solid inner electrode diameter. Both ends of the coaxial test cell are covered using Teflon caps to prevent formation of fringing electric fields. A furnace (MTI Corporation KSL-1100X) is used to house the coaxial test cell during the temperature-based impedance spectroscopy studies which is considered in the next chapter. Calibration runs were conducted on the coaxial capacitor using distilled water, tap water, silica sand and kaolin clay. Results of these calibration runs are given in figures A-1, 2, 3 and 4 in Appendix A. Having obtained an understanding of the accuracy of the functioning of coaxial capacitor using calibration data, tests were run for oil sands. For these tests, the oil sands samples were packed layer by layer between inner and outer electrode area so that a uniform packing density could be obtained. For each test, three repeated experiments of were carried out. The impedance spectroscopy was carried out by taking a total of 10-point average measurements under frequency sweep from 1 Hz to 1 MHz at a constant voltage level of 1V and no DC bias as shown in figure 3-4. Because the oil sands sample was packed very tightly and the measurements were done using a very low current, the effect of electrode impedance was considered to be negligible.

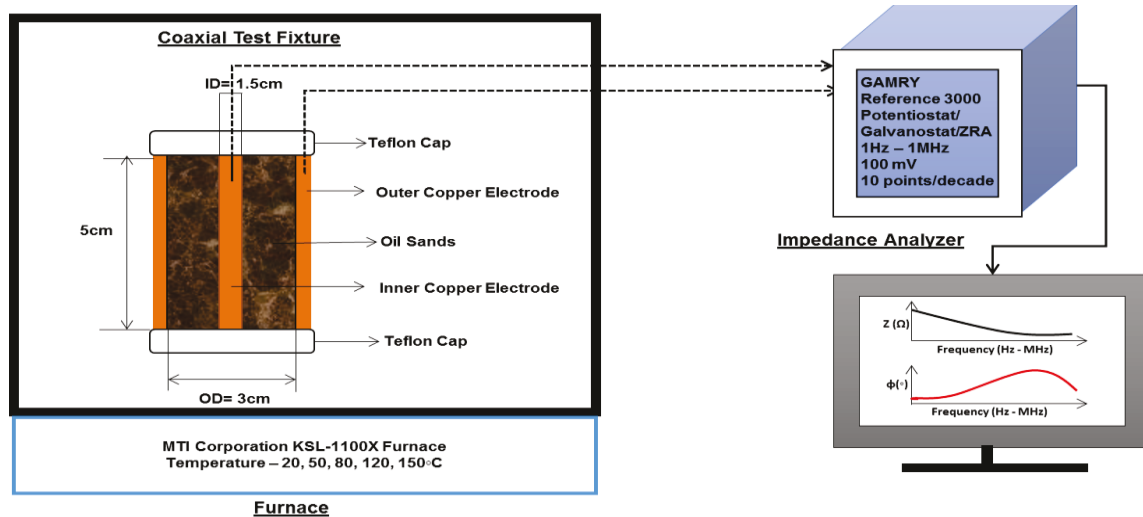


Figure 3-4. Illustration of impedance spectroscopy experiments carried out for oil sands samples at room temperature.

3.4 Results and Discussions

3.4.1 Variation of Real and Imaginary Permittivity with Frequency and Composition

Frequency dependence of the real ($\epsilon'_T = \epsilon_{eff}$) and imaginary ($\epsilon''_T = \sigma_{eff}/\omega\epsilon_0$) parts of complex permittivity is shown in figure 3-5. The real part of complex permittivity (ϵ'_T) shown in figure 3-5(a) also called dielectric constant is a measure of the total polarizations in a material which arise from electronic, atomic, molecular and interfacial mechanisms³, while the imaginary part (ϵ''_T) shown in figure 3-5(b) is a measure of the total losses in the material from conduction, interfacial polarizations and dielectric polarization mechanisms. Both (ϵ'_T) and (ϵ''_T) increase with decreasing frequency indicating the dominance of charge separation based polarizations in oil sands such as MW polarizations at interfaces or space charge polarizations at external electrodes¹. While MW polarizations is predominant in heterogeneous materials low to high concentration of ions, electrode polarizations are more dominant in cases where of high concentration of ions¹.

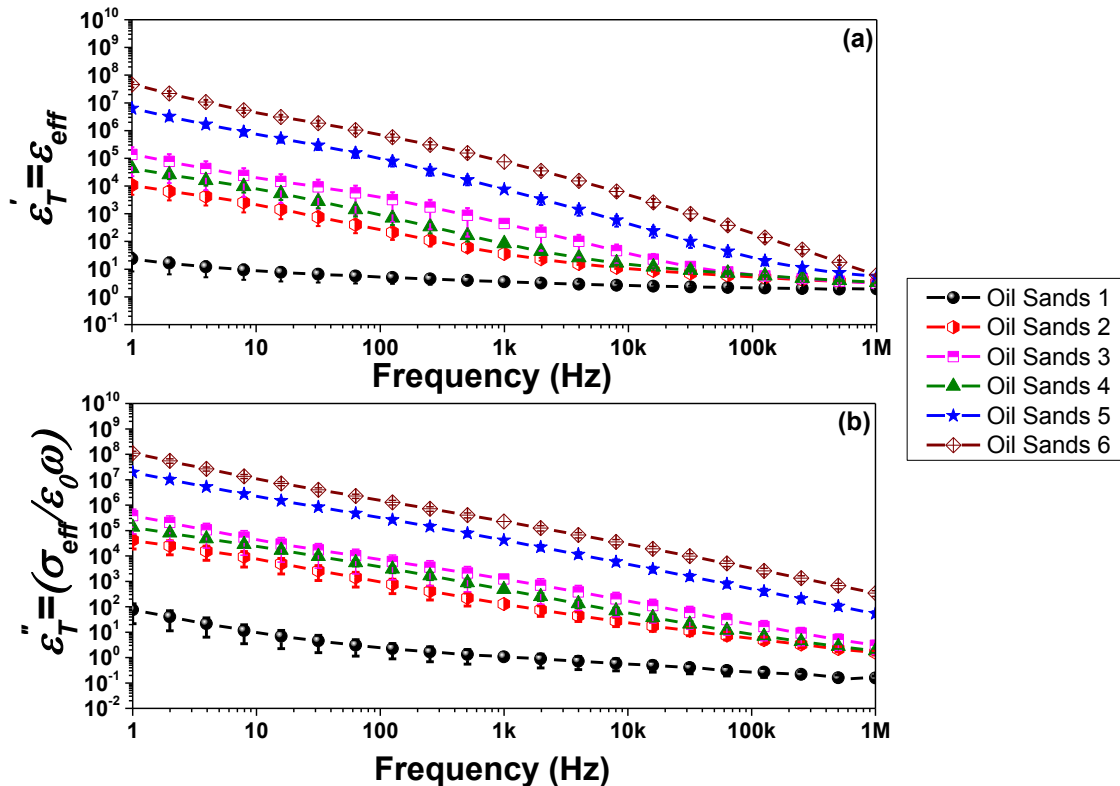


Figure 3-5. (a) Dielectric constant and (b) Dielectric losses of oil sands when swept from 1Hz to 1MHz at room temperature (20°C)

Oil Sands 1 having least water (0.3%) and clay content (1.6%), showed to have least overall complex permittivity as compared to Oil Sands 6 having most water (12%) and clay (18.6%) content. Being the richest grade, we can assume that the water in Oil Sands 1 is present mostly as bound interfacial water of 10 to 15 nm with very little concentration acting as pendular channels connecting adjacent sand grains. Due to low concentration of conducting water phase in these oil sands, the nature of the graph by following shallow fractional law at high frequencies in their response²⁰ indicate the presence of conduction relaxation at low frequencies. The linear frequency dependence of permittivity at high frequencies is referred to as nearly constant loss (NCL) regime since it corresponds to almost frequency independent dielectric loss as shown in figure 3-5. This type of behavior, was observed in disordered media and interpreted from Jonscher's power law called the Universal Dielectric Response (UDR) model^{20,21} which could be due to slowly moving hopping charge carriers. As water and clay content are increased from Oil Sands 2 to 6, we can assume that the presence of connecting pendular channels and free water present in fines cluster increases, which can contribute to dominance of the dc conduction over ac conduction and resulting MW and electrode polarizations due to it. Careful observations have led us to site MW polarizations in oil sands 2 to 4 as marked by variations in the curves in figure 3-5. High values of (ϵ'_T) and (ϵ''_T) for Oil Sands 2 to 4 at low frequencies also indicate the presence of electrode polarizations. The results shown in figures 3-6, 3-7 and 3-8 will aim at differentiating these mechanisms from each other along the frequency regime. Oil Sands 5 and 6 having most water and clay content can be assumed to offer a good conductive path for current flow and hence have dc conduction mechanisms dominating over polarization mechanisms as will become clearer from figures 3-7 and 3-8.

3.4.2 Variation of Loss Tangent with Frequency and Composition

Since we are dealing with a heterogeneous mixture having several components and interfaces, identifying the relaxations individually is a challenge due to overlapping and super positioning of more than one mechanism. The dissipation factor $\tan\delta$ shown in figure 3-6 is therefore plotted to get more clear depiction of the relaxations. It is well understood that losses due to interfacial polarizations are maximum as compared to dipole polarizations¹ in these oil sands. The dispersions due to MW polarization mechanisms seen predominantly for Oil Sands 2 to 5 can be observed clearly in Figure 3-6.

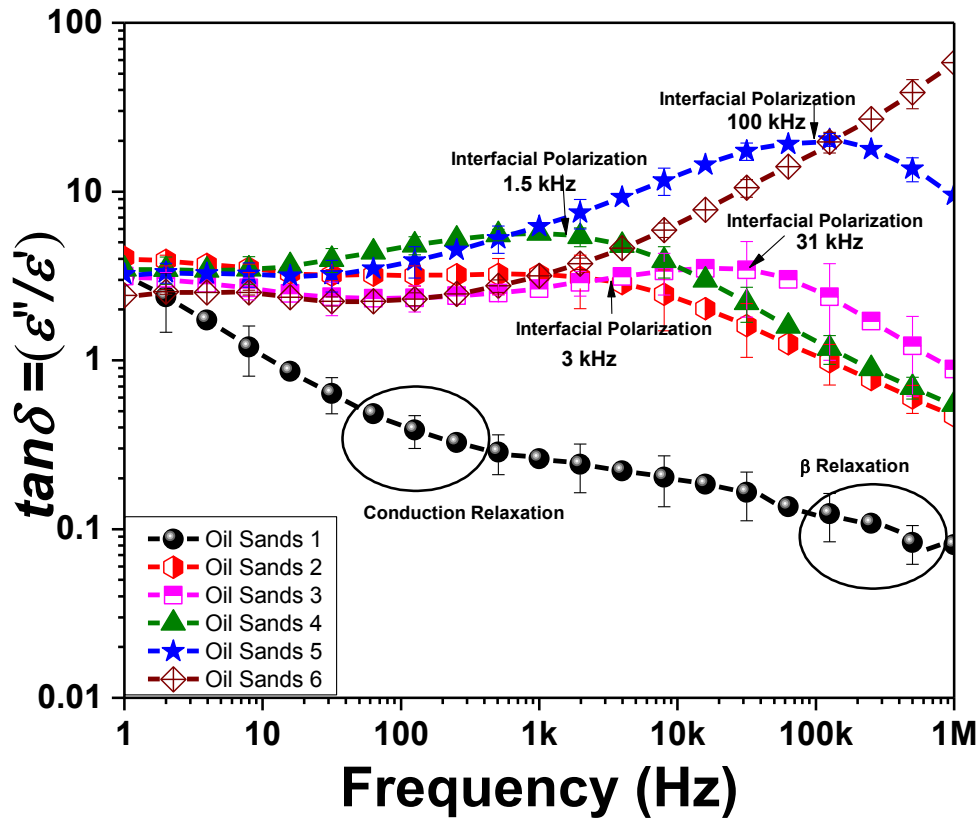


Figure 3-6. Loss tangent ($\tan\delta$) spectroscopy of oil sands at room temperature (20°C), depicting frequencies due to interfacial polarizations / MW relaxations, β relaxations and conduction relaxations

While dissipation factor also exemplifies heat generated in the material, it can be inferred that more the water and clay content of the oil sands more is the electrical heating in the material. Also carrying out electrical heating in the dispersion regime of relaxation frequency due to MW polarizations for Oil Sands 2 to 5, which lies in kHz to MHz regime, would ensure most efficient heating. When systems consists of polymeric materials such as bitumen in our case, the molecules do not undergo complete rotations but do undergo segmental motion and motion of local side chains such as α and β relaxations respectively^{1,13}. Though not very significant, we can observe a relaxation due to bitumen molecules in Oil Sands 1, which has least water and clay components in the high frequency regime between 100 kHz and 1 MHz. Such relaxations of bitumen were also reported in an earlier study²², where they attributed the observation to β relaxations due to local motion of side chains. Since bitumen is present in all oil sands samples, it may have such

relaxation peaks in the others as well, which are not visible to us due to the overshadowing effects of interfacial polarizations and conduction from water and clay. It is of interest to us to identify these relaxations due to bitumen more closely in the temperature dependent studies.

3.4.3 Variation of Conductivity with Frequency and Composition

Figure 3-7 shows the frequency dependence of conductivity and is given as $(\sigma_{eff} = \sigma_T' = \omega \epsilon_0 \epsilon_T'')$. It is observed that Oil Sands 1 to 4 have frequency dependent conductivity, whereas conductivities of Oil Sands 5 and 6 are independent of frequency.

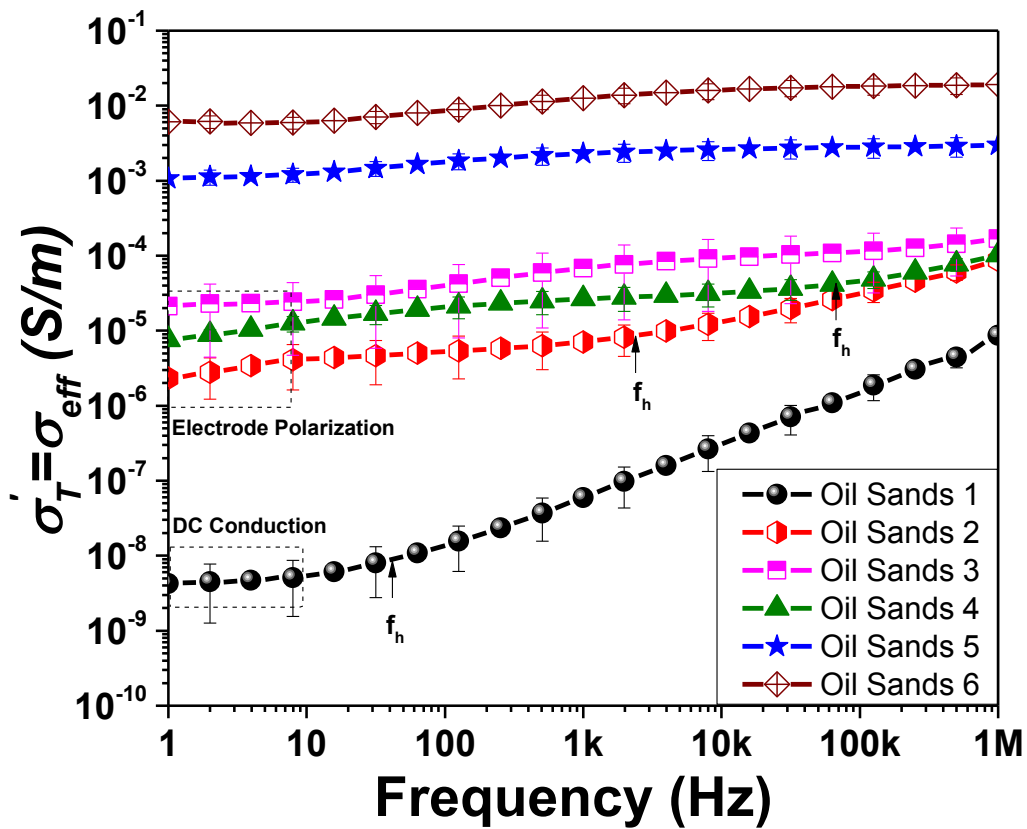


Figure 3-7. Conductivity spectra of oil sands at room temperature (20°C) depicting electrode polarizations, dc conduction and conduction relaxations.

In Oil Sands 1 to 4, a constant plateau region of conductivity in the low frequency regime indicates long-range irreversible ion diffusion indicating dc or ohmic conduction. Short time ion dynamics characterized by back and forth motion over limited ranges leads to increasing conductivity phenomena observed at higher frequencies above the hopping frequency, f_h ²¹. The overall

mechanism of ion transport when it varies in this manner with frequency could be hypothesized to be due to hopping conduction mechanism. The motion of ions through this mechanism is accompanied by a conduction relaxation whereby an ion is surrounded by negative or positive counter charge giving it a polarization cloud. The hop of an ion to a new site can only lead to a successful charge transport if the polarization cloud follows, or else the ion jumps back with high probability. This mutual movement of the ion and surrounding polarization cloud has a characteristic conduction relaxation time denoted by hopping frequency f_h . If the frequency of the electric field is lower than f_h , its effect on the ion transport averages out and long range irreversible ion diffusion characterized by random walks indicating dc conduction occurs. For frequencies higher than f_h , the relaxation of the polarization cloud is in phase with the outer electrical field resulting in short time ion dynamics characterized by back and forth motion over limited ranges²³. This total conductivity behavior which is due to hopping ion transport obeys the well-known universal dielectric response (UDR) namely Jonscher's relation²³⁻²⁵. Oil Sands 1, which has the least amount of water and clays clearly obeys Jonscher's relation²¹:

$$(\sigma'_T(f, T) = \sigma_{DC} \left[1 + (f/f_h)^s \right]) \quad (17)$$

where f_h indicates hopping frequency corresponding to the conduction relaxation time, σ_{DC} is the limiting value of σ'_T when $\omega \rightarrow 0$ and s parameter depends on temperature, morphology and composition and should be $0 \leq s \leq 1$. Following this universal law indicates that conduction in Oil Sands 1 could be a case of ion motion by activated hopping between charge compensating sites^{20,21}. It can be observed that the hopping frequency, separating the short range conduction process (ac conduction) from long range conduction process (dc conduction), shifts towards the higher frequency regime as we go from Oil Sands 2 to 4 indicating that increasing water and clay content causes dc conduction to dominate. Since these oil sands have more free charge carriers, they also show electrode polarizations as indicated by the dip in their conductivity spectra at low frequencies in figure 3-7. Such oil sands also indicate MW polarizations through slight variations in their conductivity curves. At high water and clay contents such as in Oil Sands 5 and 6, it can be observed that conduction becomes frequency independent and shows a plateau indicating that long-range dc conduction dominates through connected water channels in such oil sands for the swept frequency range.

3.4.4 Modulus Spectroscopy of Oil Sands

To eliminate the presence of electrode polarization and highlight the bulk polarizations in oil sands arising from conduction and dipole polarizations, electric modulus formalism is commonly used^{15,16}. Figure 3-8 shows the frequency dependence of M'' . In particular, peaks of M'' versus frequency highlight the time constant of relaxation time due to conduction and dielectric relaxation mechanisms. A well-defined asymmetric peak is observed around the low frequency regime for Oil Sands 1. We can attribute this peak to the presence of conduction relaxations in Oil Sands 1. Interestingly, not so well defined peaks are also observed at the high frequency end in these oil sands as was also observed for Oil Sands 1 in figure 3-6. It is assumed that this is due to molecular relaxations in bitumen evidence of which will be proved in the temperature based studies in Chapter 4. The M'' peak shifts towards the high frequency regime in Oil Sands 2 to 4 and is slightly present in Oil Sands 5, while is almost non-existent in Oil Sands 6. By convention, the low frequency side of the peak represents the range of frequencies where ions can move over long distances; i.e. ions can perform successful hopping from one site to the neighboring site. The high frequency side of the M'' peak represents the range of frequencies where ions are spatially confined to their potential wells and the ions can make localized motions within the wells¹⁵. Therefore, shifting of the M'' peak towards the high frequency for Oil Sands 2 to 4 would indicate that the increasing water and clay content have led to more long range dc conduction of ions in these oil sands and MW polarizations occurring due to the charge accumulation at boundaries of more free water zones with bitumen and silica grains. Also, lowering of these peaks indicates increasing conductivity as is seen for Oil Sands 5 and 6, for which we can say that dc or ohmic conduction mechanisms dominate over polarization mechanisms.

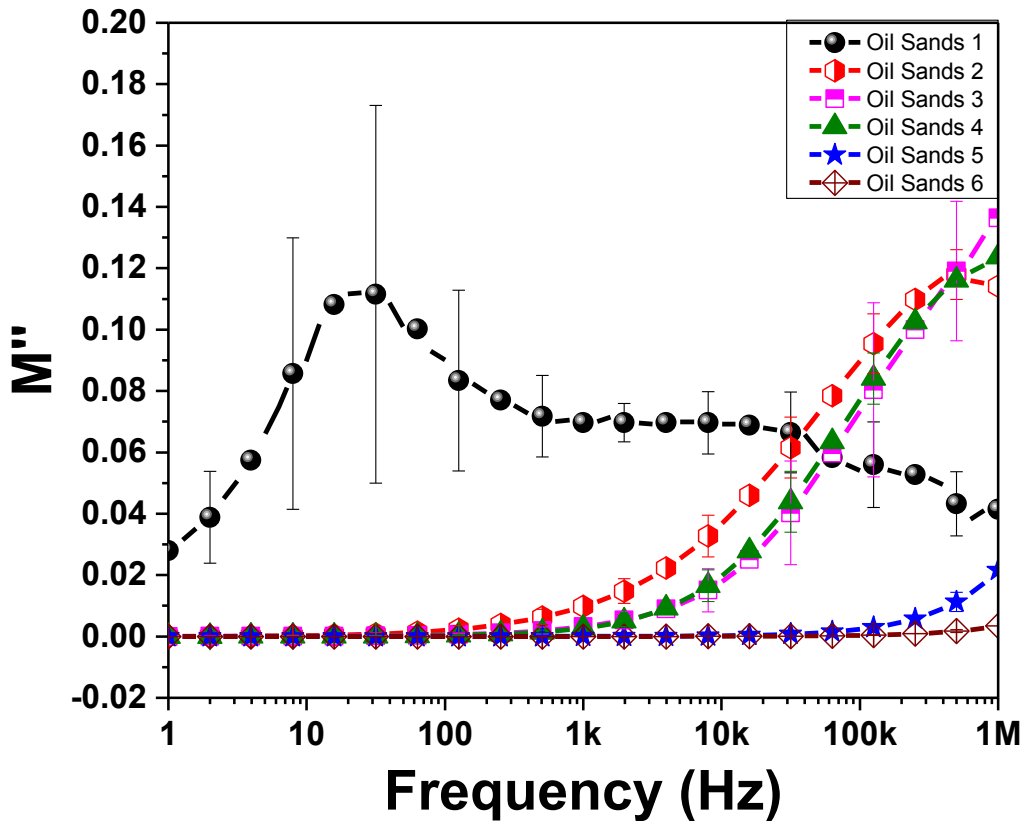


Figure 3-8. Imaginary modulus spectra of oil sands at room temperature (20°C)

3.4.5 Variation of Dielectric Constant and Conductivity with Water Concentration as a Function of Frequency

Dielectric constant (ϵ'_T) and conductivity (σ'_T) of oil sands were plotted as a function of its water content at different frequencies as shown in figure 3-9. It was observed that both properties increased as water content increased for all frequencies. In the case of dielectric constant (ϵ'_T), less difference in values were observed at low water content as compared to high water content with complementary results observed for conductivity (σ'_T). Also, for all water content dielectric constant (ϵ'_T) showed least value for 1 MHz as compared to 1 Hz while the opposite trend was observed for conductivity (σ'_T). Also 1 MHz showed least change in dielectric constant with water content as compared to 1 Hz. A slight drop was observed in both graphs when going from oil sands with 1.5% water content (Oil Sands 3) to 3% water content (Oil Sands 4). This could be because as compared to other oil sands the increase in fine solids content (<44 μ m) was significant from

Oil Sands 3 (5.5%) to Oil Sands 4 (15%) which could have hindered free conduction and resulted in a decrease of the properties.

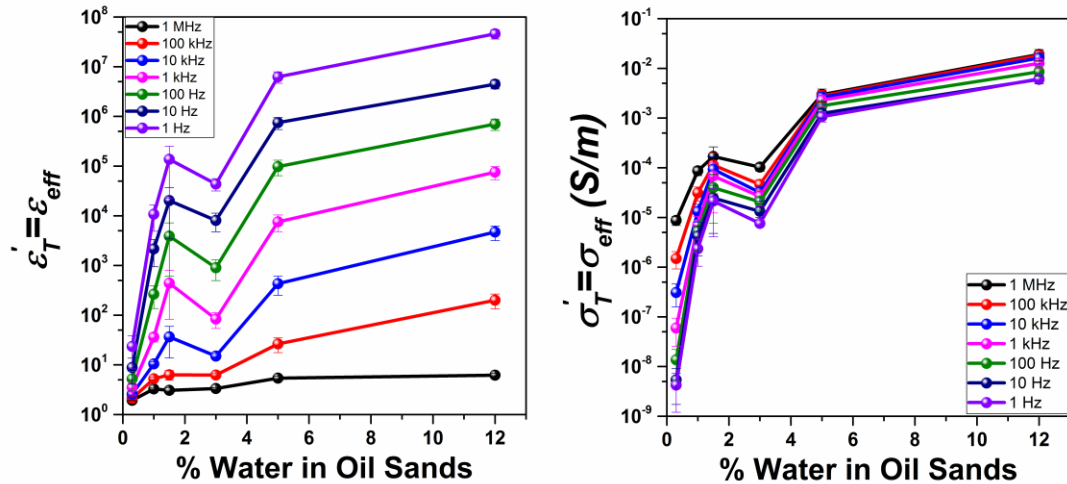
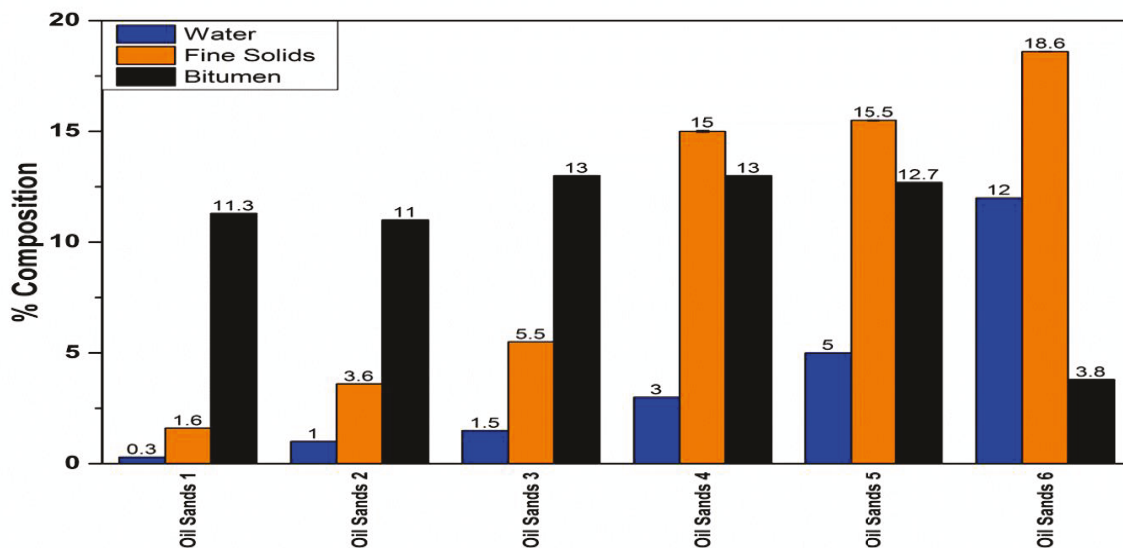


Figure 3-9. Dielectric constant and conductivity of oil sands as a function of water content at different frequencies.

3.5 Conclusions

Six oil sands were investigated for their conduction and polarization mechanisms using impedance spectroscopy. Five of the oil sands samples were rich grade with increasing water (0.3% to 5%) and clay content (1.6% to 15.5%) with similar bitumen content (11 to 13%) while the sixth one was poor grade having least bitumen (3.8%) and maximum water (12%) and clay content (19%). Oil Sands 1 having least water and clay content (0.3%) showed dominance of conduction relaxation which could be attributed to the dominance of charge carrier hopping mechanism from mobile ions in quartz minerals. Small amount of dc conduction in these oil sands at lower frequencies could be attributed to the presence of bound interfacial water between bitumen and sand grains as well as free water whose concentration is very less in these oil sands. Due to lack of water these oil sands also depicted dielectric relaxations due to molecular motion of bitumen between 100 kHz and 1 MHz. Oil Sands 2 to 4 (1-5% water) showed dominance of MW relaxations due to presence of free and bound interfacial water channels from 1 kHz to 1 MHz. Hopping frequencies appeared at higher values for these oil sands as compared to Oil Sands 1 indicating more long range ion transport as compared to short range ion transport. Oil Sands 5 and 6 (>5% water), showed dominance of the dc conduction mechanism over polarization mechanisms due to

the presence of maximum connected free water channels trapped in fine clusters. The dielectric constant and conductivity showed to increase with increasing water content of oil sands at all frequency with maximum increase of dielectric constant at 1 Hz as compared to 1MHz while the opposite was observed for conductivity. Thus it can be summarized as shown in figure 3-10 that Oil Sands 1 showed dominance of conduction relaxation mechanisms from quartz minerals and also showed evidence of bitumen polarizations; Oil Sands 2 to 4 showed dominance of MW polarizations due to interfaces between pendular connected water channels in between bitumen and sand, which showed relaxation peaks between 1 kHz and 1 MHz; whereas Oil Sands 5 and 6 showed dominance of dc conduction mechanism over the scanned frequency range due to the presence of free water channels and fine clay clusters. The next chapter discusses results of temperature based electrical behavior of oil sands shedding light on their dynamic variations due to changes in their composition and microstructural arrangement with rise in temperature.



- Conduction Relaxations at 100 to 200 Hz due to Silica
- Dipole Relaxations due to Bitumen (~200 kHz)

- Interfacial/MW Polarizations (kHz Frequency)
- Some DC Conduction
- Conduction Relaxation at very high frequency

- DC Conduction

Figure 3-10. Summary of Conduction and Polarization Mechanisms in Oil Sands with Different Composition.

3.6 References

- (1) Kremer, F.; Schönhals, A. Analysis of Dielectric Spectra. In *Broadband Dielectric Spectroscopy*; Springer-Verlag Berlin Heidelberg New York, 2003.
- (2) Revil, a.; Eppehimer, J. D.; Skold, M.; Karaoulis, M.; Godinez, L.; Prasad, M. Low-Frequency Complex Conductivity of Sandy and Clayey Materials. *J. Colloid Interface Sci.* **2013**, *398*, 193–209.
- (3) Knight, R. J.; Endres, A. L. An Introduction to Rock Physics Principles for Near-Surface Geophysics. In *Near-surface geophysics: Volume 13*; Society of Exploration Geophysicists Tulsa, 2005.
- (4) Psarras, G. C.; Manolakaki, E.; Tsangaris, G. M. Dielectric Dispersion and Ac Conductivity in - Iron Particles Loaded: Polymer Composites. *Compos. Part A Appl. Sci. Manuf.* **2003**, *34*, 1187–1198.
- (5) Chelidze, T. L.; Gueguen, Y.; Ruffet, C. Electrical Spectroscopy of Porous Rocks: A review—II. Experimental Results and Interpretation. *Geophys. J. Int.* **1999**, *137* (1), 16–34.
- (6) Hanai, T.; Koizumi, N.; Goto, R. Dielectric Constant of Emulsions. *Bulletin of the Institute for Chemical Research, Kyoto University.* 1962, pp 240–271.
- (7) Chelidze, T. L.; Gueguen, Y. Electrical Spectroscopy of Porous Rocks: A review—I. Theoretical Models. *Geophys. J. Int.* **1999**, *137* (1), 1–15.
- (8) Knight, R.; Nolte, L. J. P.; Slater, L.; Atekwana, E.; Endres, a; Geller, J.; Lesmes, D.; Nakagawa, S.; Revil, a; Sharma, M. M.; Straley, C. Geophysics At the Interface : Response of Geophysical Properties To Solid - Fluid , Fluid - Fluid , and Solid - Solid Interfaces. *Rev. Geophys.* **2010**, *48* (2007), RG4002.
- (9) Knight, R. J.; Nur, A. The Dielectric-Constant of Sandstones, 60 Khz To 4 Mhz.

- Geophysics* **1987**, 52 (5), 644–654.
- (10) Lesmes, D. P.; Morgan, F. D. Dielectric Spectroscopy of Sedimentary Rocks. *J. Geophys. Res.* **2001**, 106 (B7), 13329–13346.
- (11) Olhoeft, G. R. Low-frequency Electrical Properties. *Geophysics* **1985**, 50 (12), 2492–2503.
- (12) Revil, A. On Charge Accumulation in Heterogeneous Porous Rocks under the Influence of an External Electric Field. *Geophysics* **2013**, 78 (4), D271–D291.
- (13) Kremer, F. Dielectric Spectroscopy – Yesterday , Today and Tomorrow. **2002**, 305, 1–9.
- (14) Psarras, G. C.; Manolakaki, E.; Tsangaris, G. M. Electrical Relaxations in Polymeric Particulate Composites of Epoxy Resin and Metal Particles. *Compos. - Part A Appl. Sci. Manuf.* **2002**, 33, 375–384.
- (15) Psarras, G. C.; Manolakaki, E.; Tsangaris, G. M. Dielectric Dispersion and Ac Conductivity in - Iron Particles Loaded: Polymer Composites. *Compos. Part A Appl. Sci. Manuf.* **2003**, 34 (12), 1187–1198.
- (16) Hodge, I. M.; Ingram, M. D.; West, A. R. Impedance and Modulus Spectroscopy of Polycrystalline Solid Electrolytes. *J. Electroanal. Chem. Interfacial Electrochem.* **1976**, 74 (2), 125–143.
- (17) Tsangaris, G. M.; Psarras, G. C.; Kouloumbi, N. Electric Modulus and Interfacial Polarization in Composite Polymeric Systems. *J. Mater. Sci.* **1998**, 33 (8), 2027–2037.
- (18) Chute, F. S.; Vermeulen, F. E.; Cervenán, M. R.; McVea, F. J. Electrical Properties of Athabasca Oil Sands. *Can. J. Earth Sci.* **1979**, 16 (10), 2009–2021.
- (19) Masliyah, J.; Czarnecki, J.; Xu, Z. Physical and Chemical Properties of Oil Sands. In *Handbook on Theory and Practice of Bitumen Recovery from Athabasca Oil Sands. Vol. 1: Theoretical Basis.*; Kingsley Knowledge Publishing, 2011.
- (20) Jonscher, A. K. The Universal Dielectric Response. *Nature* **1977**, 267, 673–679.

- (21) Dyre, J. C.; Maass, P.; Roling, B.; Sidebottom, D. L. Fundamental Questions Relating to Ion Conduction in Disordered Solids. *Reports Prog. Phys.* **2009**, *72* (4), 46501.
- (22) Chen, F.; Taylor, N.; Kringos, N.; Birgisson, B. A Study on Dielectric Response of Bitumen in the Low-Frequency Range. *Road Mater. Pavement Des.* **2015**, *16* (sup1), 153–169.
- (23) Dyre, J. C.; Schröder, T. B. Universality of Ac Conduction in Disordered Solids. *Rev. Mod. Phys.* **2000**, *72* (3), 873.
- (24) Jonscher, A. K. Dielectric Relaxation in Solids. *J. Phys. D. Appl. Phys.* **1999**, *32* (14), R57–R70.
- (25) Mokni, M.; Kahouli, A.; Jomni, F.; Garden, J.-L.; André, E.; Sylvestre, A. Dielectric Investigation of Parylene D Thin Films: Relaxation and Conduction Mechanisms. *J. Phys. Chem. A* **2015**, *119* (35), 9210–9217.

Chapter 4 Temperature based Conduction and Polarization Mechanisms in Oil Sands

4.1 Introduction

It is understood that when electrical energy is applied to heterogeneous oil sands it can respond via an interplay between dc conduction and dielectric relaxation mechanisms involving conduction relaxations, interfacial polarizations and dipole polarizations. All these mechanisms in turn aid in electrical heat generation within oil sands. As temperature rises, these mechanisms also undergo changes due to changes in oil sands composition and microstructural arrangement. It is well understood from the previous chapter that the presence of water having electrolytes in oil sands can contribute to dc conduction and/or interfacial polarizations depending on their concentration and microstructural arrangement. At higher water concentrations dc conduction mechanism tends to dominate over interfacial polarization mechanisms and vice versa is true at lower concentrations. Dipole polarizations due to bitumen though predicted to be present in all oil sands are revealed only in the case where the concentration of water is very low. As temperature increases, water is the main component to get affected as it is most receptive to electrical energy due to its high conductivity and permittivity, causing it to vaporize and can be assumed to leave the oil sands mixture at temperatures greater than 100°C. Loss of water leads to discontinuation of electrical heating due to loss of conductive path between the electrodes during ohmic heating. Bitumen also changes in its physical behaviour with temperature causing it to reduce in viscosity and possibly in its polarization mechanisms. So at higher temperatures with the absence of the conductive water phase and with the presence of a more mobile dielectric bitumen phase, the oil sands becomes a heterogeneous mix of dielectric phases as shown in figure 4-1. Understanding the transition of conduction and polarization mechanisms in oil sands with increasing temperature is important to carry out an optimized and dynamically controlled electrical heating process. Therefore the aim of this study is to determine the changes in the conduction and polarization mechanisms in oil sands as temperature is raised from 20 to 200°C, with the objective of identifying operational strategies that could be carried out during the heating process.

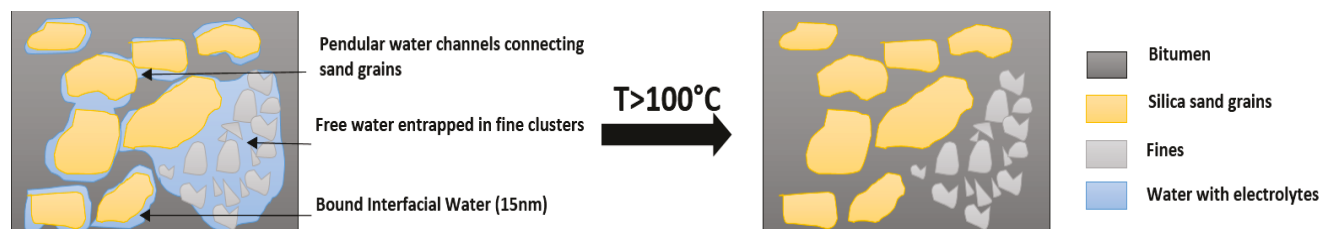


Figure 4-1. Illustration of temperature based transition of oil sands

4.2 Materials and Methods

The same materials and experimental set up discussed in Chapter 3 were used for these studies as well. Impedance spectroscopy experiments were conducted on six oil sands samples between 1Hz and 1MHz frequency at temperatures 20, 50, 80, 120, 150, 180 and 200°C by housing the coaxial test cell having the oil sands inside a furnace (MTI Corporation KSL-1100X). The furnace was automated to maintain the set temperature for 45 minutes to attain equilibrium and data was taken using the Gamry potentiostat. After taking data at 200°C, the oil sands in the coaxial test cell was cooled to room temperature to again obtain data of oil sands predicted to have lost all the water. Three repeated experimental runs was carried out for each oil sand sample, wherein similar observations were observed and one experimental run data is presented in this chapter with the results of the remaining runs given in Appendix B. The analysis of measured data was same as carried out in Chapter 3.

4.3 Results and Discussions

Temperature-based analysis was conducted to determine the role that each component plays in the conduction and dielectric relaxation process. Oil Sands 1 is initially analyzed for variation of its complex permittivity, conductivity, modulus spectrum and loss tangent with temperature for determining variations in dc conduction, bulk conduction relaxations, as well as interfacial or Maxwell Wagner (MW) and dipole polarizations. A similar analysis is followed for Oil Sands 2 to 4, where Oil Sands 2 is studied as the oil sands representing this group. While among Oil Sands 5 and 6, Oil Sands 5 is analyzed for its temperature based electrical behavior.

4.3.1 Temperature Based Impedance Spectroscopy of Oil Sands 1

Figure 4-2 shows the variation of real ($\epsilon'_T = \epsilon_{eff}$) and imaginary ($\epsilon''_T = \sigma_{eff}/\omega\epsilon_0$) parts of complex permittivity with frequency for Oil Sands 1 at different temperatures. As temperature increased from 20 °C to 120°C, the real and imaginary parts of dielectric permittivity increased

approximately by an order of magnitude at the low frequency regime below 10 kHz. However, as temperature increased from 120°C to 200°C, the permittivity values decreased. Since variation in the low frequency regime are usually indicative of interfacial polarizations we believe that the role of bound water interface dictated the trends observed in this regime. As temperature increased from 20 °C to 120 °C water mobility could have increased, eventually leading it to boil and evaporate between 100 °C and 120 °C. This increase in water mobility would have thereby affected ion mobility and interfacial energies, causing the observed increase in the trends. Beyond 120°C, the evaporation of water resulted in the reversal of trend at these low frequencies. Between 10 kHz and 1 MHz, the properties showed similar trend in the given temperature range but the magnitude of change is not substantial. However zooming in we can observe a relaxation process, which sustains and becomes more prominent as temperature is increased beyond 120 °C in the insets. Considering the presence of bitumen, the relaxation observed in high frequency regime could be indicative of motion of local side chains of bitumen as was also observed by Chen et al¹.

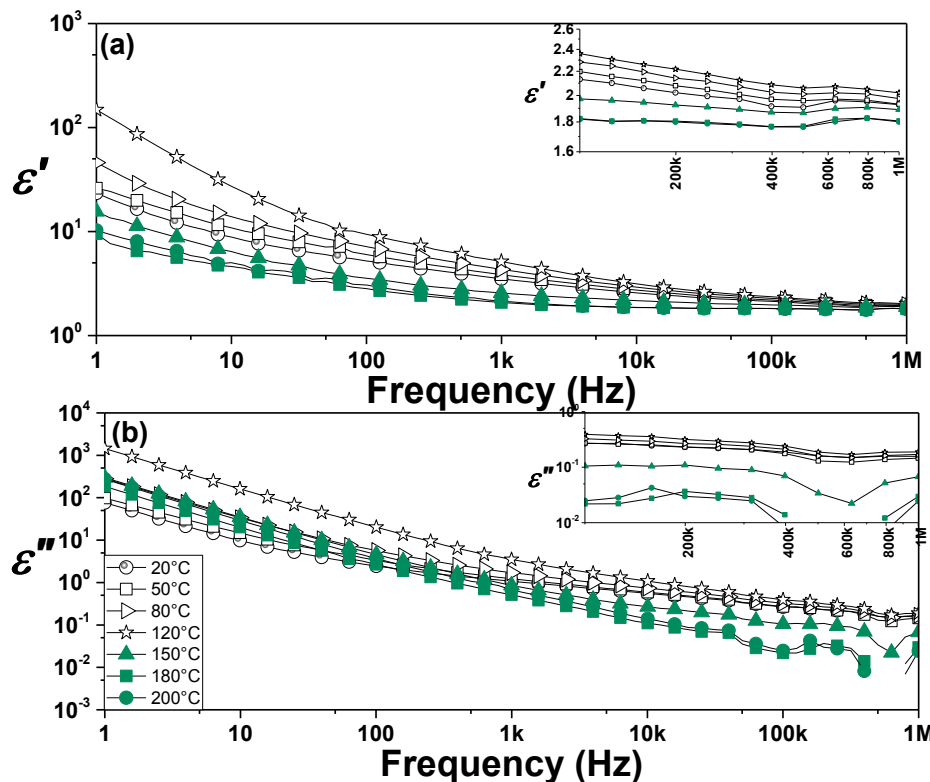


Figure 4-2. (a) Dielectric constant (b) Dielectric losses of Oil Sands 1 when swept from 1Hz to 1MHz as a function of temperature. Inset of (a) and (b) zooms into frequency regime where β relaxations are observed.

The frequency spectra of conductivity ($\sigma_{eff} = \sigma'_T = \omega \epsilon_0 \epsilon''_T$) for Oil Sands 1 at different temperatures is given in figure 4-3. The conductivity spectra with temperature shows a dispersion indicating frequency independent constant conductivity at low frequencies and frequency dependent conductivity at high frequencies varying approximately as a power of frequency. This indicates that in the given temperature range of 20 to 200°C, Jonscher's Law stays valid. As mentioned before, such conductivity dispersion is universally observed in disordered materials and is predicted to be due to hopping mechanism². It can be observed that for any given temperature, conductivity covers a range of almost four orders of magnitude with increasing frequency. As temperature is increased from 20°C to 120°C, the total conductivity increases by an order of magnitude at the low frequency edge, indicating that dc conductivity is more thermally activated. Conductivity at the high frequency edge does not change significantly with temperature, except that hopping frequency, f_h marking the onset of ac conduction also increases with temperature. As mentioned earlier, Oil Sands 1 has trace amounts of water indicating that it may be present as bound water having dissolved ions and dispersed clay particles as compared to free water channels resulting in hopping conductivity phenomena. This further supports our hypothesis about hopping conduction in oil sands discussed previously. As temperature is increased, these bound water zones become mobile, indicating increased dc conductivity. Further, from 120°C to 180°C, it is observed that the total conductivity reduces with temperature rise. This could be because all bound water must have vaporized around 120°C. Above 120°C the observed trends could be because of the conduction through charge carriers in viscosity reduced bitumen of oil sands. After observing a decreasing trend, it is also observed that from 180 to 200°C the overall conductivity increases. This could be attributed to increased mobility of charge carriers in viscosity reduced bitumen phase. At temperatures between 120°C to 200°C, it is also observed that the conductivity at the high frequency regime rises unsteadily. This could be because charge carriers in viscosity reduced bitumen undergo sub-diffusive back and forth motion.

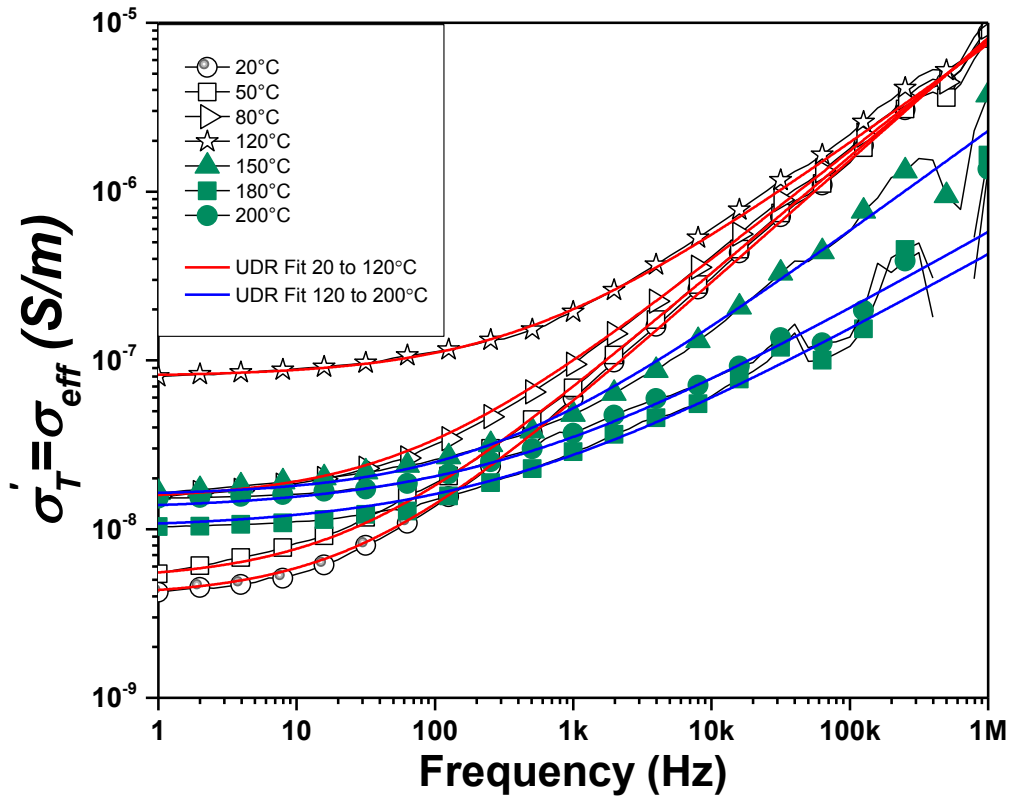


Figure 4-3. Conductivity spectra of Oil Sands 1 measured as a function of temperature and fitted with Universal Dielectric Response (UDR) or Jonscher's Law.

The modulus spectrum indicated by M'' with frequency at different temperatures gives a clear indication of conduction relaxations, MW and dipole polarizations in Oil Sands 1 as can be seen in Figure 4-4. The M'' peak observed in the low frequency regime indicate slow relaxations and could be attributed to the presence of conduction relaxations due to bound water carrying ions in these oil sands. As temperature increases from 20 °C to 120°C, the peak value reduces indicating an increase in conductivity as seen in figure 8 due to increased mobility of ions in these bound water zones. As temperature is increased from 120 °C to 200°C, the peak values start increasing, indicating reduction in conductivity as discussed in the previous paragraph. Further, the peak values also shift towards higher frequencies at these temperatures, indicating that reduced viscosity of bitumen may have allowed more long-range ion conduction through these oil sands. At greater than 100 kHz another relaxation is observed which can be attribute to be due to polarizations in

local side chains of bitumen. The reduction of these relaxations with increasing temperatures from 20 °C to 200 °C, could mean that the dipole relaxations in bitumen increased with decreasing viscosity of bitumen.

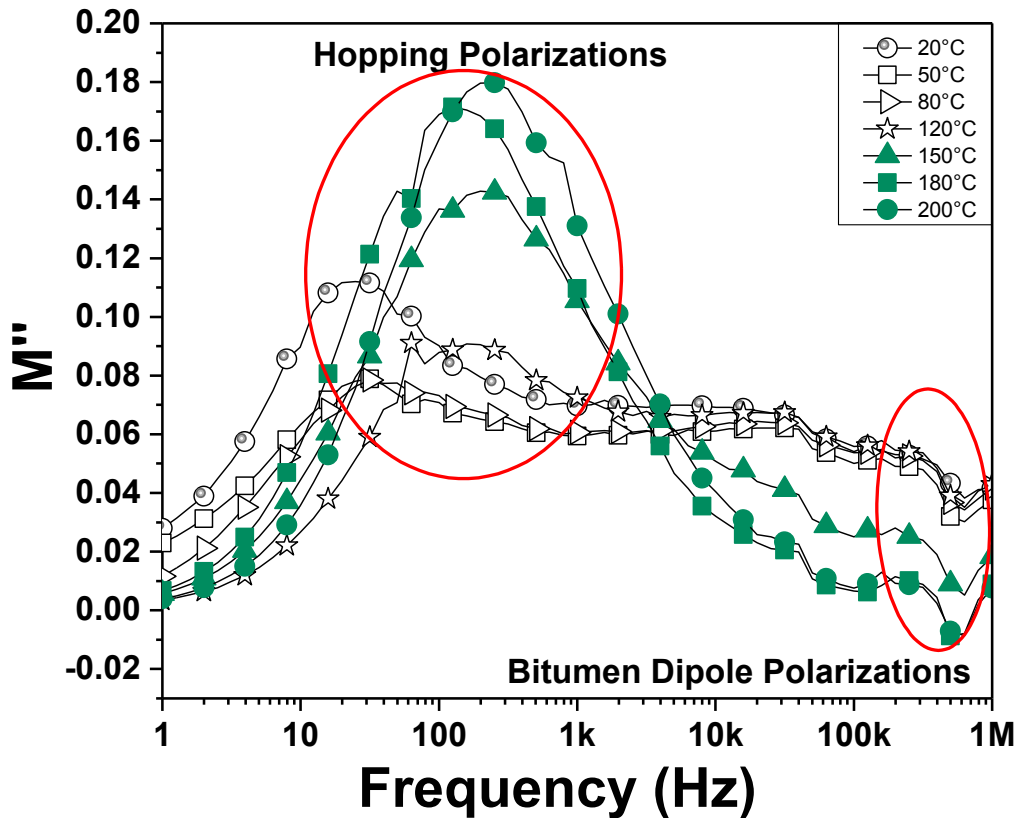


Figure 4-4. Modulus spectra of Oil Sands 1 as a function of temperature depicting hopping polarizations and bitumen dipole polarizations.

As can be seen from figure 4-5, the loss tangent of Oil Sands 1 having least water content is low at 2 at 1 Hz frequency and 0.1 at higher frequencies between 1kHz and 1 MHz. So also a relaxation is observed in this frequency range as is predicted to be due to bitumen relaxations. As temperature is increased from 20 to 120°C, it can be observed that the loss tangent increases more at 1 Hz frequency than between 1 kHz and 1 MHz. As temperature increases beyond 120°C to 200°C the data shows greater variations at frequencies around the relaxation of bitumen indicating that it undergoes physical changes at these temperatures. Thus at these temperatures, the loss tangent of

Oil Sands 1 decreases between 1 kHz and 1 MHz attributed to the role played by bitumen molecules in the system.

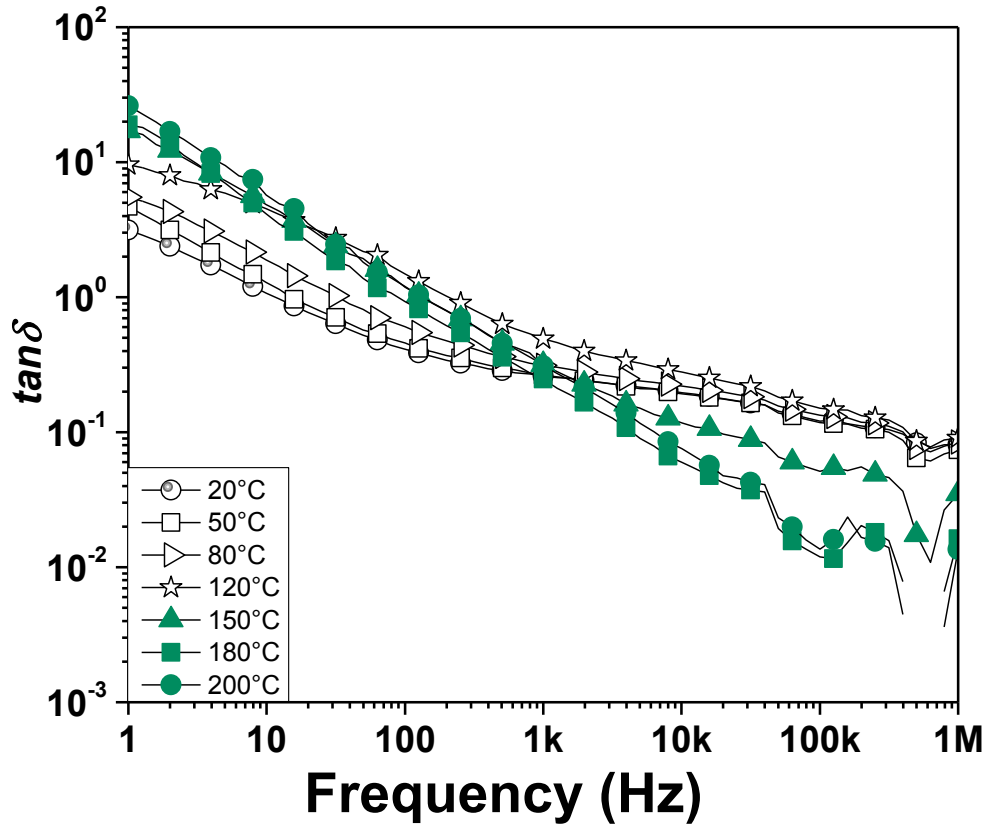


Figure 4-5. Loss tangent of Oil Sands 1 as a function of temperature.

4.3.2 Temperature Based Impedance Spectroscopy of Oil Sands 2 to 4

As mentioned earlier, since Oil Sands 2 to 4 have similar electrical behavior showing the presence of conduction relaxation, MW relaxations and electrode polarizations, it is sufficient to represent their average temperature based behavior in terms of Oil Sands 2. Since complex permittivity and conductivity are complementary to each other, we infer mechanisms from the conductivity spectra for Oil Sands 2 to 4 as they are more conductive in nature because of the increasing water and clay content in them.

Figure 4-6 depicts frequency dependence of conductivity ($\sigma_{eff} = \sigma'_T = \omega \epsilon_0 \epsilon''_T$) and imaginary part of Modulus M'' at different temperatures for Oil Sands 2. As temperature is increased from 20 to 120 °C, conductivity values given in figure 4-6 (a) increased only slightly, dominated by dc

conduction mechanism. Electrode polarization effects reduced due to increased mobility of water at these temperatures. DC conduction in Oil Sands 2 to 4 is believed to be due to the presence of more free water channels in the form of pendular connections between sand grains as compared to just the presence of isolated bound water zones in Oil Sands 1. When temperature was increased from 120 °C to 200 °C the conductivity value decreased and displayed a more sharp appearance of ac conduction relaxation frequency. Thus at temperatures above 120 °C, it was observed that Oil Sands 2 behaved similar to Oil Sands 1, due to the evaporation of water, which resulted in reduction of dc conduction and simultaneous predominance of conduction relaxation mechanism. Modulus spectroscopy in figure 4-6 (b) also depicts more clearly these effects. It can be observed that at temperatures between 20 °C and 120 °C the modulus peaks center around high frequencies indicating the dominance of long range dc conduction in free water channels before the peak frequency. The peak also signifies relaxations due to MW polarization due to interfaces formed by free water. As temperature was increased from 120 °C to 200 °C, the modulus peak shifted towards the low frequency regime indicating the presence of conduction relaxation mechanisms dominating at higher temperatures. At higher temperatures, the relaxations due to local side chains of bitumen also starts becoming visible and it can be concluded that the mechanisms in Oil Sands 2 to 4 become similar to those in Oil Sands 1 at these temperatures.

As can be seen from figure 4-7, the loss tangent of Oil Sands 2 having more water content than Oil Sands 1 is approximately 10 at 1 Hz frequency and 1 at higher frequencies between 1kHz and 1 MHz. So also a relaxation is observed in this frequency range as is predicted to be due to interfacial or MW polarizations. As temperature is increased from 20 to 120°C, it can be observed that the loss tangent does not change significantly however the peak due to interfacial polarizations does reduce indicating loss of water from the system. As temperature increases beyond 120°C to 200°C the data shows disappearance of the interfacial polarization peak and also shows greater variations at frequencies around the relaxation of bitumen indicating that it undergoes physical changes at these temperatures. Thus at these temperatures, the loss tangent of Oil Sands 2 decreases between 1 kHz and 1 MHz attributed to reduction in interfacial polarizations and increased dominance of dipole polarizations due to bitumen molecules in the system.

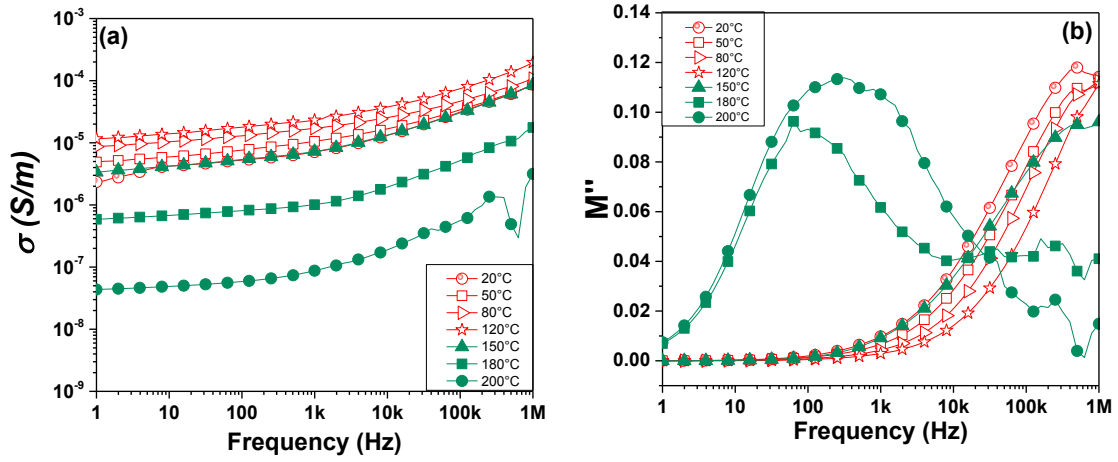


Figure 4-6. (a) Conductivity spectra and (b) Modulus spectra of Oil Sands 2 as a function of temperature

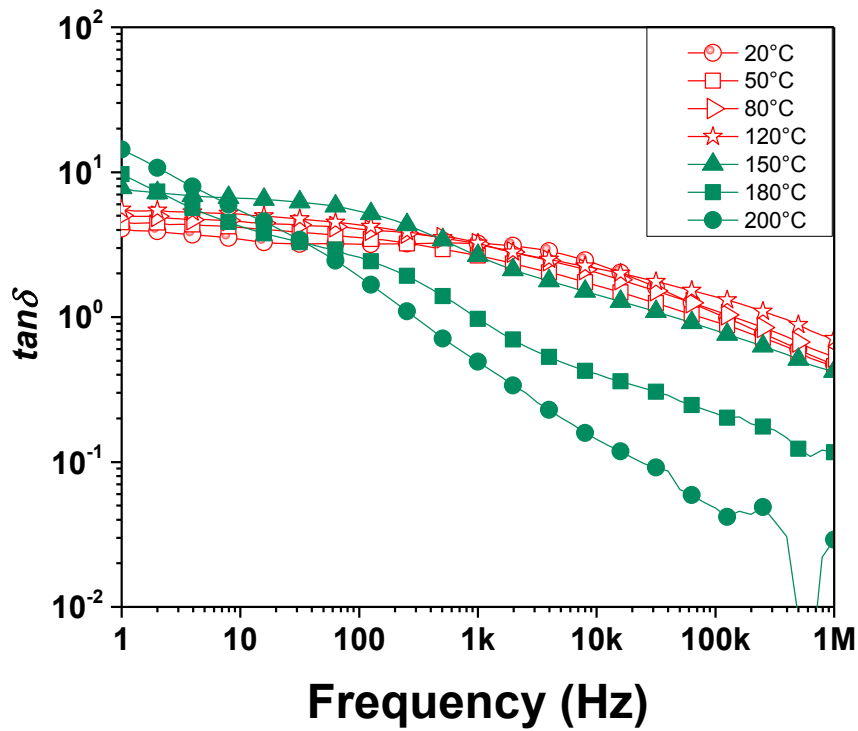


Figure 4-7. Loss tangent of Oil Sands 2 as a function of temperature.

4.3.3 Temperature Based Impedance Spectroscopy of Oil Sands 5 and 6

The temperature based electrical behavior of Oil Sands 5 and 6 having most water and clay content are represented in terms of Oil Sands 5. These oil sands having high clay content between 15 to 18% result in entrapping more water in the fine clusters and thus tend to have lots of free water zones. Figure 4-8 depicts conductivity spectroscopy ($\sigma_{eff} = \sigma_T' = \omega \epsilon_0 \epsilon_T''$) and Modulus M'' for Oil Sands 5 at different temperatures. As can be seen from the conductivity spectrum, the dc conduction seems to be the dominating mechanism with conductivity increasing only slightly when temperature is increased from 20 to 120°C. However as temperature is increased from 120 to 200°C with loss of water in the oil sands, the conductivity decreases and shows to have conduction relaxations as was shown in the previous two cases.

Modulus spectroscopy shows the absence of any bulk relaxation mechanisms except at very high frequencies near 1 MHz. This indicates the dominance of dc conduction at temperatures between 20 °C and 120 °C, over MW relaxation processes. It however clearly indicates the presence of conduction relaxation at temperatures between 120 and 200°C, indicating that at these temperatures all oil sands behave similarly.

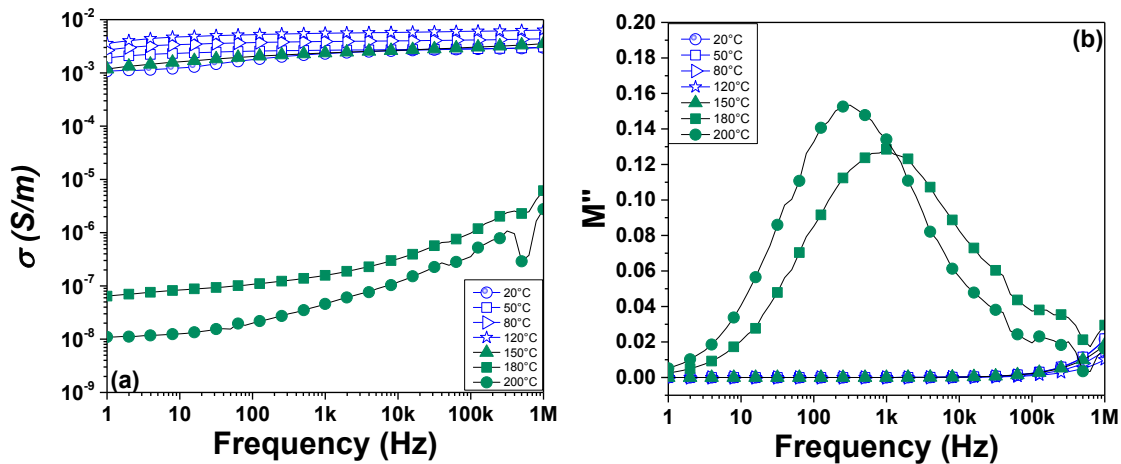


Figure 4-8. (a) Conductivity spectra and (b) Modulus spectra of Oil Sands 5 as a function of temperature

As can be seen from figure 4-9, the loss tangent of Oil Sands 5 having more water content than Oil Sands 2 to 4 as well as Oil Sands 1 is different from them due to the dominance of free water channels giving rise to dc conduction in the medium. So also a relaxation is observed in this frequency range as is predicted to be due to interfacial or MW polarizations. As temperature is increased from 20 to 120°C, it can be observed that the loss tangent increases significantly due to increased dc conduction through more mobile free water channels. As temperature increases beyond 120°C to 200°C the data shows disappearance of dc conduction and interfacial polarization peaks and also shows greater variations at frequencies around the relaxation of bitumen indicating that it undergoes physical changes at these temperatures. Thus at these temperatures, the loss tangent of Oil Sands 5 decreases between 1 kHz and 1 MHz attributed to reduction in interfacial polarizations and increased dominance of dipole polarizations due to bitumen molecules in the system.

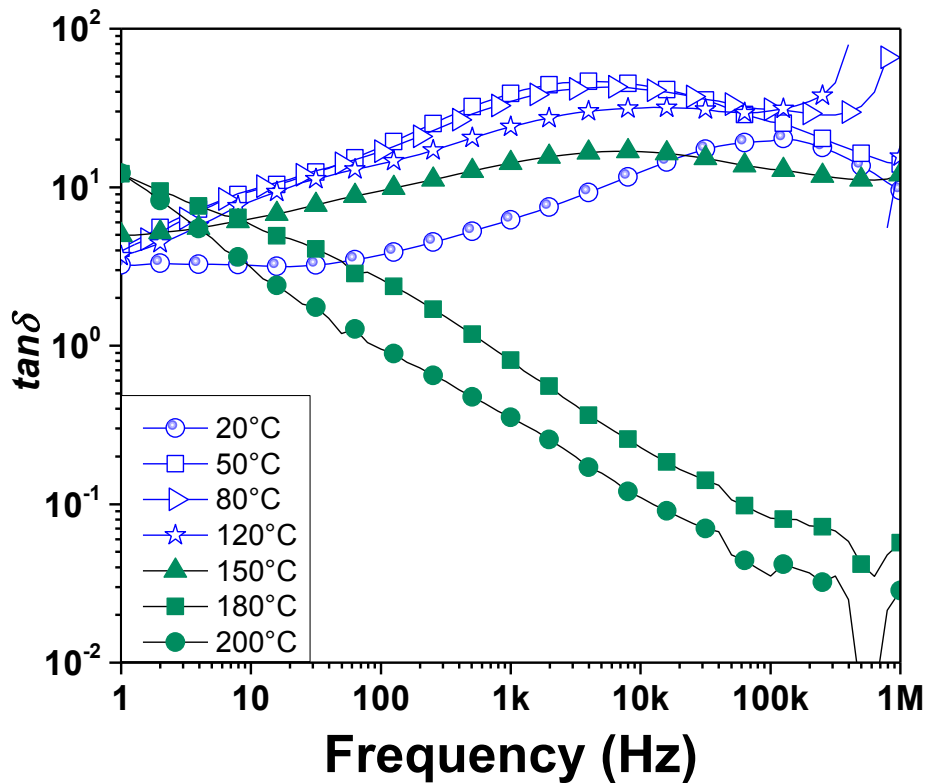


Figure 4-9. Loss tangent of Oil Sands 5 as a function of temperature.

4.3.4 Impedance Spectroscopy of Oil Sands 1 to 6 on Cooling After Heating

Since after 120 °C, the behaviour of all oil sands begin to converge, we suspected that all oil sands should behave in a similar manner at room temperature as well. Hence impedance spectroscopy was conducted on all oil sands after they were cooled down to room temperature after heating to 200 °C as shown in figure 4-10. It was observed in the above results that all oil sands showed to behave in a similar manner at 200 °C when the water was lost from its matrix, no matter what the initial grade of the oil sands was. At cooling down to room temperature, the complex permittivity of all oil sands showed to be almost constant with frequency with ϵ'_T to vary between 1 to 4 and ϵ''_T to vary between 10^{-3} to 10 as shown in figure 4-10(a) and (b), respectively. A peak variation can be seen clearly in figure 4-10 (b), which can be predicted to be due to relaxations in bitumen molecules. Earlier such relaxations were not visible in Oil Sands 2 to 6, because of the overshadowing effect of MW and conduction due to presence of water channels with clay. This implies that the relaxations in bitumen, though masked by the mentioned effects are still present in these oil sands at the frequencies between 100 kHz and 1 MHz. These dipolar relaxation effects due to bitumen are further observed in M'' and $\tan\delta$ spectrums as well in figure 4-10(d) and (e), respectively. The conductivity spectra shown in figure 4-10(c), does not show a constant dc conductivity region any more, which is attributed to the loss of conductive water phases. The increasing conductivity with frequency in these oil sands devoid of water channels can be thus attributed to the charge hopping mechanisms through bitumen and silicate minerals. Therefore as oil sands are heated to high temperatures and cooled down to room temperature, they have identical electrical conduction and polarization mechanisms, with the dominance of charge hopping ac conduction and dipole polarizations of bitumen molecules. The dc conduction, MW polarizations and electrode polarizations are thus lost due to loss of water from the system.

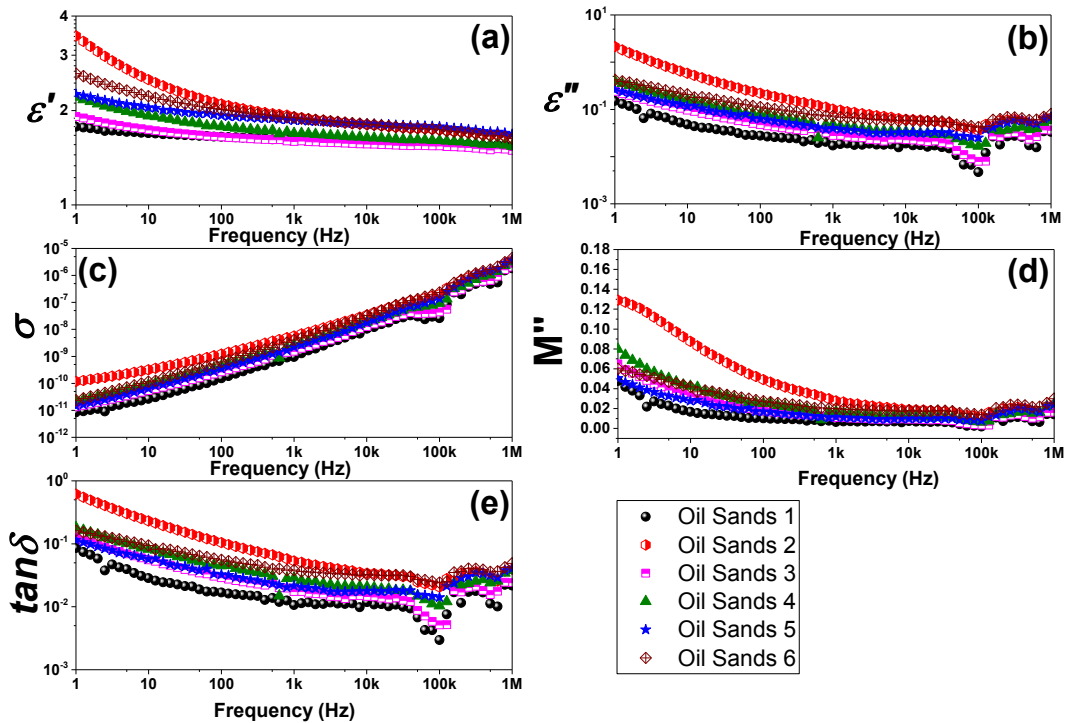


Figure 4-10. Summary of electrical properties of all six oil sands when cooled down to room temperature after heating to 200 (a) Dielectric Constant (b) Dielectric losses (c) Conductivity (d) Imaginary Modulus (e) Dissipation factor

4.4 Conclusions

DC conductivity of Oil Sands1 having least amount of water (0.3%) increased as temperature was increased from 20 to 120°C, while its ac conductivity did not change significantly indicating nearly constant loss at high frequencies. Between 120 °C and 200 °C, dc conductivity reduced significantly and the ac conductivity showed non-linear dependence at high frequency indicating that the dielectric losses were not constant any more. Oil Sands 1 also showed the presence of dielectric relaxations due to molecular motion of bitumen between 100 kHz and 1 MHz. The mechanisms suggest that capacitive heating set at frequency between 100 kHz and 1 MHz for targeting dipole relaxations in bitumen could be very suitable for such oil sands. Oil Sands 2 to 4 showed dominance of MW relaxations due to presence of interfacial and free water channels from 1 kHz to 1 MHz. Hopping frequencies appeared at higher values for these oil sands as compared

to Oil Sands 1 indicating more long range ion transport as compared to sub-diffusive motion. As temperatures were increased to 120°C, dc conduction increased and loss tangent peaks due to MW relaxations reduced in magnitude. Beyond 120°C, with loss of water in the oil sands, the effective conductivity reduced and hopping frequency shifted towards lower values. Frequency tuned capacitive heating could be a suitable method of heating such oil sands. Oil Sands 5 and 6, showed dominance of the dc conduction mechanism over polarization mechanisms due to the presence of connected free water channels trapped in fine clusters. As temperature was increased to 120°C, their dc conductivity increased. However, beyond this temperature till 200°C, effective conductivities reduced with emergence of dispersion due to conduction relaxations in these oil sands. Joule heating could be most suitable mechanism of heating such oil sands initially till they change in property after which capacitive heating can be carried out set around the dipole relaxation frequency of bitumen molecules. The dielectric constant and conductivity showed to increase with increasing water content of oil sands at all frequency with maximum increase of dielectric constant at 1 Hz as compared to 1MHz while the opposite was observed for conductivity. On cooling down to room temperature after heating to 200°C all oil sands showed the presence of dipole relaxations due to bitumen. This study would pave the way in determining optimization techniques in choosing and tuning suitable frequency regimes for carrying out efficient electrical heating on heterogeneous oil sands as was investigated in Chapters 5, 6 and 7.

4.5 References

- (1) Chen, F.; Taylor, N.; Kringos, N.; Birgisson, B. A Study on Dielectric Response of Bitumen in the Low-Frequency Range. *Road Mater. Pavement Des.* **2015**, *16* (sup1), 153–169.
- (2) Dyre, J. C.; Schröder, T. B. Universality of Ac Conduction in Disordered Solids. *Rev. Mod. Phys.* **2000**, *72* (3), 873.

Chapter 5 Characterization of Resonant Autotransformer for Conducting Capacitive Heating of Oil Sands

5.1 Introduction

The second part of the study was to investigate electrical heating pattern in oil sands in the radio frequency (RF) range so as to correlate it with the dynamic conduction and polarization mechanisms concluded from experiments discussed in Chapters 3 and 4. The results of this study are divided between Chapters 5, 6 and 7. Chapter 5 discusses the characterization studies of the radio frequency generator used for carrying out capacitive heating of oil sands whereas Chapters 6 and 7 discuss observations of heating patterns correlated to electrical to dynamic electrical behavior of oil sands as well means of controlling and optimizing the heating based on the changes. The combined results of these chapters would enable prediction of operational strategies for maintaining or improving the heating process allowing it to be uniform and continuous when implemented in a real reservoir environment.

RF heating in industries for processing various materials such as drying textiles, moisture leveling of food products, welding of plastic and heating of wood is usually fixed at 6.78, 13.56 and 27.12 MHz frequencies¹. The frequency is usually fixed at these values which pertain to the industrial, scientific and medical (ISM) radio bands. The power ratings of these RF heating equipments range from 40 to 200 kW². Conventional industrial scale RF heating systems consists mainly of two sections: a generator and an applicator. These RF heating systems fall into two categories; first and most popular being the free running oscillator system representing 99% of the RF systems used in the industry. The second being the second being the 50Ω technology employing a crystal oscillator with subsequent amplification¹.

A schematic view of a free running oscillator RF heating system is shown in figure 5-1¹. Alternating current (AC) voltage from the mains is stepped up by a transformer to several kilovolts. The output AC voltage from the transformer is then rectified to direct current (DC) voltage using a smoothed rectifier circuit which is then applied to a triode valve which is an oscillator circuit operating under class C conditions converting DC input to high frequency power at a set frequency of 13.56 MHz or 27.12 MHz. The overall system efficiency of this conversion is 50 to 60%. The high frequency power is then fed to a tank circuit consisting of a fixed inductance, a variable inductance and an applicator circuit which consists of the material to be processed placed between

capacitive electrodes. To carry out heating at the set frequency, the applicator circuit is matched to the tank circuit by changing the series or parallel variable inductance, thus allowing coupling of power from the generator to the material to be processed. Thus such a RF heating system is a fixed frequency system, disabling any frequency tuning or process monitoring capabilities during the heating process.

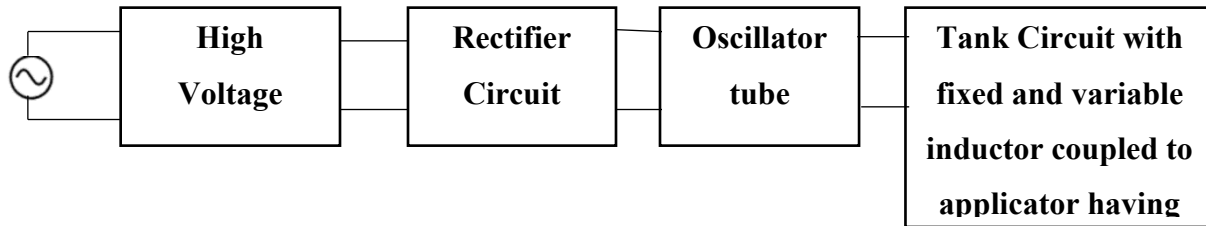


Figure 5-1. Block diagram free running oscillator used to carry out industrial RF heating¹.

In the 50Ω technology as shown in figure 5-2, a crystal oscillator provides a weak signal at a stable frequency of 27.12 MHz (again being a fixed frequency system) which is subsequently amplified and transmitted through a coaxial cable to the applicator ¹. An impedance-matching network is automatically tuned to maintain a fixed impedance of 50Ω in the applicator circuit to ensure maximum coupling of energy is achieved.

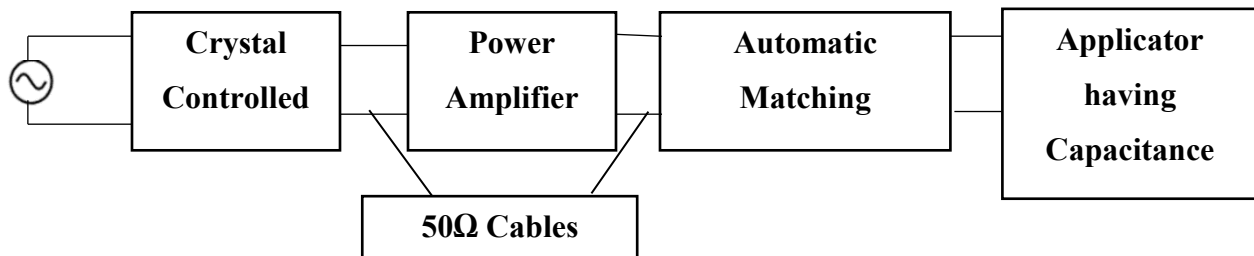


Figure 5-2. Block diagram of 50Ω technology system used for carrying out industrial RF heating ¹.

Noting that these industrial RF heaters were fixed frequency devices, they would not be useful for the purpose of our study to carry out investigations concerning the need to tune frequency following the impedance changes in oil sands arising during the heating process. There was also a need to monitor these impedance changes during the heating process, which could not be provided by the mentioned conventional RF heaters. In lieu of these requirements, a resonant

autotransformer which was essentially a distributed resonator, unlike the lumped tank circuits shown in the previous two cases for coupling with and matching impedance of the applicator was used. The resonant autotransformer was a modified Tesla Coil which had a resonance frequency of 220 kHz and could be frequency tuned. A maximum of 400 W was supplied to the resonant autotransformer which resulted in generation of sufficient electric field energy for capacitive heating of oil sands at lab scale. In order to ensure safe operations and non-interference the resonant autotransformer was placed inside a faraday cage which provided adequate shielding.. Also, any impedance changes occurring in the oil sands could be monitored via changes in the current, phase and resonance frequency which was essential to carry out the heating investigations as will be discussed in the next section. In order to ensure absolutely safe working conditions, all experimental observations were conducted from outside of the faraday cage which contained all the electromagnetic energy within it.

5.2 Resonant Autotransformer

The resonant autotransformer used in this study had the following general capabilities:

1. **Heating Capabilities:** Ability to supply sufficient electrical field energy and frequency for heating oil sands at lab scale.
2. **Probing Capabilities:** Avenues for monitoring variation in input voltage, current, phase and frequency following the changes in oil sands during the heating process.
3. **Heat Control Capabilities:** Capabilities of tuning frequency and input power to increase or maintain the heating process.

The resonant autotransformer looks like a helical coil having 260 turns of 12 AWG copper wire as shown in figure 5-3(a). Its main attributes can be summarized in calling it a “reactive near-field distributed resonator”. The characteristic features of this resonator can be best discussed by describing these terms as given below starting with the end term:

1. **Resonator** - Being a resonator it stores electrical energy in its electric and magnetic fields (via its capacitance and inductance respectively). Also, maximum storage of energy occurs at a characteristic resonant frequency which is a function of the resistance (R), capacitance (C) and inductance (L) of the system. An alternating-current (AC) power signal is applied to the resonator

at a specific frequency approximated around 220 kHz that drives the helix in resonance with its surrounding stray capacitance. When oil sands having its unique load impedance (Z) (being a function of its electrical properties and electrode configurations) is electrically connected to the resonator, the total system adjusts to a unique resonance frequency of operation. Following this, any impedance changes to the oil sands load due to increasing temperatures also reflects on the system resonance and therefore allows frequency tuning to keep up with the changes in the circuit.

- 2. Distributed Resonator** - Being a distributed resonator means that in such a system the electric and magnetic field energies are not isolated from each other but are distributed along the length of the resonator as shown in figure 5-3(b). This aids in generating high electric fields and low currents in a distributed fashion as was needed for our specific heating studies. The helix is made to function as a quarter-wave resonator, where the helix's electrical length is comparable to the wavelength of the applied signal and the input electric and magnetic fields undergo temporal and spatial phase transitions as a function of the geometry and aspect ratio of the winding. The inductance and capacitance of the helix is cumulatively distributed generating a standing wave pattern with one end of the helix fixed and the other open. Following the formulations published recently ³, the electric field, voltage, and current distribution in the helix as a function of physical turn number as shown in figure 5-3(c) were simulated based on observed phase shift, input current and voltages. The helical coil having 260 turns is able to produce an electric field of ~ 3 MV/m at the voltage anti-node, with a reduction of current to 0.004 A at the same voltage anti-node location occurring at the top of the coil when a nominal input voltage of 10V is applied. Due to conservation of energy, the current is greatly reduced but is also temporally 90 degrees out of phase with the voltage.
- 3. Near-Field Distributed Resonator** - A distinctive feature of a near-field distributed resonator is that the presence of the material load typically has a significant impact on the device's field configuration and circuit variables such as voltage, current and overall input power ⁴. In essence, the subject material, through its electrical properties, becomes a part of the circuit or an internal component to the resonating system. Therefore any changes in the electrical properties of oil sands as temperature rises is reflected on the current, voltage and phase being monitored. Further being a resonant device, the changes in the material impedance also reflects in the shift of the initial resonance frequency and therefore frequency re-tuning can be carried out to sustain or increase the heating.

4. **Reactive Near-Field Distributed Resonator** - Finally being a reactive near-field distributed resonator, this is a reactive energy system unlike a radiative energy systems, where the electrical energy that is not consumed in the oil sands is stored in the reactive near-field of the resonant autotransformer, improving the operation efficiency by reducing the overall time average electrical power consumption. Contrary to typical systems where the oil sand is considered as a load for the source to transmit power to, our system is in resonance with the oil sand element and any heating is due to the internal losses of the capacitor element (oil sands). Any energy that is not dissipated in the internal conductance/resistance is stored within the resonating system.

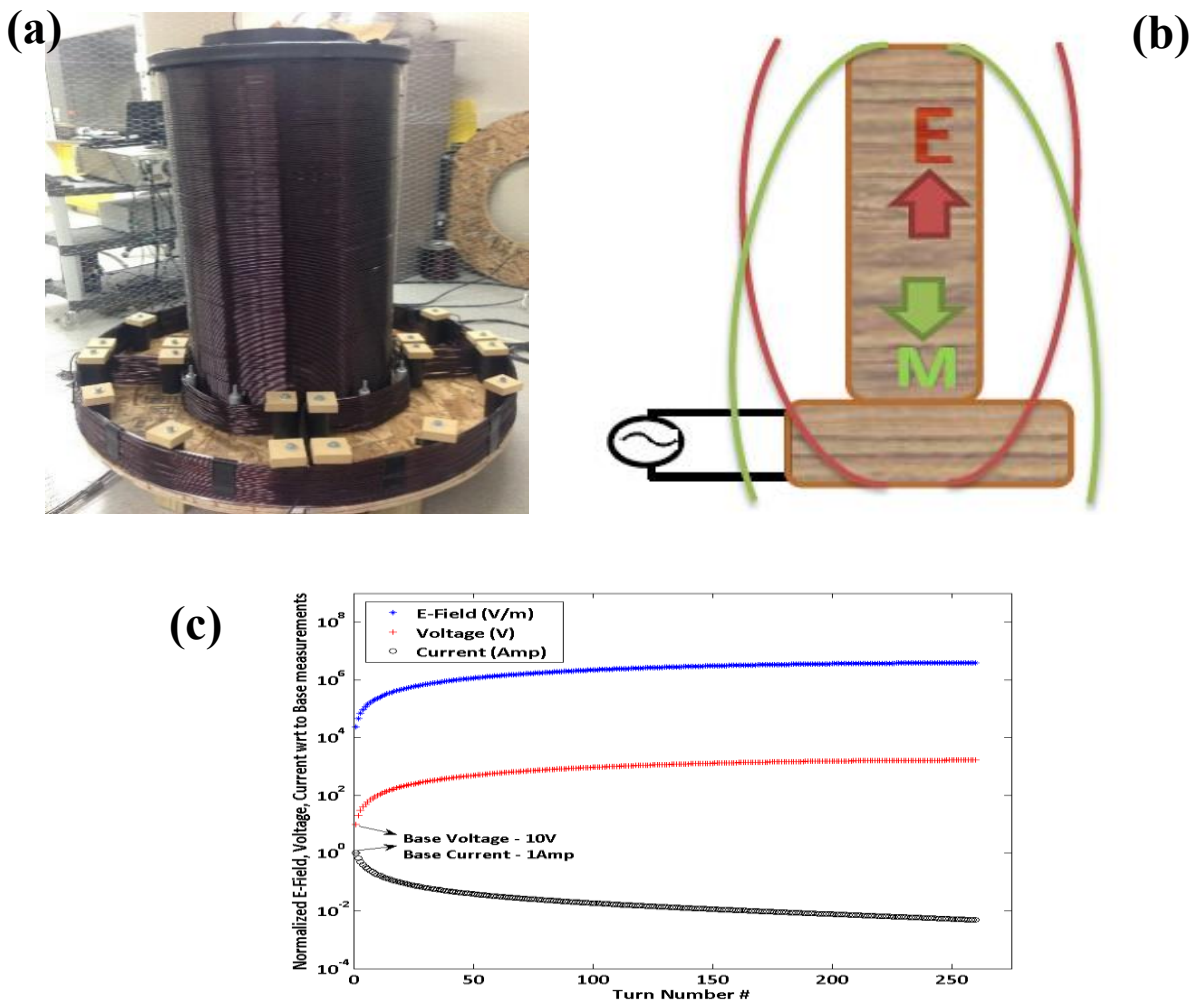


Figure 5-3. (a) Picture of resonant autotransformer placed inside a faraday cage in the backdrop. (b) Distributed nature of electric field and magnetic field in the resonant autotransformer. (c) Simulated results of electric and magnetic field magnitudes along turns of the resonant autotransformer.

5.3 Load Impedance Based Characterization Studies of Resonant Autotransformer.

In the previous section the main characteristics of the resonant autotransformer was discussed. This section will aim at understanding the variations in the working of the transformer when a load is electrically connected to it. Without the load, the resonant transformer resonates energy between the inductance of the coil and the stray capacitance of the air around it as shown in the circuit diagram in figure 5-4(a). With the load connected, which in our case is usually a dielectric material between parallel electrodes, an additional capacitance is connected to the system and it is crucial to understand how it affects the functioning of the resonator as shown in figure 5-4(b). The working of such a resonant transformer is dependent on the stray capacitance of the air around it. This makes it tough to determine the circuit behaviour in a lumped circuit method, since the system needs to be considered as a series of air capacitances distributed along the length of the coil which was out of the scope of this work. In order to determine the role of load capacitance in view of this inadequate information, this study mainly focused on how the resonance frequency and input current drawn into the overall circuit changes when load capacitance was varied. This enabled in determining suitable load capacitance and connection configuration to the transformer that would result in most efficient heating of oil sands which is considered in Chapter 6 and 7.

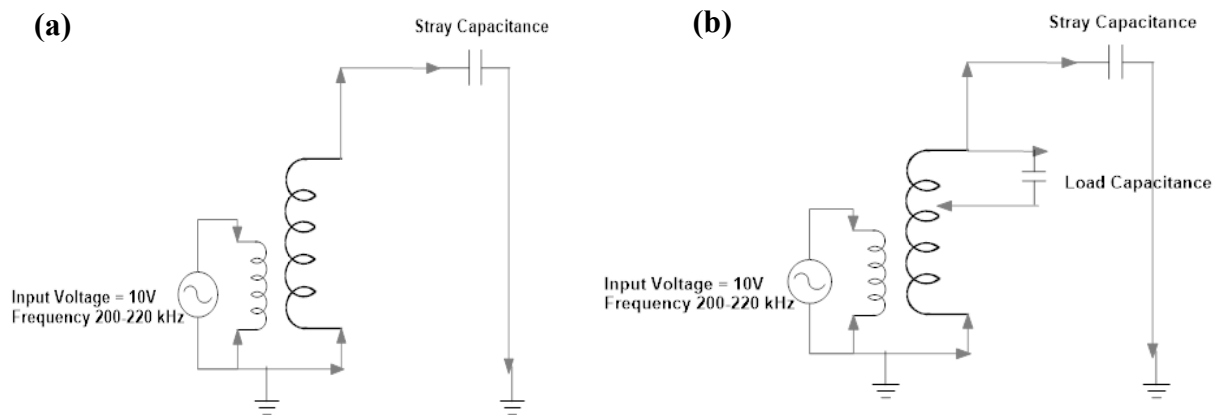


Figure 5-4, Circuit diagram of resonant autotransformer (a) without load capacitance and (b) with load capacitance

5.4 Material and Methods

The lab scale setup consists of a wall outlet supplying input power at 110V and 60 Hz to a function generator which was Agilent 33251A make having a bandwidth of 30 MHz and a power amplifier

which was an ALC Wideband Power Amplifier, 20 Hz-800 kHz, 2Vrms maximum input and 0-30Vrms output voltage. The function generator was able to tune the frequency to the required resonance frequency and stepped down the input voltage to 2Vrms. The power amplifier stepped up the input voltage of 2Vrms from the function generator to higher voltages of 5, 10, 15 or 20 V as required and was fed to the resonant autotransformer connected to the capacitance load. Frequency tuning was carried out using the function generator to keep the overall system at resonance. The input current at a specific voltage going from the power amplifier to the resonant autotransformer was measured using a current probe and oscilloscope. The oscilloscope also measured the phase angle between the input voltage and input current. The figure 5-5 given below is a block diagram of lab scale setup of resonant autotransformer with a capacitance load.

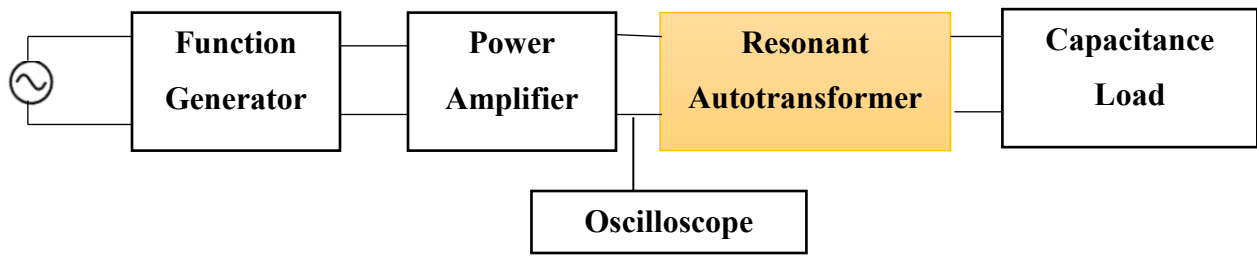


Figure 5-5. Block diagram of lab scale experimental set up for supplying the required energy to the resonant autotransformer with the capacitance load.

The capacitor load considered for this study is a parallel plate capacitor made of two circular copper electrodes having a dielectric material placed in between them as shown in figure 5-6. The edges of the copper electrodes were smoothed so that high electric fields between the electrodes would not generate sparks from the smooth edges. The position of the bottom electrode was fixed, however the top electrode could be moved along the test cell so that the required electrode spacing could be attained. The capacitor was housed inside a cylindrical test cell having 5cm inner diameter and 20 cm height. The test cell was made of virgin molded PTFE (Teflon) purchased from Enflo as Teflon is known to have extremely low dielectric loss with a loss tangent of 0.0002. This ensured that the test cell did not heat up dielectrically in the high field environment. Varying the capacitance of the load resulted in varying the overall impedance of the resonant autotransformer which affected the resonance frequency and the input current drawn into the coil. For the purpose of investigation, the capacitance of the load was varied in two ways:

1. By varying the dielectric material in the capacitor; (Air, Silica and Oil Sands)
2. By varying the spacing between electrodes in the capacitor for each type of dielectric material; (5cm, 10cm, and 20cm).

The manner in which the capacitor load was connected to the resonant autotransformer also resulted in affecting the overall working of the total system including its resonance frequency and input current drawn. Since there was no impedance matching circuit coupled between the resonant autotransformer and applicator having the capacitor load to be heated, connecting the bottom electrode of the capacitor to different turns of the helical coil helped in determining circuit connections where best impedance match could be observed for maximum energy transfer between the coil and the load. In the upcoming experiments, the top capacitor electrode was always connected to the 1st turn of the helical coil whereas the bottom electrode was connected to the 29th, 111th and 176th turn of the coil going from top to bottom respectively as shown in figure 5-6. This was studied so as to arrive at a least resistance circuit where maximum impedance match would be attained allowing maximum power transfer between the resonant autotransformer and the capacitance load. While carrying out these load characterizing experiments, the measured parameters were resonance frequency (RF), and input current (IC) using the oscilloscope. A specific dielectric material was first taken and studied for a specific electrode spacing along all three bottom electrode connection. Then the electrode spacing was changed and experiment repeated. The same procedure was carried out for the other dielectric materials investigated. The entire experimental procedure is best explained in table 5-1:

Table 5-1. Experimental Methodology for Characterising Load Based Performance of Resonant Autotransformer.

Measured Parameter	Dielectric Material	Electrode Spacing	Bottom Electrode Tapping		
			29 th	111 th	176 th
Resonance Frequency (RF)	Air ($\epsilon' = 1$) Silica ($\epsilon' = 2$ to 3)	5cm 10cm			
Input Current (IC)	Oil Sands (3% Water, 13% Bitumen, 15% fines and 69% coarse solids) ($\epsilon' = 5$)	20cm			

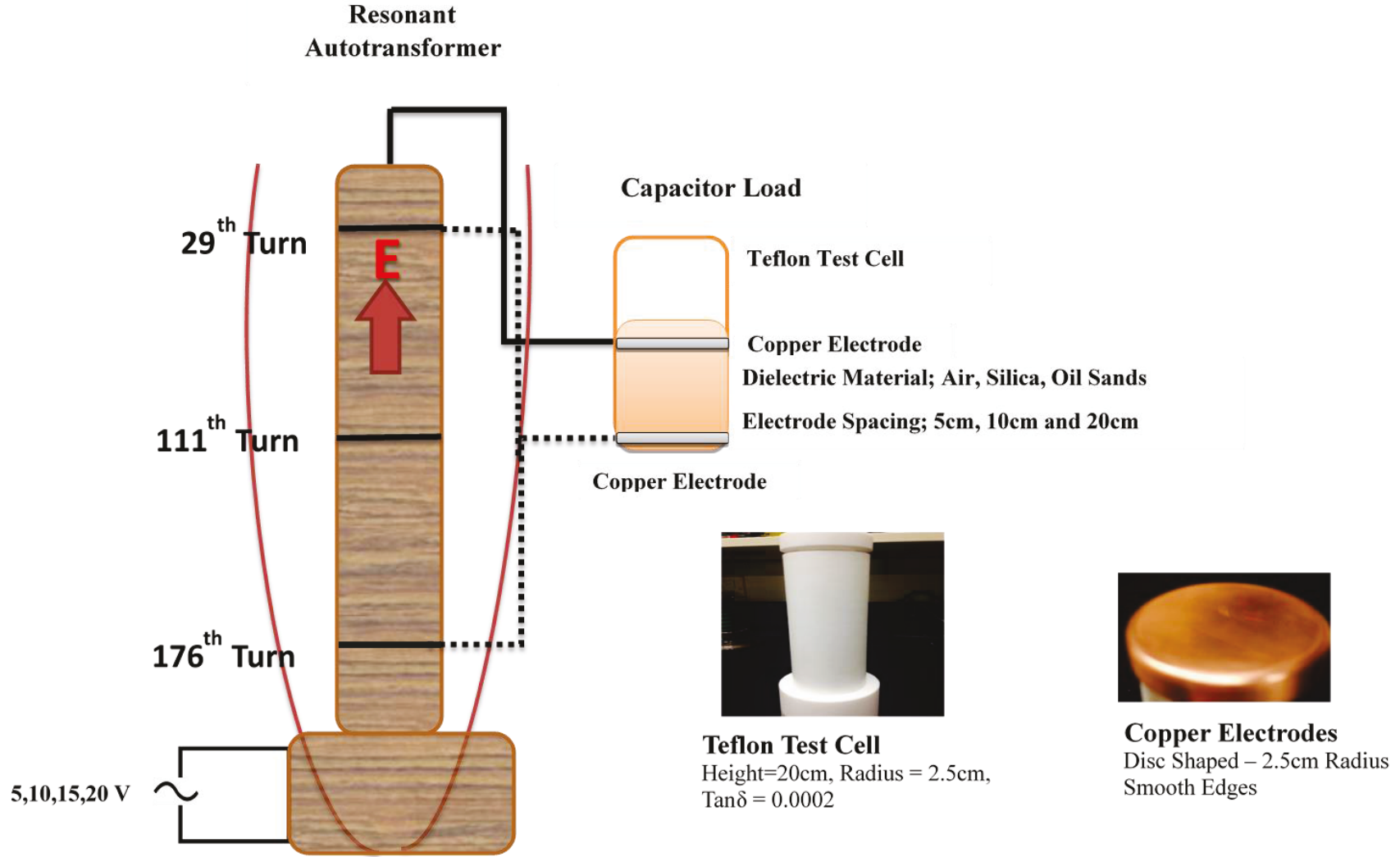


Figure 5-6. Schematic illustration of experiment conducted for characterizing working of a resonant autotransformer when connected to a capacitor load.

In the final set of experiments, the RF and IC of the resonant autotransformer system was studied in a comparative manner between the above mentioned small oil sands capacitor cell and a large sized oil sands capacitor cell by increasing the electrode area and keeping the spacing fixed at 5cm having dimensions as given in figure 5-7 below:

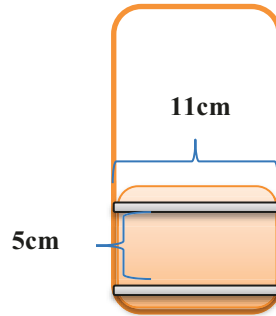


Figure 5-7. Large sized oil sands capacitor cell

The capacitance of both the big and small oil sands capacitance cell is calculated based on the equation given below and tabulated in table 5-2:

$$C = \epsilon_0 \epsilon \frac{A}{d} \quad (18)$$

Where, A is area of the capacitor electrode plate, d is the spacing between electrodes and ϵ is dielectric constant of oil sands and ϵ_0 is permittivity of free space.

Table 5-2. Capacitance of small and big oil sands capacitor cells

Parameters	Small Oil Sands Capacitor Cell	Large Oil Sands Capacitor Cell
Capacitor spacing	0.05m	0.05m
Capacitor plate area	0.0019625 m ²	0.0094985 m ²
Dielectric Constant of medium grade oil sands at 200 to 220 kHz @ 20°C	5	5
Free space permittivity	8.85E-12 F/m	8.85E-12 F/m
Capacitance	1.7 pF	8.4 pF

5.5 Results and Discussions

The initial results will be discussed in terms of the experiments conducted on the small test cell. The results will be discussed in terms of the effect of varying one experimental parameter with respect to other parameters in terms of the overall resonance frequency of the system and the input current drawn for different input voltages. For example, the effect of varying the load capacitance based on dielectric material will be initially studied based on electrode spacing and bottom electrode connection for the initial case, followed by varying the electrode spacing and later the bottom electrode connection. Following these discussions the results from comparing oil sands in small and large oil sands capacitance cell will be discussed.

5.5.1 Effect of Varying Dielectric Material

The dielectric materials considered such as air, silica and oil sands did not vary in their dielectric properties significantly as shown in table 5-1. However, even with such low variations in the dielectric constant, it was essential to understand how the resonance frequency and input current drawn by them at different input voltages would vary for a given electrode spacing and bottom electrode connection. The observations and discussions are given below:

5.5.1.1 Resonance Frequency (RF)

Figure 5-8 gives variation of RF for different dielectric materials for a given electrode spacing and a different bottom electrode connection. It can be observed that the least resonance frequency for all dielectric materials and electrode spacing occurs at 176th tap connection. This tends to indicate that the effect of load capacitance is felt most at this tapping location. It is understood from the simple relation given below that as capacitance (C) increases for a fixed inductance (L) the resonance frequency decreases:

$$\text{Resonance Frequency} = \frac{1}{\sqrt{LC}} \quad (19)$$

Since the effect of capacitance load is most felt at the 176th tapping location, it can be considered that best power transfer between the resonant transformer and capacitance load occurs when connected in such a configuration. Further, capacitance load is directly dependent on the dielectric constant of the material and inversely dependent on the electrode spacing from the relation in

equation (1). Oil Sands has the highest dielectric constant as compared to silica and air. So oil sands capacitance should be more than silica and air capacitance at a given electrode spacing. So it is observed that the resonance frequency for oil sands capacitance load is least as compared to silica and air for a given electrode spacing with maximum effect observed at the 176th tapping as seen in figure 5-8. It can be observed from figure 5-9, that at 176th tapping where the effect of capacitance is most felt, oil sands capacitance load having least electrode spacing at 5cm has least resonance frequency as well following the inverse law given in equation (1) and (2).

For all electrode spacing, the 29th connection does not show any difference in RF of the system between the three dielectric materials indicating that the effect of the capacitance load is not really felt by the resonant autotransformer at this tapping. 111th tapping also shows only slight difference between dielectric materials and electrode spacing.

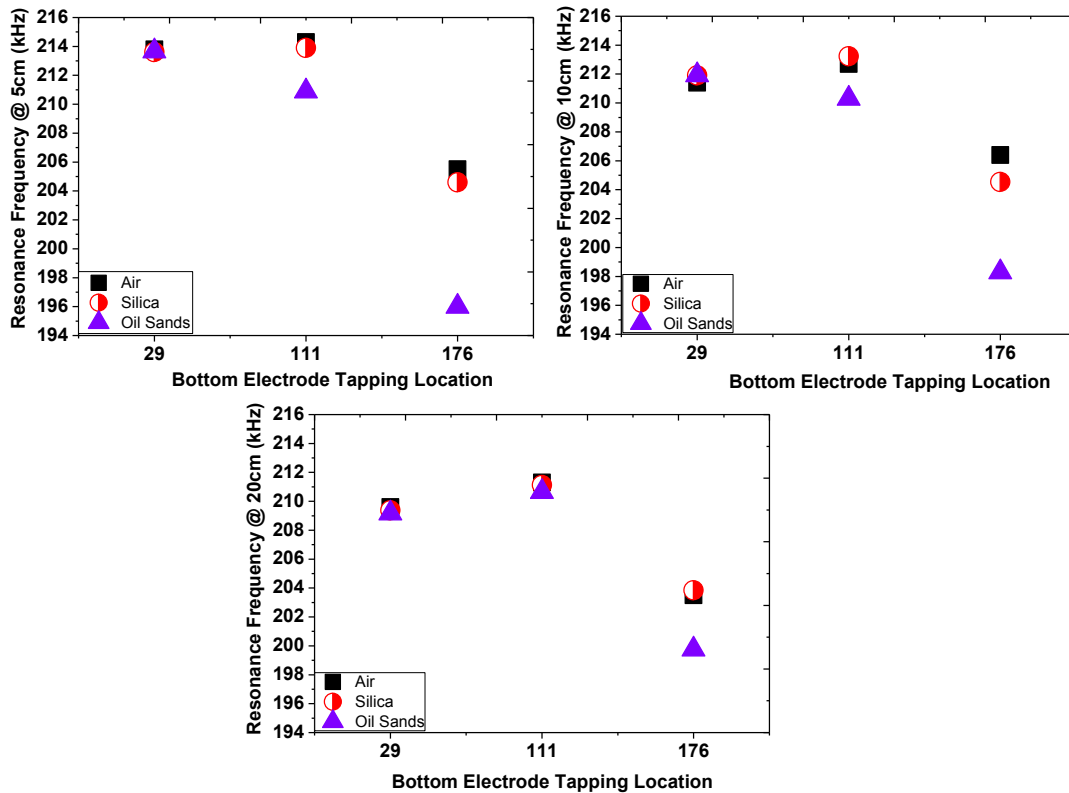


Figure 5-8. Variation of RF for different dielectric materials for a given electrode spacing when bottom electrode is connected at different turn connections.

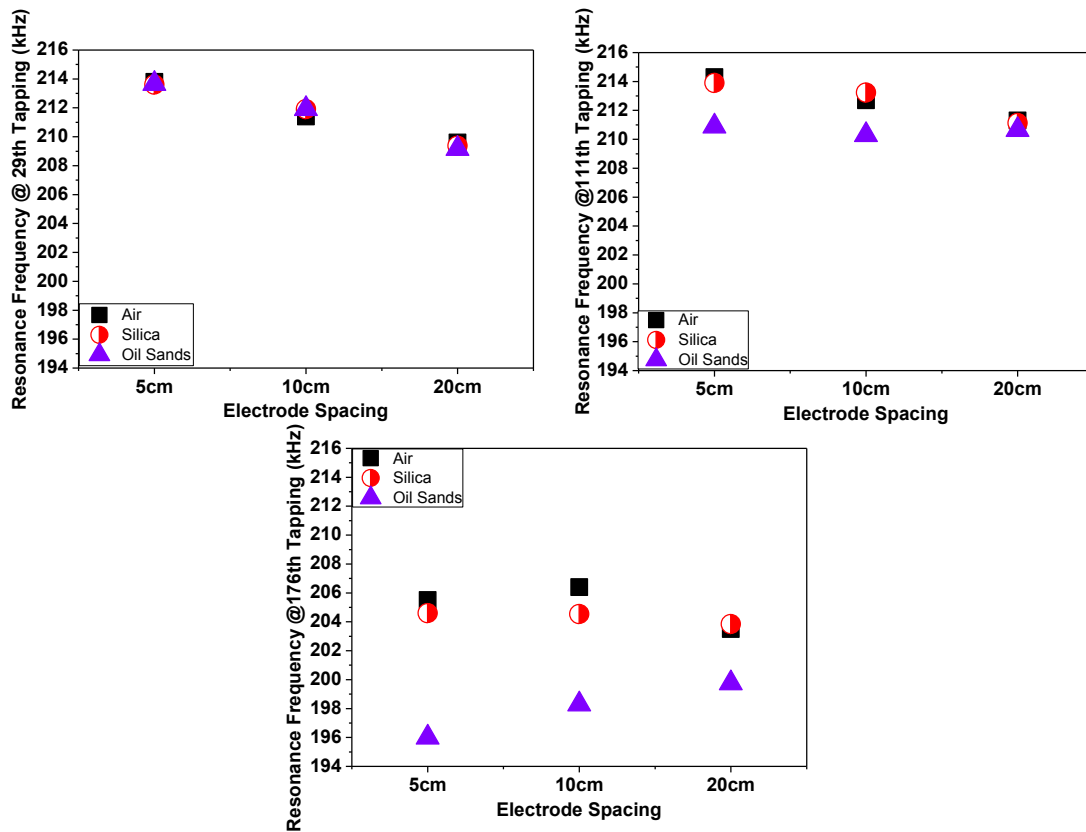


Figure 5-9. Variation of RF for different dielectric materials for a given bottom electrode connection when electrode spacing is varied.

5.5.1.2. Input Current (IC)

IC is measured at different input voltages (5, 10, 15 and 20V) for the different dielectric materials, at a given electrode spacing and bottom electrode tapping connection as shown in figure 5-10. As input voltage was increased input current showed to increase for all cases. For a given electrode spacing, oil sands seemed to draw in minimum amount of current as compared to silica and air for all bottom electrode connections. The current drawn was minimum for oil sands when connected to 176th turn as compared to the 29th turn of the coil because the effect of oil sands capacitance load was most felt at this connection as explained in the section above. At the 111th and 176th turn connections, oil sands drew least current for 5 cm electrode spacing as compared to 10cm and 20 cm electrode spacing. This could also be based on the above discussion that the least electrode spacing offered maximum capacitance and hence higher impedance to current flow into the system.

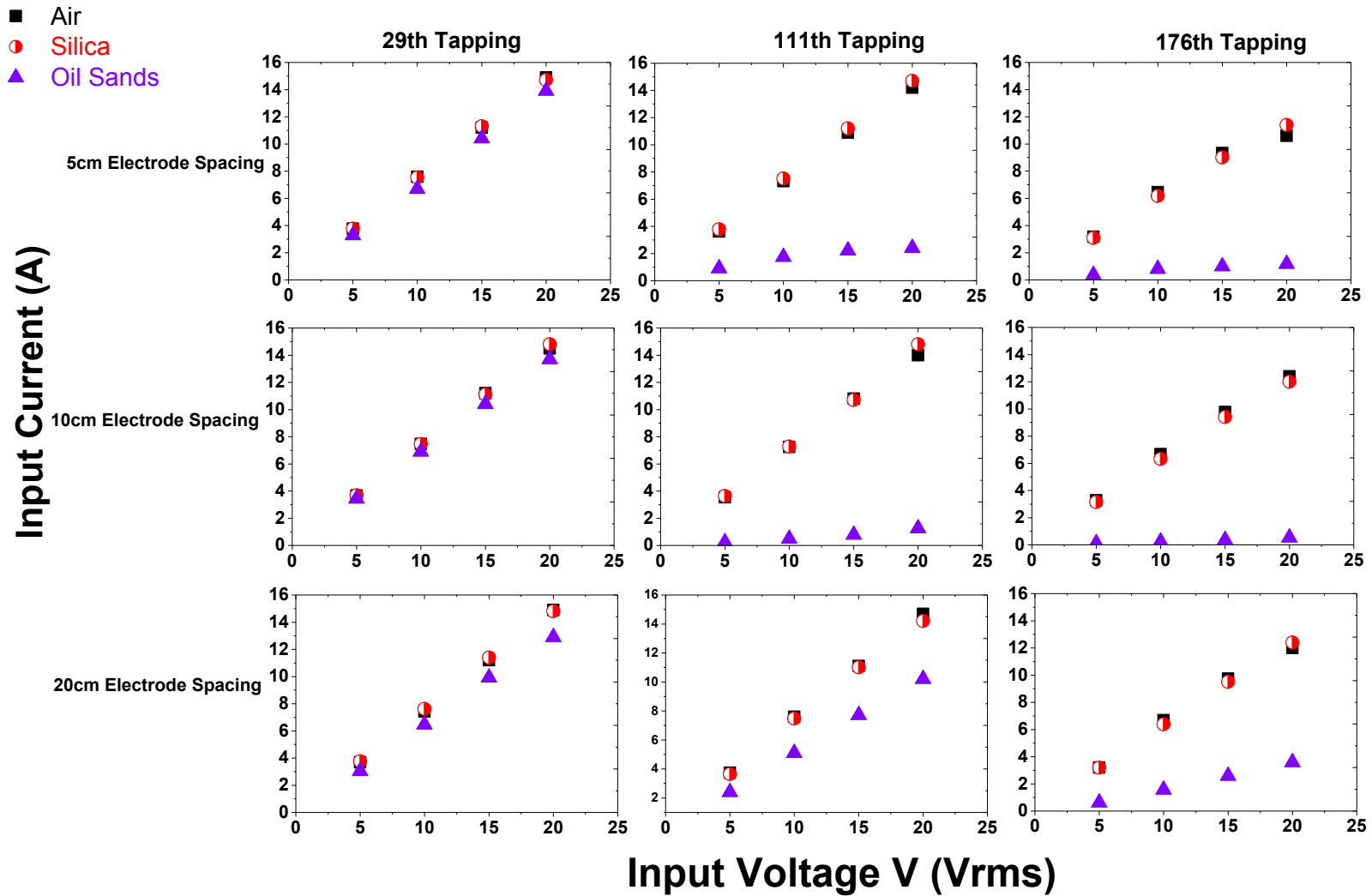


Figure 5-10. Variation of input current with voltage on varying dielectric materials for a given electrode spacing and bottom electrode connection

5.5.2 Effect of Varying Electrode Spacing

The effect of varying the electrode spacing was studied for a given dielectric material and bottom electrode connection. It was essential to understand how the resonance frequency and input current drawn by loads at different input voltages would vary for different electrode spacing for a given type of dielectric material and electrode connection. The observations and discussions are given below:

5.5.2.1 Resonance Frequency (RF)

For a given dielectric material, it can be observed from figure 5-11 that at the 29th and 111th tapping location, RF varies with electrode spacing given as 5cm>10cm>20cm indicating that least electrode spacing results in most RF in the system which is opposite to what was observed in the above case. However the difference in RF is not very significant at 176th tapping for silica and shows a reverse trend for oil sands following with the observations in the previous section.

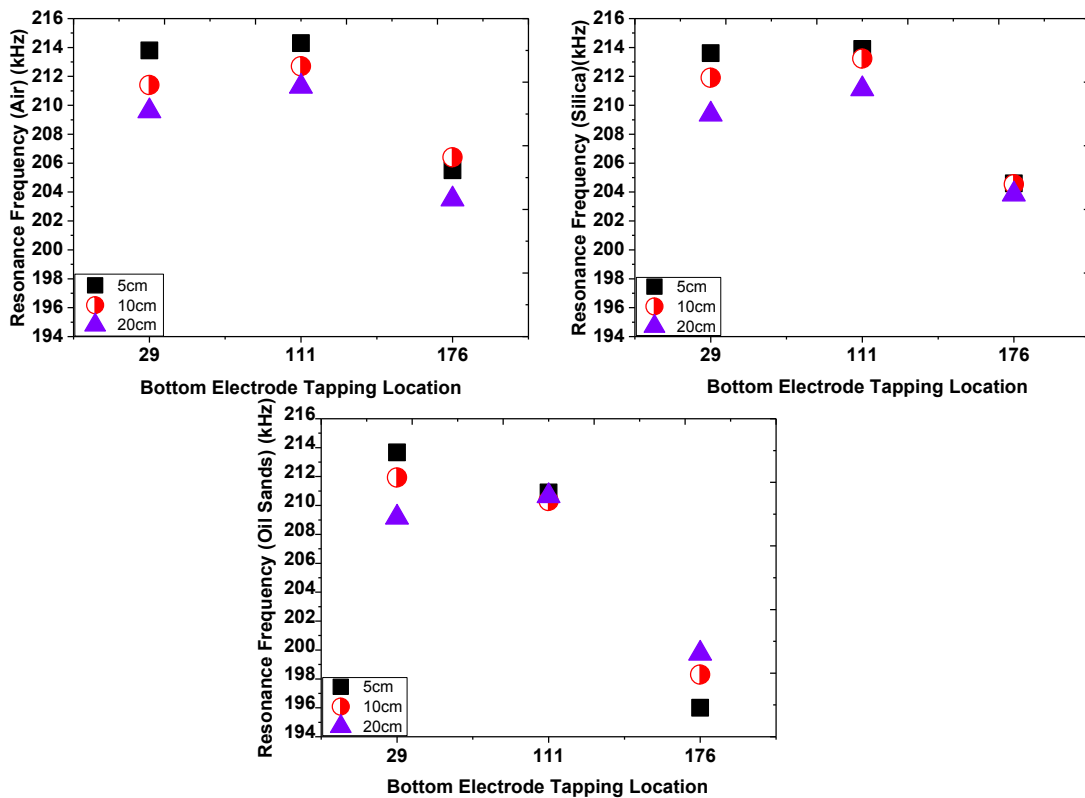


Figure 5-11. Variation of RF for different electrode spacing for a given dielectric materials when bottom electrode is connected at different turn connections.

These observations could be explained better from observations in figure 5-12. For all three dielectric materials, the difference of RF varying as 5cm>10cm>20cm is significant for 29th tapping as compared to 111th and 176th. At 176th tapping the trend reverses with RF being maximum for 20cm as compared to 5cm for oil sands. The reason for these observations could be explained on account of the complex interplay of stray capacitance and load capacitance coupled with the inductance which is not very well understood due to the abstract nature of the stray capacitance. It is understood from the above discussions that the effect of load capacitance is most felt at the 176th tapping. At the 29th and 111th tapping the effect of stray capacitance effect could be felt more than load capacitance

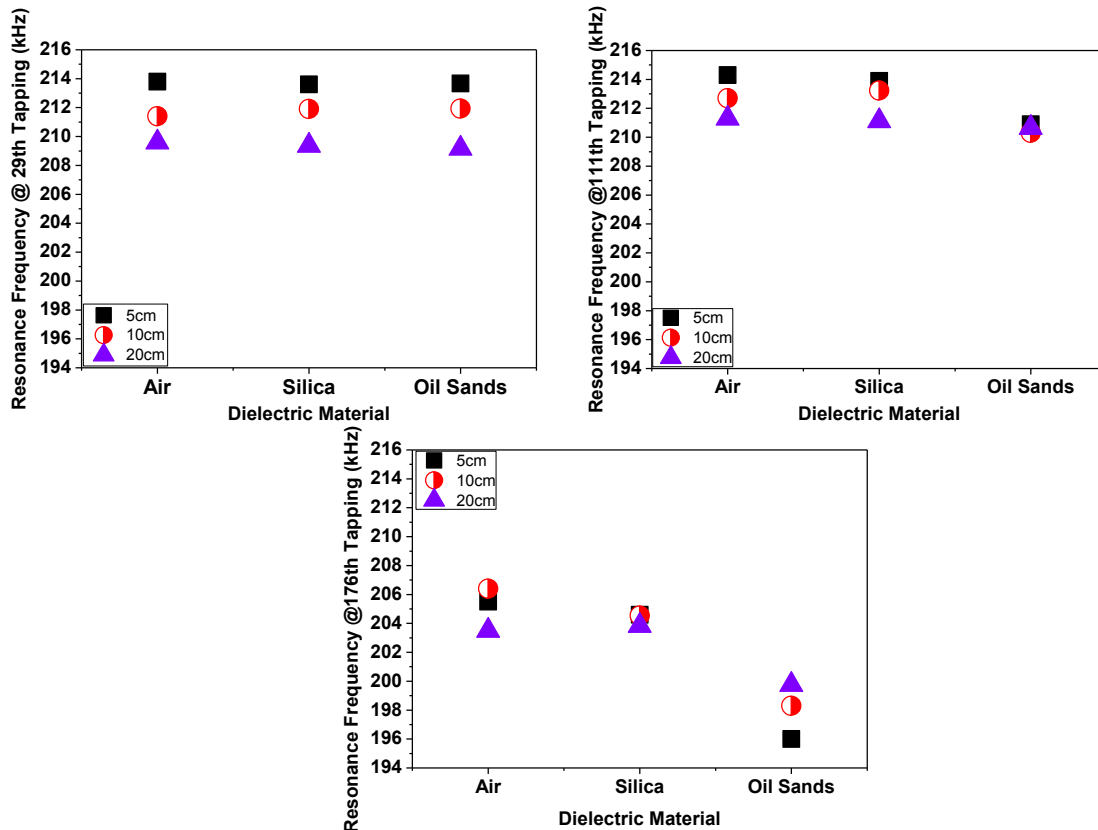


Figure 5-12. Variation of RF for different electrode spacing for a given bottom electrode connection and dielectric material.

The effect of stray capacitance felt more at the 29th and 111th tapping can be explained as follows. As electrode spacing is increased from 5cm to 20cm by fixing the bottom electrode and moving the top electrode along the length of the test cell, the spacing between the top electrode and top ground reduces in the order that 20cm<10cm<5cm. Since stray capacitance distance decreases as

the load capacitance distance increases, stray capacitance increases whereas load capacitance decreases (inverse law of capacitance with distance). As resonance frequency also follows the inverse law with capacitance, reduction in resonance frequency with decreasing cell capacitance indicates that resonance frequency is dominated by stray capacitance which increases as electrode spacing is increased and cell capacitance is decreased at the 29th and 111th tapping location, as shown in figure 5-13 below:

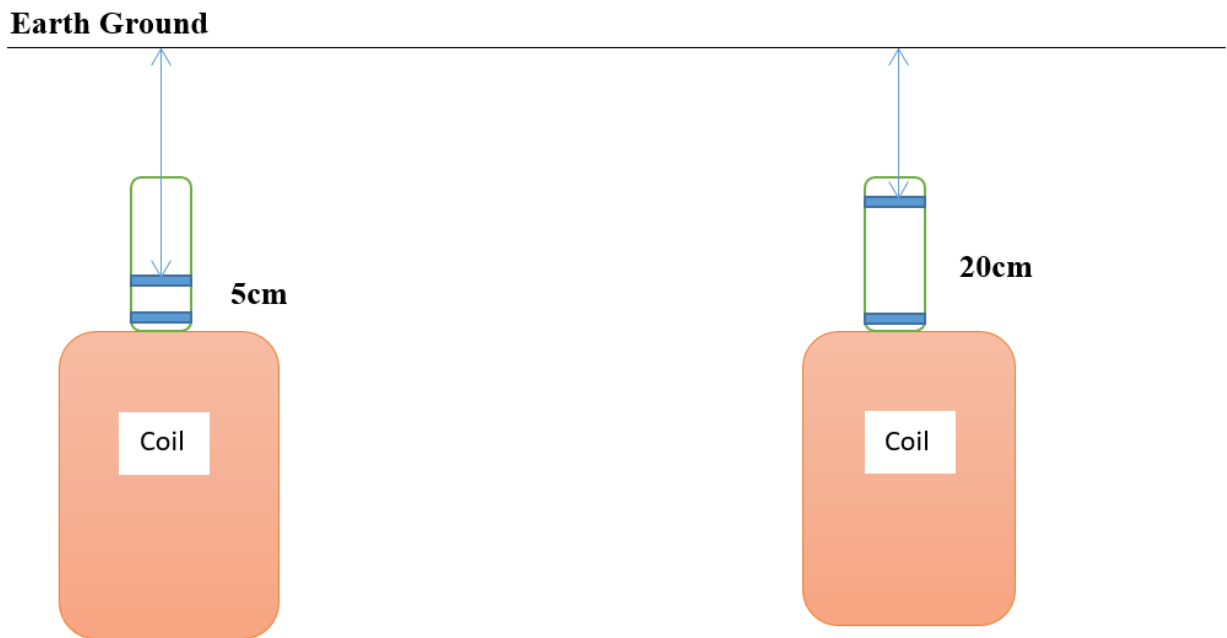


Figure 5-13. Illustration of reduced spacing between top electrode and ground as the spacing between top and bottom electrode in the capacitor is increased by fixing the bottom electrode and moving the top electrode.

5.5.2.2 Input Current (IC)

The effect of electrode spacing on the input current drawn into the resonant autotransformer as a function of dielectric material and bottom electrode tapping connection is shown in figure 5-14. It was observed that for Air and Silica, the input current drawn for all three bottom electrode tapping location was very similar for all electrode spacing. However for oil sands, the input current drawn was same for all electrode spacing at the 29th connection, the input current drawn at 20cm electrode

spacing was most in 111th and 176th connection as it offered the least impedance due to capacitor load due to inverse law relationship.

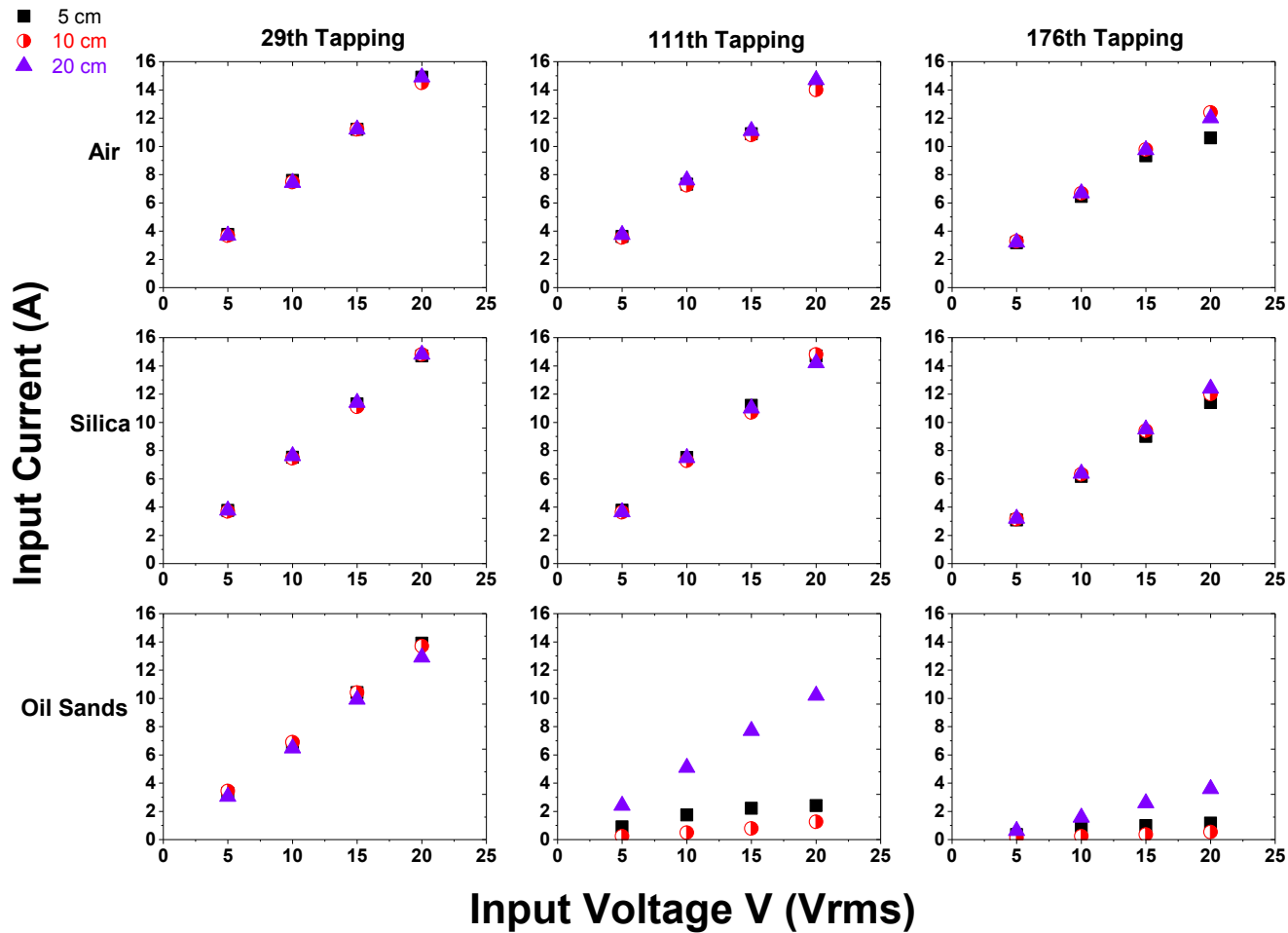


Figure 5-14. Variation of input current with voltage on varying electrode spacing for a given dielectric material and bottom electrode connection

5.5.3 Effect of Varying Bottom Electrode Connection

The effect of varying the bottom electrode connection was studied for a given dielectric material and electrode spacing. It was essential to understand how the resonance frequency and input current drawn by loads at different input voltages would vary for different electrode spacing for a given type of dielectric material and electrode connection. The observations and discussions are given below:

5.5.3.1 Resonance Frequency (RF)

It can be observed from figure 5-15 that for a given dielectric material and electrode spacing, the RF of the system is always least when the bottom electrode connection is at the 176th tapping connection with the RF being almost similar for 29th and 111th connection for all materials as was also concluded from the above results. This observation was attributed to the higher sensitivity of 176th tapping to load capacitance as compared to 29th and 111th tapping.

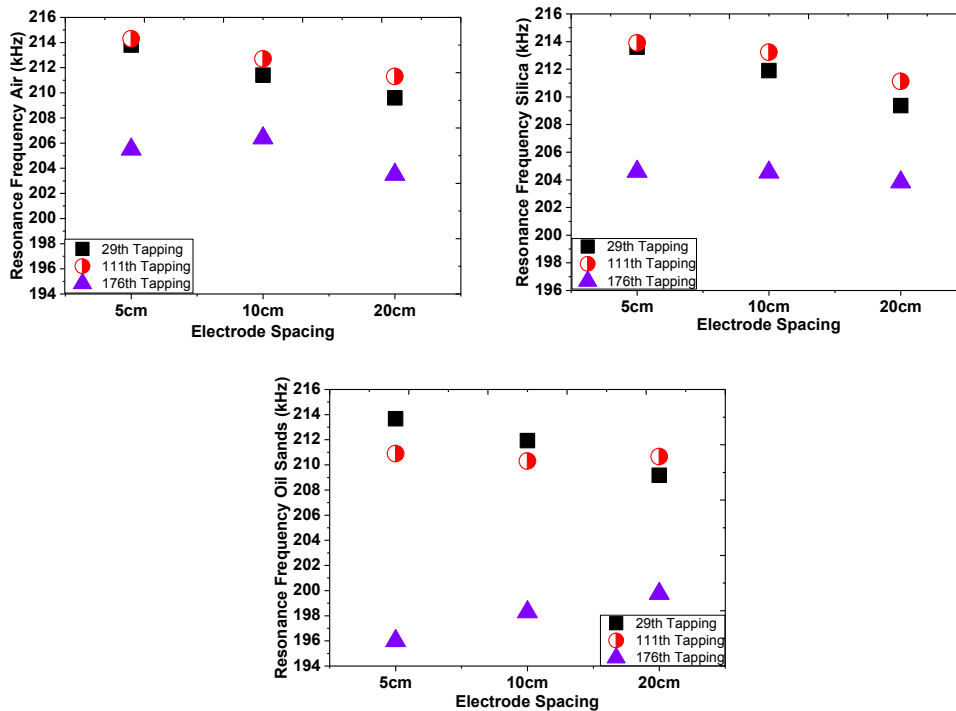


Figure 5-15. Variation of RF for different bottom electrode connections for a given dielectric materials for different electrode spacing

For a given electrode spacing, oil sands capacitor showed least RF for 176th tapping but not so much variation was observed when tapping was at 29th and 111th tapping as shown in figure 5-16. For 20cm electrode spacing, 111th tapping showed maximum resonance frequency for all dielectric materials.

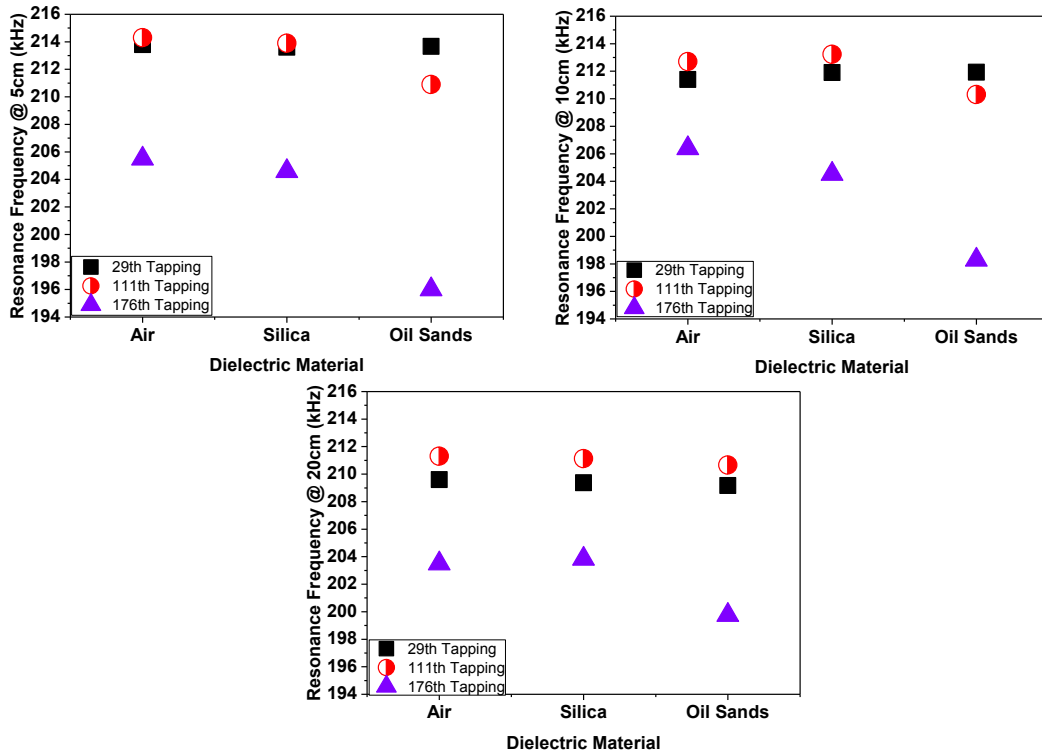


Figure 5-16. Variation of RF for different bottom electrode Tapping connections for a given electrode spacing for different dielectric materials.

5.5.3.2 Input Current (IC)

The effect of bottom electrode connection on the input current drawn into the resonant autotransformer as a function of dielectric material and electrode spacing is shown in figure 5-17. It is observed that for air and silica, the input current drawn is very similar for all electrode spacing and all bottom electrode connections. However for oil sands it is observed that the current drawn is maximum for the bottom electrode connection at the 29th tapping as compared to 111th and 176th tapping in the respective order for all electrode spacing as the effect of load capacitance is felt most at 176th tapping.

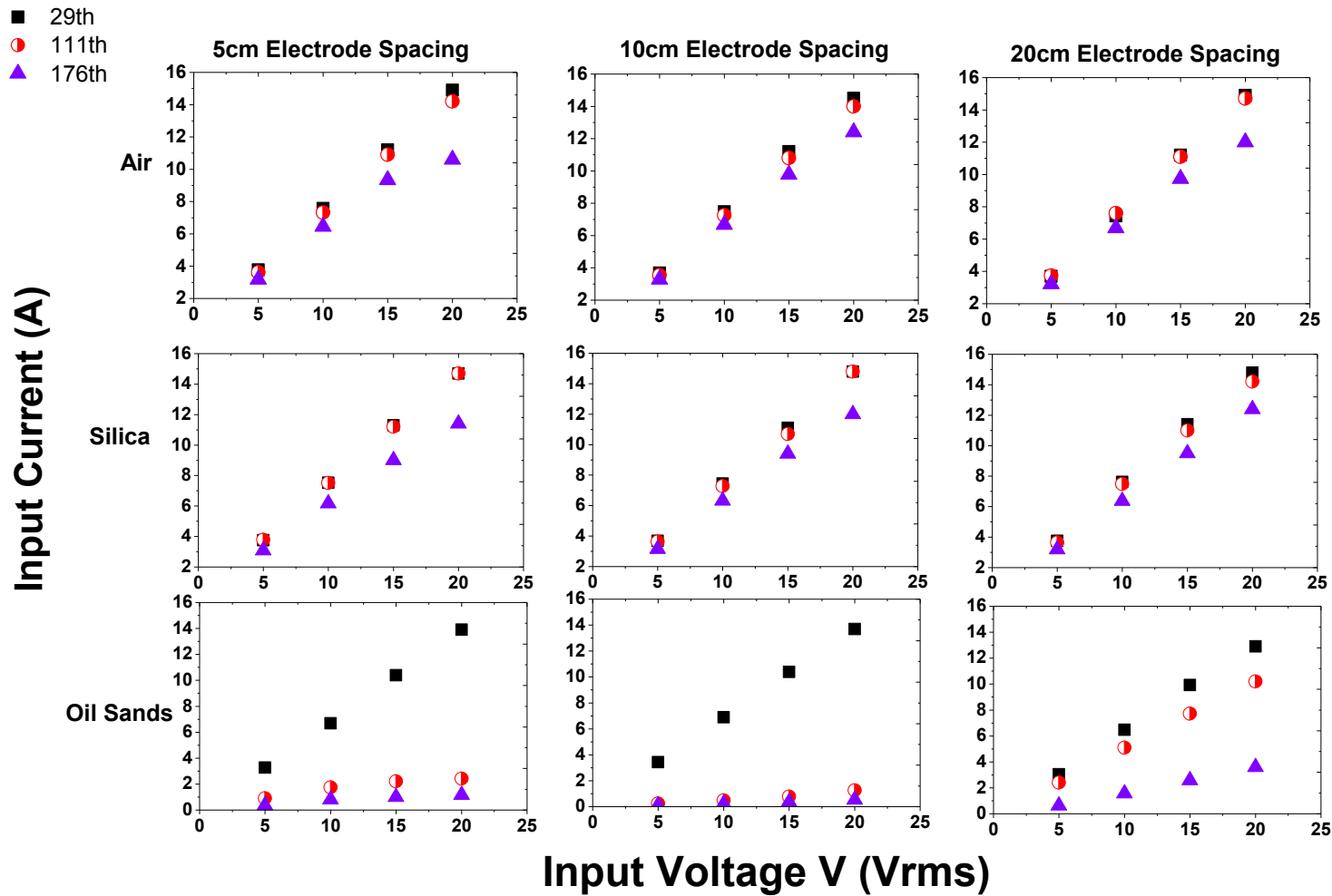


Figure 5-17. Variation of input current with voltage on varying bottom electrode connection for a given dielectric material and electrode spacing

Thus it can be concluded from these observations that for the given test cell dimensions, connecting the oil sand capacitance at the 176th tapping location resulted in best coupling of the capacitance load to the resonant autotransformer as connecting to the other tappings would result in dominance of stray capacitance over load capacitance. The RF is least when connected at 176th tapping for all dielectric materials and 5cm electrode spacing results in least RF as compared to 20cm spacing at this tapping. Input current drawn is minimum in this case too due to increased impedance due to reduced spacing at 5cm and increased dielectric constant of oil sands.

5.5.4. Effect of Changing Oil Sands Capacitance by Varying Area of Electrode

In these studies the same oil sands was used for both capacitor cells and electrode spacing was fixed at 5cm for both cells. The RF and IC measurements were taken when an input voltage of 20V was applied to both the cells as seen in figure 5-18. The electrode radius of the smaller cell was almost half of the bigger cell electrode radius. The RF for the two cells did not vary significantly for the 29th and 111th tapping since it is understood that at these tappings stray capacitance has more effect on the resonant autotransformer as compared to load capacitance. At 176th tapping where the effect of load capacitance is felt more than the effect of stray capacitance, it is seen that the RF for 8.4 pF capacitor is more than 1.7 pF capacitor. Also the input current drawn for 8.4 pF capacitor is more than that for 1.7 pF capacitor at 176th tapping indicating that a larger electrode area capacitor cell resulted in reduced overall impedance to the resonant autotransformer system as compared to the smaller electrode area capacitor cell.

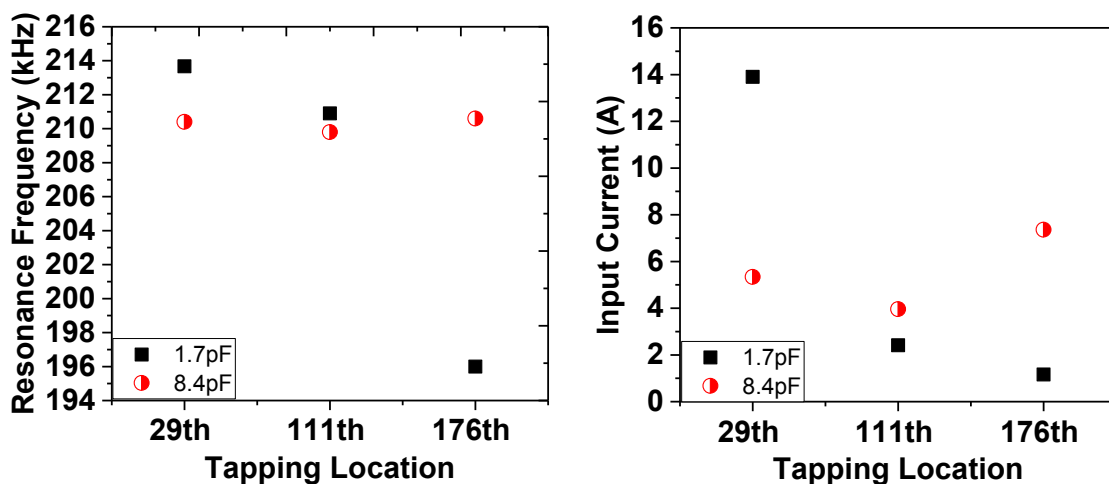


Figure 5-18. Variation of resonance frequency and input current with bottom electrode tapping location when two different oil sands capacitor sizes are used.

5.6 Conclusions

The following conclusions can be drawn from the following study regarding the capacitor load characterization of the resonant autotransformer:

1. The effect of stray capacitance is felt more strongly over load capacitance when the bottom electrode connection is made at the 29th and 111th turns of the coil. The effect of load capacitance is most strongly felt when the bottom electrode connection is made at the 176th turn of the coil.
2. Among the dielectric materials oil sands capacitor load showed to draw in least current and imparted least resonance frequency to the system for the small test cell for all spacings.
3. At 176th tapping, 5cm electrode spacing showed least resonance frequency and input current as for all dielectric materials as compared to other dielectric materials. At the 29th and 111th location the reverse trend was observed due to the dominance of stray capacitance over the load capacitance.
4. Finally between oil sands capacitor cells with fixed electrode spacing and different electrode area, it was observed that the greater electrode area resulted in reducing the capacitor impedance and aiding the development of higher resonance frequency and input current when the bottom electrode connection was at 176th tapping.

5.7 References

- (1) Yannioti, S. Microwave and Radiofrequency Heating. In *Heat Transfer in Food Processing: Recent Developments and Applications*; WTI Press, 2007; pp 101–159.
- (2) Neophytou, R. I.; Metaxas, A. C. Characterisation of Radio Frequency Heating Systems. *IEEE Proceedings-Scientific Meas. Technol.* **1997**, *144* (5), 215–222.
- (3) Van Neste, C. W.; Hawk, J. E.; Phani, A.; Backs, J. a. J.; Hull, R.; Abraham, T.; Glassford, S. J.; Pickering, a. K.; Thundat, T. Single-Contact Transmission for the Quasi-Wireless Delivery of Power over Large Surfaces. *Wirel. Power Transf.* **2014**, *1* (02), 75–82.
- (4) Mehdizadeh, M. Electric Field (Capacitive) Applicators / Probes. In *Microwave/RF Applicators and Probes, for Material Heating, Sensing, and Plasma Generation*; Elsevier, 2010; pp 67–108.

Chapter 6 Capacitive Heating Studies of Oil Sands Using Resonant Autotransformer

6.1 Introduction

Capacitive heating or heating of a dielectric medium between capacitor electrodes is the process of heating using high frequency (\geq kHz) alternating electric fields. Dielectric materials are known to have poor electrical-conduction properties but have the ability to store electrical energy via polarizations. Dielectric materials are generally also associated with poor thermal conduction properties. This results in low heat transfer rates in these materials if conventional heating methods using convection and conduction mechanisms are used. Which means that it would take a relatively long time to heat dielectric materials using conventional heating methods by applying a heat source outside the material. Thus, unlike conventional heating, dielectric or capacitive heating is considered to be fast and volumetric and is thought to be an ideal way of heating these kinds of materials. Depending on the frequency regime, temperature and the nature of the dielectric material, motion due to ionic conduction and dipole rotation of molecules tend to keep up with the alternating electric field resulting in frictional heat dissipation and are considered dominant mechanisms for dielectric heating in heterogeneous medium such as oil sands as discussed in Chapter 3 and 4. A simple schematic of a capacitive or dielectric heating system when dielectric is placed between flat capacitor plates can be seen in figure 6-1.

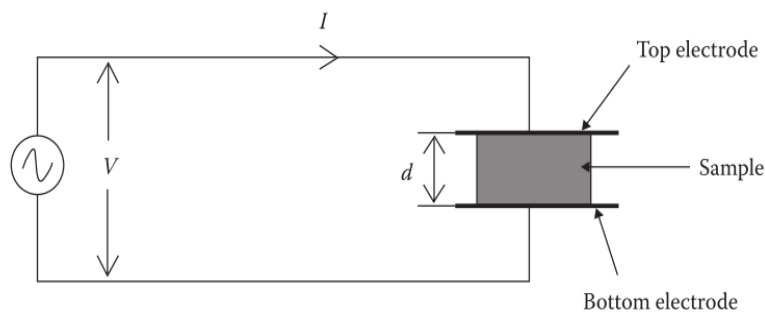


Figure 6-1. A simplified schematic of a dielectric heating system adapted from¹.

For a perfect capacitor, there is no power absorption in the dielectric between the two electrodes and the current has a phase angle of 90° with respect to the voltage because all electrical energy is stored via polarizations in the dielectric medium. But in the general case, there is bound to be some power absorption in the dielectric material due to the mentioned polarizations trying to catch up

with the alternating electric field. The dielectric material in this case would become a resistance and the current flowing through the resistance is in phase with the applied voltage. Figure 6-2 shows the circuit diagram of a dielectric heating system and the current directions, δ is known as the dielectric loss angle.

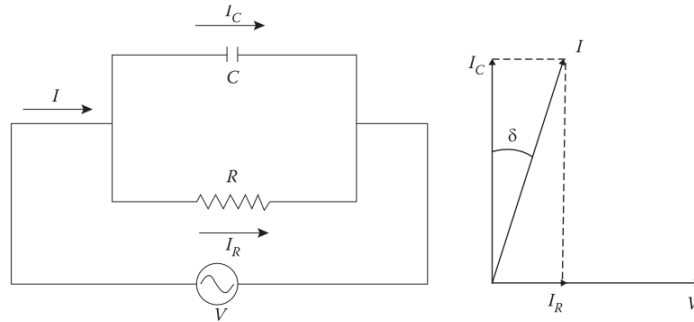


Figure 6-2. Equivalent circuit diagram of the dielectric heating system adapted from¹.

The current through the capacitor can be calculated as follows:

$$I_C = \omega VC = 2\pi fVC \quad (20)$$

Where V is the applied voltage and for the most commonly used flat capacitor, the capacitance C can be expressed as:

$$C = \frac{\epsilon_0 \epsilon' A}{d} \quad (21)$$

Where C is the capacitance (F), A is the plate surface area (m^2) and d is the electrode spacing (m) and the current through the resistance is given by:

$$I_R = I \sin \delta = I_C \tan \delta \quad (3)$$

The total power dissipated Q in the load can be expressed as:

$$Q = VI_R = VI_C \tan \delta = 2\pi fV^2 C \tan \delta \quad (4)$$

The voltage V has the following relationship with the electric field E :

$$E = \frac{V}{d} \quad (5)$$

Where E is the electric field strength (V/m) and d is the electrode spacing (m)

Substituting the equation of electric field in the power dissipated equation we get:

$$Q = 2\pi f \varepsilon_0 \varepsilon' E^2 d A \tan \delta \quad (6)$$

Where dA is the volume of load; so the power density or power dissipated per unit volume can be expressed as:

$$q = 2\pi f \varepsilon_0 \varepsilon' E^2 \tan \delta = 5.56 \times 10^{-11} f \varepsilon' E^2 \tan \delta \quad (7)$$

Where q is the power dissipation in the heated volume (W/m^3) is proportional to the applied frequency, the relative dielectric loss factor of the material and the square of the applied field strength.

In this study we investigate the resonant autotransformer's ability to carry out capacitive heating of oil sands which was discussed as one of its three attributes in Chapter 5, the second being the ability to probe changes during heating and the third being the ability to control the power and frequency input to continue the heating process by making up for the dynamic changes in the electrical behaviour of the dielectric medium. Therefore one type of oil sands sample (Oil Sands 4 with 3% water), which was studied to have a dominance of interfacial and dipole polarizations as discussed in chapter 3 and 4 was considered as a dielectric medium and used for capacitive heating in this study. The oil sands was placed between capacitor electrodes in a test cell in three types of electrode configurations and connected to the resonant autotransformer for getting heated. The resonant autotransformer has the ability of supplying high electric fields of the order of 10^4 to 10^6 V/m to the oil sands capacitor load at a system resonance frequency ranging between 190 and 220 kHz depending on the oil sands capacitor configuration and connection configuration of the electrodes to the resonant autotransformer. Electrical heating would only occur at the resonance frequency of the resonant autotransformer connected to the oil sands capacitor load. Circular parallel plate electrode configuration and bullet shaped parallel electrode configuration were used to study heating of oil sands. The latter was used with the aim of mimicking electrode wells in a

reservoir geometry. Therefore the studies presented in this chapter are purely used for observation of heat generation trends in oil sands when capacitive heating was carried out with the resonant autotransformer. This helped in informing how varying the capacitor configuration resulted in variation of electric field in the material and hence the heating profile in the oil sands. The electric field generated in the oil sands during the heating process could not be measured using any probe as this would result in interference with the working of the resonant autotransformer. Therefore the electric field causing the heating was back calculated from the temperature data obtained using a 1D steady state heat transfer equation as is discussed in section 6.3.1.

6.2 Materials and Methods

Oil sands 4 having 3% Water, 13% Bitumen, 15% fines and 69% coarse solids was used for this experiment. Due to the moderate amount of water, these oil sands showed to have a dominance of interfacial polarizations and dipole polarizations due to bitumen in the kHz frequency making them behave like dielectrics. Three capacitor configurations as shown in figure 6-3 were used to study capacitive heating of oil sands. In the first type of configuration, a cylindrical test cell being 11cm in diameter and 30 cm in height as shown in figure 6-3(a) was used for housing the oil sands between two electrodes. The test cell was made of virgin molded PTFE (Teflon) purchased from Enflo as Teflon is known to have extremely low dielectric loss with a loss tangent of 0.0002. This ensured that the test cell did not heat up dielectrically in the high field environment. The electrodes were cut into circular shapes and machined to have smooth edges. They were 10cm in inner diameter and spaced 6cm apart as shown in figure 6-3(a) to generate a capacitance of 8.4 pF. For the second set of experiments a smaller test cell was used having 5cm as inner diameter and 20cm height as shown in figure 6-3(b). The electrodes were again disc shaped and placed 10cm apart generating a capacitance of 1.7 pF. For the third experiment, bullet shaped electrodes having 6cm length and 6cm as inner diameter with diameter of the bullet head hemisphere being 4 cm were used and spaced at a distance of 10 cm as shown in figure 6-3(c). Both electrodes had smooth edges to prevent electric field breakdown due to sharp edges. In all three experimental configuration, the oil sands were tapped layer by layer to obtain a tight packing each time the experiment was carried out. Neoptix fiber optic temperature sensors T1S-02 having a resolution of 0.1°C were used to measure the temperature. These were chosen for thermometry over thermocouples as they have ability to withstand high electric fields present in the system. For the first and second set of experiments using parallel plate electrodes in the big test cell, three fiber

optic temperature sensors were placed axially in the oil sands at the center of the test cell to monitor spatial and temporal temperature profiles. The middle sensor was placed halfway between the packing and the top and bottom sensors were placed at the boundaries near the electrodes. Heating rates were observed for these oil sands with this electrode configurations by fixing the input voltage at 20V and varying the bottom electrode connection at three different tapping points along the coil that is at 29th, 111th and 176th tapping. For the third set of experiments using the bullet electrode, seven fibre optic temperature sensors were placed in the oil sands as shown in figure 6-3(c). The top most sensor was in the oil sands layer above the top bullet electrode, second being below it, third below the second sensor and fourth in the middle between the electrodes, fifth below the middle sensor, sixth just above the bottom electrode and seventh below the bottom electrode. The temperature sensors were placed strategically to determine the temperature rise around the electrodes in such a configuration. Heating rates were observed for these oil sands with this electrode configurations by fixing the input voltage at 20V and varying the bottom electrode connection at two different tapping points along the coil that is at 111th and 176th tapping. For this particular configuration, some heating studies were done without the presence of the faraday cage around the resonant autotransformer for increasing the electrical energy served to the oil sands load reasons for which will be explained in section 6.4.3. The experimental layout of capacitive heating studies carried out using resonant autotransformer for capacitor configurations shown in figure 6-3 is shown in figure 6-4.

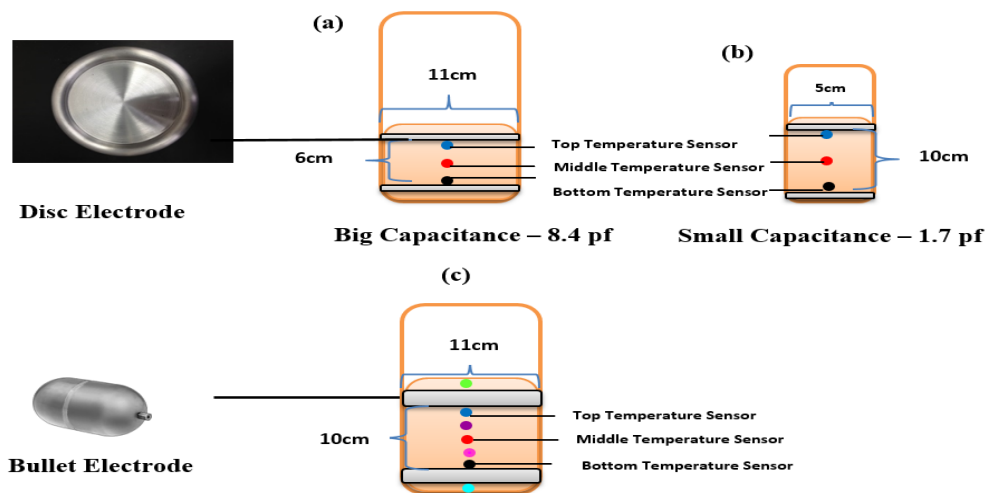


Figure 6-3. (a) Big oil sands capacitor of 8.4 pF made of disc electrodes spaced 6cm apart (b) Small oil sands capacitor of 1.7 pF made of disc electrodes spaced 10cm apart (d) Capacitor made of bullet electrodes spaced 10cm apart

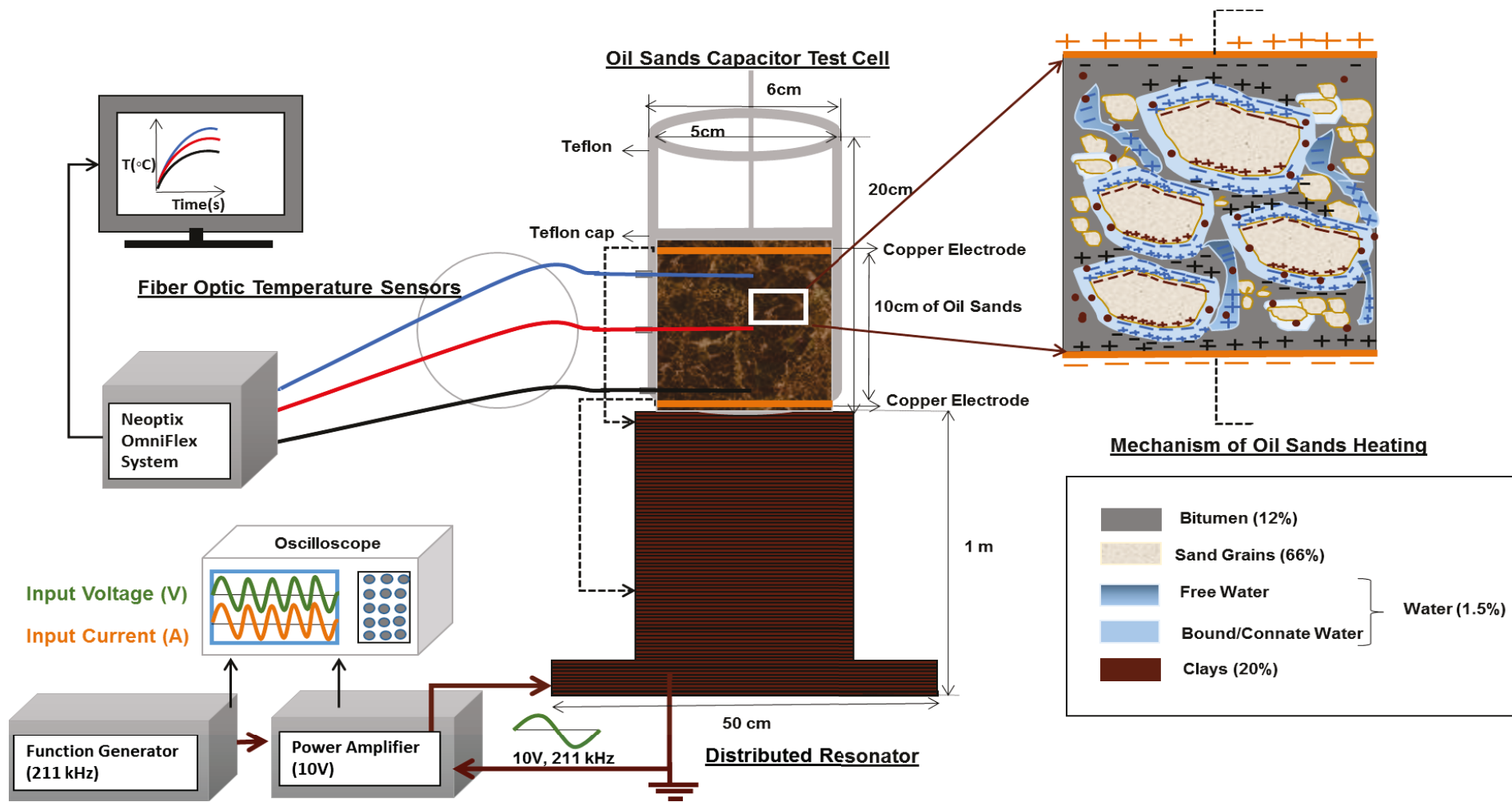


Figure 6-4. Schematic illustration of experiment used to carry investigation of capacitive heating pattern in oil sands when heating using resonant autotransformer.

6.3 1D Steady State Heat Transfer Equation with Dielectric Heat Generation in the System

It is important to determine the electric field within the oil sands which causes temperature rise during capacitive heating of oil sands. Since the quarter-wave helical coil generator is a distributed resonator in its functioning, it is difficult to correlate the input energy given to the resonator to the output potential that it generates which translates to the electric field within and outside of the oil sands test cell. By developing a 1-D steady state heat transfer equation for the given heating that happens within the oil sands, the information of temperature obtained can be used to estimate the approximate order of electric field being concentrated within the oil sands. This would be beneficial in characterising the distributed resonators ability to generate such fields. Description of the control volume is shown in figure 6-5. The following assumptions are made in the model:

- Heat conduction losses occur only along 1 dimension i.e along the z-direction.
- Thermal conductivity is considered to be constant with temperature.
- Steady state condition is observed i.e. temperature is not varying with time
- Heat losses from the surface of test cell occur due to convective losses.
- Radiation from surface is assumed to be negligible.
- Uniform electric field is considered for the sake of getting an order of estimate, though we know that a non-uniform field is imparted in the oil sands due to the distributed voltage from the resonant autotransformer.

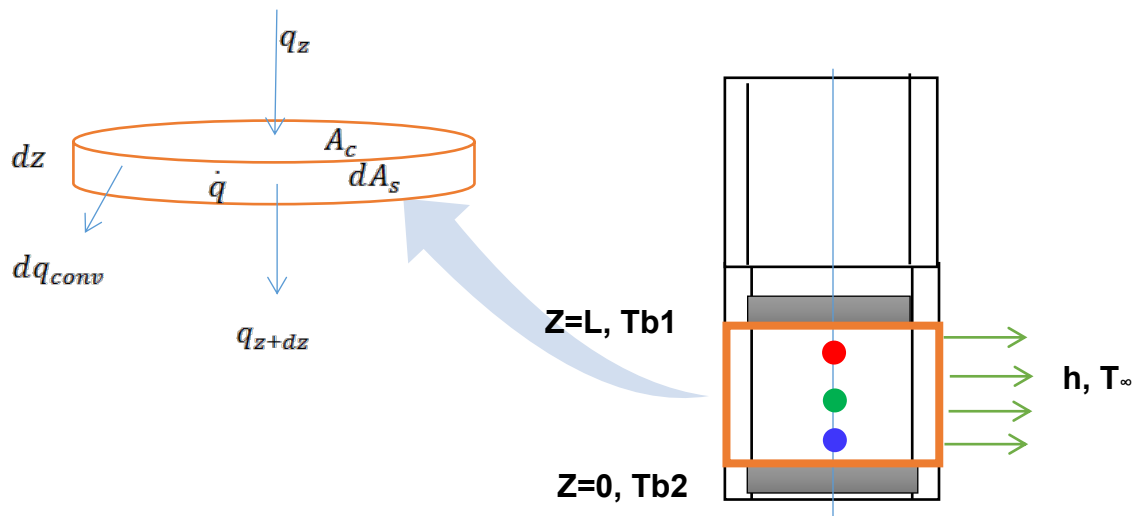


Figure 6-5. Depiction of Control Volume across which Heat Transfer model is developed.

The energy balance equation for 1-D steady state with heat generation and convective losses from the surface can be given as:

$$q_z - q_{z+dz} + qdzA_c - dq_{conv} = 0 \quad (8)$$

Where:

Energy entering the control volume by conduction:

$$q_z = -kA_c \frac{dT}{dz}$$

Energy leaving the control volume by conduction:

$$q_{z+dz} = q_z + \frac{dq_z}{dz} dz = -kA_c \frac{dT}{dz} - kA_c \frac{d^2T}{dz^2} dz$$

k = Thermal conductivity of oil sands [$\frac{W}{m} \text{ } ^\circ\text{C}$]

$A_c = \pi r^2$; where r = radius of oil sands test cell.

Energy leaving the control volume by convection from the outer curved surface of the test cell:

$$dq_{conv} = h dA_s (T - T_\infty)$$

h = Convective heat transfer coefficient [$\frac{W}{m^2} \text{ } ^\circ\text{C}$]

A_s = Curved surface area of oil sands test cell = $2\pi zr$

q = Heat energy generated in the oil sands control volume due to electrical heating

Putting these values in equation (8), we get:

$$\frac{d^2T}{dz^2} + \frac{q}{k} - \frac{2h}{kr} (T - T_\infty) = 0 \quad (9)$$

Consider:

$$m = \sqrt{\frac{2h}{kr}}$$

$$\theta = (T - T_{\infty})$$

Substituting these in the model equation (9) can be given as a second order in-homogeneous differential equation:

$$\frac{d^2\theta}{dz^2} + \frac{q}{k} - m^2\theta = 0 \quad (10)$$

Solution for this equation can be given as:

$$\theta = C_1e^{mz} + C_2e^{-mz} + \frac{qr}{2h} \quad (11)$$

Boundary Conditions are:

$$z = 0; \theta(0) = T_{b2} - T_{\infty}$$

$$z = L; \theta(L) = T_{b1} - T_{\infty}$$

Solution for 1-D steady state heating with heat generation and convective losses determined analytically is given as:

$$q = \left[\frac{\theta(0)\sinh(mz) + \theta(L)\sinh(m(L-z)) - \theta(z)\sinh(mL)}{\frac{r}{2h}(\sinh(m(L-z)) + \cosh(mz) + \sinh(mL))} \right] \quad (12)$$

Assuming uniform electric field E , the power density q determined from equation (12) can be substituted in equation (7) to determine E as given below:

$$E = \sqrt{\frac{q}{2\pi f \epsilon_0 \epsilon' \tan \delta}} \quad (122)$$

The assumptions considered and the experimental data of $\theta(z)$ used for estimating the overall electric field generated in the material is given in Appendix D

6.4 Results and Discussions

6.4.1 Heating Profile for Disc Electrode Configuration in Big Oil Sands Capacitor (8.4 pF)

Heating was carried out on driving the power amplifier at 20V input voltage. When the bottom electrode was connected to different tapping locations on the resonant autotransformer being 29th, 111th and 176th turns, the different circuit configuration resulted in different potential difference and thereby different electric fields in the capacitor. Using the 1D steady state heat transfer model, the electric field in the oil sands was estimated using the spatial temperature data and is given in table 6-1. Greater the electric field, greater was the temperature rise in the medium. The maximum temperature and rate obtained becomes a function of the electric field, frequency, dielectric properties of oil sands and heat losses due to conduction and convection from the walls of the test cell as given in table 6-2. As can be seen from figure 6-6, the temperature increased as the bottom electrode connection was varied from 29th to 111th and 176th tapping. The current drawn in the case of 29th tapping and 176th tapping were similar at 8A however the maximum temperatures attained at both these tapping locations were different with maximum temperature of 150°C attained for 176th tapping as compared to 72°C attained for tapping at 29th turn. This indicates that tapping at the bottom turns of the coil resulted in better coupling of capacitor load with the resonant autotransformer resulting in greater power transfer to the load and hence generation of higher electric field in the oil sands capacitor for almost similar input powers considered at 160W. The current drawn when bottom electrode was tapped at 111th tapping was lower than the other two connections, however the temperature rise was higher than that at 29th tapping indicating that better energy coupling or power transfer between the oil sands capacitor load and resonant autotransformer occurred at this turn connection as compared to the 29th connection. Therefore with this it can be inferred that as the bottom electrode connection was varied along the length of the coil, it resulted in better capacitive heating efficiency for the given oil sands capacitor load. As is estimated the electric field in the oil sands was in the kV/m range for the given input power. The general trend of temperature rise observed was that initially the temperature rise was fast and varied with time and then the rate of rise was stable resulting in a steady state in all three cases. The degree of heating uniformity varied in these oil sands depending on the non-uniformity of the electric field created in the oil sands due to the different voltages applied at the two electrodes due to the distributed nature of the resonant autotransformer.

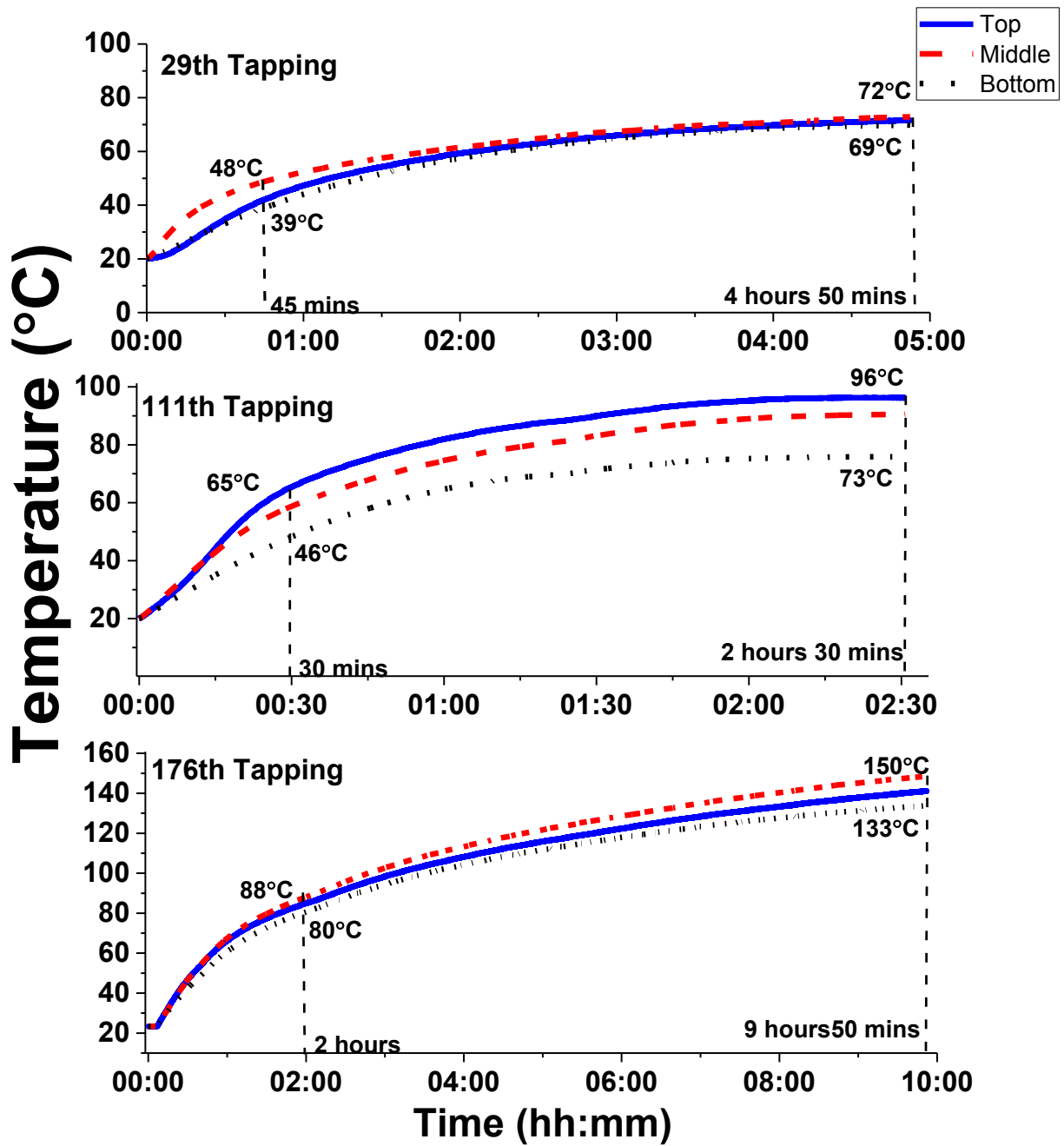


Figure 6-6. Heating profile of Oil Sands 4 when capacitive heating was carried out between disc electrodes placed 5cm apart, with bottom electrode connection varied between 29th, 111th and 176th turns

Table 6-1. Input power and power dissipated as heat in oil sands based on the electric field generated in the oil sands when bottom electrode connection was varied along the resonant autotransformer for big capacitance.

Tapping Location	Input Voltage (V)	Input Current (A)	Input Power (W)	Resonance Frequency (Hz)	Electric Field (V/m)	Power Dissipated in Heating (W)
29th	20	8.2	164	210200	29,119	24
111th	20	4.6	92	207900	36,884	38
176th	20	8	160	210600	53,064	79

Table 6-2. Tabulation of temperature profile during capacitive heating of oil sands carried out at different input electric field varied by varying the bottom electrode connection along the resonant autotransformer.

Tapping Location	Bottom Boundary Temperature at Z=0 at steady state (°C)	Top Boundary Temperature at Z=0.05m at steady state (°C)	Oil Sands Temperature at Z=0.025 m at Steady State (°C)	Initial Rate of Heating (°C/min)	Degree of Non-Uniformity of Temperature at steady state (°C)
29th	69	70	72	1.1	3
111th	73	96	90	2.1	23
176th	133	140	150	0.73	17

6.4.2. Heating Profile with Disc Electrode Configuration in a Small Oil Sands Capacitor (1.7pF)

For the second set of experiment input power variations were studied when the small oil sands capacitor of 1.7 pF was coupled with the resonant autotransformer. For this investigation the capacitance was tapped at 29th, 111th and 176th turns of the resonator keeping connection at the top fixed and varying the bottom connection. When oil sands is connected to the resonator, varying electric fields for each turn connection would translate to different heating magnitudes. Figure 6-7 shows spatial and temporal heating pattern when the bottom electrode was connected at the 29th turn, 111th and 176th turn. Table 6-3 is a comparative assessment of the input power and electric field generated in the oil sands estimated from the heat transfer model. It is observed that connecting the Oil Sands 1 capacitor to 111th turn resulted in better heating efficiency at the corresponding input voltage as low input power was used to obtain higher temperature, more uniform heating and a faster rate of heating as compared to connection at 29th turn.

A 1-dimensional steady state analytical capacitive heating model as shown in section 6.3.1 was developed to estimate the electric field within the capacitive cell from the temperature data. When the connection was at the 29th turn, the oil sands were exposed to a lower mean electric field of 13 kV/m (electric field information obtained from analytical model), and the maximum mean temperature attained was 41°C. Maximum mean temperature of heating was achieved in about 1 hour 45 minutes which results in a temperature rise of 0.9°C/minute for each kg of oil sands exposed to the electric field. When the connection was at 111th turn of the helical resonator, an increased mean electric field of 30 kV/m was applied to the cell. A maximum mean temperature of 85°C was obtained. Maximum temperature was achieved in about 30 minutes of high field exposure which translates to a heating rate of 7°C/minute per kg of oil sands. When connected to 176th tapping the temperature rise was lower at 70°C than 111th tapping with an electric field of 17 kV/m generated in the oil sands. Maximum temperature was attained in 60 minutes which translates to a heating rate of 1.2°C/minute. This indicates that for the small oil sands capacitor, best connection was at 111th tapping. Table 6-4 clearly indicate that connecting at the 111th turn of the resonator resulted in lower input power and better heating pattern translating to better heating efficiency of oil sands using the resonator at the corresponding input voltage. Again a varying degree of non-uniform heating was achieved in this oil sands capacitor cell owing to the distributed nature of the resonant autotransformer imparting non-uniform electric fields as discussed in the previous section.

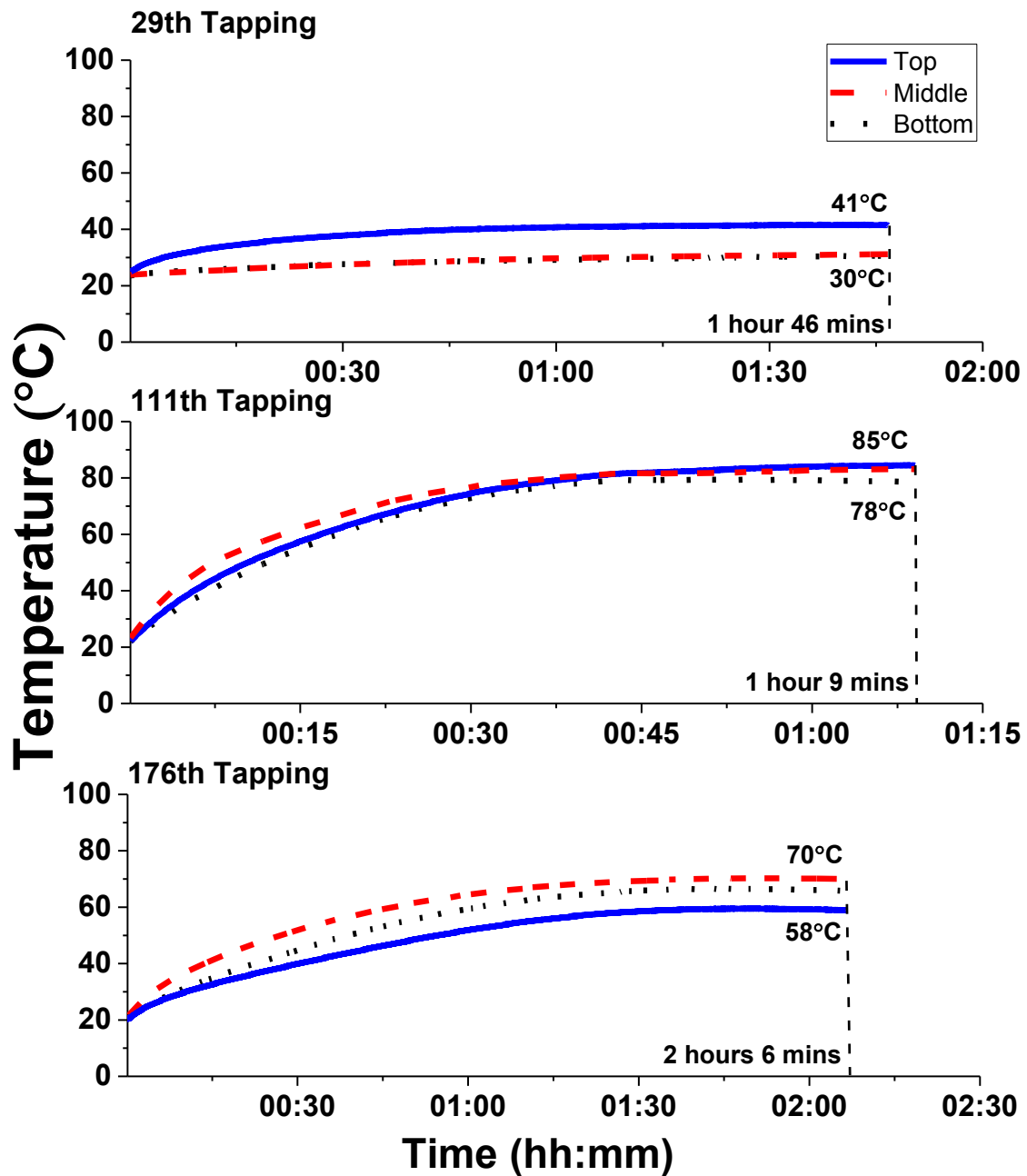


Figure 6-7. Heating profile of Oil Sands 4 when capacitive heating was carried out between disc electrodes placed 10cm apart, with bottom electrode connection varied between 29th, 111th and 176th turns

Table 6-3. Input power and power dissipated as heat in oil sands based on the electric field generated in the oil sands when bottom electrode connection was varied along the resonant autotransformer for small capacitance.

Tapping Location	Input Voltage (V)	Input Current (A)	Input Power (W)	Resonance Frequency (Hz)	Electric Field (V/m)	Power Dissipated in Heating (W)
29th	20	5.54	110.8	215000	13,098	5
111th	20	4.03	80.6	218500	30,103	26
176th	20	4.6	92	204900	17,776	9

Table 6-4. Tabulation of temperature profile during capacitive heating of oil sands carried out at different input electric field for small capacitance.

Tapping Location	Bottom Boundary Temperature at Z=0 at steady state (°C)	Top Boundary Temperature at Z=0.1m at steady state (°C)	Oil Sands Temperature at Z=0.05 m at Steady State (°C)	Initial Rate of Heating (°C/min)	Degree of Non-Uniformity of Temperature at steady state (°C)
29th	30	44	32	0.9	11
111th	78	84	85	7	7
176th	70	58	60	1.2	12

6.4.3 Heating Profile with Bullet Electrode Configuration

When capacitive heating was carried out using the bullet shaped electrodes to simulate a cylindrical well environment, the heating profile was observed as given in figure 6-7. The electrodes were placed 10cm apart and this time the bottom electrode connections were at 111th and 176th turns only. Heating profile at 29th turn connection was not studied as it was understood that higher electric fields were generated at 111th and 176th turns resulting in better heating efficiency. However, interestingly both connection configurations showed a maximum temperature rise of 52 to 55°C when an input voltage of 20V was supplied to the resonant autotransformer.

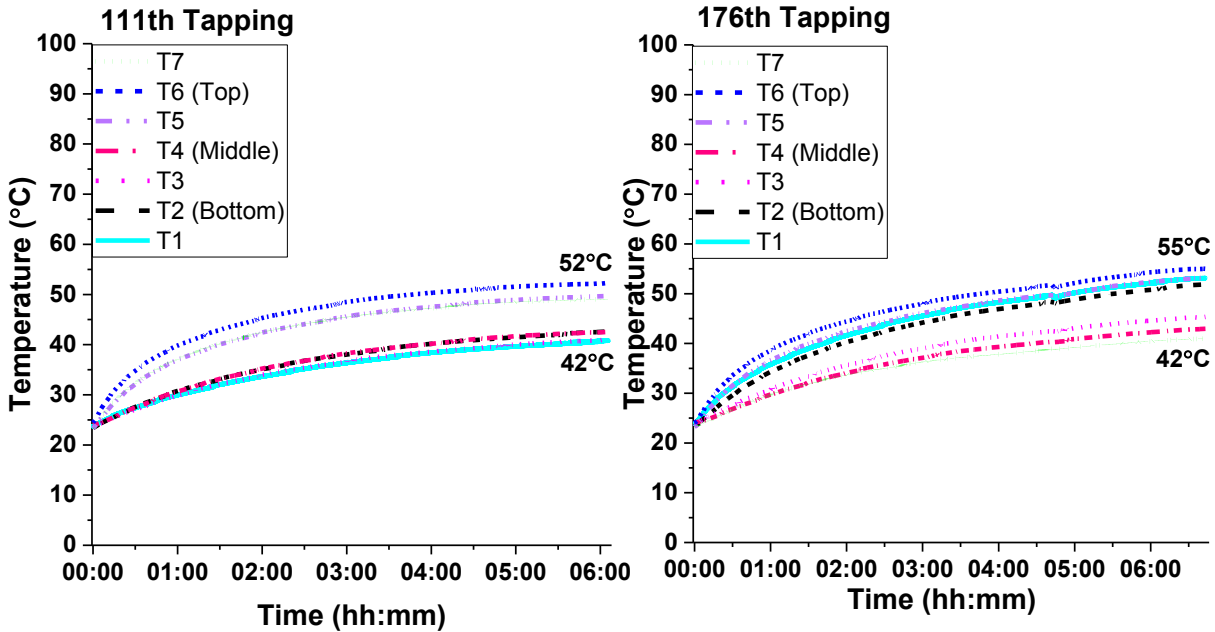


Figure 6-8. Heating profile of Oil Sands 4 when capacitive heating was carried out between bullet electrodes placed 10cm apart, with bottom electrode connection varied between 111th and 176th turns

This indicated that using this electrode configuration the heating of oil sands was not so good, which could be attributed to poor impedance matching or coupling of capacitor load with resonant autotransformer and also to the development of a non-uniform electric field generation around the cylindrical electrode. The temperature profile also indicated that heating was more around the electrodes as compared to within the oils sands. This was observed for both top and bottom electrodes indicating that in such a configuration the region around the electrodes get heated more than the region in the centre of the oil sands. Also the rate of heating was very slow indicating that the electric field within the oil sands was very less in such a configuration.

Table 6-5. Tabulation of input power supplied and heating profile in the oil sands when bullet electrodes were used to carry out capacitive heating.

Tapping Location	Input Voltage (V) (Volts)	Input Current (I) (Ampere)	Input Power (VI) (Watts)	Resonance Frequency (f) (Hz)	Maximum Steady State Temperature (°C)	Degree of Non-Uniformity of Temperature (°C)
111th	20	4.3	86	252300	52	11
176th	20	3	60	236200	55	13

In order to see if better heating could be obtained using such a configuration, it was decided to increase the power supplied to the resonant autotransformer. However the power amplifier could not be ramped up more than 20V input voltage. So, in view of this limitation, it was decided to carry out heating sans the faraday cage which provided some amount of impedance and limited the current that could be supplied to the oil sands capacitor using this electrode configuration. The heating results obtained with this experimental step is shown in figure 6-8. It can be observed that oil sands heated well to a high temperature of 100 to 106°C.

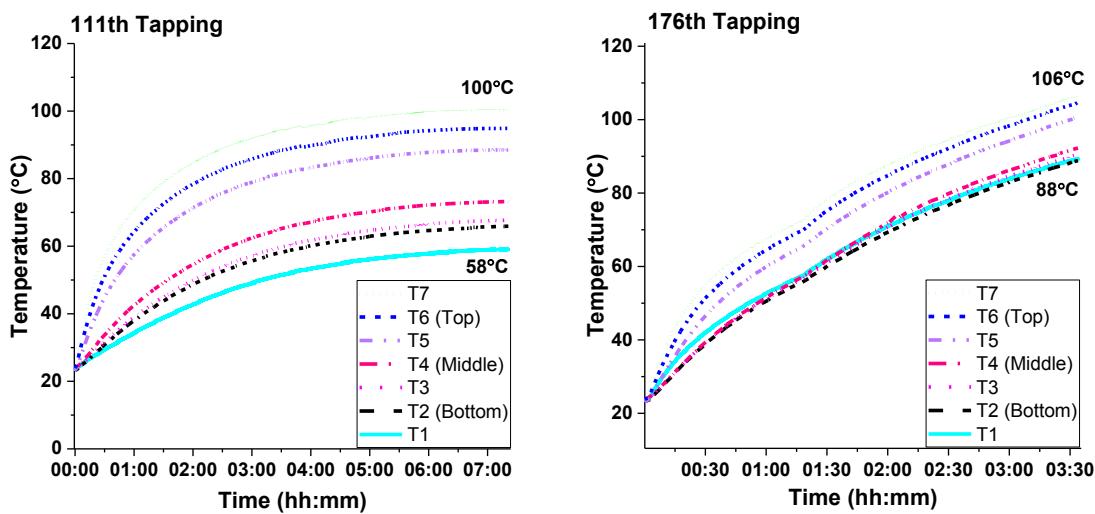


Figure 6-9. Heating profile of Oil Sands 4 when capacitive heating was carried out between bullet electrodes placed 10cm apart, with bottom electrode connection varied between 111th and 176th turns in the absence of the faraday cage.

It is observed from table 6-6 that the input current drawn for both cases in the absence of faraday cage was higher, given as 14A and 10A respectively when bottom electrode connection was at 111th and 176th tapping location. This time it was observed from figure 6-9 that the heating was more distributed along the oil sands with the highest temperature near the top electrode and lowest near the bottom electrode which was similar to the result obtained for disc electrode configuration. These results thus indicate that for bullet electrode configuration the oil sands capacitor load is better heated when the electrical energy supplied to the resonator was higher.

Table 6-6. Tabulation of input power supplied and heating profile in the oil sands when bullet electrodes were used to carry out capacitive heating in the absence of faraday cage

Tapping Location	Input Voltage (V)	Input Current (A)	Input Power (W)	Resonance Frequency (Hz)	Maximum Steady State Temperature (°C)	Degree of Non-Uniformity of Temperature (°C)
111th	20	14	280	217500	94	30
176th	20	10	200	209300	104	16

6.5 Conclusions

The heat generated in oil sands while carrying out capacitive heating using the resonant autotransformer was investigated in these studies. While fixing Oil Sands 4 having 3% water, 13% bitumen and 81% solids as the dielectric medium different capacitor electrode configurations were tested in this study to determine the best heating configuration. Two parallel plate capacitor configurations were tested having 8.4pF and 1.7pF capacitances respectively. A third configuration with bullet electrodes were also tested to replicate cylindrical horizontal well like configuration which are used in field cases. For all these electrode configurations, the bottom electrode connection was varied along the different turns of the resonant autotransformer. This was done to observe the circuit connection which resulted in best impedance match for the given capacitor load resulting in maximum power transfer and hence generation of greatest electric field in the oil sands which resulted in maximum heating of it. Since electric field generated in the oil sands dielectric could not be measured, it was analytically calculated using a 1D steady state heat transfer model based on the spatial temperature profile developed in the oil sands.

The results indicated that the parallel plate capacitance of 8.4 pF resulted in maximum temperature rise in the oil sands at 150°C when the bottom electrode connection was at 176th tapping. The smaller parallel plate capacitance of 1.7 pF resulted in highest temperature rise of 85°C when the bottom electrode connection was at 111th tapping. For bullet electrode configuration the best heating with maximum temperature of 106°C and better uniformity of heating was observed when the bottom electrode connection was at 176th turn in the absence of the faraday cage which resulted in higher electric field in the oil sands for the same input power. In all cases the electric field generated within the oil sands was analytically calculated to be 13 to 55 kV/m indicating that for a nominal input voltage of 20V the resonant autotransformer had the ability to generated very high

electric fields in the oil sands as mentioned above making it a suitable dielectric heating equipment for lab scale applications.

6.6 References

- (1) Yannioti, S. Microwave and Radiofrequency Heating. In *Heat Transfer in Food Processing: Recent Developments and Applications*; WTI Press, 2007; pp 101–159.

Chapter 7 Controlled Capacitive Heating of Oil Sands Based on Its Probed Dynamic Electrical Behaviour

7.1 Introduction

Having conducted capacitive heating on a given oil sands using the alternating electric field generated from the resonant autotransformer, it was of interest to use its other two attributes namely, its probing and heat control abilities to detect dynamic variations in oil sands and optimize electrical heating accordingly. This was done by carrying out heating studies of oil sands with different compositions with their dynamically changing electrical response during the heating process. Inferring the results from Chapter 3, Oil sands having least water content (0.5%) was studied to have a dominance of conduction relaxations and dipole polarization mechanisms and was considered as a good dielectric. With increasing water concentration (between 0.5 and 5%), the oil sands was known to have a dominance of interfacial polarizations along with dipole polarizations and was also considered to be a good dielectric, however dependent on the behaviour of water during the heating process. The oil sands having greater than 5% water was considered to have more connected water channels which resulted in a dominance of dc conduction mechanism making them a good electrical conductor. However, results from Chapter 4 show that as temperature is increased to 120°C, all oil sands converge to behave more like low loss dielectric medium presumably because of evaporation of water and increase in the mobility of bitumen.

Hence the probing capabilities of the resonant autotransformer were utilized in this study to investigate the dynamic nature of variation of electrical mechanisms during electrical heating of all these oil sands having different compositions. Having probed the changes, energy input was controlled via power or frequency tuning to carry out increased heating of the oil sands. This was done for studying the hypothesis that different heating strategies should be applied to oil sands based on their heat generation mechanisms; and also as their electrical properties changed during the heating process.

As was discussed the resonant autotransformer is a reactive near-field distributed resonator, resonating at approximately 220 kHz without a capacitor load and having the ability to produce electric field at 10^6V/m . This system utilizes electrical standing waves to maximize the electric field between the electrodes in the oil sands. As reported (Mehdizadeh 2009) a distinctive feature of a near-field resonator is that the presence of the material load typically has a significant impact on the device's field configuration and circuit variables such as current drawn for a given input

voltage (overall input power) and the system resonance frequency. In essence, the subject material, through its electrical properties, becomes a part of the circuit. The oil sands capacitor coupled with the near field standing wave in a resonant manner at a characteristic resonance frequency depending on the grade of oil sands and capacitor geometry. Heating was observed only once system resonance was achieved. Once maximum temperature was achieved for a given resonance frequency and voltage, the electrical properties and over all impedance of the oil sands changed which impacted the resonance of the system. Based on these changes the system could be re-tuned to a new characteristic resonance frequency to maintain or increase temperature. Experiments were conducted to determine the rate of re-tuning resonance frequency of the system for different moisture grade oil sands during the heating process as their compositions changed dynamically. This helped in informing strategies of carrying out electrical heating at suitable frequencies for given oil sands grade.

7.2 Materials and Methods

The investigation of capacitive heating of oil sands using the resonant autotransformer was conducted as shown in figure 6-4 of Chapter 6. As described in section 6-3(b) of chapter 6, the oil sands capacitor was contained in a cylindrical test cell used for housing the oil sands between two copper electrodes for practical experimentation purpose. The test cell was made of virgin molded PTFE (Teflon) purchased from Enflo as Teflon is known to have extremely low dielectric loss with a loss tangent of 0.0002. This ensured that the test cell did not heat up dielectrically in the high field environment. The oil sands were tapped layer by layer to obtain a tight packing each time the experiment was carried out. Neoptix fiber optic temperature sensors T1S-02 having a resolution of 0.1°C were used to measure the temperature. These were chosen for thermometry over thermocouples as they have ability to withstand high electric fields present in the system. For most of the experiments, three fiber optic temperature sensors were placed axially in the oil sands at the center of the test cell to monitor spatial and temporal temperature profiles. The middle sensor was placed halfway between the packing and the top and bottom sensors were placed at the boundaries near the electrodes. In certain experiments, only two temperature sensors were used with one placed near the top electrode and the other placed near the bottom electrode.

Two types of experiments were conducted to carry out controlled capacitive heating of oil sands based on its probed dynamic electrical behavior. The first type of experiment investigated the

variation in system resonance frequency with changes in the electrical behaviour of oil sands as temperature increased. As discussed before, this was possible because of the near field characteristics of the resonant autotransformer. The resonance imparted by the system to the resonator and oil sands would shift depending on the compositional and microstructural changes in the oil sands with increasing temperature. Therefore it was of interest to identify these frequency shifts so as to get information about changes in the electrical behavior of oil sands. For this, 10cm spacing between the capacitor electrodes was fixed and three of the six types of oil sands having different electrical mechanisms due to their composition and microstructural arrangement as investigated in Chapters 3 and 4 were used for this experiment. The composition of these oil sands samples were determined using Dean Stark extraction method and Oil Sands 1, Oil Sands 3 and Oil Sands 5 were used as given in Table 7-1. For all types of oil sands the bottom electrode was connected to the 111th turn of the coil thought to be optimum for maximum energy transfer for the used capacitor size and input voltage of 10 V was supplied.

Table 7-1. Composition of oil sands used for carrying out re-tuning resonance frequency experiments.

Type	Bitumen (%)	Water (%)	Coarse Solids (%)	Fines (%)	Electrical Mechanism
Oil Sands 1	13%	0.3%	85%	1.7%	Conduction Relaxation, Dipole Polarization
Oil Sands 3	13%	1.5%	80%	5.5%	Interfacial Polarization
Oil Sands 5	12.7%	5%	66.8%	15.5%	DC Conduction

In the second set of experiments, the electrical energy drawn during the capacitive heating process for heating oil sands was monitored in terms of the input current and the phase angle between the input voltage and input current and correlated to the changes in the electrical impedance of the oil sands with temperature as investigated in Chapter 4. For this experiment Oil Sands 1 and Oil Sands 4 investigated in Chapter 3 and 4 was used, whose composition is given below in table 7-2. With this understanding, frequency tuning or power tuning was carried out to increase heating.

Table 7-2. Composition of oil sands used for carrying out experiments for investigating heating by varying bottom electrode connection.

Type	Bitumen (%)	Water (%)	Coarse Solids (%)	Fines (%)	Electrical Mechanism
Oil Sands 4	13%	3%	69%	15%	Interfacial Polarization

Repeated results of the findings are given in Appendix D.

7.3 Results and Discussions

7.3.1 Resonance Frequency based Probing and Controlling of Capacitive Heating of Oil Sands

7.3.1.1 Power Tuned Controlled Capacitive Heating of Oil Sands Having Dominance of Conduction Relaxations and Dipole Polarization

For the first set of experiment the variation of system resonance frequency during the heating process for different types of oil sands were investigated. It was observed that Oil Sands 1 heated at a resonance frequency of 203 kHz and maintained a steady rise of temperature as shown in figure 7-1. As steady state temperature was attained, the system did not really go out of resonance indicating that the impedance of Oil Sands 1 having least amount of water i.e. 0.5% did not really change as much during the heating process. So in order to increase the heating process, the input voltage to the system was increased as shown in figure 7-1 from initial 10V to 15V which resulted in more heating of the oil sands. This experiment thus showed that when water was least in oil sands making it more like a good dielectric, frequency re-tuning was not really needed to increase the heating process after steady state temperature was attained. In these oil sands, since water was very less, it was assumed that the steady state heating occurred due to polarizations in bitumen which showed to have a relaxation frequency in 200 to 400 kHz regime. Thus it could be concluded from these observations that Oil Sands 1 having least amount of water heated in a steady manner when capacitive heating was carried out because polarizations in bitumen could have resulted in the heat generation in the oil sands.

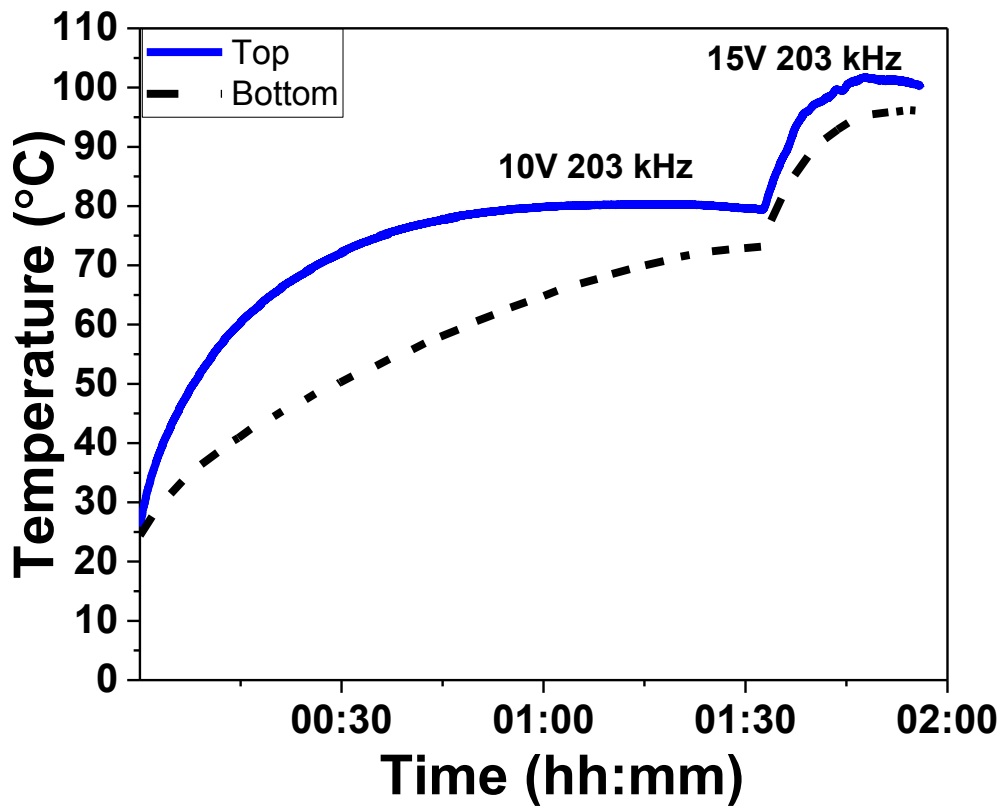
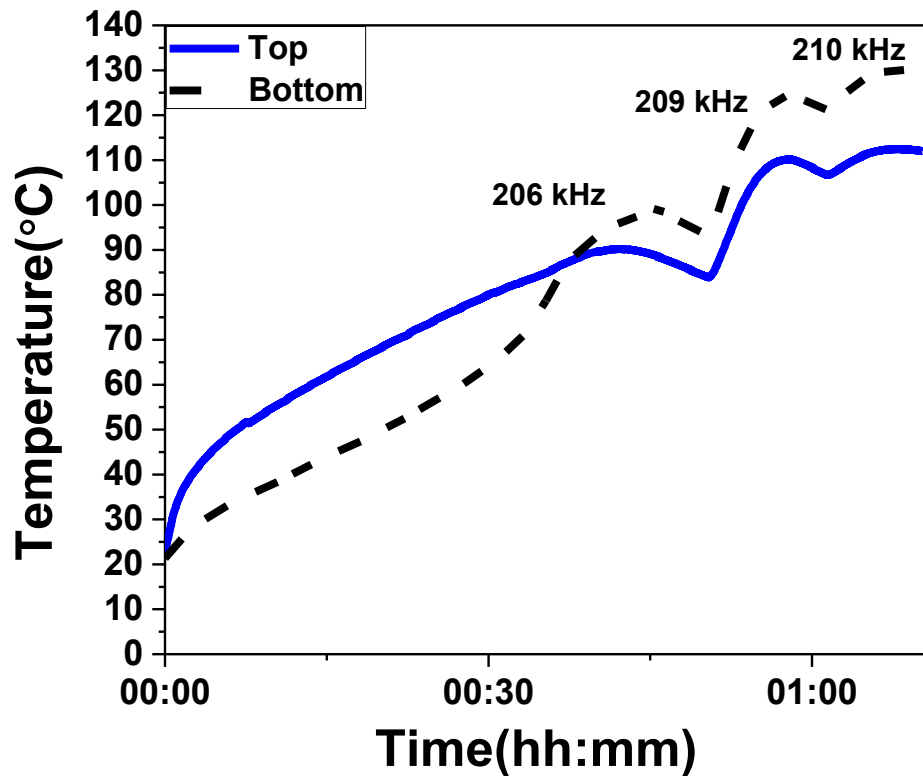


Figure 7-1. Capacitive heating data of Oil Sands 1 indicating voltage tuning to increase the heating process.

7.3.1.2 Frequency Tuned Controlled Capacitive Heating of Oil Sands Having Dominance of Interfacial Polarizations

It was observed that Oil Sands 3 having 1.5% water known to have a dominance of interfacial polarizations started heating at a system resonance frequency of 206 kHz as shown in figure 7-3. This time a maximum input voltage of 20V was fed to the system. It was observed that after steady state temperature was attained in these oil sands, the system went out of resonance indicating that the impedance of Oil Sands 3 had changed. To get the system back into resonance, the frequency was re-tuned to 209 kHz as shown in figure 7-2. This resulted in increasing the temperature of the oil sands till a temperature saturation was further attained. At this resonance frequency the input power was maintained constant. Further to increase temperature again, frequency re-tuning was again carried out from 209 kHz to 210 kHz, whereby temperature showed to increase again. Therefore, this experiment indicated that the interfacial polarization in these oil sands could be dominating the impedance changes in them assumed to be due to vaporization of water as

temperature increased and thereby resulted in shifting of the system resonance frequency. In such oil sands where interfacial polarizations dominate, frequency tuned capacitive heating could result in efficient heating.



b

Figure 7-2. Capacitive heating data of Oil Sands 3 indicating frequency tuning to increase the heating process.

7.3.1.3 Rapid Frequency Tuned Controlled Capacitive Heating of Oil Sands Having Dominance of DC Conduction

It was observed that Oil Sands 5, having 5% water started heating at a resonance frequency of 326 kHz and as maximum temperature was attained for this frequency, the system went out of resonance. So in order to increase the rate of heating the frequency had to be re-tuned to a new frequency as shown in figure 7-3. The rate of re-tuning frequency was more in this type of oil sands as can be seen that the frequency increased from 326 kHz to 434 kHz with several frequency re-tuning steps in between. The heating process in this case was not very stable due to the dominance of the water present as connected water channels in this case. Along with the presence of a higher concentration of fines, the increased water content increased the overall conductivity

of the oil sands as shown in Chapter 3 which prevented adequate capacitive heating due to interfacial polarizations from dominating the system. Also, a higher degree of non-uniform heating arises in these oil sands due to combined effect of non-uniform electric field and high water content in the oil sands which only gets heated where the field intensity is high. In such oil sands, utilizing low frequency joule heating could be more useful in carrying out the heating process. The unique frequency response for heating of Oil Sands 1,3 and 5 was thought to be attributed to the difference in water and fines content both of which were low in Oil Sands 1 as compared to Oil Sands 3 followed by Oil Sands 5. A repetition of this experiment can be seen in figure D-3 of Appendix D.

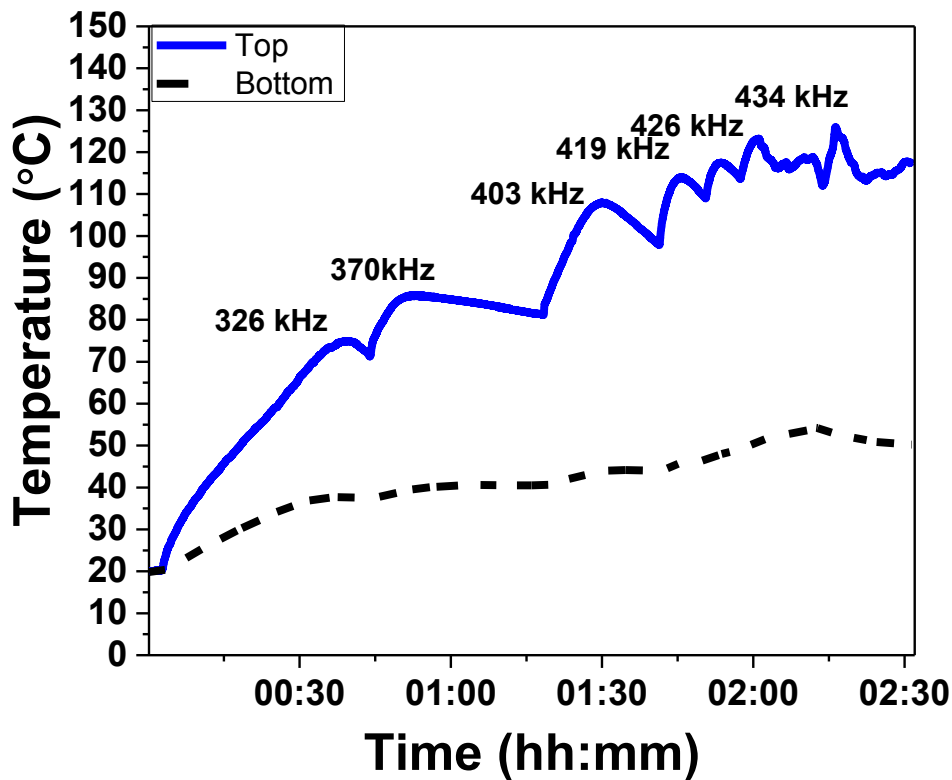


Figure 7-3. Capacitive heating data of Oil Sands 5 indicating more rapid frequency tuning to increase the heating process.

7.3.2. Input Current and Phase Angle Based Probing of Dynamic Variations in Oil Sands Impedance during Capacitive Heating

Having probed the shift in resonance frequency based on the changes in the oil sands electrical behavior with increasing temperature, it was of interest to probe the variations in input current and phase angle between the input voltage and current drawn by the resonant autotransformer with the

oil sands load during the heating process. This would help in clarifying the type of changes occurring in the oil sands during the heating process. Oil Sands 5 showing dominance of dc conduction was not considered for this study because it was evident from the previous results that capacitive heating would not be suitable for such oil sands. Joule or ohmic heating would be most suitable for these oil sands in the initial stages till most of the water is vaporized, after which capacitive heating could be a suitable method of heating such oil sands. So for this study, Oil Sands 1 having dominance of conduction relaxations and dipole polarizations were considered and probed for the variations in input current and phase. Oil Sands 4 known to have a dominance of interfacial polarizations was also considered for this study and probed for the variations in input current and phase. It was understood from the above section that Oil Sands 1 did not change the resonance frequency of the system on getting heated, whereas Oil Sands 3 which is similar to Oil Sands 4 in having interfacial polarization did show a change. Therefore it was of interest to understand the corresponding changes in the input current and phase based on changes in the impedance of the materials.

7.3.2.1 Probing of Dynamic Electrical Behaviour of Oil Sands Having Conduction Relaxations and Dipole Polarizations during Capacitive Heating.

The results of impedance spectroscopy at room temperature of Oil Sands 1 as determined from Chapter 3 is summarized in figure 7-4. It can be seen that these oil sands have very low dielectric constant and loss tangent at frequencies in kHz to MHz regime. Also it was learned from previous results that dipole polarizations due to bitumen showed up in these oil sands above 100 kHz. Also a look at the conductivity spectrum indicates that these oil sands had a dominance of ac conduction by hopping polarizations at frequencies in the kHz to MHz regime attributed to the presence of charge carriers in quartz minerals. Due to lack of water in the oil sands, hopping polarizations and dipole polarizations seemed to be the dominant mechanism making these oil sands good low loss dielectrics which could be expected to heat steadily while carrying out capacitive heating.

When capacitive heating was carried out on Oil Sands 1 at 203 kHz which showed dominance of hopping polarizations due to quartz minerals and dipole polarizations due to bitumen, it was observed that the input current drawn into the system and the phase did not change significantly during the capacitive heating process as shown in figure 7-5(a).

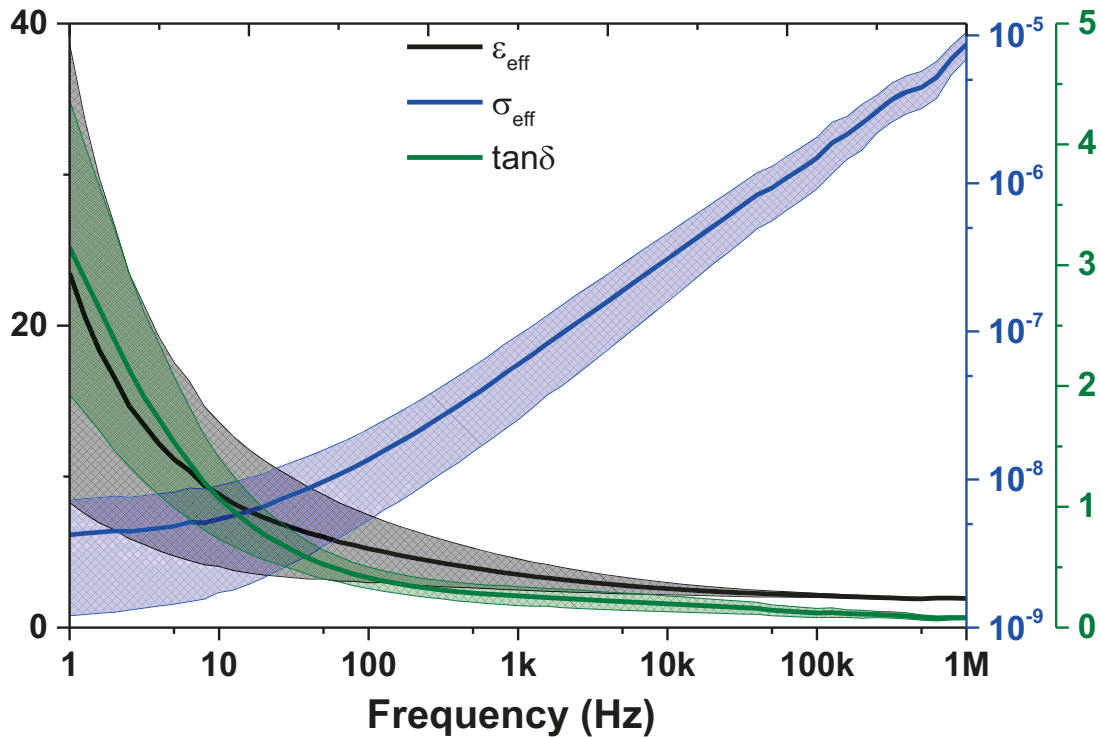


Figure 7-4. Effective permittivity, conductivity and loss tangent of Oil Sands 1 at 20°C

This indicates that the heating in these oil sands was primarily due to polarizations with hardly any charge conduction occurring in them. This substantiates the fact that these oil sands are good dielectrics and could be heated well in the presence of alternating electric fields. It can be observed from temperature based impedance spectroscopy results of Oil Sands 1 at 200 kHz in figure 7-5(b) that the permittivity, conductivity and loss tangent of Oil Sands 1 did not change significantly in the given temperature range which could be attributed to the lack of water in these oil sands. When temperature saturation was attained, the frequency was not retuned this time, instead the power input was increased by tuning the voltage from 10 to 15V which resulted in increased current being drawn into the system to increase the temperature. In order to support the understanding that bitumen polarizations could have contributed significantly to the rise in temperature in these oil sands, bitumen was heated separately as discussed below in figure 7-6.

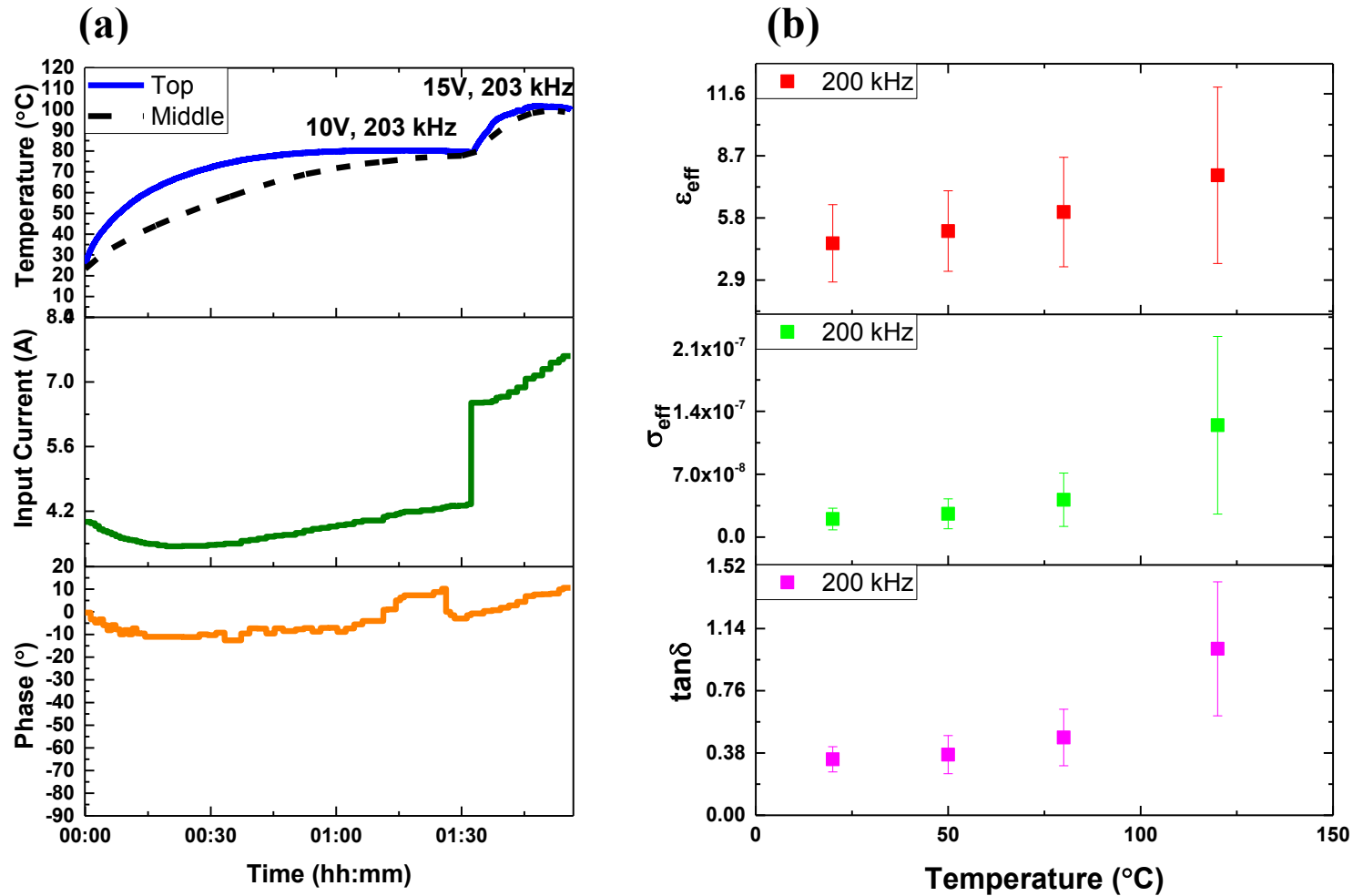


Figure 7-5. (a) Capacitive heating results of Oil Sands 1 with input current and phase variations (b) Variation in effective permittivity, conductivity and loss tangent of Oil Sands 1 with temperature at 200 kHz as determined from impedance spectroscopy.

It was observed that when 100ml of bitumen was exposed to the high alternating electric field from the resonant autotransformer by exposing it to two parallel circular electrodes, placed vertically in a beaker as shown in figure 7-6 (a), it showed to heat up as shown in figure 7-6(b). The resonance frequency of the system was 218 kHz. It was believed that bitumen heated up because its relaxation frequency where the dielectric losses are maximum were around these frequencies.

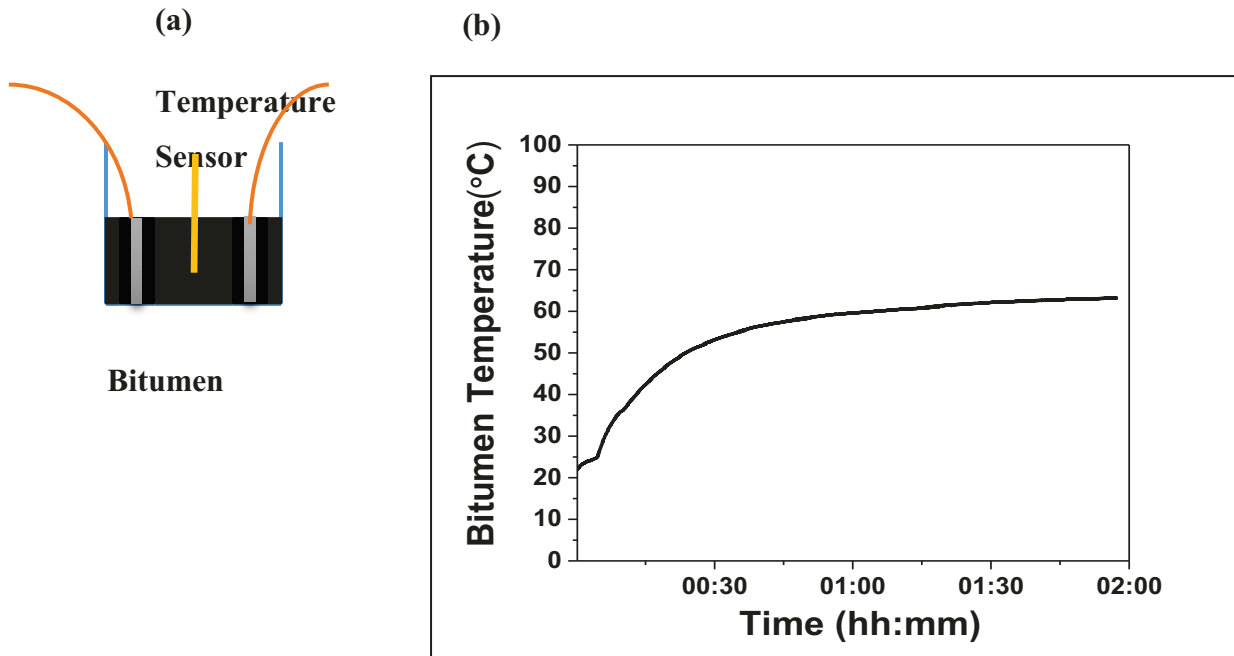


Figure 7-6.(a) Experimental setup used to carry out capacitive heating of bitumen (b) Temperature profile attained during capacitive heating of bitumen.

A repeated experiment of input current and phase probed capacitive heating of Oil Sands 1 was carried out using the same configuration and the results of which are given in figure D-1 of Appendix D.

7.3.2.2 Probing of Dynamic Electrical Behaviour of Oil Sands Having Interfacial Polarizations during Capacitive Heating.

Results of impedance spectroscopy for Oil Sands 4 discussed to have a dominance of interfacial polarizations in Chapter 3 and 4 were considered for this study. These experiments were conducted as a precursor to understand the probed variations in input current, phase and system resonance frequency with changes in the electrical behaviour of oil sands during capacitive heating

experiments. The results of impedance spectroscopy at room temperature of Oil Sands 4 as determined from Chapter 3 is summarized in figure 7-7 to identify the general electrical energy storage and loss behavior of these oil sands as well as to identify a frequency dispersion range of the relaxation due to interfacial polarizations of the given oil sands and their variations with temperature. This was done in order to select an optimum radio-frequency for heating experiments as well as an optimum frequency tuning pattern to continue the heating process.

It can be seen that the dielectric constant of the sample oil sands showed very high values of 10^5 at low frequency of 1Hz as compared to low value of 1 at high frequency of 1MHz which is indicative electrochemical, electrode and interfacial polarization mechanisms occurring in heterogeneous oil sands. Conductivity increased slightly from 10^{-4} to 10^{-3} S/m when frequency was increased from 1Hz to 1MHz. The rise in conductivity is very less because irreversible ion migrations are frequency independent. The loss tangent curve shows a relaxation peak averaging at 65 kHz for the given sample of rich grade oil sands. This relaxation frequency at 65 kHz had an average loss tangent value of 7 and could be indicative of Maxwell Wagner polarizations at bitumen, water and silica interfaces¹⁻³. The dispersion regime of relaxation peak at 65 kHz has a full width at half maximum of 2 decades of frequency. Carrying out heating in this dispersion regime of 65 kHz relaxation peak would prove useful in ensuring greater heat losses in oil sands. The resonator is designed to work at resonant frequency of 220 kHz without any oil sands load. When the Oil Sands 4 filled capacitor cell load with its electrodes are connected in circuit to the resonator its total system resonance shifts to 211 kHz. This frequency lies within the full width at half maximum of the dielectric relaxation dispersion range of the given oil sands and hence is suitable for heating.

Figure 7-8 shows results of temperature based changes to loss tangent ($\tan\delta$) spectroscopy for given oil sands averaged over three repeated experiments along with their error bars. As observed in results of figure 7-7, the sample oil sands showed a mean relaxation peak averaging around 65 kHz at room temperature. As temperature is increased from 20 to 150 °C, this relaxation peak is seen to vary in magnitude and shift in position. This could be attributed to several reasons such as: increased ionic mobility, increased thermal motion and phase changes of water as well as viscosity reduction of bitumen. As temperature is increased from 20 to 50 °C a shift in the relaxation peak, as well as, a reduction in the magnitude of loss tangent, ($\tan\delta$) is observed. These observations could be attributed to reduction in Maxwell Wagner polarizations

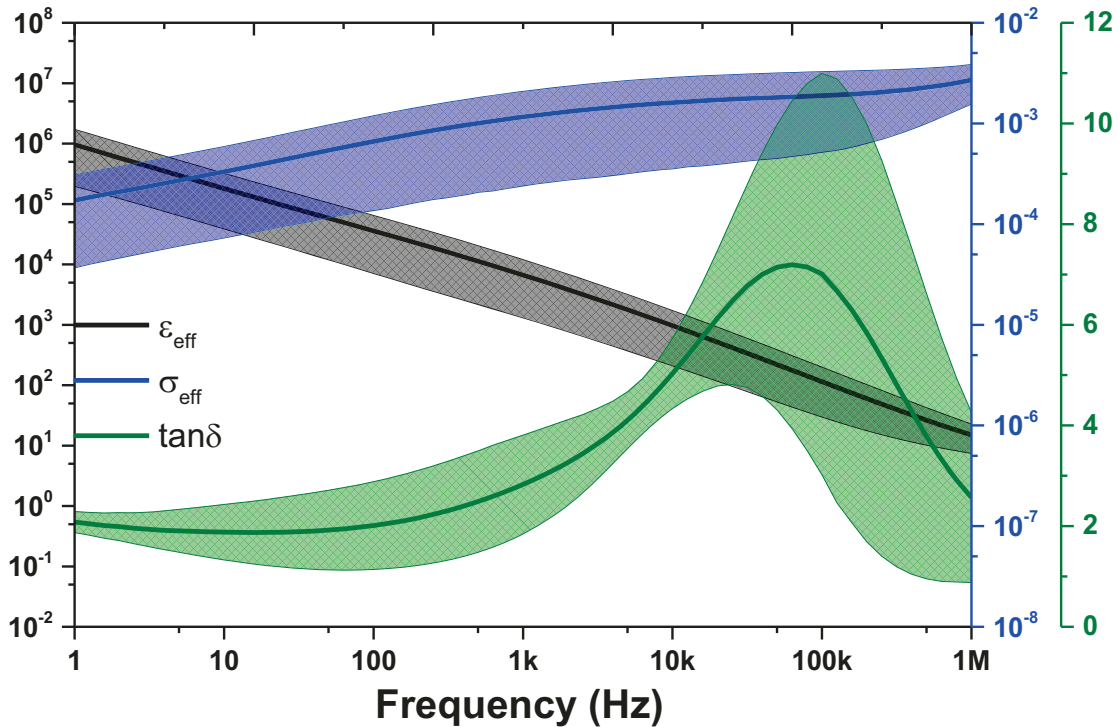


Figure 7-7. Effective permittivity, conductivity and loss tangent of Oil Sands 4 at 20°C

between water, bitumen and silicate minerals as temperature increased thermal motion of water molecules and reduced bitumen viscosity. As temperature is increased from 50 °C to 80 °C the relaxation peak further shifts in position towards lower frequency and also decreases in magnitude. It is known from literature⁴ that bitumen starts to phase transition at 70 °C. It can be assumed that as temperature was increased to 120 °C, the water phase in oil sands converted to vapor and viscosity of bitumen reduced further causing lighter components to start vaporizing. Any relaxation behavior observed could be attributed to the role of bitumen interface with silicate minerals and clays. At 120 °C, it can be seen that the relaxation peak becomes widely dispersed and also reduced in magnitude from initial case. This relaxation peak could be reasoned to be due to Maxwell Wagner polarizations arising from charge carriers in less viscous bitumen and silica interfaces with the disappearance of water interface. At 150 °C it is observed that the relaxation peak initially at 65 kHz completely disappears and oil sands appears to become a low loss dielectric

material. At this temperature, bitumen starts breaking down into other distillable components and also further reduces in viscosity. The interface between bitumen and silicate minerals becomes more prominent in the absence of water.

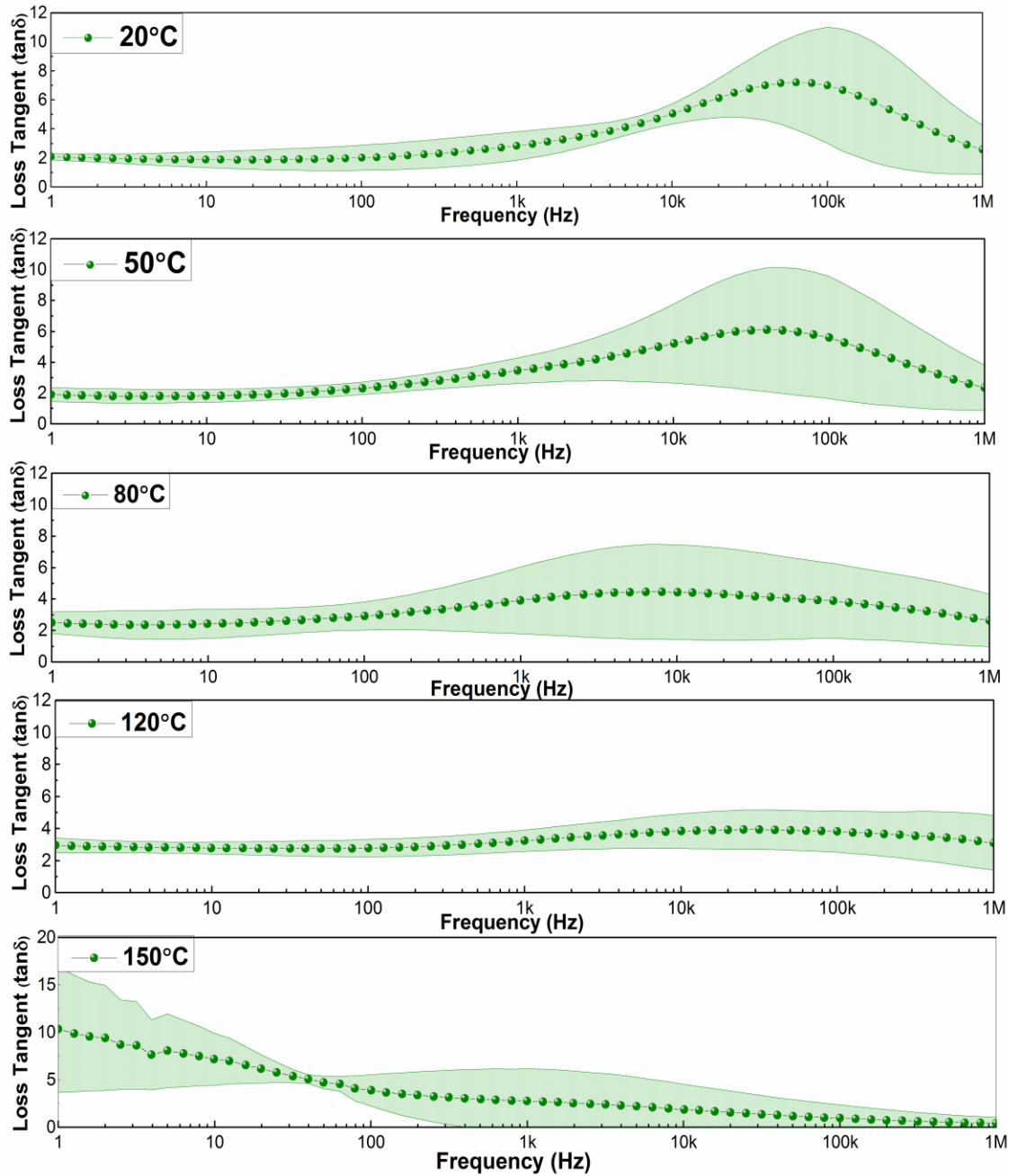


Figure 7-8. Loss tangent spectroscopy of Oil Sands 4 at different temperatures

The dispersion regime of relaxation process around 65 kHz was further chosen to be suitable for carrying out radio frequency heating. Since the full width at half maximum extended to 2 decades of frequency, operating at any frequency in this regime could prove to be useful in the heating process. This also ensured that re-tuning the applied frequency according to changed relaxation times with temperature would ensure optimized and efficient heating. These interesting observations of temperature based variations of relaxation peaks indicated changes in polarization mechanisms as fluid mobilities, phases and interfaces changed and gave us a strong reason to carry out frequency tuned heating of oil sands.

Capacitive heating results of the given oil sands are summarized in figure 7-9. Figure 7-9(a) shows the summary of oil sands temperature rise as a function of heating time at the top, middle and bottom parts of the test cell. Capacitive heating of oil sands began as the distributed resonator along with the oil sands load was tuned to the system resonance frequency of 211 kHz. The input voltage supplied was kept constant at 10V throughout the heating experiment. As temperature rose in Oil Sands 4, the input current drawn as well as the phase angle between the input current and input voltage increased and followed the temperature rise curve, becoming steady when temperature became steady as shown in figure 7-9(a). As steady state temperature was reached for the given oil sands for the given input power, we believed that the impedance of the oil sands had changed thereby changing its relaxation frequency. This led to the next step of frequency re-tuning from 211 kHz to 212 kHz at 1 hour and 15 minutes during capacitive heating of oil sands. This step helped to account for the temperature based changes in relaxation frequency of oil sands and caused further heating of it as shown in figure 7-9(a). The frequency tuning from 211 to 212 kHz was not conducted exactly according to temperature-based shifts in relaxation frequencies as shown in figure 7-8. This was because the resonator was also a part of the circuit and had its inherent resonance frequency which needed to be accounted for while re-tuning. Thereby re-tuning the frequency by 1000 Hz to observe a system resonance compensated for changes in oil sands relaxation frequencies as well and caused temperature rise in the oil sand. Thus re-tuning the frequency helped in catching up with the changed relaxation peaks of oil sands where maximum heat dissipation occurred and hence helped in establishing that electrical heating could be carried out by tuning radio frequency to match the dielectric relaxation changes of oil sands with temperature. This could be advantageous in terms of energy efficiency and can prove to be an apt operational strategy while carrying out electrical heating.

Temperature based impedance spectroscopy results of Oil Sands 4 at 200 kHz in terms of its effective permittivity, conductivity and loss tangent can be observed in figure 7-9(b). These oil sands seemed to have higher conductivity of which varied as temperature increased which could be attributed to the concentration and arrangement of water in these oil sands. The combined effect of the total losses to the total storage as temperature increased was reflected in the loss tangent which decreased as temperature rose indicating that the ratio of heat generated to energy stored in the given oil sands decreased as temperature rose. This also implies that for a given input power, the ability of given oil sands to heat up decreases as temperature increases. In this case frequency tuning at the given input power could be a suitable method of increasing heating as was done in our experiment. Therefore when temperature saturation was attained, the frequency was retuned which resulted in increased current being drawn into the system to increase the temperature and the phase went back to original value.

A repetition of this experiment was conducted and results are given figure D-2 of Appendix D.

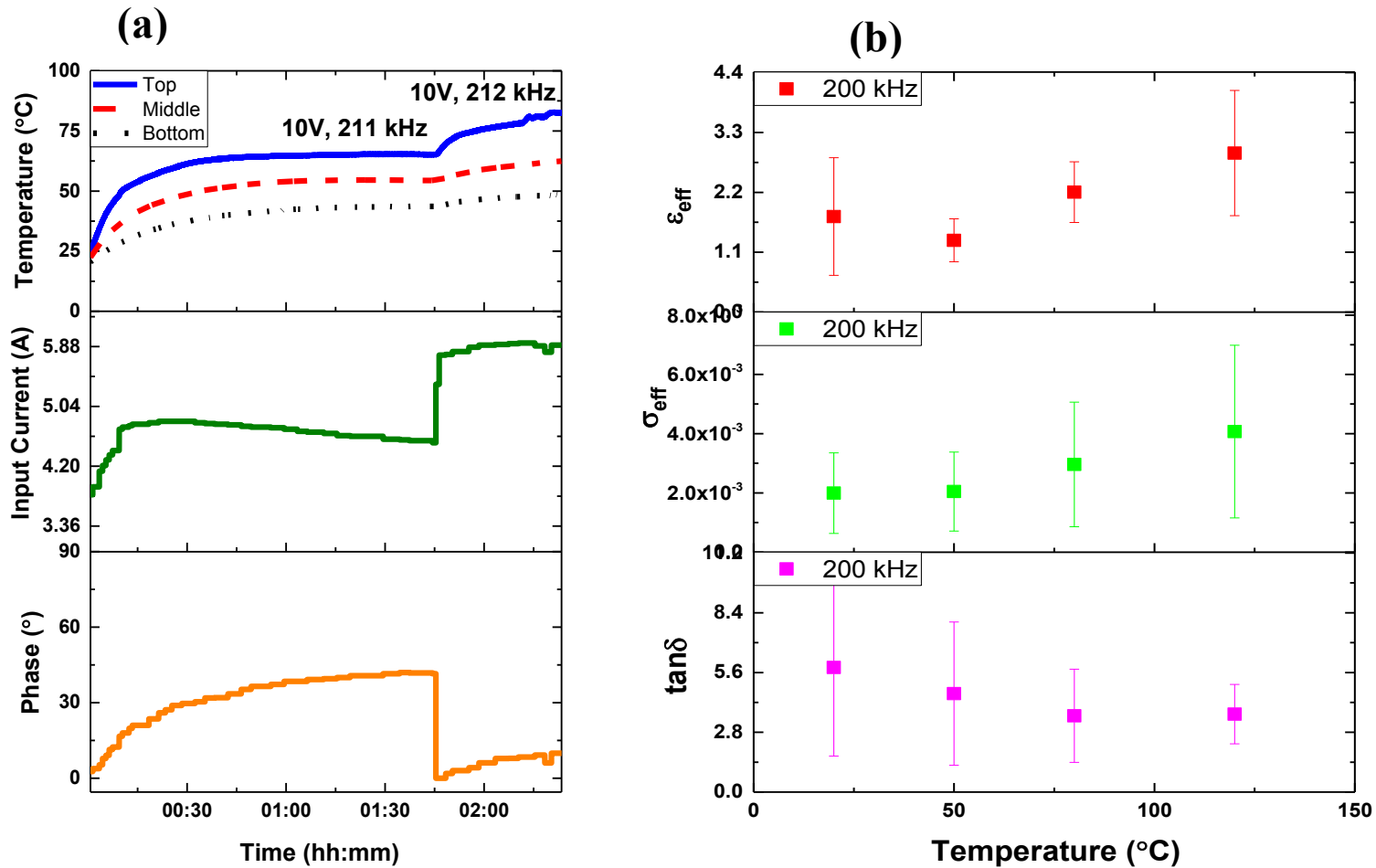


Figure 7-9. (a) Capacitive heating results of Oil Sands 4 with input current and phase variations (b) Variation in effective permittivity, conductivity and loss tangent of Oil Sands 4 with temperature at 200 kHz as determined from impedance spectroscopy.

7.4 Conclusions

In this study the dynamic variations in the electrical behavior of oil sands was probed using the resonant autotransformer while carrying out capacitive heating. Based on the probed changes, the capacitive heating of oil sands was optimised by frequency or power tuning to increase or maintain the heating process. All three types of oil sands i.e. Oil Sands 1, Oil Sands 3, 4 and Oil Sands 5 studied to have three different dominating electrical mechanisms i.e. hopping and dipole polarizations, interfacial polarizations and dc conduction respectively were considered for this study. It can be concluded that each type of oil sands heated at a unique system resonance frequency depending on its conduction and polarization mechanisms which varied based on its composition and microstructural arrangement.

Oil Sands 1 which had least water content ($<0.5\%$) showed to heat in a very steady manner which could be attributed to its good dielectric like nature attributed to the presence of hopping and dipole polarization due to quartz minerals and bitumen respectively. The system resonance frequency, input current or phase did not seem to change for these oil sands on attaining increasing temperature indicating that their electrical behavior did not change with increasing temperature. Therefore for such oil sands capacitive heating was further controlled by increasing the input voltage supplied to the system which resulted in further temperature rise.

Oil Sands 3 and 4 which showed to have a dominance of interfacial polarization due to presence of isolated water channels owing to its concentration (0.5 to 5%) also showed to heat in a steady manner. These oil sands could be considered as lossy dielectrics with dominance of interfacial polarizations over dc conduction. It was probed that the system resonance frequency, input current and phase changed during capacitive heating of these oil sands which was attributed to the changes in the interfacial polarization as water vaporized in these oil sands. In order to continue the heating process on attaining steady state frequency tuning needed to be carried out in these oil sands for increasing the temperature.

Oil Sands 5 which had the highest water content ($>5\%$) seemed to modify the resonator's response to a higher resonance frequency of 326 kHz to begin heating. It was also observed that these oil sands increased in temperature rapidly and shifted out of resonance at the same rate requiring rapid frequency tuning to keep up with the heating process. Due to this rapid frequency tuning and unsteady heating pattern, it was understood that carrying out capacitive heating of such oil sands was not advantageous as it resulted due to conduction of current through the connected water

channels in these oils sands. Joule/ohmic heating was thought to be the best method of heating these oil sands up to temperatures where water reduces in them and then capacitive heating would be a suitable method of carrying out further steady heating.

7.5 References

- (1) Lesmes, D. P.; Morgan, F. D. Dielectric Spectroscopy of Sedimentary Rocks. *J. Geophys. Res.* **2001**, *106* (B7), 13329–13346.
- (2) Chelidze, T. L.; Gueguen, Y. Electrical Spectroscopy of Porous Rocks: A review—I. Theoretical Models. *Geophys. J. Int.* **1999**, *137* (1), 1–15.
- (3) Levitskaya, T. M.; Sternberg, B. K. Polarization Processes in Rocks: 1. Complex Dielectric Permittivity Method. *Radio Sci.* **1996**, *31* (4), 781.
- (4) Masson, J. F.; Polomark, G. M. Bitumen Microstructure by Modulated Differential Scanning Calorimetry. *Thermochim. Acta* **2001**, *374* (2), 105–114.

Chapter 8 Conclusions

8.1 Concluding Remarks

Although electrical heating of oil sands reservoir has many foreseeable advantages over currently used water based thermal technologies, it is not yet a commercialized technology. Since electrical heating is highly dependent on the electrical behaviour of the oil sands reservoir, it is essential to gain a good understanding of the fundamental electrical energy conduction, storage and dissipation mechanisms in oil sands. Two approaches were taken in this study improve the feasibility of electrical heating of oil sands. The first approach investigated oil sands as a heterogeneous dielectric system for its conduction and polarizations mechanisms. These mechanisms dominate depending on the composition, microstructural arrangement and temperature of oils sands. This understanding would give a comprehensive account of the dynamic electrical behaviour of oil sands which is crucial for downhole electrical applicators and devising operational strategies to carry out an efficient and sustainable electrical heating process. The second approach was to determine the electrical heating patterns in oil sands which varied dynamically based on different conduction and polarization mechanisms. For this purpose capacitive heating of oil sands using a resonant autotransformer was conducted which also had the ability to probe and control the electrical changes in oil sands. These studies helped at arriving at conclusions about the oil sands electrical heating patterns and informed operational strategies that could help in maintaining continuous heating during dynamic changes in their behaviour.

8.1.1 Conduction and Polarization Mechanisms in Oil Sands

Impedance spectroscopy between 1 Hz and 1 MHz and for temperatures between 20 and 200°C was done to determine the dominance of conduction and polarization mechanism in oil sands which lead to heat generation during electrical heating process. Five rich grade oil sands sample having increasing water (0.3 to 5%) and fines content (1.6 to 15.5%) but similar bitumen content (11 to 13%) along with one poor grade sample (12% water, 19% fines and 4% bitumen) were used for this study. It was shown that oil sands with least water content (<0.5%) showed dominance of conduction relaxation mechanisms due to quartz minerals or silica sand grains and also showed evidence of bitumen polarizations; oil sands having 1-5% water showed dominance of interfacial or Maxwell-Wagner (MW) polarizations due to interfaces between pendular connected water

channels in between bitumen and sand, which showed relaxation peaks between 1 kHz and 1 MHz; whereas oil sands having >5% water showed dominance of dc conduction mechanism over the scanned frequency range due to the presence of free water channels and fine clay clusters. As temperature was increased from 20 to 120°C, the dc conduction and dielectric constant of all oil sands increased indicating the increased mobility of water, irrespective of their concentration in the oil sands. From 120 to 200°C, the mentioned properties reduced indicating the loss of water making the oil sands dominant in conduction relaxations and bitumen polarizations. Though these polarizations are present in all oil sands irrespective of their water content, they are not observed because of the dominating role of water which depicts dominance of dc conduction in oil sands with >5% water and interfacial polarizations in oil sands with 0.5 to 5% water. Having understood the dynamic electrical behavior of oil sands based on their conduction and polarizations dependent on their composition, microstructural arrangement and temperature, it was of interest to determine their electrical heating patterns when considered as a heterogeneous dielectric medium during capacitive heating. Results of which are discussed below.

8.1.2 Capacitive Heating of Oil Sands Using Resonant Autotransformer

Electrical heating of all the oil sands samples were carried out via capacitive heating method using a resonant autotransformer. The resonant autotransformer was used because of its threefold abilities; (1) Heating Ability- could produce 10^{4-6} V/m of electric field from kHz to MHz frequency; (2) Probing Ability – could probe dynamic variations in the electrical behaviour of oil sands via monitoring of resonance frequency, input current and phase; (3) Control Ability – could control the heating process based on the probed changes in the electrical behavior via frequency or power tuning. The oil sands was placed as a dielectric medium between two parallel capacitor electrodes. Flat disk shaped and bullet shaped electrodes were considered as variations in electrode shapes and flat disc electrode configurations were varied in spacing and area of electrode plate to test two different capacitor sizes (1.7 pF and 8.4 pF). The initial study involved characterization of the working parameters of resonant autotransformer when different dielectric mediums (air, silica, oil sands), capacitor electrode spacings (5cm, 10cm, 20cm) and connections of the bottom electrode to different turns of the transformer (29th turn, 111th turn and 176th turn) were varied. These studies helped in optimizing the capacitor load configuration for carrying out capacitive heating of oil sands. The heating studies for different capacitor geometries showed that 8.4 pF capacitance oil sands showed greater temperature rise (maximum of 150°C) as compared to 1.7

pF capacitance, indicating that bigger capacitances resulted in better impedance match with the resonant autotransformer and hence caused more generation of electric fields in them. Bullet electrode configuration was considered as a step towards replicating cylindrical well like configuration found in the field. These showed uniform heating in the oil sands and significantly high temperatures were attained in the oil sands. For carrying out controlled capacitive heating based on probed changes in the oil sands electrical behavior, three oil sands i.e Oil Sands 1, Oil Sands 3,4 and Oil Sands 5 were chosen as they had dominance of three different electrical mechanisms i.e. conduction relaxations and bitumen polarizations, interfacial polarizations and dc conduction respectively. It was observed that Oil Sands 1 heated in a steady manner as a low loss dielectric and it was probed that the resonance frequency, input current and phase did not change during the heating process indicating that the electrical behaviour of these oil sands did not change owing the dominance of conduction relaxations and dielectric relaxations due to bitumen due to the low amount of water present in them. When temperature saturation was attained for these oil sands, power tuning was carried out to increase their temperature. Oil Sands 3,4 also heated very steadily however it was probed that the resonance frequency shifted during the heating process and input current as well as phase followed the temperature rise in the oil sands indicating a dynamic change in the electrical behavior of these oil sands owing to the presence of isolated water zones giving rise to interfacial polarizations with changed with temperature. Frequency tuned capacitive heating was carried out for these oil sands to increase the temperature once saturation was attained for the given input power. Oil Sands 5 having maximum amount of water showed to heat up in a very unsteady fashion during capacitive heating requiring rapid frequency tuning to keep up with the changes in the oil sands owing to increased mobility and vaporization of water channels. So it was understood that carrying out capacitive heating of these highly conducting oil sands would not be feasible and required Joule or ohmic heating in such cases. Concluding, these studies indicate that oil sands with less than 5% water heated in a steady manner owing to polarization mechanisms and capacitive heating or frequency tuned capacitive heating could be a suitable means of heating these oil sands. Also, for greater than 5% water content oil sands carrying out ohmic heating would be suitable in the initial stages followed by capacitive heating after much of the water has got vaporized.

8.2 Major Contributions

1. Considered oil sands as a heterogeneous dielectric medium having conductive water present in varied composition and microstructural arrangements according to Takamura's model and determined the conduction and polarization mechanisms in them based on these factors.
2. Identified dominance of conduction relaxations due to hopping polarizations from quartz minerals and bitumen polarizations in oil sands having less than 0.5% water. Identified interfacial polarization as the dominating electrical mechanism in oil sands having 0.5 to 5% water owing to their presence as isolated or remotely connected interfacial water. Also identified dc conduction to be to dominating mechanism in oil sands having greater than 5% water owing to presence of connected free water channels.
3. Determined that conductivity and dielectric constant of all oil sands increase as temperature increases from 20 to 120°C owing to increased motion and vaporization of water. From 120 to 200°C all oil sands decrease in these properties due to loss of water and become more like low loss dielectrics having dominance of hopping polarization and bitumen polarizations.
4. Identified relaxation peaks due to bitumen polarizations to be present in all oil sands in between 200 to 600 kHz but are not revealed in cases where water concentration is high. Carrying out electrical heating in this frequency regime would be useful in obtaining more uniform heating of oil sands.
5. Determined that electrical heating of oil sands should be customized to the dominant electrical mechanism in the given reservoir and operational strategies should be considered to keep up with the dynamically changing electrical behavior. Where water content is higher than 5%, ohmic heating should be conducted and as water gets vaporized in these oil sands with increasing temperature the operational strategy should be to switch to capacitive method of heating. For oil sands having 0.5 to 5% water having dominance of interfacial polarizations, frequency tuned capacitive heating should be carried out and for oil sands with less than 0.5% water power tuned capacitive heating should be carried out in the frequency regime of relaxation due to bitumen polarizations. These strategies are summarised in the figure below:

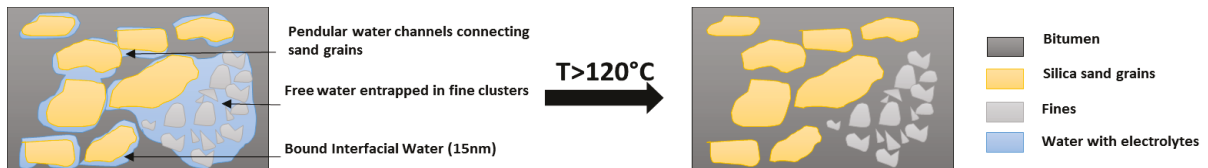
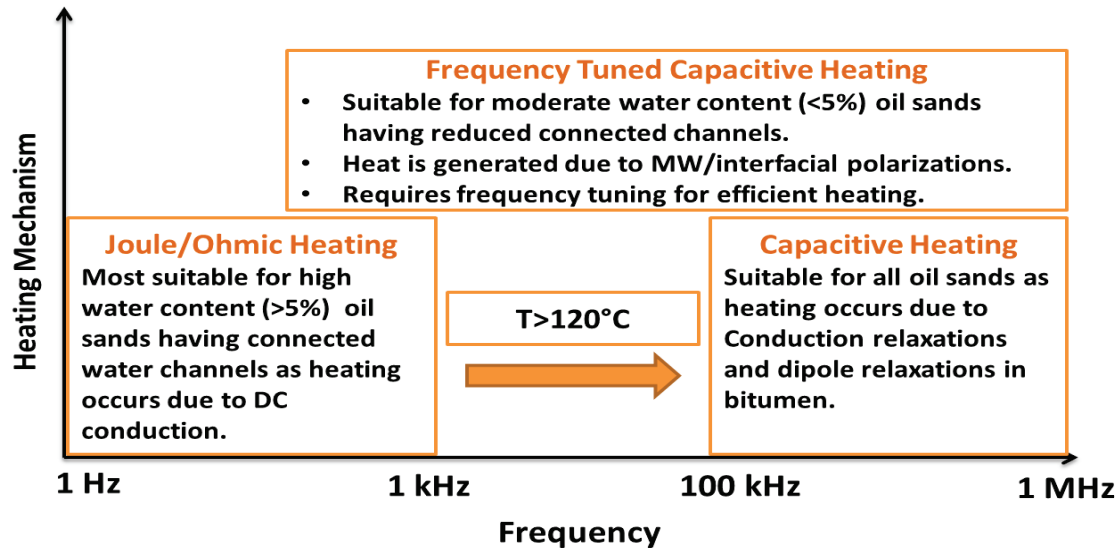


Figure 8-1. Operational strategies for carrying out electrical heating of oil sands based on their dynamic electrical behavior.

8.3 Recommendations for Future Research

1. More research should be conducted to identify polarization mechanisms in bitumen.
2. The role of clay particularly in electrochemical polarizations in oil sands should be studied.
3. These findings should be incorporated in reservoir simulations to depict realistic electrical behavior of oil sands and hence obtain more accurate predictions of electrical heating of oil sands.
4. Scale up models should be studied for their conduction and polarization behaviors as well as electrical heating patterns based these behaviors.
5. The proposed strategies could be applied to in situ reservoirs based on their electrical impedance and corresponding changes in their relaxation behavior during the heating process. The main advantages envisioned could be volumetric heat generation hence uniform and faster heating, less dependence on ionic conduction in connected water channels, optimized frequency tuned heating to increase electrical efficiency, feasible penetration depths for reservoir scales as well as better control and less wasteful reservoir heating.

Bibliography

Abernethy, E. R. Production Increase of Heavy Oils by Electromagnetic Heating. *J. Can. Pet. Technol.* **1976**, 3 (12), 91–97.

Al-Bahlani, A.-M.; Babadagli, T. SAGD Laboratory Experimental and Numerical Simulation Studies: A Review of Current Status and Future Issues. *J. Pet. Sci. Eng.* **2009**, 68 (3-4), 135–150.

B.Awuah, G.; Ramaswamy, H. S.; Tang, J. Radio-Frequency Heating in Food Processing, Principals and Applications; CRC Press, Taylor & Francis Group, 2015.

Bera, A.; Babadagli, T. Status of Electromagnetic Heating for Enhanced Heavy Oil/bitumen Recovery and Future Prospects: A Review. *Appl. Energy* **2015**, 151, 206–226.

Betancourt-Torcat, A.; Almansoori, A.; Elkamel, A.; Ricardez-Sandoval, L. Stochastic Modeling of the Oil Sands Operations under Greenhouse Gas Emission Restrictions and Water Management. *Energy and Fuels* **2013**, 27 (9), 5559–5578.

Bientinesi, M.; Scali, C.; Petarca, L. Radio Frequency Heating for Oil Recovery and Soil Remediation. IFAC-PapersOnLine **2015**, 48 (8), 1198–1203.

Bogdanov, I.; Cambon, S.; Prinnet, C.; Total, S. A. Analysis of Heavy Oil Production by Radio-Frequency Heating. In SPE International Heavy Oil Conference and Exhibition; Society of Petroleum Engineers: 8-10 December 2014, Magaf, Kuwait; pp 1–13.

Bridges, J.; Stresty, G.; Taflove, A.; Snow, R. Radio-Frequency Heating to Recover Oil from Utah Tar Sands. In First Intl.Conference on the Future of Heavy Crude and Tar Sands; New York City: McGraw-Hill Book Co. Inc., 1979; pp 396–409.

Bridges, J.; Taflove, A.; Snow, R. Method for In Situ Heat Processing of Hydrocarbonaceous Formations. 4140180, 1979.

Bruggeman, V. D. A. G. Calculation of Various Physics Constants in Heterogenous Substances I Dielectricity Constants and Conductivity of Mixed Bodies from Isotropic Substances. *Ann. Phys.* **1935**, 24 (7), 636–664.

- Butler, R. M.; Yee, C. T. Progress in the in Situ Recovery of Heavy Oils and Bitumen. *J. Can. Pet. Technol.* **2002**, 41 (1), 31–40.
- Butler, R. Steam and Gas Push (SAGP). *J. Can. Pet. Technol.* **1999**, 38 (3), 54–61.
- Carlson, R. D.; Blase, E. F.; McLendon, T. R. Development of the IIT Research Institute RF Heating Process for In Situ Oil Shale Tar Sand Fuel Extraction - An Overview; **1981**.
- Carrizales, M. A.; Lake, L. W.; Johns, R. T. Multiphase Fluid Flow Simulation of Heavy Oil Recovery by Electromagnetic Heating. In SPE Improved Oil Recovery Symposium; 24–28 April 2010, Tulsa, Oklahoma, USA; pp 568–580.
- Carrizales, M. a; Lake, L. W.; Johns, R. T. Production Improvement of Heavy-Oil Recovery by Using Electromagnetic Heating. In SPE Annual Technical Conference and Exhibition; 21–24 September 2008, Denver, Colorado, USA; pp 1–16.
- Chelidze, T. L.; Gueguen, Y. Electrical Spectroscopy of Porous Rocks: A review—I. Theoretical Models. *Geophys. J. Int.* **1999**, 137 (1), 1–15.
- Chelidze, T. L.; Gueguen, Y.; Ruffet, C. Electrical Spectroscopy of Porous Rocks: A review—II. Experimental Results and Interpretation. *Geophys. J. Int.* **1999**, 137 (1), 16–34.
- Chen, F.; Taylor, N.; Kringos, N.; Birgisson, B. A Study on Dielectric Response of Bitumen in the Low-Frequency Range. *Road Mater. Pavement Des.* **2015**, 16 (sup1), 153–169.
- Chute, B. F. S. On the Electromagnetic Heating of Low Loss Materials Using Induction Coils. *Can. Electr. Eng. J.* **1981**, 6 (1), 20–28.
- Chute, F. S.; Vermeulen, F. E. Electrical Heating of Reservoirs. In AOSTRA Technical Handbook on Oil Sands, Bitumen and Heavy Oils; Hepler, L. G., Hsi, C., Eds.; Alberta Oil Sands Technology and Research Authority, 1991; pp 337–373.
- Chute, F. S.; Vermeulen, F. E.; Cervenak, M. R.; McVea, F. J. Electrical Properties of Athabasca Oil Sands. *Can. J. Earth Sci.* **1979**, 16 (10), 2009–2021.
- Crowson, F. L.; Gill, W. G. Method and Apparatus for Secondary Recovery of Oil. US3605888, 1971.

Dakin, T. W.; Auxier, R. . Dielectric Heating – Application of Dielectric Measurements to Cellulose and Cellulose Filled Phenolic Laminating Materials. *Ind. Eng. Chem.* **1945**, 37 (3), 268–275.

Das, M.; Thapar, R.; Rajeshwar, K.; DuBow, J. Thermophysical Characterization of Oil Sands: 3. Electrical Properties. *Can. J. Earth Sci.* **1981**, 18 (4), 742–750.

Das, S. Electro-Magnetic Heating in Viscous Oil Reservoir. In SPE International Thermal Operations and Heavy Oil Symposium; 20–23 October 2008, Calgary, Alberta, Canada; pp 1–11.

Davison, R. J. Electromagnetic Stimulation of Lloydminster Heavy Oil Reservoirs: Field Test Results. *J. Can. Pet. Technol.* **1995**, 34 (1), 15–24.

Davletbaev, A.; Kovaleva, L.; Babadagli, T. Heavy Oil and Bitumen Recovery Using Radiofrequency Electromagnetic Irradiation and Electrical Heating : Theoretical Analysis and Field Scale Observations. In Canadian Unconventional Resources & International Petroleum Conference; 19–21 October 2010, Calgary, Alberta, Canada; pp 1–14.

Davletbaev, A.; Kovaleva, L.; Babadagli, T. Mathematical Modeling and Field Application of Heavy Oil Recovery by Radio-Frequency Electromagnetic Stimulation. *J. Pet. Sci. Eng.* **2011**, 78 (3-4), 646–653.

Deng, X. Recovery Performance and Economics of Steam/Propane Hybrid Process. In SPE International Thermal Operations and Heavy Oil Symposium; 1-3 November, 2005, Calgary, Alberta, Canada; pp 1–7.

Department of Energy. Alberta Energy: Facts and Statistics
<http://www.energy.alberta.ca/oilsands/791.asp> (accessed Apr 6, 2016).

Duryee, L. M. Some Economic Aspects of Radio-Frequency Heating. *Trans. Am. Inst. Electr. Eng.* **1948**, 67 (1), 105–112.

Dyre, J. C.; Maass, P.; Roling, B.; Sidebottom, D. L. Fundamental Questions Relating to Ion Conduction in Disordered Solids. *Reports Prog. Phys.* **2009**, 72 (4), 46501.

- Dyre, J. C.; Schröder, T. B. Universality of Ac Conduction in Disordered Solids. *Rev. Mod. Phys.* **2000**, 72 (3), 873.
- El-Feky, S. A. Theoretical and Experimental Investigation of Oil Recovery by the Electrothermic Technique, University of Missouri, Rolla, **1977**.
- Environmental Protection Agency (EPA), A Citizen's Guide to In Situ Thermal Treatment; **2012**, EPA 542-F-12-013.
- Environmental Protection Agency (EPA). Engineering Paper: In Situ Thermal Treatment Technologies: Lessons Learned; **2014**.
- Fanchi, J. R. Feasibility of Reservoir Heating by Electromagnetic Irradiation. In 65th Annual Technical Conference and Exhibition of the Society of Petroleum Engineers; 23-26 September, 1990, New Orleans, USA, 1990; pp 1–12.
- Findlay, J. P. The Future of the Canadian Oil Sands; **2016**, OIES Paper: WPM-64
- Fisher, S. Solid Fossil-Fuel Recovery by Electrical Induction Heating in Situ: A Proposal. *Resour. Recover. Conserv.* **1980**, 4 (4), 363–368.
- Fisher, S. T. Electrical Induction Heating for the Processing of Fossil Fuels. *Electron. Power* **1978**, 527–530.
- Fisher, S. T. Processing of Solid Fossil-Fuel Deposits by Electrical Induction Heating. *IEEE Trans. Ind. Electron. Control Instrum.* **1980**, IECI-27 (1), 19–26.
- Fisher, S. T.; Fisher, C. B. Induction Heating of Underground Hydrocarbon Deposits. 3,989,107, **1976**.
- Fisher, S. T.; Fisher, C. B. Method for Induction Heating of Underground Hydrocarbon Deposits Using a Quasi Toroidal Conductor Envelope. 4,008,761, **1977**.
- Flock, D. L.; Tharin, J. Unconventional Methods of Recovery of Bitumen and Related Research Areas Particular to the Oil Sands of Alberta. *J. Can. Pet. Technol.* **1975**, 14 (3), 17–27.

Foll, H. Electronic Materials http://www.tf.uni-kiel.de/matwis/amat/elmat_en/index.html (accessed Jul 1, 2016).

Francis Eugene Parsche. Electromagnetic Heat Treatment Providing Enhanced Oil Recovery. US 8,701,760 B2.

Gasbarri, S.; Diaz, A.; Guzman, M. Evaluation Of Electric Heating On Recovery Factors In Extra Heavy Oil Reservoirs Low-Medium Frequency Current Low Frequency Current High Frequency Current Resistive Inductive Microwave Ohmic Radio Frequency. In SPE Heavy Oil Conference and Exhibition; 12–14 December 2011, Kuwait City, Kuwait; pp 1–17.

Gates, I.; Wang, J. Evolution of In Situ Oil Sands Recovery Technology: What Happened and What's New? In SPE Heavy Oil Conference and Exhibition; 12–14 December 2011, Kuwait City, Kuwait; pp 1–10.

Gill, H. The Electrothermic System for Enhancing Oil Recovery. In First International Conference on the Future of Heavy Crude and Tar Sands; New York City: McGraw-Hill Book Co. Inc., 1979; pp 469–473.

Godard, A.; Rey-Bethbeder, F. Radio Frequency Heating , Oil Sand Recovery Improvement. In SPE Heavy Oil Conference and Exhibition; 12–14 December 2011, Kuwait City, Kuwait; pp 1–8.

Goual, L. Impedance Spectroscopy of Petroleum Fluids at Low Frequency Impedance Spectroscopy of Petroleum Fluids at Low Frequency. *Energy & Fuels* **2009**, 23 (4), 2090–2094.

Grinstead, L. Dielectric Heating by the Radio Frequency Method. *J. Br. Inst. Radio Eng.* **1945**, 128–145.

Haagensen, D. B. Sub-Surface Heating System. US3104711, 1963.

Hagedorn, A. R. Oil Recovery by Combination Steam Stimulation and Electrical Heating. US3,946,809, 1976.

Haimbaugh, R. E. Theory of Heating by Induction. In Practical Induction Heat Treating; ASM International, 2001; pp 5–18.

Hale, A.; Sandberg, C.; Kovscek, A. History and Application of Resistance Electrical Heating in Downhole Oil Field Applications. In SPE Western Regional & AAPG Pacific Section Meeting 2013 Joint Technical Conference; 19-25 April 2015, Monterey California, USA; pp 1–10.

Hanai, T.; Koizumi, N.; Goto, R. Dielectric Constant of Emulsions. Bulletin of the Institute for Chemical Research, Kyoto University. **1962**, pp 240–271.

Harvey, A. H.; Arnold, M. D.; El-Feky, S. A. Selective Electric Reservoir Heating. *J. Can. Pet. Technol.* **1979**, 18 (3), 47–57.

Hascakir, B.; Acar, C.; Akin, S. Microwave-Assisted Heavy Oil Production: An Experimental Approach. *Energy & Fuels* **2009**, 23 (18), 6033–6039.

Hascakir, B.; Babadagli, T.; Akin, S. Experimental and Numerical Simulation of Oil Recovery from Oil Shales by Electrical Heating. *Energy & Fuels* **2008**, 22 (11), 3976–3985.

Hascakir, B.; Babadagli, T.; Akin, S. Field-Scale Analysis of Heavy-Oil Recovery by Electrical Heating. In International Thermal Operations and Heavy Oil Symposium; 20–23 October 2008, Calgary, Alberta, Canada; pp 131–142.

Hiebert, A. D.; Vermeulen, F. E.; Chute, F. S.; Capjack, C. E. Numerical Simulation Results for the Electrical Heating of Athabasca Oil-Sand Formations. *SPE Reserv. Eng.* **1986**, 1 (01), 76–84.

Hodge, I. M.; Ingram, M. D.; West, A. R. Impedance and Modulus Spectroscopy of Polycrystalline Solid Electrolytes. *J. Electroanal. Chem. Interfacial Electrochem.* **1976**, 74 (2), 125–143.

Holly, C.; Soni, S.; Mader, M.; Toor, J. Alberta Energy, Alberta Energy Oil Sands Production Profile 2004-2014; **2016**.

Hulls, P.; Shute, R. Dielectric Heating in Industry Application of Radio Frequency and Microwaves. *IEE Proc. A - Phys. Sci. Meas. Instrumentation, Manag. Educ. - Rev.* **1981**, 128 (9), 583–588.

Jonscher, A. K. Dielectric Relaxation in Solids. *J. Phys. D. Appl. Phys.* **1999**, 32 (14), R57–R70.

Jonscher, A. K. The Universal Dielectric Response. *Nature* **1977**, 267, 673–679.

- K. N. Jha, A. Chakma. Heavy-Oil Recovery from Thin Pay Zones by Electromagnetic Heating. *Energy Sources* **1999**, 21 (1-2), 63–73.
- Kasevich, R. S.; Price, S. L.; Faust, D. L.; Fontaine, M. F. Pilot Testing of a Radio Frequency Heating System for Enhanced Oil Recovery from Diatomaceous Earth. In SPE 69th Annual Technical Conference and Exhibition; 25-28 September 1994, New Orleans, USA, 1994; pp 105–119.
- Kern, L. R. Method of Producing Bitumen from a Subterranean Tar Sand Formation. US3,848,671, 1974.
- Killough, J. E.; Gonzalez, J. A. A Fully-Implicit Model for Electrically Enhanced Oil Recovery. In 61st Annual Technical Conference and Exhibition of the Society of Petroleum Engineers; 5-8 October, 1986, New Orleans, USA, 1986; pp 1–16.
- Kinzer, D. E. In Situ Processing of Hydrocarbon Bearing Formations with Variable Frequency Automated Capacitive Radio Frequency Dielectric Heating. US7091460B2, 2006.
- Knight, R. J.; Endres, A. L. An Introduction to Rock Physics Principles for Near-Surface Geophysics. In Near-surface geophysics: Volume 13; Society of Exploration Geophysicists Tulsa, 2005.
- Knight, R. J.; Nur, A. The Dielectric-Constant of Sandstones, 60 Khz To 4 Mhz. *Geophysics* **1987**, 52 (5), 644–654.
- Knight, R.; Nolte, L. J. P.; Slater, L.; Atekwana, E.; Endres, a; Geller, J.; Lesmes, D.; Nakagawa, S.; Revil, a; Sharma, M. M.; Straley, C. Geophysics At the Interface : Response of Geophysical Properties To Solid - Fluid , Fluid - Fluid , and Solid - Solid Interfaces. *Rev. Geophys.* **2010**, 48 (2007), RG4002.
- Koolman, M.; Huber, N.; Diehl, D.; Wacker, B. Electromagnetic Heating Method To Improve Steam Assisted Gravity Drainage. In SPE International Thermal Operations and Heavy Oil Symposium; 20–23 October 2008, Calgary, Alberta, Canada, 2008; pp 1–12.
- Kremer, F. Dielectric Spectroscopy – Yesterday , Today and Tomorrow. **2002**, 305, 1–9.

Kremer, F.; Schönhals, A. Analysis of Dielectric Spectra. In *Broadband Dielectric Spectroscopy*; Springer-Verlag Berlin Heidelberg New York, 2003.

Lesmes, D. P.; Friedman, S. P. Relationships between the Electrical and Hydrogeological Properties of Rocks and Soils: In *Hydrogeophysics*; Springer, 2005; pp 87–128.

Lesmes, D. P.; Morgan, F. D. Dielectric Spectroscopy of Sedimentary Rocks. *J. Geophys. Res.* **2001**, 106 (B7), 13329.

Levitskaya, T. M.; Sternberg, B. K. Polarization Processes in Rocks: 1. Complex Dielectric Permittivity Method. *Radio Sci.* **1996**, 31 (4), 781.

Lupi, S.; Forzan, M.; Aliferov, A. Induction and Direct Resistance Heating: Theory and Numerical Modeling; Springer, 2015.

Masliyah, J.; Czarniecki, J.; Xu, Z. Physical and Chemical Properties of Oil Sands. In *Handbook on Theory and Practice of Bitumen Recovery from Athabasca Oil Sands. Vol. 1: Theoretical Basis.*; Kingsley Knowledge Publishing, 2011.

Masson, J. F.; Polomark, G. M. Bitumen Microstructure by Modulated Differential Scanning Calorimetry. *Thermochim. Acta* **2001**, 374 (2), 105–114.

McGee, B. C. W. Electro-Thermal Pilot in the Athabasca Oil Sands: Theory versus Performance. In *Canadian International Petroleum Conference*; 17-19 June 2008, Calgary, Alberta Canada, 2008; Vol. 229, pp 47–54.

McGee, B. C. W.; McDonald, C. W.; Little, L. Comparative Proof of Concept Results for Electrothermal Dynamic Stripping Process : Integrating Environmentalism With Bitumen Production. In *International Thermal Operations and Heavy Oil Symposium*; Calgary, 2009; pp 141–145.

McGee, B. C. W.; McDonald, C. W.; Little, L. Electro-Thermal Dynamic Stripping Process. In *The SPE International Thermal Operations and Heavy Oil Symposium*; 20-23 October, 2008, Calgary, Alberta, Canada; pp 1–8.

- Mcgee, B. C. W.; Vermeulen, F. E. The Mechanisms of Electrical Heating for the Recovery of Bitumen from Oil Sands. *J. Can. Pet. Technol.* **2007**, 46 (1), 28–34.
- McGee, B. C. W.; Vermeulen, F. E.; Yu, L. Field Test of Electrical Heating with Horizontal and Vertical Wells. *J. Can. Pet. Technol.* **1999**, 38 (3), 46–53.
- McPherson, R. G.; Chute, F. S.; Vermeulen, F. E. Recovery of Athabasca Bitumen With the Electromagnetic Flood (Emf) Process. *J. Can. Pet. Technol.* **1985**, 24 (1), 44–51.
- Mcqueen, B. Y. G.; Parman, D.; Williams, H. A Case Study of Enhanced Oil Recovery of Shallow Wells. *Tyco Thermal Controls IEEE Industry Applications Magazine*. **2012**, pp 18–25.
- Mehdizadeh, M. Electric Field (Capacitive) Applicators / Probes. In *Microwave/RF Applicators and Probes, for Material Heating, Sensing, and Plasma Generation*; Elsevier, 2010; pp 67–108.
- Meyer, R.; Attansi, E.; Freeman, P. Heavy oil and natural bitumen resources in geological basins of the world. <http://pubs.usgs.gov/of/2007/1084/> (accessed Jul 1, 2016).
- Mokni, M.; Kahouli, A.; Jomni, F.; Garden, J.-L.; André, E.; Sylvestre, A. Dielectric Investigation of Parylene D Thin Films: Relaxation and Conduction Mechanisms. *J. Phys. Chem. A* **2015**, 119 (35), 9210–9217.
- Mukhametshina, A.; Martynova, E. Electromagnetic Heating of Heavy Oil and Bitumen: A Review of Experimental Studies and Field Applications. *J. Pet. Eng.* **2013**, No. 476519, 1–7.
- Mustafina, D.; Koch, A.; Danov, V.; Sotskiy, S.; Ag, S. Mechanism of Heavy Oil Recovery Driven by Electromagnetic Inductive Heating. In *SPE Heavy Oil Conference Canada*; 11–13 June 2013, Calgary, Alberta, Canada, 2013; pp 1–9.
- Neophytou, R. I.; Metaxas, A. C. Characterisation of Radio Frequency Heating Systems. *IEEE Proceedings-Scientific Meas. Technol.* **1997**, 144 (5), 215–222.
- Newbold, F. R.; Perkins, T. K. Wellbore Transmission of Electrical Power. *J. Can. Pet. Technol.* **1978**, 3 (3), 39–53.
- Olhoeft, G. R. Electrical Properties of Rocks. *Phys. Chem. Rocks Miner.* **1976**, 262–278.

- Olhoeft, G. R. Low-frequency Electrical Properties. *Geophysics* **1985**, 50 (12), 2492–2503.
- Ovalles, C.; Fonseca, A.; Lara, A.; Alvarado, V.; Urrecheaga, K.; Ranson, A.; Mendoza, H. Opportunities of Downhole Dielectric Heating in Venezuela: Three Case Studies Involving Medium Heavy and Extra-Heavy Crude Oil Reservoirs. In SPE International Thermal Operations and Heavy Oil Symposium and International Horizontal Well Technology Conference held; 4–7 November 2002, Calgary, Alberta, Canada; pp 1–10.
- Pasalic, D.; Vaca, P.; Okoniewski, M.; Diaz-Goano, C. Electromagnetic Heating : A SAGD Alternative Strategy to Exploit Heavy Oil Reservoirs. In World Heavy Oil Congress; 24 -26 March, 2015, Edmonton, Alberta, Canada; pp 1–13.
- Peraser, V.; Patil, S. L.; Khataniar, S.; Dandekar, A. Y.; Sonwalkar, V. S. Evaluation of Electromagnetic Heating for Heavy Oil Recovery From Alaskan Reservoirs. In SPE Western Regional Meeting; 19–23 March 2012, Bakersfield, California, USA; pp 1–15.
- Pinder, K. Induction and Dielectric Heating. *Electr. Eng.* **1947**, 66 (2), 149–160.
- Pizarro, J. O. S.; Trevisan, O. V. Electric Heating of Oil Reservoirs. Numerical Simulation and Field Test Results. *J. Pet. Technol.* **1990**, 1320–1326.
- Pritchett, W. C. Method And Apparatus for Producing Fluid by Varying Current Flow Through Subterranean Source Formation. US3,948,319, 1976.
- Psarras, G. C.; Manolakaki, E.; Tsangaris, G. M. Dielectric Dispersion and Ac Conductivity in - Iron Particles Loaded: Polymer Composites. *Compos. Part A Appl. Sci. Manuf.* **2003**, 34, 1187–1198.
- Psarras, G. C.; Manolakaki, E.; Tsangaris, G. M. Electrical Relaxations in Polymeric Particulate Composites of Epoxy Resin and Metal Particles. *Compos. - Part A Appl. Sci. Manuf.* **2002**, 33, 375–384.
- Revil, A. On Charge Accumulation in Heterogeneous Porous Rocks under the Influence of an External Electric Field. *Geophysics* **2013**, 78 (4), D271–D291.

Revil, A.; Eppheimer, J. D.; Skold, M.; Karaoulis, M.; Godinez, L.; Prasad, M. Low-Frequency Complex Conductivity of Sandy and Clayey Materials. *J. Colloid Interface Sci.* **2013**, 398 (November 2015), 193–209.

Rice, S. A.; Kok, A. L.; Neate, C. J. A Test of the Electric Heating Process As a Means of Stimulating the Productivity of an Oil Well in the Schoonebeek Field. *Pet. Soc. CIM* **1992**, 4, 1–16.

Ritchey, H. W. Radiation Heating. US2757738, 1956.

Sandberg, C. Benefits of Heating Heavy Oil with Medium-Voltage Mineral Insulated Cables. *Oil & Gas Engineering*. **2015**, pp 8–9.

Sandberg, C.; Thomas, K.; Hale, A. Advances in Electrical Heating Technology for Heavy Oil Production. In SPE Heavy Oil Conference-; 10-12 June 2014, Alberta Canada; pp 1–6.

Sastry, S. K. Overview of Ohmic Heating. In Ohmic Heating in Food processing; Ramaswamy, H. S., Marcotte, M., Sastry, S., Abdelrahim, K., Eds.; CRC Press, Taylor & Francis Group, 2014.

Scott, G. W. The Role of Frequency in Industrial Dielectric Heating. *Electr. Eng.* **1945**, 64 (8), 558–562.

Sen, P. N.; Chew, W. C. The Frequency Dependent Dielectric and Conductivity Response of Sedimentary Rocks. *J. Microw. Power* **1983**, 18 (1), 97.

Singhal, A. K.; Ito, Y.; Kasraie, M. Screening and Design Criteria for Steam Assisted Gravity Drainage (SAGD) Projects. In SPE International Conference on Horizontal Well Technology; 1-4 November 1998, Calgary, Alberta, Canada; pp 1–7.

SPE International. Electromagnetic heating of oil
http://petrowiki.org/Electromagnetic_heating_of_oil#cite_note-r4-4 (accessed Jun 1, 2016).

Spencer, H. L.; Isted, R. E. Electrical Induction Heating of Heavy Oil Wells Using the Triflux System. **1998**, pp 1–6.

Sresty, G.; Dev, H.; Snow, R.; Bridges, J. Recovery of Bitumen From Tar Sand Deposits With the Radio Frequency Process. *SPE Reserv. Eng.* **1986**, 1 (1), 85–94.

- Svrcek, W. Y.; Mehrotra, A. K. One Parameter Correlation for Bitumen Viscosity. *Chem. Eng. Res. Des.* **1988**, 66 (4), 323–327.
- Takamura, K. Microscopic Structure of Athabasca Oil Sand. *Can. J. Chem. Eng.* **1982**, 60, 538–545.
- Todd, J. C.; Howell, E. P. Numerical Simulation Of In-Situ Electrical Heating To Increase Oil Mobility. *J. Can. Pet. Technol.* **1978**, 2 (1), 31–41.
- Towson, D. The Electric Preheat Recovery Process. In Second International Conference on Heavy Crude and Tar Sand,; 7-17th February, 1982, Caracas, Venezuela, 1982; pp 1–10.
- Trautman, M.; Ehresman, D. T.; Edmunds, N.; Taylor, G.; Cimolai, M. Effective Solvent Extraction System Incorporating Electromagnetic Heating. US 2012/0118565 A1, 2012.
- Trautman, M.; Macfarlane, B. Experimental and Numerical Simulation Results from a Radio Frequency Heating Test in Native Oil Sands at the North Steepbank Mine. In World Heavy Oil Congress; 5-7 March 2014, New Orleans USA; pp 1–14.
- Tsangaris, G. M.; Psarras, G. C.; Kouloumbi, N. Electric Modulus and Interfacial Polarization in Composite Polymeric Systems. *J. Mater. Sci.* **1998**, 33 (8), 2027–2037.
- Van Neste, C. W.; Hawk, J. E.; Phani, A.; Backs, J. a. J.; Hull, R.; Abraham, T.; Glassford, S. J.; Pickering, a. K.; Thundat, T. Single-Contact Transmission for the Quasi-Wireless Delivery of Power over Large Surfaces. *Wirel. Power Transf.* **2014**, 1 (02), 75–82.
- Vermeulen, F. E.; Chute, F. S. Electrical Extraction of Oil From Tar Sand. *IEEE Trans. Ind. Appl.* **1977**, IA-13 (6), 604–607.
- Vermeulen, F. E.; Chute, F. S. Electromagnetic Techniques in the in-Situ Recovery of Heavy Oils. *J. Microw. Power* **1983**, 18 (1), 15–29.
- Vermeulen, F. E.; Chute, F. S. The Induction Heating of Fossil Fuels in-Situ by Electric and Magnetic Fields. *Can. Electr. Eng. J.* **1985**, 10 (4), 147–151.
- Vermeulen, F. E.; Mcgee, B. C. W. In Situ Electromagnetic Heating for Hydrocarbon Recovery and Environmental Remediation. *J. Can. Pet. Technol.* **2000**, 39 (8), 25–30.

Vinsome, K.; W. McGee, B.; Vermeulen, F.; Chute, F. Electrical Heating. *J. Can. Pet. Technol.* **1994**, 33 (4), 29–36.

Wacker, B.; Helget, A.; Torlak, M.; Karmeileopardus, D.; Trautmann, B. Electromagnetic Heating for In-Situ Production of Heavy Oil and Bitumen Reservoirs. In Canadian Unconventional Resources Conference; 15–17 November 2011, Calgary, Alberta, Canada; pp 1–14.

Wadadar, S. S.; Islam, M. R. Numerical Simulation of Electromagnetic Heating of Alaskan Tar Sands Using Horizontal Wells. *Pet. Soc. CIM AOSTRA* **1991**, 35, 1–14.

Wattenbarger, R. A.; McDougal, F. W. Oil Production Response To In Situ Electrical Resistance Heating (Erh). *J. Can. Pet. Technol.* **1988**, 6 (3), 45–50.

Williams, G.; Thomas, D. K. Phenomenological and Molecular Theories of Dielectric and Electrical Relaxation of Materials. *Novocontrol Appl. Note Dielectr.* 1998, 3, 1–29.

Wise, S.; Patterson, C. Reducing Supply Cost With Eseeih TM Pronounced Easy. In SPE Canada Heavy Oil Technical Conference held; Society of Petroleum Engineers: 7–9 June 2016, Calgary, Alberta, Canada; pp 1–12.

Yannioti, S. Microwave and Radiofrequency Heating. In *Heat Transfer in Food Processing: Recent Developments and Applications*; WTI Press, 2007; pp 101–159.

Yu, C. L.; Mcgee, B. C. W.; Chute, F. S.; Vermeulen, F. E. Electromagnetic Reservoir Heating with Vertical Well Supply and Horizontal Well Return Electrodes. Patent Number: 5,339,898, 1994.

Zahabi, A.; Gray, M. R.; Dabros, T. Heterogeneity of Asphaltene Deposits on Gold Surfaces in Organic Phase Using Atomic Force Microscopy. *Energy & Fuels* **2012**, 26 (5), 2891–2898.

Zhao, Y.; Park, J. A. E. W.; Wells, J. H. Using Capacitive (Radio Frequency) Dielectric Heating in Food Processing and Preservation - A Review. *J. Food Process Eng.* **1999**, 23 (860), 25–55.

Appendix A

Table A-1. Experimental data of three runs carried out for estimating the composition of Oil Sands 1 to 6 using the Dean Stark Extraction Method.

Components	Run 1	Run 2	Run 3	Average	Standard Deviation
Oil Sands 1					
Bitumen	11.8%	11.8%	11.6%	11.7%	0.001155
Water	0.3%	0.3%	0.5%	0.4%	0.001155
Coarse Solids	86.2%	86.2%	86.4%	86.3%	0.001155
Fine Solids	1.7%	1.7%	1.5%	1.6%	0.001155
Oil Sands 2					
Bitumen	9.2%	9.6%	9.2%	9.3%	0.002309
Water	1.0%	1.2%	1.0%	1.1%	0.001155
Coarse Solids	85.3%	85.9%	85.8%	85.7%	0.003215
Fine Solids	4.0%	3.3%	3.5%	3.6%	0.003606
Oil Sands 3					
Bitumen	13.0%	12.7%	13.0%	12.9%	0.001732
Water	1.5%	1.5%	1.5%	1.5%	0
Coarse Solids	79.5%	80.8%	80.0%	80.1%	0.006557
Fine Solids	6.0%	5.0%	5.5%	5.5%	0.005
Oil Sands 4					
Bitumen	13.0%	13.0%	13.0%	13.0%	0
Water	3.0%	3.0%	2.0%	2.7%	0.005774
Coarse Solids	64.0%	69.0%	75.0%	69.3%	0.055076
Fine Solids	20.0%	15.0%	10.0%	15.0%	0.05
Oil Sands 5					
Bitumen	12.0%	13.0%	13.0%	12.7%	0.005774
Water	5.2%	4.0%	5.5%	4.9%	0.007937
Coarse Solids	64.0%	69.0%	68.0%	67.0%	0.026458
Fine Solids	18.8%	14.0%	13.5%	15.4%	0.029263
Oil Sands 6					
Bitumen	3.7%	4.0%	3.7%	3.8%	0.001732
Water	12.0%	11.2%	12.0%	11.7%	0.004619
Coarse Solids	64.3%	68.8%	64.3%	65.8%	0.025981
Fine Solids	20.0%	16.0%	20.0%	18.7%	0.023094

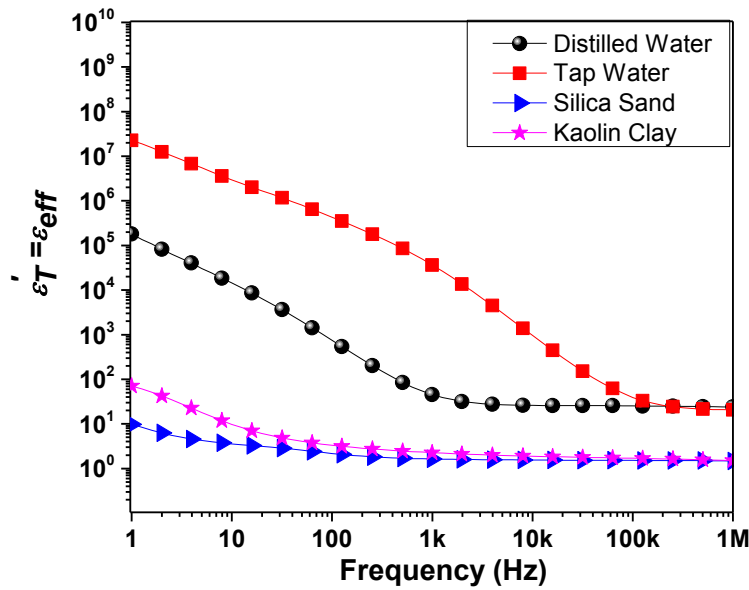


Figure A-1. Calibrated values of dielectric constant for known components when swept from 1Hz to 1MHz at room temperature (20°C).

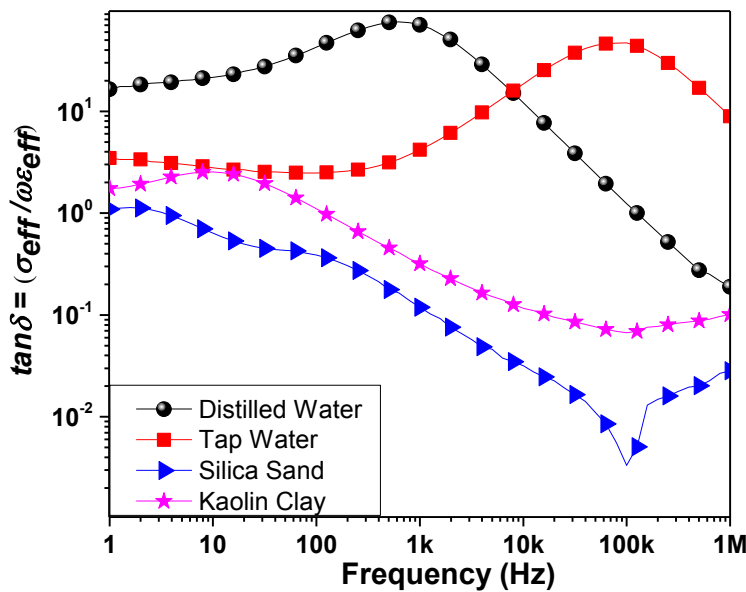


Figure A-2. Calibrated values of Loss tangent for known components when swept from 1Hz to 1MHz at room temperature

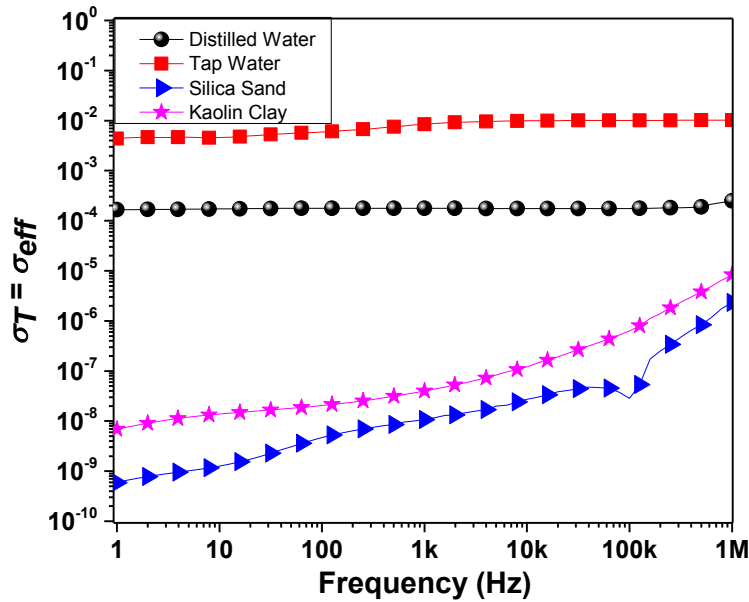


Figure A-3. Calibrated values of conductivity for known components when swept from 1Hz to 1MHz at room temperature.

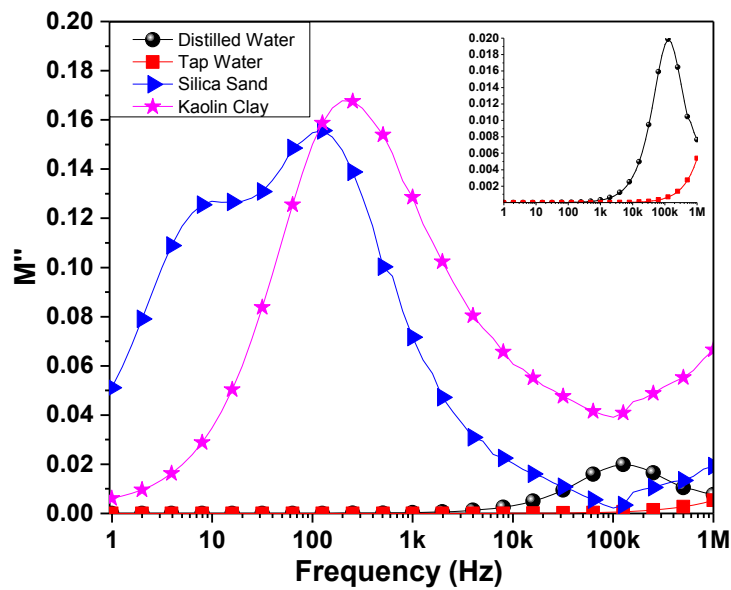


Figure A-4. Calibrated values of modulus spectra for known components when swept from 1Hz to 1MHz at room temperature.

Appendix B

Oil Sands 1

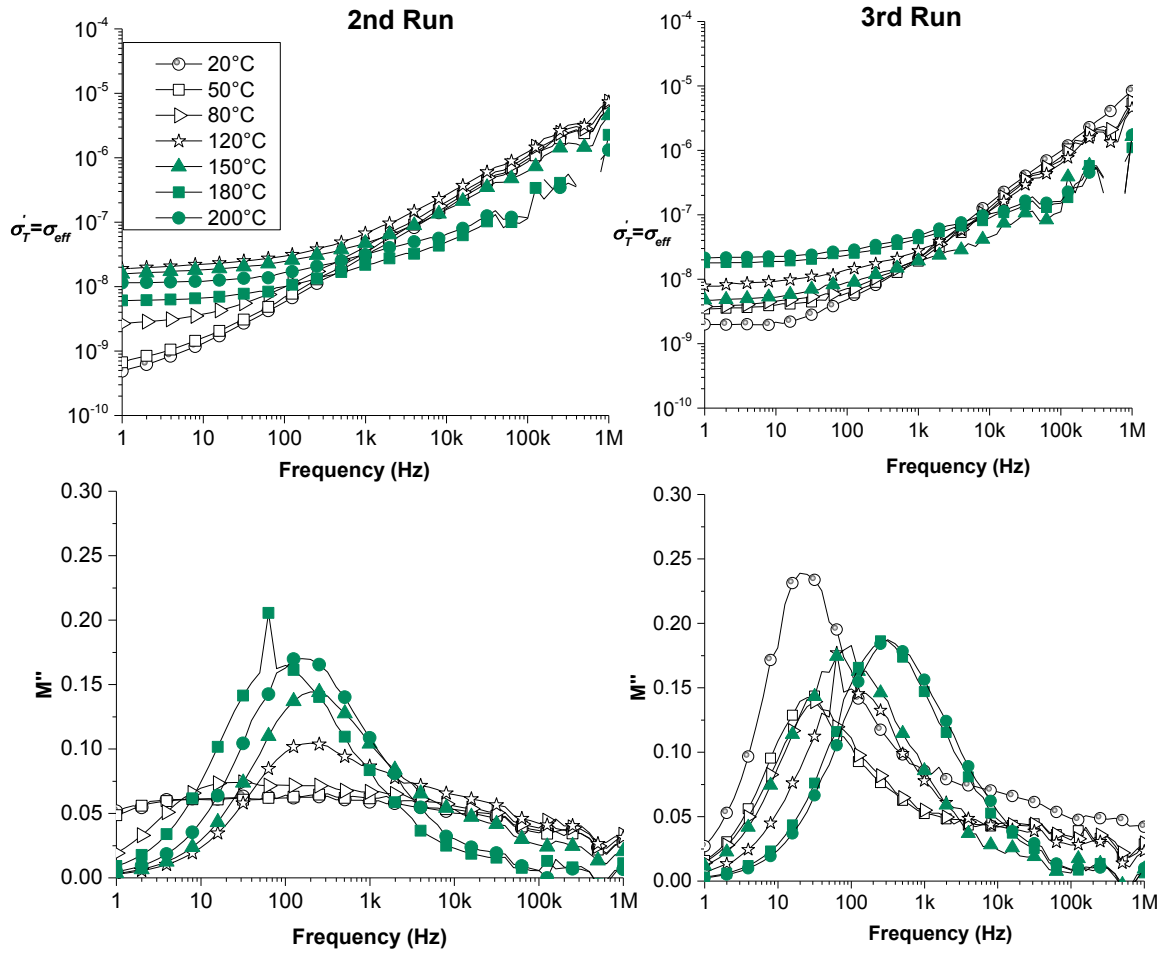


Figure B-5. Results of 2nd and 3rd runs of temperature based conductivity and modulus spectra of Oil Sands 1.

Oil Sands 2

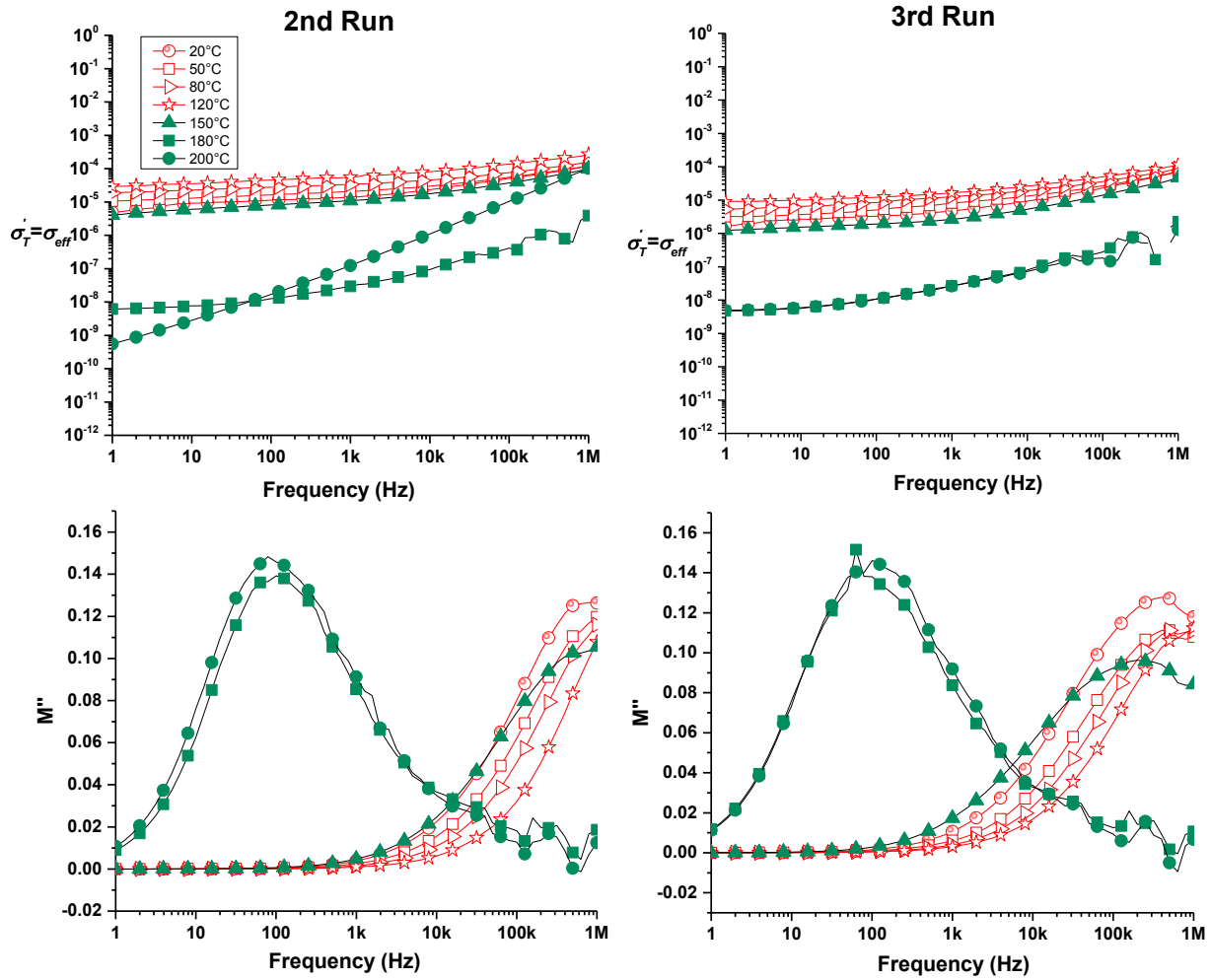


Figure B-6. Results of 2nd and 3rd runs of temperature based conductivity and modulus spectra of Oil Sands 2

Oil Sands 3

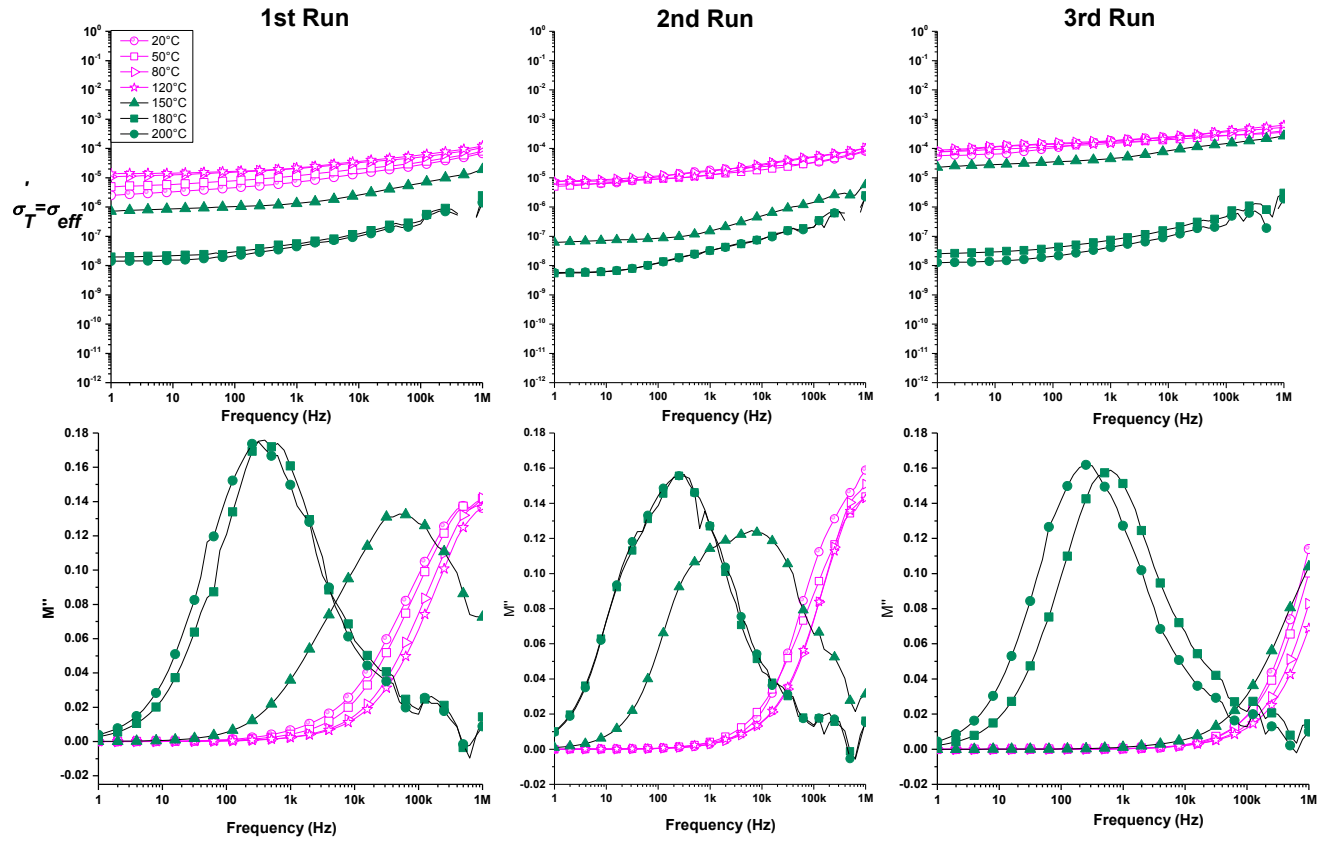


Figure B-7. Results of 1st, 2nd and 3rd runs of temperature based conductivity and modulus spectra of Oil Sands 3

Oil Sands 4

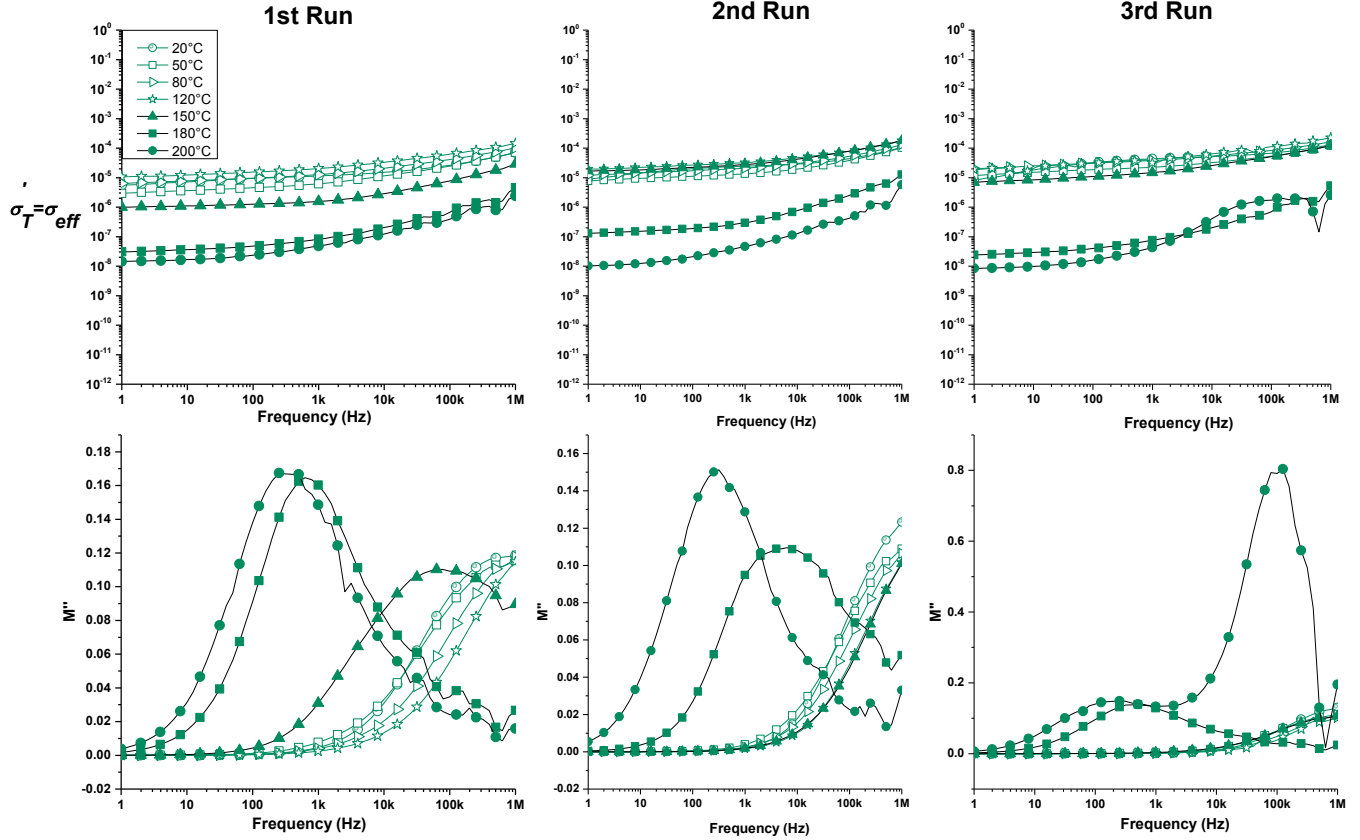


Figure B-8. Results of 1st, 2nd and 3rd runs of temperature based conductivity and modulus spectra of Oil Sands 4

Oil Sands 5

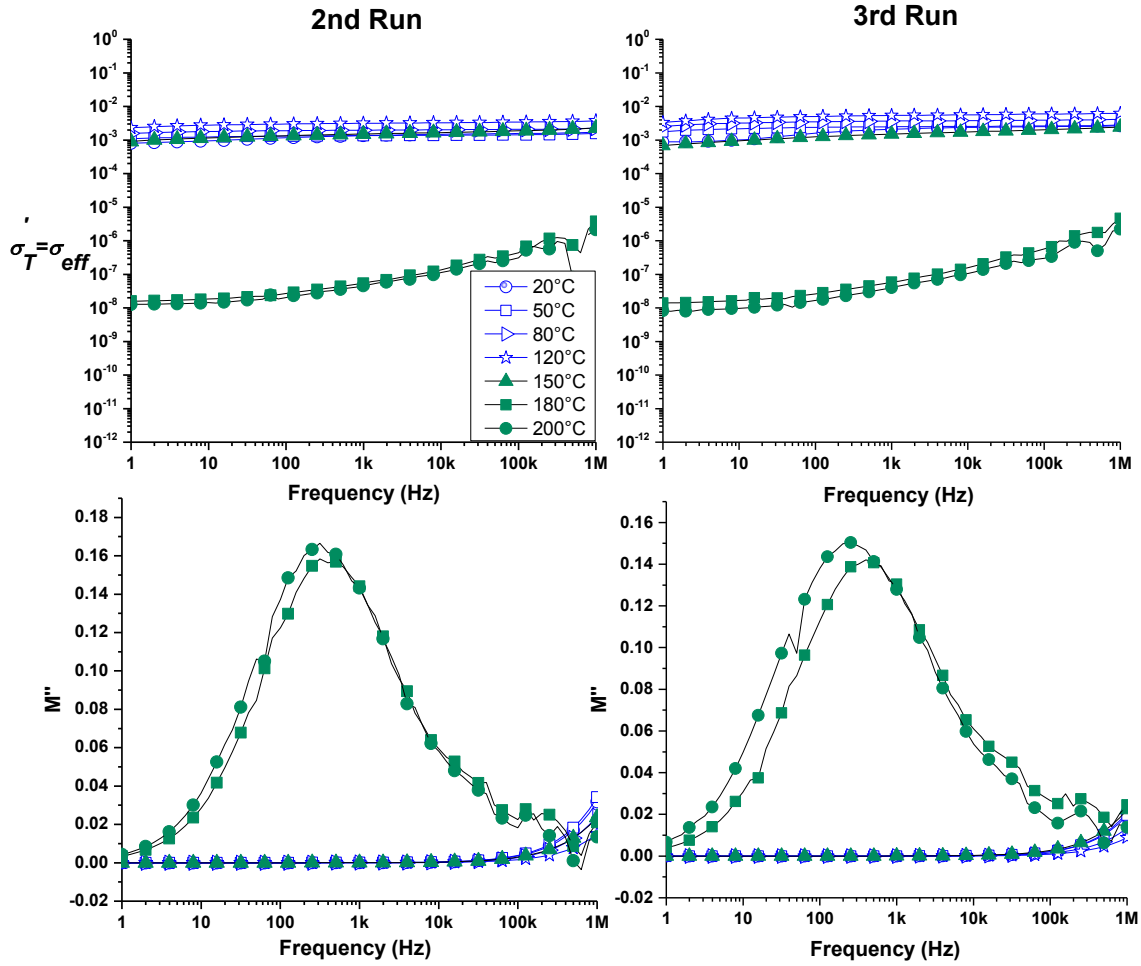


Figure B-9. Results of 2nd and 3rd runs of temperature based conductivity and modulus spectra of Oil Sands 5

Oil Sands 6

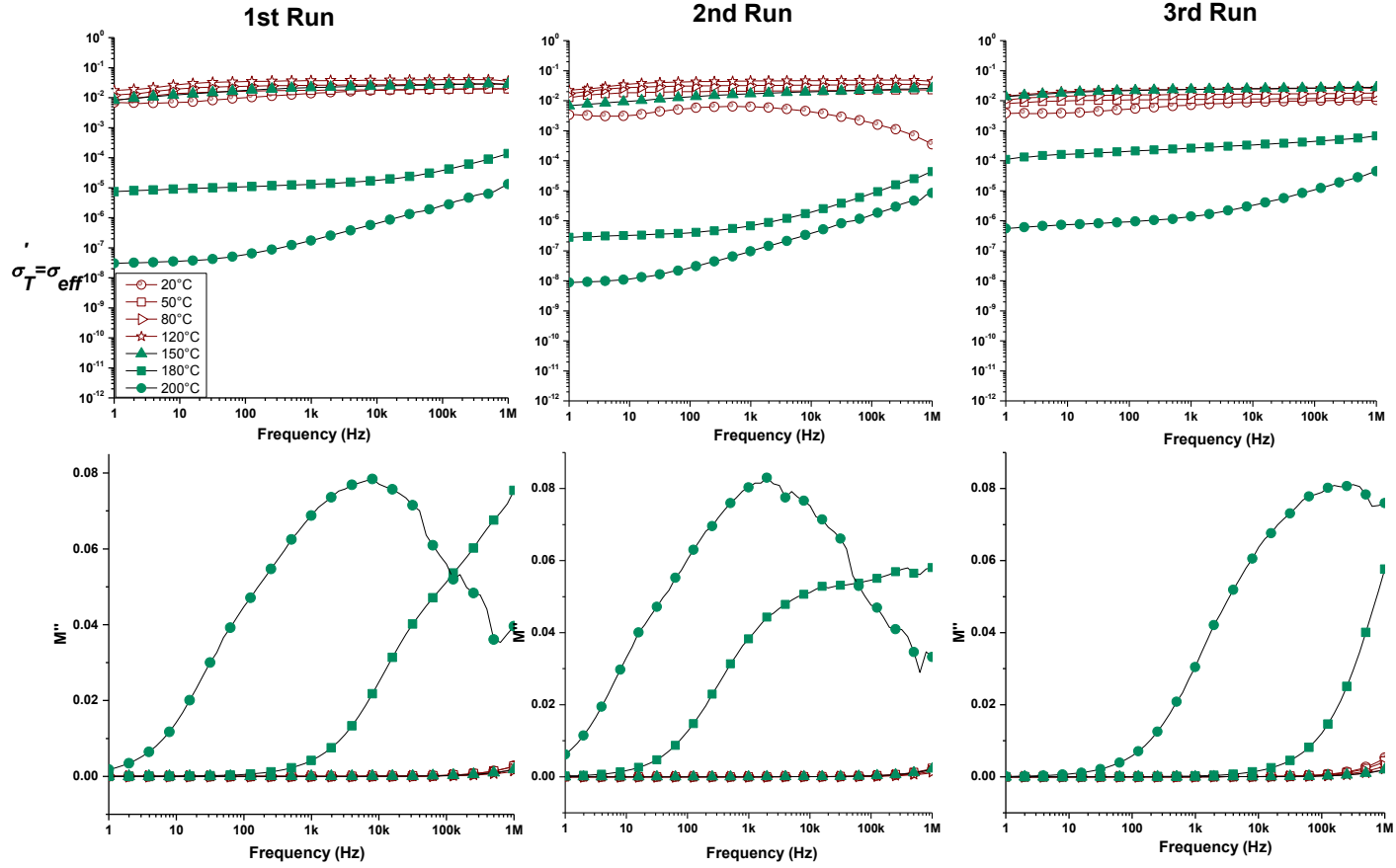


Figure B-10. Results of 1st, 2nd and 3rd runs of temperature based conductivity and modulus spectra of Oil Sands 6

Appendix C

C.1 Assumptions and Experimental Data considered for estimating Electric Field in Big Oil Sands Capacitor Load

$$h = 20 \frac{W}{m^2 \cdot ^\circ C}$$

$$k = 1.72 \text{ W/m}^\circ\text{C} \text{ (CERVENAN, VERMEULEN, and CHUTE 1981)}$$

$$r = 5.5 \text{ cm}$$

$$m = \sqrt{\frac{2h}{kr}} = 20$$

$$\varepsilon' = 5$$

$$\tan \delta = 1.01$$

Table C-2. Estimation of Electric Field in Big Oil Sands Capacitor based on Spatial Temperature Profile at Steady State Condition.

Tapping Location	Bottom Boundary Temperature at steady state ($^\circ\text{C}$)	Top Boundary Temperature at steady state ($^\circ\text{C}$)	Oil Sands Temperature at Steady State (T_z @ $z=0.025 \text{ m}$) ($^\circ\text{C}$)	Heat generated q (W/m^3)	Electric Field in the oil sands (V/m)
29th	69	70	72	49,825	29,119
111th	73	96	90	79,069	36,884
176th	133	140	150	165,780	53,064

C.2 Assumptions and Experimental Data considered for estimating Electric Field in Small Oil Sands Capacitor Load

$$h = 20 \frac{W}{m^2 \cdot ^\circ C}$$

$$k = 1.72 \text{ W/m}^\circ\text{C} \text{ (CERVENAN, VERMEULEN, and CHUTE 1981)}$$

$$r = 2.5 \text{ cm}$$

$$m = \sqrt{\frac{2h}{kr}} = 30$$

$$\varepsilon' = 5$$

$$\tan\delta = 1.01$$

Table C-3. Estimation of Electric Field in Small Oil Sands Capacitor based on Spatial Temperature Profile at Steady State Condition.

Tapping Location	Bottom Boundary Temperature at steady state (°C)	Top Boundary Temperature at steady state (°C)	Oil Sands Temperature at Steady State (Tz @ z=0.025 m) (°C)	Heat generated q (W/m³)	Electric Field in the oil sands (V/m)
29th	30	44	32	10,312	13,098
111th	78	84	85	55,354	30,103
176th	70	58	60	18,100	17,776

Appendix D

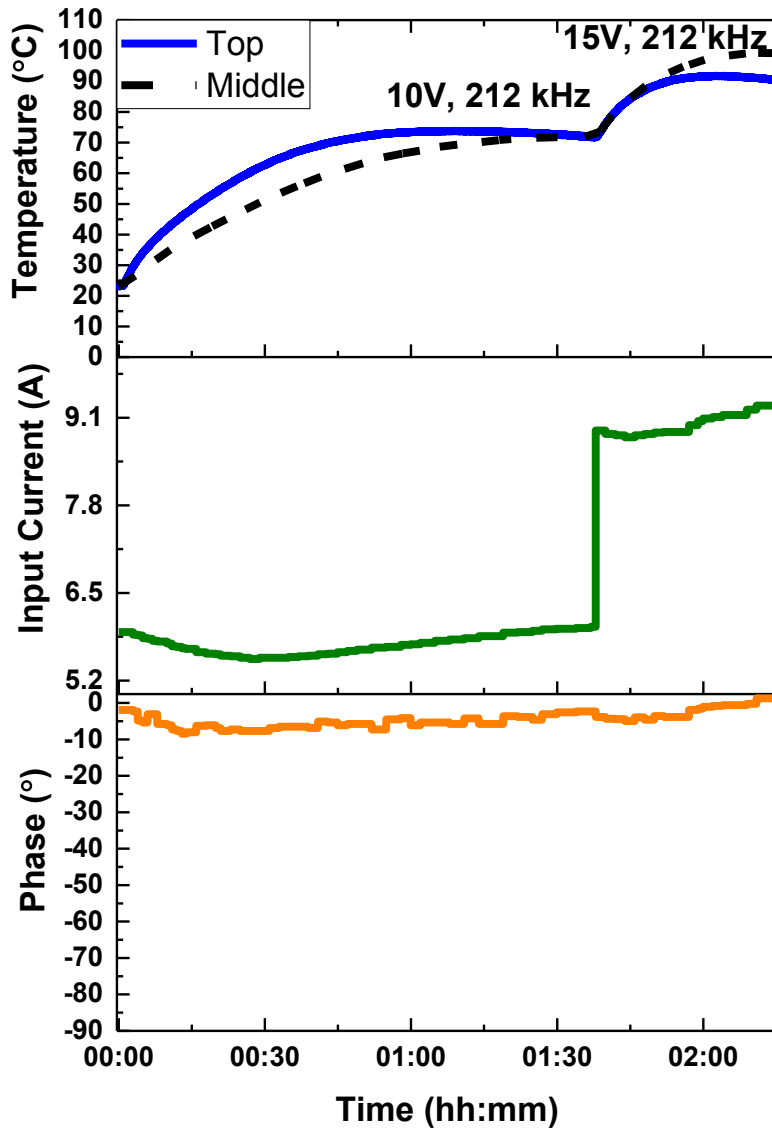


Figure D-11. Capacitive heating results of Oil Sands 1 with input current and phase variations from repeated experiment.

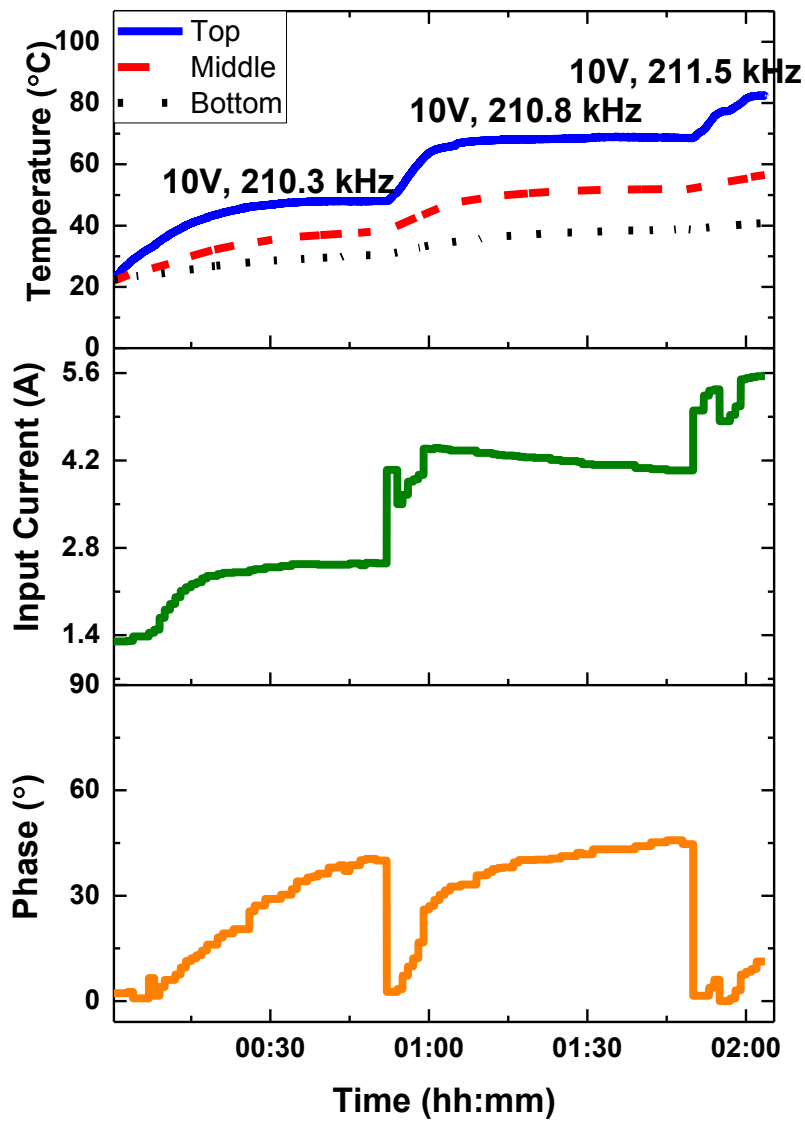


Figure D-12. Capacitive heating results of Oil Sands 4 with input current and phase variations from repeated experiment.

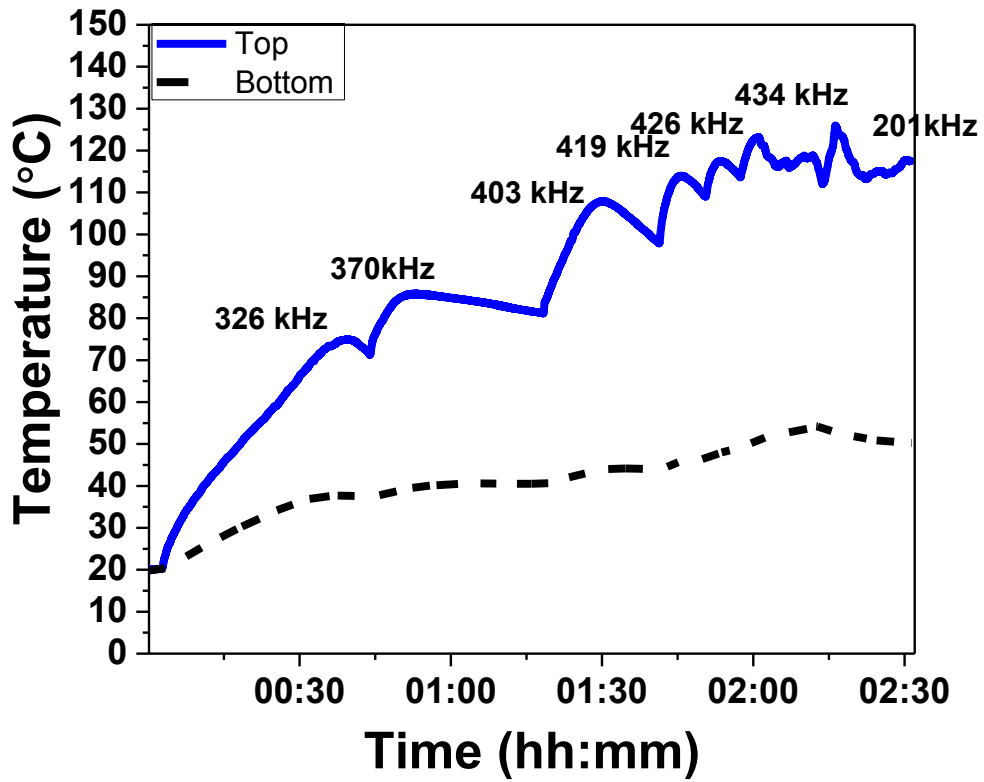


Figure D-13. Capacitive heating results of Oil Sands 5 requiring rapid frequency tuning from repeated experiment